Heterogeneously Catalyzed Oxidation Reactions Using Molecular Oxygen

Beier, Matthias Josef

Publication date:
2011

TECHNICAL UNIVERSITY OF DENMARK (DTU)

Heterogeneously Catalyzed Oxidation Reactions Using Molecular Oxygen

Matthias Josef Beier

Ph.D. Thesis

Supervisors:	Jan-Dierk Grunwaldt	(Karlsruhe Institute of Technology, Germany)
	Anker Degn Jensen	(DTU)
	Georgios M. Kontogeorgis	(DTU)

Department of Chemical and Biochemical Engineering
Combustion and Harmful Emission Control Research Centre

für meine Oma

in Dankbarkeit und liebender Erinnerung

Preface

The present dissertation summarizes the research activities between February 2008 and February 2011 performed as a member of the Combustion and Harmful Emission Control (CHEC) research centre at The Department of Chemical and Biochemical Engineering at the Technical University of Denmark (DTU) and is submitted as a partial fulfillment for obtaining the Ph.D. degree at the DTU. The dissertation was supervised by Jan-Dierk Grunwaldt (Karlsruhe Institute of Technology, Germany), Anker D. Jensen (DTU) and Georgios M. Kontogeorgis (DTU). Experimental work was mainly carried out at DTU and at ETH Zürich (Switzerland) in the group of Professor Alfons Baiker. Financial support was granted by MP_2T Graduate School in Chemical Engineering, DTU, Det Frie Forskningsråd/ Teknologi og Produktion (FTP) and Haldor Topsøe A/S.

Kgs. Lyngby, February 11th, 2011

Excerpts of the thesis were already published:

M.J. Beier, T.W. Hansen, J.-D. Grunwaldt, "Selective liquid phase oxidation of alcohols catalyzed by a silver-based catalyst in the presence of ceria", J. Catal. 2009, 266, 320-330.

M.J. Beier, B. Schimmoeller, T.W. Hansen, J.E.T. Andersen, S.E. Pratsinis, J.-D. Grunwaldt, "Selective side-chain oxidation of alkyl aromatic compounds catalyzed by cerium modified silver catalysts", J. Mol. Catal. A 2010, 331, 40-49.

I. Tsivintzelis, M.J. Beier, J.-D. Grunwaldt, A. Baiker, G.M. Kontogeorgis, "Experimental Determination and Modeling of the Phase Behavior for the Selective Oxidation of Benzyl Alcohol in Supercritical CO_2", Fluid Phase Equilibr., available at doi:10.1016/j.fluid.2010.10.001.

Summary

Heterogeneously catalyzed selective oxidation reactions have attracted a lot of attention in recent time. The first part of the present thesis provides an overview over heterogeneous copper and silver catalysts for selective oxidations in the liquid phase and compared the performance and catalytic properties to the widely discussed gold catalysts. Literature results were summarized for alcohol oxidation, epoxidation, amine oxidation, phenol hydroxylation, silane and sulfide oxidation, (side-chain) oxidation of alkyl aromatic compounds, hydroquinone oxidation and cyclohexane oxidation. It was found that both copper and silver can function as complementary catalyst materials to gold showing different catalytic properties and being more suitable for hydrocarbon oxidation reactions. Potential opportunities for future research were outlined.

In an experimental study, the potential of silver as a catalyst for the selective oxidation of alcohols was investigated. By using a straightforward screening approach, silver supported on silica prepared by impregnation was found to be catalytically active in a mixture with nano-sized ceria. The collaborative effect between ceria and silver was traced back to direct physical contact while leaching could be excluded. The silver catalyst was most active when calcined over a short time at 500 °C potentially due to the formation of silver-oxygen species. Removal of these species might be a deactivation mechanism as was suggested by X-ray absorption spectroscopy (XAS) analysis. XAS revealed that silver was in the metallic state. Silver particle sizes estimated from XAS were significantly smaller (2-3 nm) than from transmission electron microscopy (TEM) and X-ray diffraction (XRD; ca. 30 nm). It was proposed that silver-oxygen species might cause local disorder which would lead to an underestimated particle size by XAS. Based on catalytic studies, a simplified preliminary mechanism was proposed following the dehydrogenation mechanism over gold and palladium catalysts. Comparison of the performance of the silver catalyst with commercial palladium and gold catalysts revealed that all catalysts were more active in combination with ceria nanoparticles and that under the tested reaction conditions silver was equally or even more efficient than the gold catalysts.

Calcination at 900 °C of silver on silica prepared by impregnation afforded a catalyst which was used in the selective side chain oxidation. Toluene, *p*-xylene, ethylbenzene and cumene were oxidized to the corresponding hydroperoxides, alcohols, carbonyl compounds and carboxylic acids most likely

following a radical autoxidation mechanism. *p*-Xylene conversion was promoted by ceria nanoparticles in combination with a carboxylic acid resulting in TONs of up to 2000. In the absence of the carboxylic acid, ceria inhibited the reaction exhibiting radical scavenger properties. Contrary to *p*-xylene, neither ethylbenzene nor cumene conversion was promoted by ceria even in the presence of a carboxylic acid. Substantial leaching of silver was observed with the impregnated silver catalyst. By using silver supported on CeO_2-SiO_2 prepared by flame spray pyrolysis, leaching could be limited significantly. XAS investigation revealed that the active catalyst is most likely metallic silver. Compared to silver on silica calcined at 500 °C (*vide supra*) the particle size obtained from XAS for the impregnated catalyst calcined at 900 °C (> 5 nm) was in qualitative agreement with TEM and XRD results.

Oxidation reactions like the previously described alcohol oxidation can profit from the use of pressurized CO_2 as a solvent. Phase behavior in CO_2 containing systems was previously shown to be important for catalytic reactions. Using the Cubic plus Association (CPA) Equation of State the phase behavior of ternary systems consisting of benzyl alcohol – O_2 – CO_2 and benzaldehyde – H_2O – CO_2 were modeled. Dew points of the latter system occurred in general at lower pressures than the former. Good agreement between experimental data measured at catalysis-relevant conditions and the model was found. Experimental dew points occurred at (slightly) lower pressures as predicted by the model. The usefulness of the model was further evaluated in a continuous catalytic study with Pd/Al_2O_3 as catalyst where the conversion of benzyl alcohol was monitored as a function of pressure. Indeed the reaction rate differed significantly depending on whether the system was mono- or biphasic. The CPA model predictions therefore assist in locating the pressure regime with the highest catalytic activity in a rational manner making extensive trial-and-error experiments unnecessary. Biphasic conditions close to the dew point gave the highest catalytic activity for benzyl alcohol oxidation over Pd/Al_2O_3 while rates were lower under single phase conditions. A reason for this behavior might be overoxidation of palladium or blocking of surface sites by byproducts with low solubility under single phase conditions. Under biphasic conditions the substrate was found to accumulate in the reactor (and the overall experimental setup) leading to longer residence times.

Compared to alcohol oxidation the epoxidation of olefins with molecular oxygen is more difficult. Using *N*,*N*-dimethylformamide (DMF) as a solvent the Co-based metal-organic framework (MOF) STA-12(Co) catalyzed the epoxidation of styrene, (*E*)- and (*Z*)-stilbene. While the stilbene isomers were converted with good selectivity, styrene probably underwent oligomerization as a major side reaction. DMF was oxidized correlating with the olefin conversion thus functioning as a sacrificial reductant. Due to the high Co loading of the MOF, high conversions were achieved with considerably

lower absolute catalyst amounts compared to previous literature results. Higher reaction rates were observed with increasing temperature, substrate concentration and oxygen supply while the amount of catalyst only had a limited influence. Some cobalt leaching was observed though the MOF in general exhibited good stability as suggested by scanning electron microscopy (SEM), XRD and XAS. Amines (from DMF) deactivated the catalyst. The MOF catalyst featured an induction period which was not observed with homogeneously dissolved cobalt. During the induction, the catalyst was activated by benzaldehyde forming as a side-product which led to the interesting effect that co-epoxidation of (*E*)-stilbene proceeded faster in the presence of styrene since styrene is more easily oxidized to benzaldehyde. Further catalytic studies allowed the formulation of a tentative reaction mechanism.

Dansk Resumé

Denne afhandling giver indledningsvist et overblik over heterogene kobber og sølv katalysatorer til selektiv oxidation i væskefase og sammenligner virkningsgraden og katalytiske egenskaber af disse med den i vidt omfang benyttede guld katalysator. Resultater fra litteraturen er opsummeret for alkohol oxidation, epoxidation, amin oxidation, fenyl hydroxylation, silan og sulfid oxidation, (side-kæde) oxidation af alkyl aromatiske stoffer, hydroquinon oxidation samt cyklohexan oxidation. Det er blevet fundet at både kobber og sølv kan fungere som komplementære katalysatormaterialer til guld, idet de udviser andre katalytiske egenskaber og er bedre egnede til kulbrinte oxidationsreaktioner. Potentielle muligheder for fremtidig forskning er heraf blevet skitseret.

Potentialet af sølv som katalysator til selektiv oxidation af alkoholer er blevet undersøgt eksperimentelt. Sølv imprægneret på en silika bærer er ved en screeningsmetode fundet katalytisk aktiv sammen med en blanding af nano-størrelse ceriumoxid. Resultaterne indikerer at den synergistiske virkning mellem ceriumoxid og sølv skyldes den fysiske kontakt imellem de to stoffer hvorimod udludning kunne udelukkes. Sølv katalysatoren udviste højest aktivitet når den var kalcineret i kort tid ved 500 °C, sandsynligvis på grund af dannelsen af sølv-ilt specier. Fjernelsen af disse specier kan muligvis være en deaktiveringsmekanisme, hvilket blev antydet efter analyse med Røntgen-absorbtionsspektroskopi (X-ray absorption spectroscopy, XAS). XAS afslørede at sølv var tilstede i metallisk form. Sølv partikelstørrelserne bestemt med XAS var betydeligt mindre (2-3 nm) end de ved transmission elektronmikroskopi (TEM) samt Røntgen-diffraktion (XRD) bestemte størrelser (ca. 30 nm). En mulig grund kunne være at sølv-ilt specier skabte en lokal uorden, hvilket kunne betyde at XAS underestimerede partikelstørrelsen. En foreløbig mekanisme for dehydrogenering på guld og palladium katalysatorer er blevet foreslået baseret på et katalystisk studium. Til sammenligning med kommercielle palladium og guld katalysatorer var de her dannede sølv katalysatorer mere aktive når de var til stede med ceriumoxid nanopartikler og under de testede reaktionsbetingerlser var sølv mindst lige så godt, og endda i visse tilfælde mere effektive, end guld katalysatoren.

Kalicinering ved 900 °C af sølv imprægneret på silika gav en katalysator der kunne anvendes i selektiv sidekæde oxidation. Toluen, *p*-xylen, etylbenzen samt cumen blev alle oxideret så de dannede de respektive hydroperoxider, alkoholer, karbonyl og karboxylsyre grupper, højst sandsynlig ved fri

radikal autoxidation. *p*-xylen omdannelsen blev fremmet af ceriumoxid nanopartikler i kombination med en karboxylsyre hvilket gav *turn-over*-tal (TON) op til 2000. Uden karboxylsyren inhiberede ceriumoxid derimod reaktionen idet det eliminerede de nødvendige frie radikaler. I modsætning til *p*-xylen blev hverken ethylbenzen eller cumen omdannelsen fremmet af ceriumoxid, selv i kombination med en karboxylsyre. En betydelig udludning af sølv blev observeret for de imprægnerede sølv katalysatorer. Ved at anvende sølv på ceriumoxid-silika fremstillet ved flamme-spray pyrolyse, kunne udludning imidlertid kraftigt begrænses. XAS undersøgelser viste at den aktive katalysator højst sandsynligt var metallisk sølv. I forhold til sølv på silika kalcineret ved 500 °C (*vide supra*) var partikelstørrelsen bestemt med XAS for den imprægnerede katalysator kalicineret ved 900 °C (> 5nm) i kvalitativ overensstemmelse med TEM og XRD.

Oxidationsreaktioner som den førnævnte alkoholoxidation kan fremmes ved brug af tryksat CO_2 som opløsningmiddel. Faseegenskaberne i CO_2 holdige systemer er tidligere vist at være vigtige for de katalytiske egenskaber. Ved brug af en tilstandsligning (cubic-plus-association, CPA) er faseegenskaberne blevet modelleret i ternære systemer bestående af benzylalkohol-ilt-CO_2 og benzylaldehyd-vand-CO_2. Dugpunkter af sidstnævnte system lå generelt ved lavere tryk. Der blev observeret god overenstemmelse mellem de målte og eksperimentelle data ved reaktionsrelevante betingelser. Eksperimentelt fundne dugpunkter lå ved (en smule) lavere end tryk end forudsagt af modellen. Modellens anvendelighed blev yderligere evalueret ved undersøgelse af en Pd/Al_2O_3 katalysators egenskaber vedkontinuerte omdannelse af benzylalkohol i en flow reaktor, hvori omdannelsen blev fulgt som funktion af trykket. Reaktionshastighederne var betydeligt forskellige afhængig af hvorvidt systemet indeholdt en eller to faser. CPA modellens forudsigelser kan derfor anvendes til at bestemme tryk betingelser i hvilket den højeste katalytiske aktivitet kan opnås, hvilket overflødiggør ofte meget omfattende og gentagne eksperimentelle forsøg. Tofase betingelser tæt ved dugpunktet gav den højeste katalystiske aktivitet for oxidation af benzylalkohol på en Pd/Al_2O_3 katalysator, mens etfase betingelser gav en lavere reaktionshastighed. En af grundene for dette er muligvis en overoxidation af palladium eller en overfladeblokering med sideprodukter af lav opløslighed under etfase betingelser. Ved tofase betingelser blev reaktanterne akkumuleret i reaktoren hvilket gav længere opholdstider af væskefasen og lange tider til stabil drift.

I forhold til alkoholoxidation er epoxideringen af olefiner med molekylært ilt vanskeligere. Ved at bruge N,N-dimethylformamid (DMF) som opløsningsmiddel kunne en Co-baseret metalorganisk gitter (MOF) [STA-12(Co)] katalysere epoxideringen af styren, (E) og (Z)-stilben. Hvor stilben isomererne blev omdannet med god selektivitet, gennemgik styren formentlig en oligomerisering som en betydelig

sidereaktion. Derudover blev DMF også oxideret under olefin omdannelsen og virkede dermed yderligere som et i stort overskud tilgængeligt reduktionsmiddel. På grund af det høje indhold af Co i MOF'en, kunne høje omdannelsesgrader opnås ved betydeligt lavere absolutte mængder katalysator i forhold til tidligere resultater fra litteraturen. Højere reaktionshastigheder blev observeret ved øget temperatur, reaktantkoncentration og iltforsyning, hvorimod mængden af katalysator kun havde en begrænset indflydelse. En vis cobolt udludning blev observeret, selv om MOF'en generelt udviste en god stabilitet (som set i SEM, XRD og XAS). Det blev også fundet at aminer deaktiverede katalysatoren. MOF katalysatoren havde en opstartsperiode der ikke sås tilsvarende for homogent opløst cobolt. Under opstartsperioden blev katalysatoren aktiveret af benzylaldehyd der dannedes som sideprodukt hvilket gav den interessante effekt at sam-epoxideringen af (E)-stilben skete hurtigere ved tilstedeværelsen af styren eftersom styren lettere oxideres til benzylaldehyd. Yderligere katalytiske studier gjorde det muligt at opstille en foreløbig reaktionsmekanisme.

Table of Contents

Chapter 1

Introduction

With its great influence on society, heterogeneous catalysis has been a political issue for more than 100 years. Like many scientific areas, catalysis also has a tragic history. The Haber-Bosch process developed for ammonia synthesis kept the German artillery firing almost 100 years ago and around 25 years later, the coal liquefaction processes by Bergius-Pier and Fischer-Tropsch allowed the German tanks to keep rolling causing death and suffering for millions. The societal impact of catalysis has shifted by now. Haber-Bosch is feeding the world and Fischer-Tropsch is intended to make the world a greener place. Indeed, catalysis is a key to the development of environmentally benign and sustainable processes and a cornerstone in the concept of "Green Chemistry" [1-3].

First and foremost, catalysis is part of our everyday life and contributes substantially to our societal wealth. It is therefore not surprising that many basic processes e.g. hydrogenation and oxidation reactions are of constant interest both in academia and industry bringing forth more and more effective catalysts, new technologies and an ever increasing in-depth understanding of fundamental catalytic principles. Heterogeneous catalysis taking place at the interface between two phases is difficult to study. Detailed knowledge is available on important gas-phase reactions like ammonia synthesis and CO oxidation and was recently awarded with the Nobel prize for Gerhard Ertl [4].

The present thesis concentrates on studying liquid phase oxidation catalysis. Oxidation catalysis is a mandatory tool (Figure 1-1) for the production of fine chemicals [5], functionalization of petrochemical feedstocks [6] and for harmful emission control [7] and will contribute to the development of new target compounds from biomass [8]. The capability of catalysts to activate environmentally benign and inexpensive oxidants such as hydrogen peroxide and especially molecular oxygen has added a great deal to the attractiveness of catalysts eliminating toxic and atom-inefficient oxidants like hexavalent chromium. On an industrial scale, both homogeneous and heterogeneous

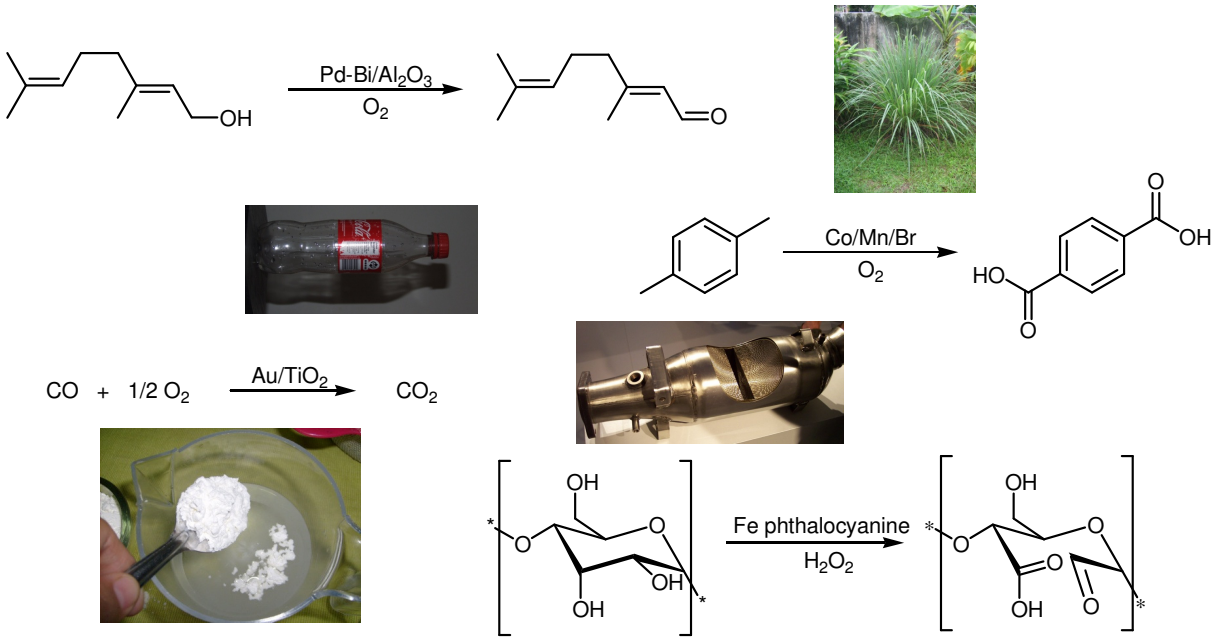

Figure 1-1: Catalytic oxidation reactions.

catalysts found their field of application. Homogenous transition metal catalysts being present in the same phase as the substrate(s) afford high reaction rates and variation of the ligand sphere is often an effective and relatively simple way of tailoring catalyst properties. In some cases, homogenous catalysts are highly active already in minimal concentrations which make a catalyst separation step dispensable. Zirconocenes ("Kaminsky catalysts") used in olefin polymerization [9] are an often cited example for catalysts with such remarkable activities. Within oxidation catalysis cobalt salts are used initiating the radical autoxidation of hydrocarbons. In combination with manganese salts and a bromide source inexpensive cobalt salts form the basis of the AMOCO process producing terephthalic acid from *p*-xylene [10]. Due to the nature of a radical autoxidation only small quantities of catalyst are necessary to achieve high conversions and – in terms of figures – enormous turn-over frequencies. When catalysts are less active and production costs or mandatory end product qualities require separation of the catalyst, heterogeneous catalysts are advantageous. Grafting of homogeneous catalysts is a possibility [11] but the usually observed higher stability and the significantly lower production costs make this a key research area of inherently heterogeneous catalysts – minerals, oxides, (supported) nanoparticles, metal foams etc.

In order to achieve high efficacy, selectivity is often regarded to be more important and harder to achieve than activity. Selectivity in terms of heterogeneously catalyzed oxidation reactions includes the selective formation of one partial oxidation product, the chemoselective oxidation of only one oxidizable moiety within a molecule (though to several different products, e.g. the selective side-chain

oxidation of alkyl aromatic compounds, *cf.* Chapter 4) and the selective oxidation of one type of compound within a mixture of several (e.g. CO oxidation in H_2 containing atmosphere [12]) [13]. Due to the capability of many noble metals to adsorb and activate molecular oxygen, supported noble metal nanoparticles were especially successful and play a key role in selective oxidation catalysis affording numerous impressive results. Platinum group metal catalysts are dominating in the selective oxidation

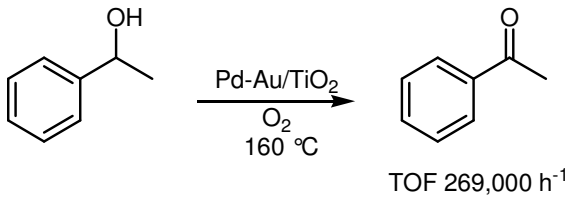

Scheme 1-1: High turn-over frequencies for alcohol oxidation [14].

of alcohols [5]. Very high turn-over frequencies for benzyl alcohol oxidation were obtained over palladium-gold bimetallic catalysts [14] under solvent-free high-temperature conditions. TOFs as high as 269,000 h^{-1} for 1-phenylethanol (Scheme 1-1) and 86,500 h^{-1} for benzyl alcohol at 160 °C were reported (though without stating the selectivities). Despite these impressive numbers it should not be forgotten that the tested alcohols are model compounds for more complex (often solid) substrates thus mild temperatures and the use of a solvent are frequently required. Benzaldehyde production as such is more feasible from an economical viewpoint *via* toluene oxidation with cobalt catalysts or hydrolysis of benzal chloride [15].

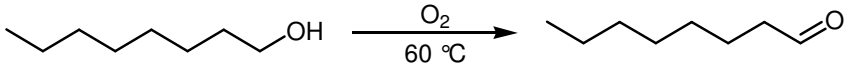

	Conversion	Selectivity
5%Pt/Al_2O_3	34 %	94 %
5%Pt-1%Bi/Al_2O_3	66 %	87 %

Scheme 1-2: Oxidation of 1-octanol over 5%Pt/Al_2O_3 with and without Bi promotion [18].

Promotion of either palladium or platinum catalysts by bismuth or lead [16] made the catalysts industrially relevant resulting in a large amount of patents. Alcohols highly susceptible to overoxidation can be oxidized with good selectivity (Scheme 1-2). There are different suggestions for the role of the

promoter. As an example, promoters may block highly active sites thereby stabilizing the catalyst against poisoning [17].

Heterogeneous ruthenium catalysts stand out due to excellent selectivities achieved e.g. over Ru/Al_2O_3 exceeding 97 % for a number of aliphatic and benzylic alcohols at full conversion. Even electron-poor alcohols were oxidized efficiently under relatively mild conditions [19]. The use of platinum group metals is of course not limited to alcohol oxidation, Ru/Al_2O_3 also catalyzes amine oxidation [20], stabilized platinum nanoparticles oxidize hydroquinones with oxygen [21] and palladium can be used to insert oxygen in alkynes [22] just to name a few (Scheme 1-3). Still, alcohol oxidation is the most intensively studied reaction (especially for palladium) within liquid phase oxidations.

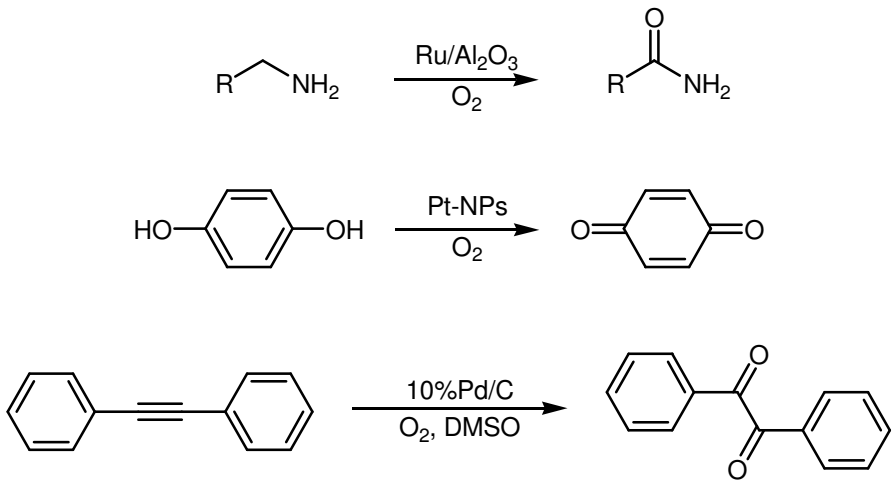

Scheme 1-3: Oxidation reactions over platinum group metals.

The interest in gold as a catalyst material has reached out from low-temperature CO oxidation [7, 23, 24]. From there the use of gold was broadened to liquid phase transformations of course including the selective oxidation of alcohols [25, 26] but gold has also shown interesting activity in epoxidation reactions activating molecular oxygen directly without the need for a sacrificial reductant like H_2, hydrocarbons or aldehydes [27-29]. While a high focus was laid on gold in liquid phase oxidation reactions, the other coinage metals – silver and copper – have received less attention. The literature review in Chapter 2 will show if this is justified highlighting the strengths and opportunities of these lighter coinage metals. Chapter 3 and 4 evaluate the performance of silver catalysts for the oxidation of alcohols and alkyl aromatic compounds, respectively. By a special screening approach an interesting promoter effect of nano-sized ceria was found which in the case of alcohol oxidation was also observed

with palladium and gold catalysts. Whether ceria was a promoter or inhibitor depended on the substrate for the side-chain oxidation of alkyl aromatic compounds.

A fairly new field of research is the use of pressurized – often slightly simplified called "supercritical"[1] – CO_2 (Figure 1-2) as a solvent in combination with molecular oxygen [30, 31]. The use of CO_2 can have various advantages; one certainly is the increased safety making last but not least working in the laboratory with oxygen and organic substrates at high pressures considerably more comfortable. The high solubility of oxygen can increase rates of reactions limited by oxygen mass transport though a high oxygen availability can also deactivate the catalyst due to overoxidation [32-36]. Pressurized CO_2 is

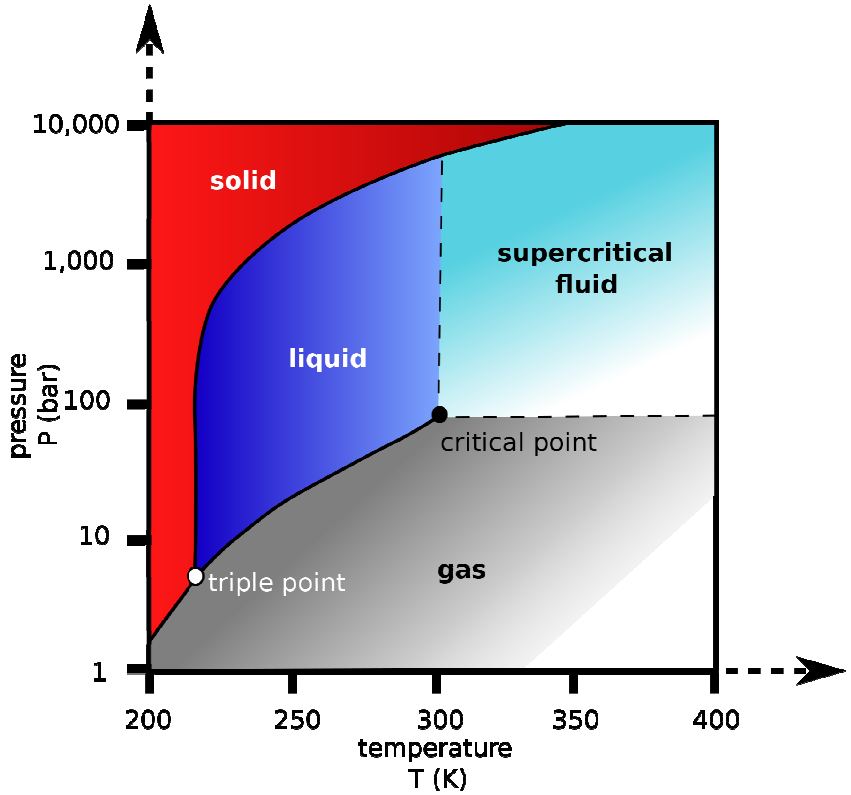

Figure 1-2: Phase diagram of carbon dioxide. Above the critical temperature liquefaction of CO_2 is not possible [37].

a good solvent for non-polar organic substrates. The solvent power of CO_2 depends on the pressure and hence, all reactants can be present in a single phase (except of course the heterogeneous catalyst) or exist as a multiphasic mixture. This influences reaction rates and therefore knowledge about the phase behavior is desirable. Chapter 5 shows an approach using the Cubic plus Association Equation of State

[1] "Supercritical" applies strictly speaking only to pure compounds.

for modeling the phase behavior of ternary mixtures relevant in the oxidation of benzyl alcohol. The usefulness of phase modeling is evaluated in a continuous oxidation of benzyl alcohol over an alumina supported palladium catalyst, a catalytic process which has shown high sensitivity to pressure changes [38, 39].

While catalysts readily catalyze the oxidation of alcohols with molecular oxygen, there are only few analogue examples in epoxidation catalysis. In rare cases, gold catalysts [27, 40] were found to activate oxygen (*vide supra*) but often a sacrificial reductant is necessary. Also epoxidation in *N*,*N*-dimethylformamide with cobalt catalysts require no additional sacrificial reductant but there is some debate to what the role of the solvent is. Chapter 6 summarizes investigations with a highly active cobalt-based metal-organic framework which give some new insights. In addition, benzaldehyde as a side-product of olefin epoxidation played a special role activating the catalyst.

References

[1] J.H. Clark, Green Chem. 1 (1999) 1.

[2] P.T. Anastas, M.M. Kirchhoff, Acc. Chem. Res. 35 (2002) 686.

[3] C.H. Christensen, J. Rass-Hansen, C.C. Marsden, E. Taarning, K. Egeblad, ChemSusChem 1 (2008) 283.

[4] G. Ertl, Angew. Chem. 120 (2008) 3578.

[5] T. Mallat, A. Baiker, Chem. Rev. 104 (2004) 3037.

[6] W. Partenheimer, Adv. Synth. Catal. 351 (2009) 456.

[7] M. Haruta, T. Kobayashi, H. Sano, N. Yamada, Chem. Lett. (1987) 405.

[8] S.R. Collinson, W. Thielemans, Coord. Chem. Rev. 254 (2010) 1854.

[9] J. Herwig, W. Kaminsky, Polym. Bull. 9 (1983) 464.

[10] W. Partenheimer, Catal. Today 23 (1995) 69.

[11] M.J. Beier, W. Knolle, A. Prager-Duschke, M.R. Buchmeiser, Macromol. Rapid Comm. 29 (2008) 904.

[12] M.M. Schubert, V. Plzak, J. Garche, R.J. Behm, Catal. Lett. 76 (2001) 143.

[13] I. Hermans, E.S. Spier, U. Neuenschwander, N. Turra, A. Baiker, Top. Catal. 52 (2009) 1162.

[14] D.I. Enache, J.K. Edwards, P. Landon, B. Solsona-Espriu, A.F. Carley, A.A. Herzing, M. Watanabe, C.J. Kiely, D.W. Knight, G.J. Hutchings, Science 311 (2006) 362.

[15] F. Ullmann, "Ullmann's encyclopedia of industrial chemistry", 6th edition, Wiley-VCH, Weinheim, 2003.

[16] H. Fiege, K. Wedemeyer, Angew. Chem. Int. Ed. 20 (1981) 783.

[17] T. Mallat, A. Baiker, Catal. Today 19 (1994) 247.

[18] R. Anderson, K. Griffin, P. Johnston, P.L. Alsters, Adv. Synth. Catal. 345 (2003) 517.

[19] K. Yamaguchi, N. Mizuno, Angew. Chem. Int. Edit. 41 (2002) 4538.

[20] J. Kim, K. Yamaguchi, N. Mizuno, Angew. Chem. Int. Edit. 47 (2008) 9249.

[21] H. Miyamura, M. Shiramizu, R. Matsubara, S. Kobayashi, Angew. Chem. Int. Edit. 47 (2008) 8093.

[22] S. Mori, M. Takubo, T. Yanase, T. Maegawa, Y. Monguchi, H. Sajiki, Adv. Synth. Catal. 352 (2010) 1630.

[23] M. Haruta, N. Yamada, T. Kobayashi, S. Iijima, J. Catal. 115 (1989) 301.

[24] M. Haruta, S. Tsubota, T. Kobayashi, H. Kageyama, M.J. Genet, B. Delmon, J. Catal. 144 (1993) 175.

[25] A. Corma, H. Garcia, Chem. Soc. Rev. 37 (2008) 2096.

[26] C. Della Pina, E. Falletta, L. Prati, M. Rossi, Chem. Soc. Rev. 37 (2008) 2077.

[27] M.D. Hughes, Y.J. Xu, P. Jenkins, P. McMorn, P. Landon, D.I. Enache, A.F. Carley, G.A. Attard, G.J. Hutchings, F. King, E.H. Stitt, P. Johnston, K. Griffin, C.J. Kiely, Nature 437 (2005) 1132.

[28] S. Bawaked, N.F. Dummer, N. Dimitratos, D. Bethell, Q. He, C.J. Kiely, G.J. Hutchings, Green Chem. 11 (2009) 1037.

[29] M. Turner, V.B. Golovko, O.P.H. Vaughan, P. Abdulkin, A. Berenguer-Murcia, M.S. Tikhov, B.F.G. Johnson, R.M. Lambert, Nature 454 (2008) 981.

[30] T. Seki, M. Baiker, Chem. Rev. 109 (2009) 2409.

[31] A. Baiker, Chem. Rev. 99 (1999) 453.

[32] C. Keresszegi, T. Burgi, T. Mallat, A. Baiker, J. Catal. 211 (2002) 244.

[33] C. Keresszegi, D. Ferri, T. Mallat, A. Baiker, J. Phys. Chem. B 109 (2005) 958.

[34] M. Caravati, J.-D. Grunwaldt, A. Baiker, Catal. Today 126 (2007) 27.

[35] J.-D. Grunwaldt, C. Keresszegi, T. Mallat, A. Baiker, J. Catal. 213 (2003) 291.

[36] C. Keresszegi, J.-D. Grunwaldt, T. Mallat, A. Baiker, J. Catal. 222 (2004) 268.

[37] Obtained from "http://en.wikipedia.org/wiki/Carbon_dioxide", last accessed on January, 24th, 2011.

[38] M. Caravati, J.-D. Grunwaldt, A. Baiker, Catal. Today 91-2 (2004) 1.

[39] M. Caravati, J.-D. Grunwaldt, A. Baiker, Phys. Chem. Chem. Phys. 7 (2005) 278.

[40] R.M. Lambert, F.J. Williams, R.L. Cropley, A. Palermo, J. Mol. Catal A 228 (2005) 27.

Chapter 2

All That Glitters is not Gold – Selective Liquid-Phase Oxidation Catalysis with Heterogeneous Copper and Silver Catalysts in Comparison to Gold

Abstract

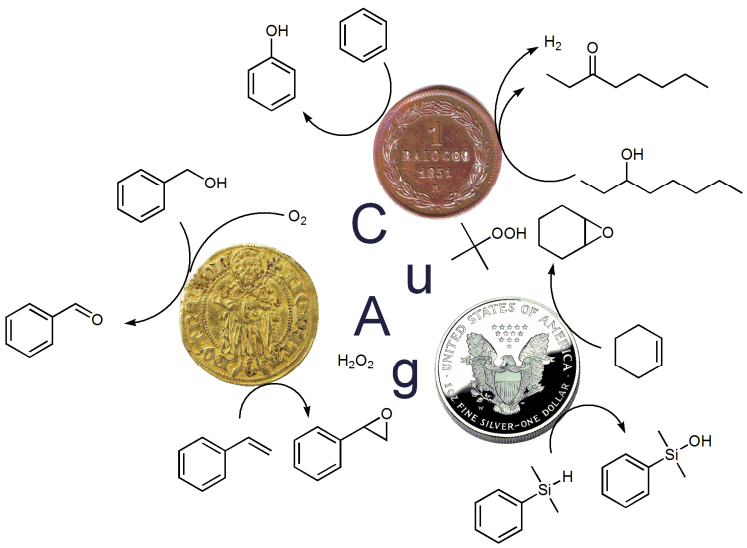

Coinage metal catalysts.

Gold as an active material for oxidation catalysis has received a great deal of attention in the recent years. This overview will focus on silver and copper, covering all coinage metals. Both metals also have shown a considerable potential as heterogeneous catalysts for different selective oxidation reactions in the liquid phase. For many oxidation reactions, the efforts which were put in gold-related research have brought forward gold catalysts with high catalytic performance. Cu and Ag can profit from the extensive knowledge on Au catalysts due to similarities between the coinage metals. As an example, alcohol oxidation which was first studied over gold catalysts can also be efficiently catalyzed by silver. Synthesis techniques from gold catalysts can be adapted for copper and silver but their complex

chemistry requires specialized routes for catalyst synthesis. Thus, common synthesis techniques will be summarized highlighting important design principles. Available literature on oxidation reactions catalyzed by silver and copper and – if not already described by other recent reviews – gold will be summarized. The strengths and opportunities of the three metals will be discussed and compared stressing out the chances of Cu and Ag thereby showing that the two metals are not necessarily competitors of gold but often complementary. Opportunities for further research will be outlined.

2.1 Introduction

Ever since Haruta *et al.* [1-3] disproved the prejudice of gold being a beautiful but essentially inert metal in catalysis, a huge run on gold started – first with the in-depth investigation of the Au catalyzed gas phase CO oxidation proceeding already at room temperature or even below. The use of gold as a potent heterogeneous oxidation catalyst was extended to selective liquid phase oxidations resulting in an immense amount of literature [4-10]. But the origin of the fascination of gold is also its strongest burden: its low availability and high price (apart from the color and the gold-digger myths). Despite the tremendous knowledge on gold catalyzed reactions, there are only few examples where gold is industrially competitive [11]. On the other hand, the smaller siblings of gold – silver and copper – have long been applied for important catalytic processes in industry, silver being used in methanol oxidation as well as ethylene epoxidation and copper e.g. for methanol synthesis. However in academics, both silver and copper received far less attention and thus have not made it to step out of the shadow of gold especially in selective liquid-phase oxidations. Considering that silver is roughly 2 orders and copper even 4 orders of magnitude less expensive than gold makes industrial applications much more likely. Establishing new processes on the background of the discussion on “Green Chemistry” is certainly important and the price of a catalyst is a crucial factor in making a process sustainable. With respect to CO oxidation, both silver [12-15] and copper [16-19] have proven their ability to catch up with gold. Applications of heterogeneous copper and silver catalysts in the total oxidation of harmful organic compounds in wastewater effluents [20-23] underline their potential in liquid phase oxidations. Recently, the potential of the coinage metals mainly in gas phase reactions was summarized in two reviews [4, 10]. This chapter will concentrate on liquid-phase oxidations and compare heterogeneous silver and copper catalysis with the broad field of gold catalysis. The intention is to show the niches and individual strengths of silver and copper but also supplying a short overview over important features of liquid-phase gold catalysis. Opportunities for future research will be described, benefitting from the broad knowledge on gold catalysis.

Focus has been laid on selective oxidations by intrinsically heterogeneous catalysts. Thus, total oxidations and immobilized complexes being an extensive topic especially for Cu catalysis will only be covered where it supports the argumentation. After providing a short summary of synthesis techniques towards the different catalysts the most important selective oxidation reactions will be described where one or more of the coinage metals play a significant role as a catalyst material. A discussion with respect to important parameters for catalyst synthesis, differences between the catalytic properties and performance of the metals and finally opportunities for future work will complete this chapter.

2.2 Catalyst synthesis for oxidation reactions

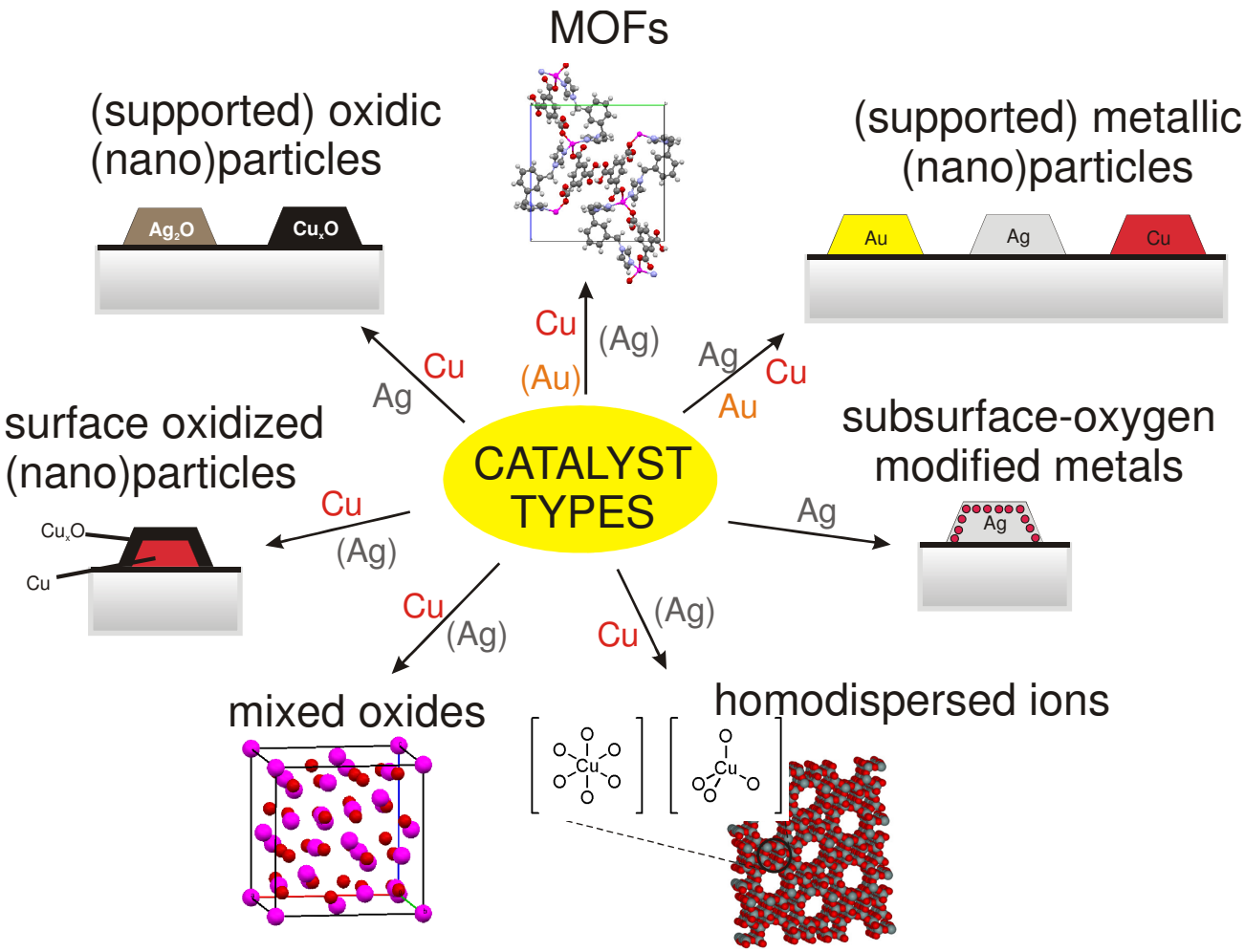

Figure 2-1: Schematic overview over catalyst types synthesized from coinage metals.

Due to the high standard potential of gold, the most prevalent type of gold catalysts consists of metallic gold nanoparticles distributed on a high-surface area support material. For silver and especially for copper, ionic species also play a role and thus the types of catalysts derived from those metals feature a higher versatility. A simplified schematic overview over the most abundant types of catalysts is given in Figure 2-1. Supported metallic nanoparticles are common for all metals. By high-temperature treatment in oxygen, subsurface silver-oxygen species (among others) are generated. Due to (mostly) ionic character of Cu under oxidizing conditions, a variety of Cu catalysts can be synthesized. Hence, fully and surface-oxidized metal nanoparticles are used as catalysts though these are usually prone to leaching problems. Combination with other metals affords mixed oxides which can of course also be dispersed on a support. Cu catalysts with highly dispersed Cu centers are mostly synthesized *via* ion exchange. The metal-organic frameworks (MOFs) constitute a relatively new type of catalyst class. Synthesis routes for the different catalysts will be summarized in this section. Note that the boundaries between the different types are fluid since e.g. the oxidation state of the metal can change during the catalytic reaction.

2.2.1 Synthesis of gold catalysts

Gold has attracted much interest and high efforts were put into developing efficient gold catalysts which undoubtedly contributed to the success of this noble metal. The most prevalent method to synthesize supported noble metal catalyst, i.e. (dry) impregnation usually affords undesirable large particles when used for Au catalysts. Therefore, other techniques were developed in order to synthesize Au nanoparticles on various supports such as deposition-precipitation, adsorption of colloidal Au, vacuum deposition, grafting and reduction, etc. An extensive overview over these techniques was given in two reviews [4, 24]. Catalysts featuring metallic copper and silver particles can be prepared similarly; e.g. colloidal methods where pre-reduced metal nanoparticles are adsorbed on a support.

2.2.2 Synthesis of copper catalysts

The most prominent types of Cu catalysts feature Cu as (1) homodisperse ionic Cu species, (2) supported (potentially metallic) Cu nanoparticles and (3) (mixed) oxides or other bulk ionic materials (e.g. phosphates [25]). Note that often several Cu species are abundant in one catalyst, e.g. both Cu_xO particles and isolated Cu

ions (Figure 2-2). Therefore the categorization into different catalyst types and hence synthesis techniques shall only be understood as a rough classification.

Copper catalysts with isolated Cu centers are most abundant and catalytically active in many oxidation reactions and often more stable against leaching than oxidic Cu nanoparticles. These species are frequently synthesized by ion exchange of zeolites [26-30], similar porous materials [31, 32] and other minerals with ion exchanger properties like clays [33] or hydroxyapatite [34]. The ion exchange procedure is straightforward and therefore industrially applicable; the parent material is treated with a solution of the desired ion followed by filtration and drying. A higher concentration of the active metal can be obtained by repeating this treatment several times [27, 31] though high metal concentrations and/or calcination treatment can afford Cu domains which are often undesired due to the aforementioned leaching issue. In principal, supports modified by organic linkers can also be ion-exchanged in order to graft Cu complexes [35, 36] but this class of catalysts will not be covered here.

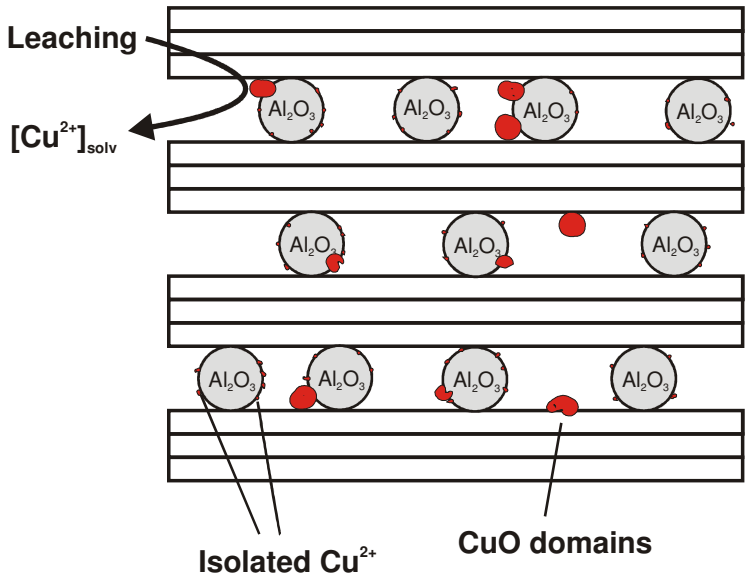

Figure 2-2: Isolated Cu sites and CuO present simultaneously in a catalyst where CuO domains are often prone to leaching; schematic model of Cu-doped montmorillonite consisting of regular layers and Al_2O_3 pillars [33].

Sol-gel, hydrothermal and coprecipitation synthesis methods allow simultaneous synthesis of support and incorporation of the catalytically active metal and also afford Cu species with high dispersion when Cu is applied in low concentrations. All three methods are based on precipitating the catalyst from a homogeneous solution. Sol-gel methods are based on the hydrolysis and subsequent condensation of a precursor (e.g.

tetraethyl orthosilicate) often under controlled pH. The solvent can be removed by simple air-drying but also more complex strategies like supercritical drying are used. High surface areas can be achieved by this approach. Addition of other metal ions allows doping; pore structures can be induced by bulky organic additives. Sol-gel synthesis is often used for synthesizing Cu-doped silica materials. Fast hydrolysis of the copper precursor compared to the SiO_2 precursor may be problematic. Cu additives have a negative influence on MCM-41 materials decreasing the surface area [37, 38]. This can partly be compensated by addition of Al ions [31, 38] forming acidic sites with ion exchange properties binding to Cu(II) [39] which also stabilizes Cu species against leaching (Figure 2-3). Sol-gel synthesis is of course not limited to doped silicas [40]. Hydrothermal synthesis, i.e. reaction of precursors to the desired product in an autoclave at elevated temperatures and pressures, is also useful for preparing homodisperse Cu species in a heterogeneous matrix as was done for the synthesis of copper-substituted aluminophosphate molecular sieves [38, 41]. (Cu-based) metal-organic frameworks are also frequently synthesized *via* a solvothermal approach [42]. Cu incorporated in alumina can be synthesized by coprecipitating Cu and Al [43]. Coprecipitation requires no special (e.g. high-pressure) equipment and starts from a solution of two (or more) metal oxides. Precipitation is (most often) induced by a change in pH. Prominent examples for this synthesis route are the Cu-ZnO-Al_2O_3 catalysts for industrial methanol synthesis [11]. The final structure is tunable both by the pH during precipitation and the aging time.

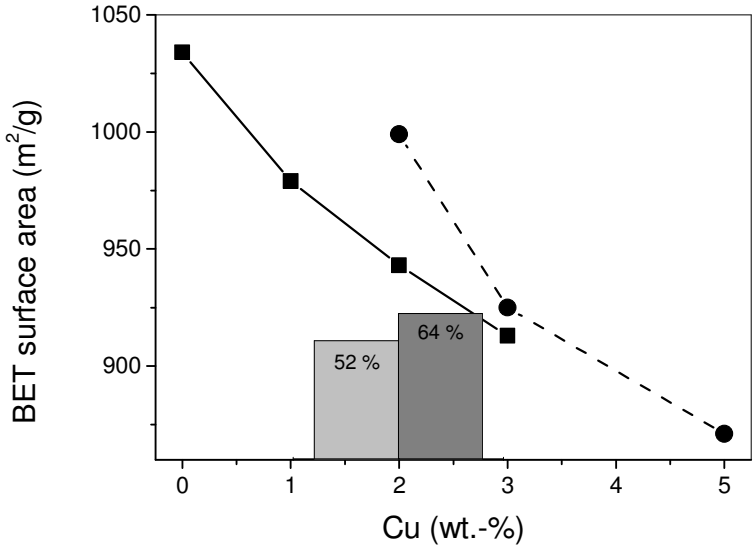

Figure 2-3: BET surface area of MCM-41 as a function of Cu doping; (■) Cu doping only (●) Cu and Al doping (same wt.-% as Cu); columns: 2,3,6-trimethylphenol conversion with 2% Cu-MCM-41 (left) and 2% Cu-2%Al-MCM-41 (right) [38].

Coprecipitation is a flexible method. Where supported Cu_xO nanoparticles are desired these can be obtained by increasing the Cu concentration when aiming for CuO/Al_2O_3 [43, 44] and other catalysts [40] which is also true for the other synthesis methods described in the previous section, i.e. sol-gel and hydrothermal synthesis. Another method frequently used is impregnation of a solid support [43, 45-50]. Interestingly, CuO supported on Al_2O_3 is the catalyst synthesized most often by impregnation, though in many reports impregnation was shown to afford inferior catalysts compared to other synthesis techniques. A method which is often used for the synthesis of nanogold catalysts is deposition-precipitation. This method is also useful for synthesizing metallic Cu nanoparticles on a support [51-53]. Briefly, deposition-precipitation is done by mixing a dispersion of the support with a solution of the Cu ion followed by subsequent increase of the pH to a moderately alkaline level causing precipitation. After filtration and drying, metallic finely dispersed Cu nanoparticles are obtained by hydrogen treatment at elevated temperatures. Colloidal methods are reported by the group of Schüth [54]. Nanoparticles in the range of 5 nm were obtained by reduction of copper acetylacetonate with trialkylaluminium which also serves as a stabilizer. Note that metallic copper particles are oxidized when exposed to oxygen. Their use is therefore limited to oxidation reactions under oxygen-lean conditions. Of course, Cu_xO particles or metallic-core/oxidic shell particles can be obtained from oxidation of metallic nanoparticles [55].

The third class of Cu catalysts, i.e. Cu (mixed) oxides – e.g. spinels – and phosphates are mostly obtained from coprecipitation (or precipitation for Cu_xO only) [56-58] and hydrothermal synthesis [59, 60]. Supported mixed oxides were synthesized by deposition-precipitation [61] ($Cu_{1.5}Mn_{1.5}O_4$ spinel on Al_2O_3) or impregnation [47]. Note that the boundaries between a supported copper oxide and a mixed oxide (where Cu is situated not only on the surface and might also form a new compound with the other metal oxide) often overlap.

2.2.3 Synthesis of silver catalysts

Silver catalysts are structurally closer to gold catalysts. Both noble metals are mostly present as nanoparticles on a support. Partly due to the antibacterial properties of silver, many sophisticated synthesis strategies were developed for the preparation of silver nanoparticles [64, 65]. Silver was also used unsupported in catalysis e.g. as nanoparticles with different morphologies or Ag monoliths [66] prepared in the liquid phase by (high-temperature) reduction of $AgNO_3$ in the presence of a surfactant (Figure 2-4) [62, 63]. A very common

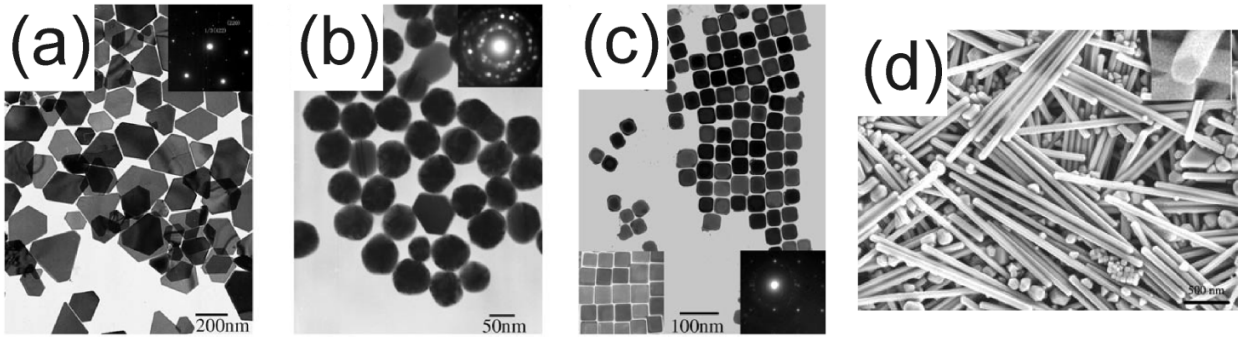

Figure 2-4: Silver nanomaterials with different morphologies: (a) truncated triangular nanoplates, (b) near-spherical particles, (c) nanocubes (all from ref. [62]); reprinted with permission from Wiley VCH © 2006), (d) silver nanowires ([63]; reprinted with permission from Springer © 2007).

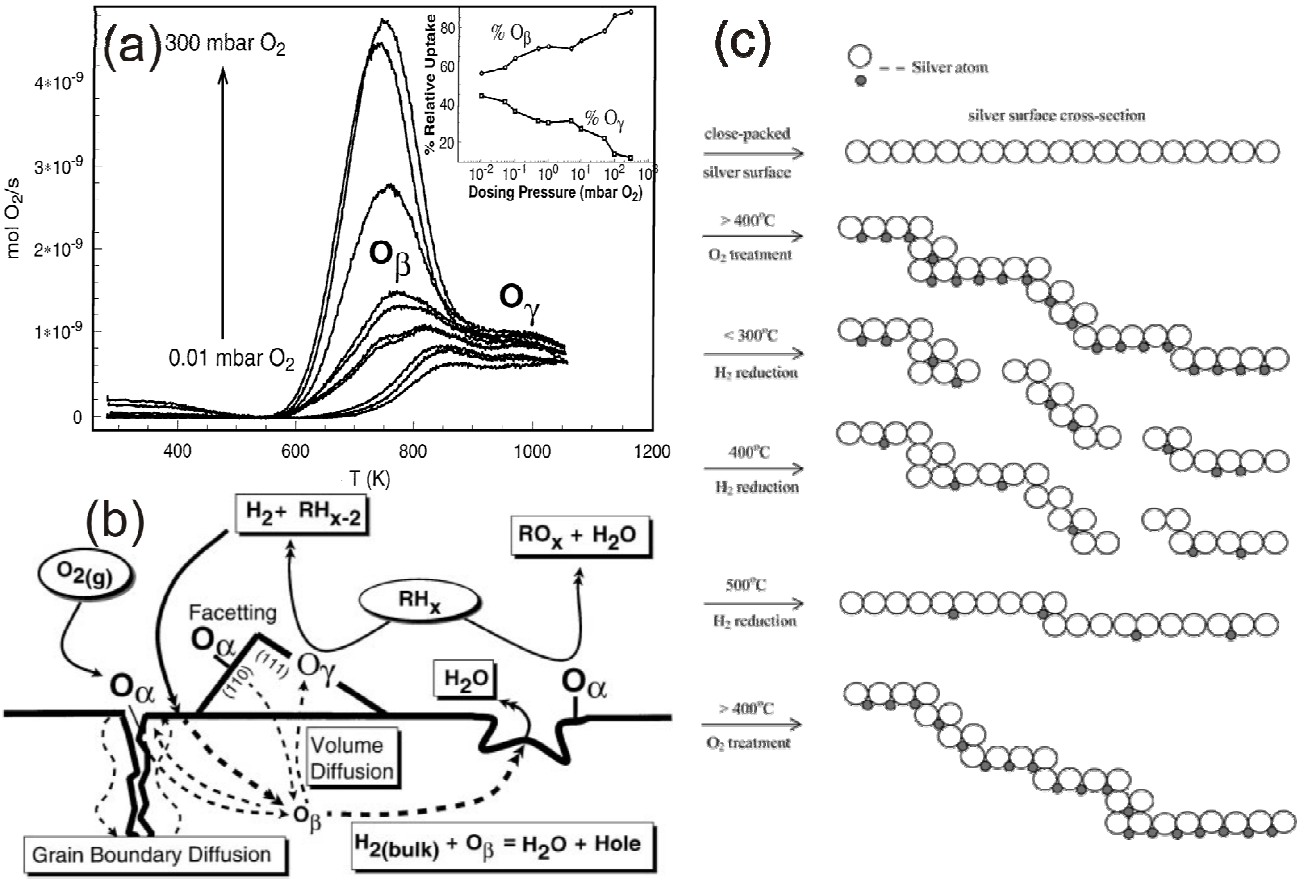

Figure 2-5: Interaction of oxygen with metallic silver: (a) oxygen species generated by oxygen treatment of silver (500 °C) differ in their thermal desorption behavior [77]; (b) Schematic overview over different silver-oxygen species: O_α surface adsorbed oxygen; O_β bulk adsorbed oxygen; O_γ subsurface oxygen [77]; (c) schematic overview over the formation of silver-oxygen species upon O_2 treatment and redispersion of silver particles by low-temperature hydrogen treatment [13]; reprinted with permission from the American Chemical Society © 1999 and Elsevier © 2005.

technique for silver catalyst preparation is impregnation [67-70] often followed by air/oxygen calcinations around 500 °C affording metallic silver [71] (calcinations at 300 °C yielded supported Ag_2O [72]) and sometimes subsequent hydrogen treatment at lower temperatures potentially improving the metal dispersion [13]. This treatment generates (among others) subsurface silver-oxygen species [12, 73-77] influencing the catalytic properties of the silver catalyst (Figure 2-5). The relatively high stability of subsurface oxygen allows redispersion of silver particles by low-temperature hydrogen treatment (Figure 2-5c). Often, silver particle sizes obtained *via* this approach are large potentially due to the high mobility of silver nanoparticles at elevated temperatures [78]. Other "classical" methods used are sol-gel synthesis ([79], for Ag/TiO_2-SiO_2) and various colloid methods where – similar to gold – Ag nanoparticles are generated in solution by reduction (e.g. chemically [80, 81] or *via* radiation [65, 82]) and then supported on a carrier. Another interesting technique is electrografting, demonstrated for Ag/carbon nanotubes [83]: Ag ions are adsorbed on an electrode consisting of carbon nanotubes *via* a linker and then electrochemically reduced on the surface (Figure 2-6).

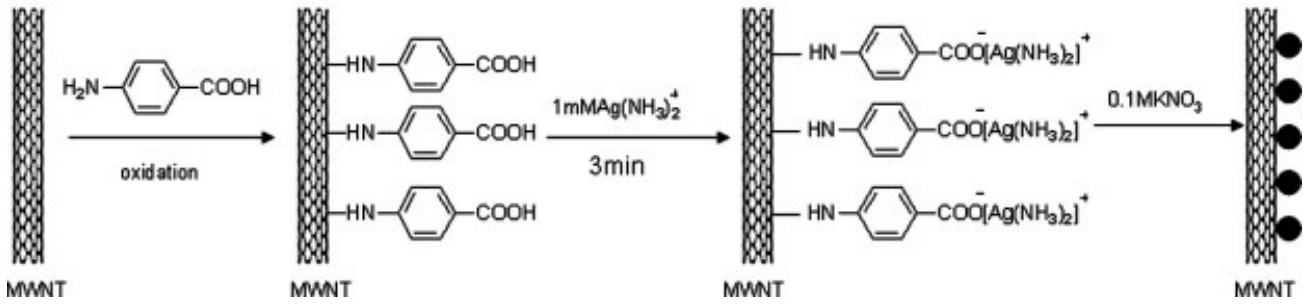

Figure 2-6: Procedure for the preparation of Ag nanoparticles on multi-walled carbon nanotubes (MWNT) with intermediate linker [83]; reprinted with permission from Elsevier © 2007 (no higher image resolution available).

Ion-exchange can also be employed and yields catalysts with ionic Ag [84, 85]. Reducing silver in ion-exchanged materials in hydrogen atmosphere afforded catalysts with very small silver particles in selected cases [86, 87]. Supported silver particles can also be synthesized by flame-spray pyrolysis e.g. with Ag/SiO_2 (Figure 2-7) [88, 89]. Addition of CeO_2 to the SiO_2 support during flame synthesis afforded smaller silver particles [91]. Silver in combination with vanadium in polyoxometallates has attracted considerable attention. This material can be flexibly synthesized so that silver is either in metallic or ionic state (Scheme 2-1). For metallic silver, vanadium in $H_5PV_2Mo_{10}O_{40}$ is first reduced with Zn. Treatment with ionic silver re-oxidizes vanadium forming silver particles on the surface [92]. The analogue with oxidized silver is prepared by ion

exchange either in solution by "metathesis precipitation" (2a) [93] or by calcination of a mixture of a homogeneous mixture of $AgNO_3$ and $H_5PV_2Mo_{10}O_{40}$ (2b) [94].

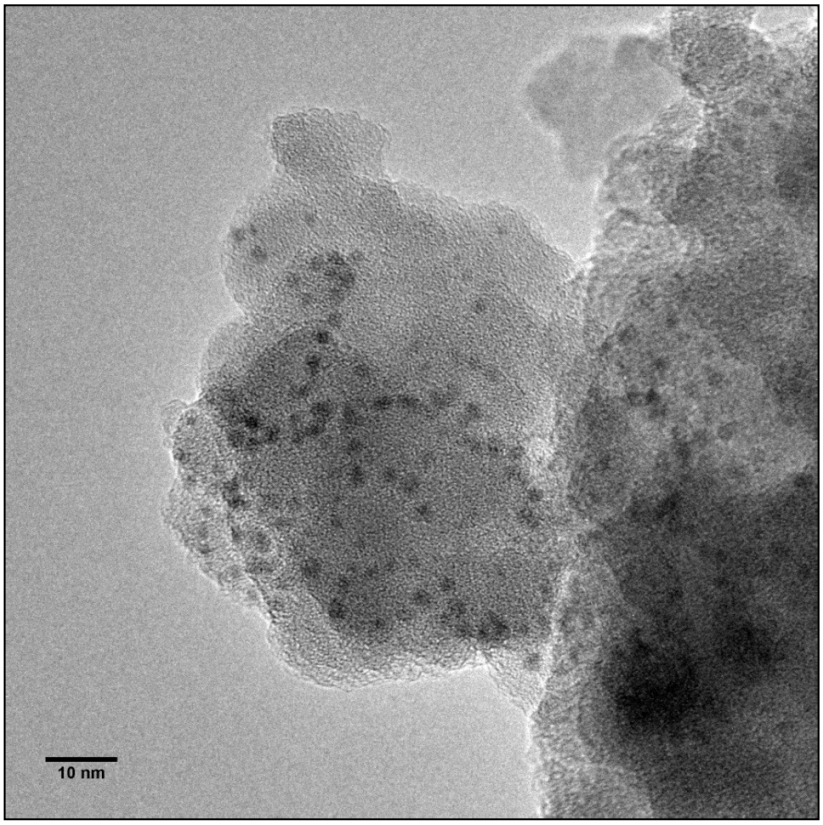

Figure 2-7: Silver on SiO_2 prepared by flame-spray pyrolysis [90].

(1) $H_5PV_2Mo_{10}O_{40} + Zn \xrightarrow{H_2O} ZnH_3PV_2Mo_{10}O_{40} \xrightarrow{Ag^+} Ag_n\text{-}ZnH_3PV_2Mo_{10}O_{40}$

(2a) $Na_5PV_2Mo_{10}O_{40} + AgNO_3 \longrightarrow Ag_5PV_2Mo_{10}O_{40}\downarrow + NaNO_3$

(2b) $H_5PV_2Mo_{10}O_{40} + AgNO_3 \xrightarrow{\Delta} Ag_5PV_2Mo_{10}O_{40}$

Scheme 2-1: Synthesis strategies for Ag-doped polyoxometallates [92-94].

2.3 Selective liquid-phase oxidation reactions

The most intensively studied liquid phase oxidations (Scheme 2-2) are alcohol oxidation, olefin epoxidation and alkyl aromatics oxidation. Aerobic alcohol oxidation is a prominent field of research in gold catalysis. Silver and

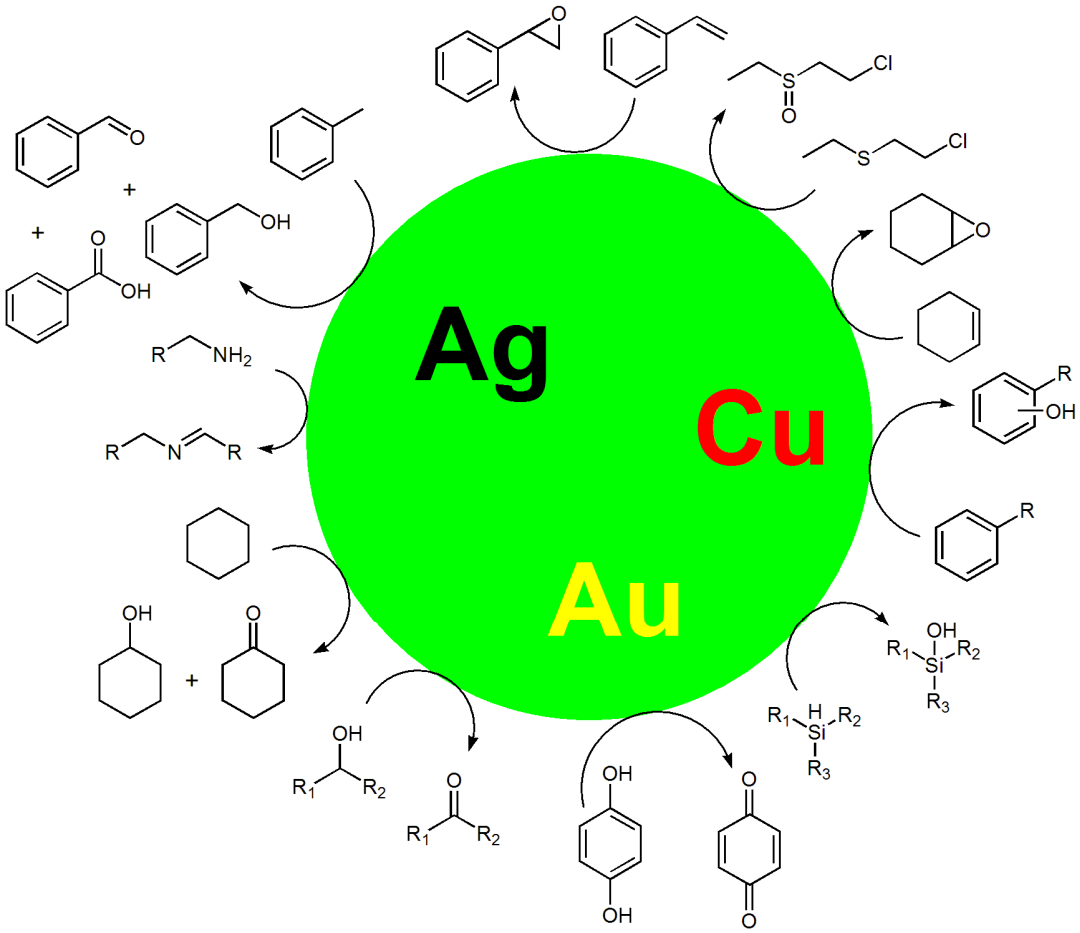

Scheme 2-2: Schematic overview over the covered oxidation reactions.

copper offer an alternative way by catalyzing the anaerobic dehydrogenation of alcohols achieving other chemoselectivites in selected cases. Olefin epoxidation by molecular oxygen is difficult to achieve in the absence of a sacrificial reductant; there are some examples with Au, but most studies rely on the use of peroxides as oxidants where the reaction rates are considerably higher. The radical side-chain autoxidation of alkyl aromatic compounds was mainly investigated with silver and copper but gold also showed some potential which may be further deepened in the future. Another important metal-induced autoxidation is cyclohexane oxidation to K/A oil. Gold was mainly used in combination with oxygen. Literature sees its catalytic activity somewhere between outstanding and almost negligible. Cu catalysts often require *tert.*-butyl hydroperoxide

(TBHP) as oxidant. Especially for Cu, ring hydroxylation of aryl compounds was extensively studied and is also summarized here. Analogue examples with Ag and Au are rare. Au-catalyzed amine oxidation has emerged greatly in the recent years and may also offer opportunities for the other coinage metals. Finally, benzoquinone, sulfide and silane oxidation are fields were the amount of literature is still limited; silane oxidation is remarkable since water could be used as the oxidant.

The comparison of the performance of different catalysts is difficult, since the catalyst activity greatly depends on the chosen reaction conditions and hence, on the degree of optimization of a catalytic reaction. Following the proposition by Mallat and Baiker [7], it will be assumed that the catalysts were tested close to optimal conditions. Where the reported data allow it, turn-over frequencies (TOFs) will be used to describe and compare the catalytic activity based on the overall amount of transition metal. Thus, metal dispersions etc. will not be taken into account as these data are only rarely available. Especially in oxidation catalysis, the meaning of a TOF as a microkinetic description of chemical processes at the active site is limited since the nature of the active site is often unknown and, even more, many oxidation reactions are at the origin of a radical autoxidation which was merely induced by the transition metal catalyst. Thus, the TOF will function primarily as a performance comparison. TOFs presenting essentially a reaction rate are highly dependent on the experimental conditions, varying greatly for the same reaction when measured at high or low conversion. Thus, the respective tables will not only give TOFs but also the conversions at which these were obtained.

2.3.1 Alcohol oxidation

The oxidation of alcohols with molecular oxygen has been intensively studied in the recent years with a great interest in gold catalysis and is described extensively in a number of reviews [5, 6, 95]. The strength of gold catalysts compared to e.g. Pt group members is the high selectivity to the intermediate oxidation product, i.e. the aldehyde or ketone. Au nanoparticles supported on nanosized CeO_2 gave impressive results [96] with TOFs higher than 400 h^{-1} for 3-octanol oxidation and >99 % selectivity. Often significantly lower reaction rates are reported. As an example, Enache *et al.* investigated a number of standard supports including SiO_2, TiO_2, CeO_2 and activated carbon where TOFs were between 10 – 80 h^{-1} for benzyl alcohol oxidation at 100 °C [97] which settles gold catalysts in the proximity of silver catalysts (*cf.* Table 2-1, entry 9 and 19). Many gold catalysts require a strong base in order to facilitate alcohol oxidation which is why basic supports often are beneficial for the Au catalyzed alcohol oxidation [7].

Table 2-1: Overview over alcohol oxidation reactions.

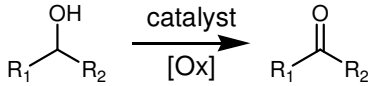

Entry	Catalyst	Substrate	Product	Oxidant	Solvent	T (°C)	Rct. time (h)	Conversion	Selectivity	TOF (h^{-1})	Reference
1	8%Cu/SiO_2	3-octanol	3-octanone	-	toluene	90	20	100%	100%	0.3	[100]
2	8%Cu/Al_2O_3	3-octanol	3-octanone	styrene	toluene	90	1.5	100%	100%	4	[101]
3	8%Cu/Al_2O_3	carveol	carvone	styrene	toluene	90	1.5	100%	95%	3.5	[101]
4	7%Cu/MgO	1-octanol	octanal	styrene	mesitylene	150	3	58%	>99%	1.7	[51]
5	8%Cu/La_2O_3	1-octanol	octanal	styrene	mesitylene	150	2	63%	100%	2.4	[53]
6	CuAl/HT	benzyl alcohol + benzamine	dibenzyl amine	-	-	150	14	72%[c]	-	1.3	[102]
7	CuAl/HT	benzyl alcohol + *p*-nitro-benzamine	*N*-benzyl-*N*-(4-nitrophenyl)amine	-	-	160	9	98%[c]	-	2.7	[102]
8	Cu/HT	cyclooctanol	cyclooctanone	-	-	180	8	85%[c]	-	390	[52]
9	Ag/HT	benzyl alcohol	benzaldehyde	-	xylene	130	24	>99%	90%	250	[86]
10	5%Ag/Al_2O_3	benzyl alcohol	benzaldehyde	-	toluene	111	24	100%	82%	2.1	[67]
11	Cu-OMS-2	2-propanol	acetone	O_2	water	55	3	40%	Ca. 50%	-	[84]
12	$Cu_xMn_yO_z/Al_2O_3$	benzyl alcohol	benzaldehyde	O_2	toluene	100	4	91%	99%	0.8	[61]
13a	CuO	1-phenylethanol	acetophenone	O_2	-	200	1	78%	100%	1.6	[103]
13b	CuO/Y	1-phenylethanol	(*E*)-1,2-dimethylstilbene	O_2	-	200	1	100%	85%	2.1	[103]
14*	$Cu_{0.4}Co_{0.6}Fe_2O_4$	benzyl alcohol	benzaldehyde	H_2O_2	ACN	60	8	80%	98%	-	[104]
15	CuCr/LDH (layered double OH)	benzyl alcohol	benzaldehyde	TBHP	-	94	5	51%	75%	-	[105]
16	Cu-Al-HT/BINOL[d]	benzyl alcohol	benzaldehyde	O_2	-	RT	10	99%[c]	-	-	[106]
17	0.5% Ag-zeolite	2-propanol	acetone	O_2	water	55	5	30%	80%	-	[84]
18	0.6%Ag/pumice	benzyl alcohol	benzaldehyde	O_2	ACN	75	-	-	-	0.5	[69]
19	10%Ag/SiO_2 + CeO_2	benzyl alcohol	benzaldehyde	O_2	xylene	140	2	98%	95%	21	[71]
20	Ag-V-MPA	cinnamyl alcohol	cinnamaldehyde	O_2	toluene	90	10	93%[c]	-	1.2	[94]
21	2%Ag/Al_2O_3 + TEMPO	MGP	MGPA[b]	PDS	water	25	15	78%	99%	8	[107]
22	$CuCl_2$-SILP-SiO_2 + TEMPO	benzyl alcohol	benzaldehyde	O_2	dibutyl-ether	65	14	99%	99%	1.4	[108]

*No standard use reported. [a]Methyl-α-D-glucopyranoside. [b]Methyl-α-D-glucopyrasiduronic acid. [c]Yield. [d]K_2CO_3 added.

2.3.1.1 Anaerobic alcohol oxidation

The selective oxidation of alcohols is also readily catalyzed by silver and copper. Many reports describe alcohol oxidation under anaerobic conditions, i.e. either by using a hydrogen acceptor or no oxidant giving H_2 as a side product. This approach is especially attractive where the intermediate aldehyde is highly susceptible to overoxidation by molecular oxygen. Anaerobic dehydrogenation with silver and copper catalysts is long known in gas phase catalysis [11]. The oxidant-free lactonization of 1,5-pentandiol to *δ*-valerolactone was already described in 1947 by Schniepp and Geller [99] using copper chromite (Scheme 2-3). High temperatures above 200 °C were necessary to facilitate the reaction which is in general observed due to the highly endothermic nature of the oxidant-free alcohol dehydrogenation. High temperatures can limit the selectivity, e.g. polymeric

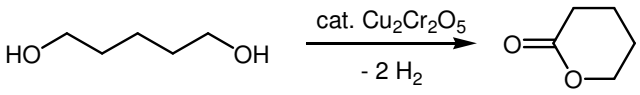

Scheme 2-3: Anaerobic dehydrogenation of 1,5-pentandiol [99].

side products were obtained during 1,5-pentandiol conversion. Continuing these studies, Zaccharia *et al.* investigated the dehydrogenation of 3-octanol and other alcohols at low temperatures of 90 °C [100, 101] with Cu/Al_2O_3 (Table 2-1 , entry 1). In a closed reactor, only low conversions over long reaction times were achieved because of thermodynamic limitations caused by remaining H_2. Removal of hydrogen by either reactor venting or, more effectively, addition of styrene as hydrogen acceptor resulted in quantitative conversion and a TOF of 4 h^{-1} (entry 2). Cyclooctanol dehydrogenation proceeded especially readily with a TOF of 12.5 h^{-1} at full conversion. Substrates bearing double bonds can also be used as hydrogen acceptors, the catalyst thus affording an isomerization product as was demonstrated with carveol (entry 3, Scheme 2-4). With styrene as "external" hydrogen acceptor, the selectivity could be tuned to the dehydrogenated product. Primary benzylic

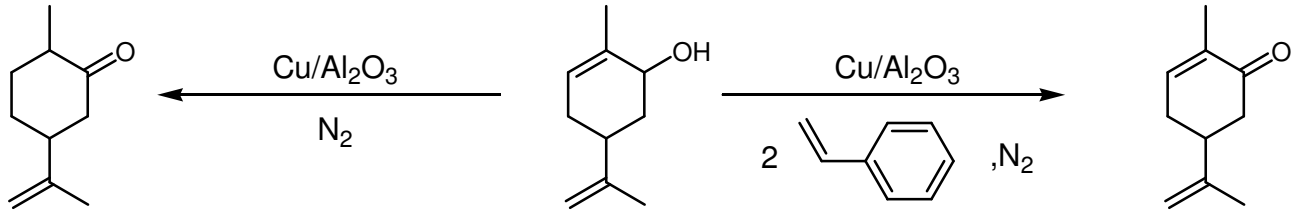

Scheme 2-4: Anaerobic oxidation/ isomerization of carveol over Cu/Al_2O_3 [101].

alcohols reacted slowly (benzyl alcohol 51.5% conversion (20 h); cyclohexanol 99% conversion (3h)) [100] in contrast to aerobic alcohol oxidation over Au catalysts where similar or higher reaction rates were often observed for benzylic alcohols (Figure 2-8) [98, 109, 110]. While in this report primary alcohols exhibited low reactivity, Cu supported on basic supports, i.e. MgO (entry 4) [51] and La_2O_3 (entry 5) [53] were suitable for primary aliphatic alcohols like 1-octanol at high reaction temperatures (150 °C), also with styrene as hydrogen acceptor. Both Cu catalysts were stable against leaching. Cu was fully reduced in these studies.

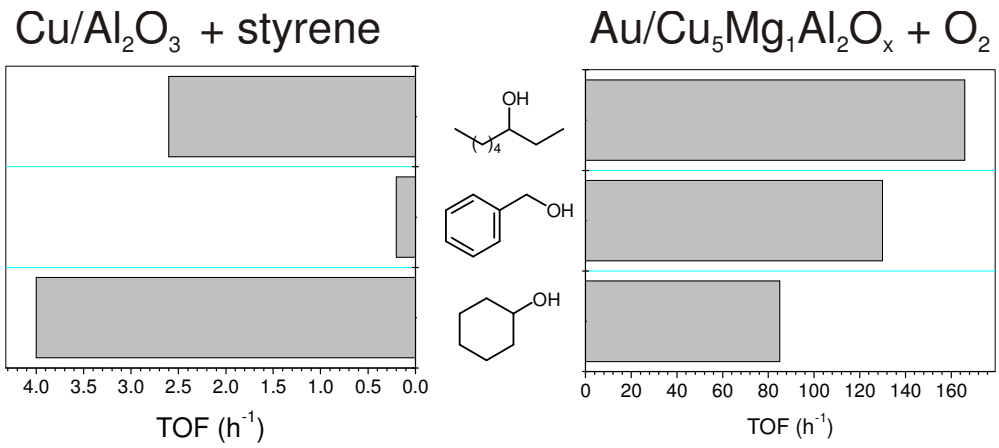

Figure 2-8: Different reactivities of alcohols on gold [98] and copper [100] catalysts.

The hydrogen transfer principle offers interesting reaction routes. Copper-aluminum hydrotalcite was used as a catalyst for the amination of primary alcohols (Scheme 2-5) which proceeds *via* the imine (Table 2-1, entry 6) [102]. K_2CO_3 as a base was necessary under the harsh reaction conditions (160 °C).

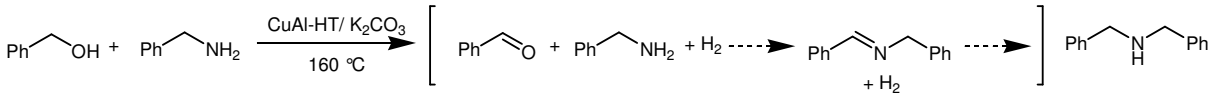

Scheme 2-5: Reaction scheme for the amination of primary alcohols [102]. Note that the proposed imine was not observed as an intermediate.

Benzyl alcohols both with electron-donating and electron-withdrawing substituents (entry 7) were aminated with similar reaction rates. Secondary alcohols were unreactive under the described reaction conditions which is in contrast to the previously described studies on alcohol dehydrogenation where secondary alcohols were always more reactive. Hydrogen-acceptor free dehydrogenation was investigated in more detail in a recent paper using metallic Cu nanoparticles also supported on hydrotalcite [52]. As in the previous studies, primary

benzylic alcohols were less reactive than secondary aliphatic alcohols. High temperatures were required (≥130 °C). At 180 °C, neat cyclooctanol could be transferred to cyclooctanone in 87 % yield with a TOF of 388 h^{-1} (entry 8). A related publication from the same group used Cu catalysts for the anaerobic lactonization of diols [111]. Hydrotalcite prepared by hydrothermal synthesis gave the best results but also other supports such as SiO_2, TiO_2 and Al_2O_3 exhibited good catalytic activity in mesitylene solvent at 150 °C.

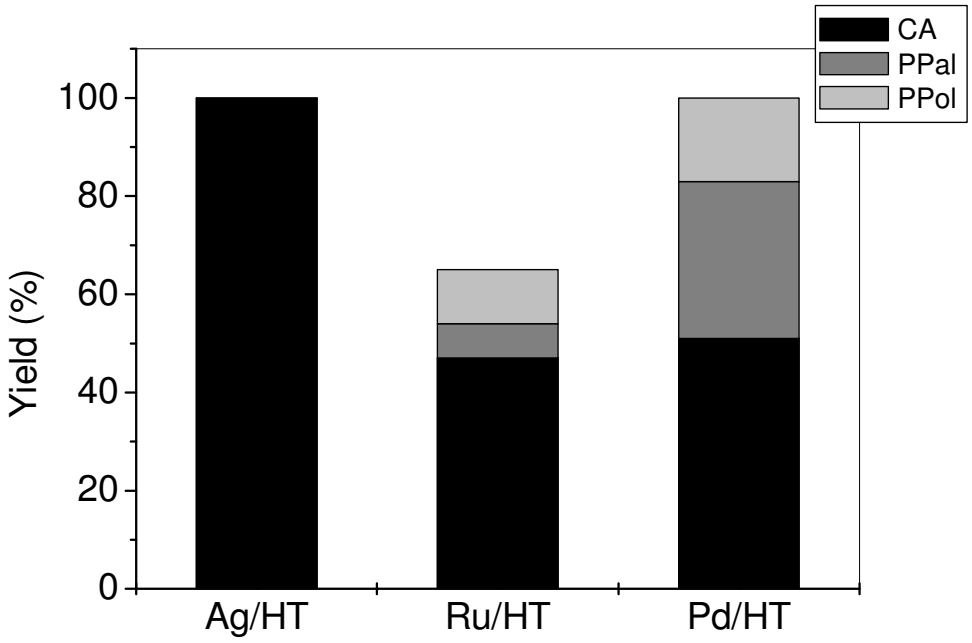

Figure 2-9: Oxidant-free dehydrogenation of cinnamic alcohol over Ag/Ht, Ru/HT and Pd/HT [86]; CA: cinnamic aldehyde, PPal: 3-phenylpropanal, PPol: 3-phenylpropan-1-ol.

In analogy to Cu/HT catalysts, Ag nanoparticles supported on hydrotalcites are also capable of facilitating the dehydrogenation of a broad variety of samples [86] with very high selectivity. Due to the low silver loading (0.005 wt.-%), high TOFs were obtained, e.g. for benzyl alcohol oxidation (Table 2-1, entry 9). Despite the low loading TEM images with silver nanoparticles could be recorded and revealed an average Ag particle size of 3.3 nm. Based on the catalyst mass, however, the catalyst activity appears only moderate. Usually 0.10 g of catalyst were required to convert 1 mmol of substrate over 24 h. Cinnamyl alcohol containing a double bond which could be susceptible to transfer hydrogenation was converted to cinnamaldehyde with 100 % selectivity potentially due to the weak interaction between H_2 and the Ag surface [112]. Ru/HT and Pd/HT on the contrary afforded large amounts of isomerization or hydrogenated products (Figure 2-9).

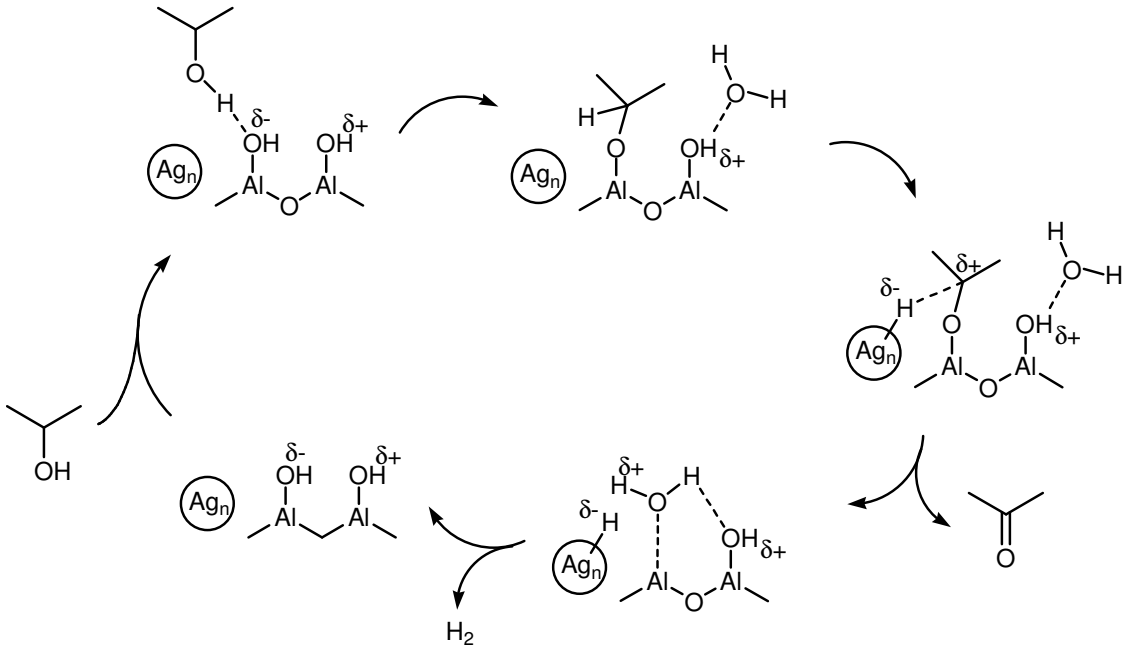

Scheme 2-6: Dehydrogenation mechanism over Ag/Al_2O_3 featuring basic and acidic sites, adapted from ref. [67].

Ag/Al_2O_3 was thoroughly investigated at lower temperatures (100 °C) where also the evolution of H_2 was proved (Table 2-1, entry 10) [67]. High selectivies were obtained for various alcohols. Based on IR investigations, a reaction mechanism was proposed which involved both acidic and basic sites on the catalyst support (Scheme 2-6). The catalyst deactivated during the reaction. Reactivation was achieved by treatment with O_2 at 600 °C and subsequent hydrogen treatment, which might indicate the involvement of subsurface silver-oxygen species in the reaction. These are specifically formed under the air treatment conditions and stable towards low-temperature hydrogen treatment [12, 13]. EXAFS analysis suggested unusually small Ag particle sizes < 1nm. Note that Ag-O species might interfere with the EXAFS analysis (*vide infra*) [71] affording underestimated Ag particle sizes. Ag/Al_2O_3 could also be used for oxidant-free amide synthesis from alcohols and amines [68].

Note that the oxidant-free oxidation of alcohols is also catalyzed by palladium [113, 114] though there are some important differences. Side reactions observed over palladium are the C-O bond cleavage of the alcohol by surface-adsorbed hydrogen (affording e.g. toluene in benzyl alcohol oxidation). Additionally, CO as a side product from alcohol oxidation poisons the palladium catalysts being oxidatively removed under aerobic conditions. Both effects limit the selectivity and the catalytic activity, respectively, and were not reported over Ag and Cu.

2.3.1.2 Aerobic alcohol oxidation

While with Ag/HT [86] also aerobic oxidation was performed very effectively (TOF 6000 h^{-1} for benzyl alcohol), similar experiments for the corresponding Cu catalysts are not reported. A reason might be that the usually metallic copper nanoparticles are oxidized and hence deactivated under elevated temperature aerobic conditions while silver is stable against deep oxidation. Hence, aerobic alcohol oxidation is reported only with oxidic copper species. An early example is the oxidation of 2-propanol to acetone with Cu-exchanged octahedral molecular sieves (Table 2-1, entry 11) [84]. In $Cu_{1.5}Mn_{1.5}O_4$ spinel supported on Al_2O_3 a collaborative effect of Mn and Cu was found where Cu was assumed to activate oxygen [61]. TOFs obtained with this catalyst are quite low (entry 12). Cu was also used as a mixed oxide together with Mg as a support for Au [98] forming a highly active catalyst. The exact nature of the beneficial influence of Cu could not be identified and might be connected to its influence on surface basicity, redox activity or an influence on the net charge of Au particles (which were, however, assumed to be the primary active species). In another study, Y-zeolite encorporated CuO particles were used at very high temperatures (200 °C) for the oxidation of e.g. 1-phenylethanol [103] for which CuO and CuO/Y exhibited significantly different behavior: CuO afforded acetophenone (entry 13a), CuO/Y gave mainly 2,3-diphenyl-but-2-ene (entry 13b). The difference in selectivity was assigned to the interaction of lewis-acid/ -base sites on the zeolite and CuO particles, respectively. Cu-containing mixed oxides were further used with H_2O_2 (entry 14) [104] and TBHP (entry 15) [105] though this approach appears less attractive given the activities obtained already with molecular oxygen. Room temperature aerobic oxidation was described with Cu-Al-hydrotalcite which was co-impregnated with *rac*-BINOL as a ligand (entry 16) [106]. Due to the low temperatures long reaction times were required but aldehydes were obtained with excellent selectivity under neat conditions. Steric constraints afforded a high selectivity for primary alcohols. The catalyst was reusable so apparently leaching of copper and the required co-impregnated ligand was low.

Compared to gold catalysis, the literature on silver catalysts for the selective aerobic alcohol oxidation is scarce. This is astonishing since silver has long been used as an industrial methanol oxidation catalyst in gas phase reactions proving the principal feasibility of silver. In one of the first studies, polystyrene crosslinked Ag-exchanged natural zeolite was successfully used under mild conditions for the oxidation of simple alcohols such as *iso*-propanol and 2,3-butandiol (Table 2-1, entry 17). In the latter case, C-C cleavage was observed as the main reaction pathway thus giving acetaldehyde [84]. The reactions were carried out under mild conditions (55 °C) in water. Various reports found unmodified metallic silver to be inactive for alcohol oxidation [69-71]. Liotta *et al.* found that metallic silver can be activated by treatment in air with molecular oxygen at 500 °C (entry 18) [69] which was confirmed in a recent study (entry 19) [71]; however, air treatment did not bulk-

oxidize silver. The complex interaction of silver with oxygen and thus the formation of stable silver-subsurface oxygen (so-called *γ*-oxygen) species might account for the prominent change in reactivity [74, 75, 115, 116]. These species are also connected to the catalytic activity in gas phase methanol oxidation [73].

Palladium is a highly active metal in alcohol oxidation. Combinations of Pd and Ag supported on pumice were tested for benzyl alcohol oxidation [69]. Addition of Ag to Pd/pumice dramatically decreased the alcohol oxidation activity. On the other hand, Ag/pumice and Pd/pumice applied as a physical mixture exhibited a remarkable synergistic effect. Leaching of the metal species as a source for this observation was not investigated. Similarly, the addition of CeO_2 nanoparticles to Ag/SiO_2 increased the benzyl alcohol conversion more than ten-fold [71]. High reaction temperatures were required and the catalytic activity was only moderate likely connected to the poor Ag dispersion; here, EXAFS analysis significantly underestimated particle sizes (2-3 nm) while TEM and XRD agreed well suggesting particle sizes around 30 nm. However, 10 % Ag/SiO_2 was similarly active as gold catalysts (containing only 1 wt.-% gold thus giving higher TOFs) and exhibited high selectivity. Details on this study can also be found in Chapter 3. Later, Ag catalysts synthesized *via* flame-spray pyrolysis with smaller Ag particles (*cf*. Figure 2-7) resulted in similar TOFs [90]. CeO_2 turned out to be a general, easily applicable dopant, i.e. also Au/TiO_2, Au/Al_2O_3, Au/ZnO and Pd/Al_2O_3 exhibited a significantly higher catalytic performance when used with nanosized ceria. The effect of the dopant was assumed to be *via* direct physical contact; leaching of either Ag or Ce species could be excluded. No alcohol dehydrogenation activity was observed under anaerobic conditions. Silver in combination with vanadium is a frequently used oxidation catalyst. Also silver-exchanged molybdovanado phosphoric acid showed considerable catalytic activity for the selective oxidation of various allylic alcohols with moderate to high selectivity. Neither leaching nor deactivation was observed. Both silver and copper can interact with TEMPO and thus mediate alcohol oxidation. Due to steric constraints, primary alcohols are most susceptible to reaction. In the presence of peroxodisulfate, the oxidation of sugars proceeded at room temperature [107], $CuCl_2$ dissolved in an ionic liquid used in a SILP catalyst required low reaction temperatures (65 °C) with O_2 as the oxidant [108].

Finally, it should be noted that the aerobic *N*-acylation of amines with methanol (methanol thus being oxidized) is also facilitated by coinage metal catalysts, i.e. with supported Au nanoparticles [117], copper hydroxyl salts as heterogeneous catalysts [56] and principally also by metallic silver surfaces [118]. The acylation occurs *via* transformation of methanol to H_2 and CO_2 reacting with the amine. [119]

2.3.2 Oxidation of alkenes

The oxidation of alkenes in the gas phase is well-established over silver catalysts for the oxidation of ethylene to ethylene oxide where molecular oxygen can be used. In liquid phase olefin oxidations, oxygen often has to be supplied in an activated form, e.g. as *m*-chloroperoxybenzoic acid. Catalysts have been developed to use less expensive peroxides, typically hydrogen peroxide and TBHP [11]. Also procedures using an additional sacrificial reductant, e.g. an aldehyde or H_2, in combination with and in order to activate molecular oxygen are described, but examples for catalysts achieving epoxidation with molecular oxygen only are rare. Typical substrates used in epoxidation studies are cyclohexene and styrene. Epoxidation reactions can be catalyzed by Cu, Ag and Au. Au epoxidation catalysis is already widely covered by recent reviews on Au catalysis [4-6] and thus will only shortly be disscussed here. Typical substrates are styrene and cyclohexene (Table 2-2 and Table 2-3).

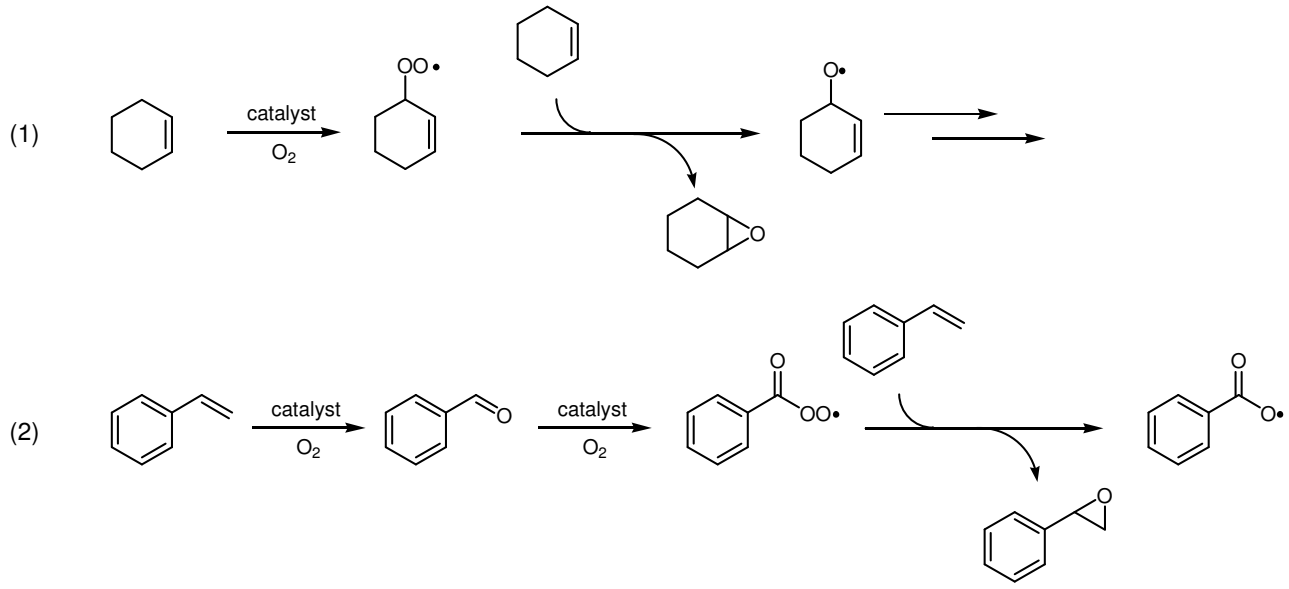

Scheme 2-7: Schematic reaction pathway for secondary epoxidation via primary oxidation products for cyclohexene (1) and styrene (2).

2.3.2.1 Oxidation of aliphatic olefines

High epoxide selectivities are difficult to obtain for cyclohexene and other aliphatic substrates since allylic C-H bonds easily break in the presence of radicals typically occurring in this type of oxidation reaction. Especially with molecular oxygen, peroxo radicals or peroxides can form as intermediates which can serve as the primary epoxidizing agent (Scheme 2-7) being principally also conceivable for styrene. This reaction pathway can only be excluded when the epoxide selectivity is high. The group of Hutchings successfully applied Au/graphite,

Au/SiO_2 and Au/TiO_2 catalysts for the aerobic oxidation of cyclohexene and cyclooctene [97]. The reaction was greatly depending on the choice of solvent and required catalytic amounts of TBHP suggesting that the underlying mechanism was based on radicals. Epoxides were only formed to a significant amount with 1,2,3,5-tetramethylbenzene and hexafluorobenzene as solvents, the former giving a selectivity of 50 % to the epoxide (Table 2-2, entry 1). The high selectivity excludes the epoxidation to occur *via* the mentioned cyclohexenylperoxo/ -peroxide as the main reaction pathway. Apparently, oxygen supply by leaving the reaction vessel open to air was sufficient. Cyclooctene could be epoxidized with selectivities around 80 % even under solvent-free conditions, TOFs of up to 35 h^{-1} were achieved [120] at temperatures around 80 °C (Table 2-2, entry 2). Gold nanoparticles supported on La-doped manganese oxide octahedral molecular sieves applied for solventless oxidation of cyclohexene yielded mostly allylic oxidation products (entry 3, small amounts of epoxide were also formed) showing that gold has no intrinsic aerobic epoxidation activity [122]. Gold and copper modified silicon nanowires (Au/ and Cu/SiNWs), respectively, were tested in the aerobic epoxidation in the absence of solvent [123] for both cyclohexene and cyclooctene with TBHP as radical initiator in an open reactor system. Outstanding selectivities to the epoxide with Au/SiNWs for cyclooctene oxidation (>90 %), TOFs being in the range of 50 h^{-1} and higher (entry 4a) were reported. In strong contrast, for cyclohexene with Au/SiNWs exclusively allylic oxidation products were observed (entry 4b). Cu/SiNWs also afforded only allylic oxidation products (entry 5a,b). No internal standard was used, so substrate evaporation occurring over the long reaction time (24 h) at elevated temperatures (80 °C) might have interfered. As an alternative to the direct reaction with oxygen, the combination of Au/CeO_2 as a peroxide generating catalyst and Ti-MCM-41 as an epoxidizing catalyst was proposed [124]. The formation of gold-peroxy species from reaction with azo-bis(isobutyronitrile) (AiBN) on the surface of Au nanoparticles was evidenced by IR investigations and assumed to be responsible for the formation of cumene hydroperoxide from cumene. With cumene as sacrificial reductant, selectivities in 1-octene oxidation approached 90 %. TOFs close to 50 h^{-1} were obtained at low conversion at 100 °C (entry 6, Scheme 2-8).

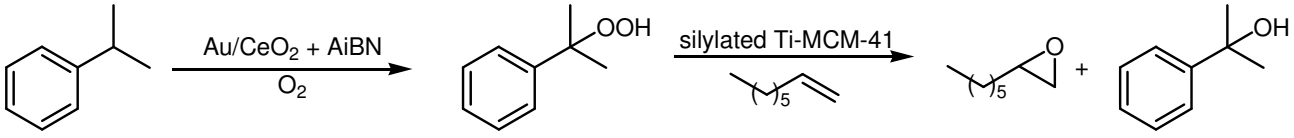

Scheme 2-8: Epoxidation of 1-octene by oxygen activated by cumene with Au/CeO_2 and Ti-MCM-41 in a one-pot synthesis [124].

Table 2-2: Oxidation of aliphatic olefins.

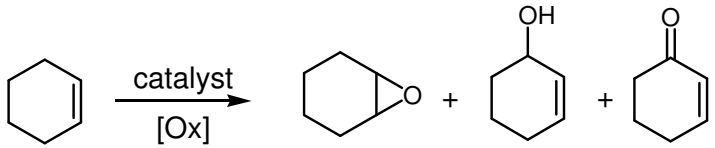

Entry	Catalyst	Oxidant	Solvent	T (°C)	Rct. time (h)	Conversion	Selectivity			TOF (h^{-1})	Ref.
							Ox[a]	Ol[b]	On[c]		
1	Au/graphite[d]	O_2	1,2,3,5-TMB[e]	80	24	30%	50%	0%	26%	13	[121]
2	Au/graphite[d]	O_2	-	80	72	20%	77%	5%	5%	35	[120]
3	Au/La-OMS	O_2	-	80	24	48%	2.5%	40%	44%	170	[122]
4a*	Au/SiNWs[f,g]	O_2	-	80	24	38%[h]	90%	-	7%	-	[123]
4b*	Au/SiNWs[f,g]	O_2	-	80	24	93%	0.2%	25%	75%	-	[123]
5a*	Cu/SiNWs[f,g]	O_2	-	80	24	98%	0.1%	46%	54%	-	[123]
5b*	Cu/SiNWs[f,g]	O_2	-	80	24	28%[h]	0.2%	25%	75%	-	[123]
6	Au/CeO_2 + Ti-MCM-41[g,i]	O_2	-	90	5	5.3%[j]	88%	9.6%		230[k]	[124]
7*	$Cu_2(OH)PO_4$	O_2	-	80	4	29%	5.0%	27%	39%	-	[60]
8	Ag-VP-POM/ α-Al_2O_3	O_2	trifluoro -toluene	160	1	20%	50%	-	-	135	[92]
9*	Ag-γ-ZrP	TBHP	ACN	82	12	96%	-	94%	-	45	[125]
10	Cu-Nb_2O_5	TBHP	ACN	60	-	14%	1.8%	2.2%	80%	n.a.	[126]
11*	$Cu_3(BTC)_2$	TBHP	ACN	50	20	50%	~ 60%	-	~ 40%	n.a.	[127]
12*	$[Cu(H_2btec)(bipy)]_\infty$	TBHP	DCE	75	24	65%	73%	7.7%	19%	110	[42]

*No standard use reported. [a]Cyclohexene oxide. [b]Cyclohexenol. [c]Cyclohexenone. [d]Catalytic amounts of TBHP added. [e]Tetramethylbenzene. [f]Si-nanowires. [g]AiBN as initiator. [h]*Cis*-cyclooctene as substrate. [i]Cumene added. [j]1-octene as substrate. [k]Based on the amount of Au.

$Cu_2(OH)PO_4$ and $Cu_4O(PO_4)_2$ were investigated as catalysts in O_2 atmosphere at 80 °C for cyclohexene oxidation [60, 128]. A selectivity to the epoxide around 5 % for cyclohexene was found, products resulting mainly from allylic oxidation. The reaction proceeded faster with acetonitrile solvent. EPR investigations proved the presence of ·OH radicals under reaction conditions. On the contrary, Cu/Al_2O_3 synthesized *via* impregnation was catalytically inactive for the aerobic oxidation of cyclohexene [49]. Cu catalysts obtained by impregnation feature mainly Cu_xO particles which might be responsible for the low activity. Aerobic epoxidation was also investigated with silver as metallic nanoparticles on a V-containing polyoxometalate ($H_5PV_2Mo_{10}O_{40}$) which itself was supported on α-Al_2O_3 (Table 2-2, entry 8) [92]. Under the harsh reaction conditions (160 °C) the catalyst deactivated rapidly. The catalyst epoxidized numerous aliphatic olefins with yields between 5-66 %. Cyclohexene was converted with 50 % selectivity (entry 8). No primary allylic oxidation products were found. In the absence of a catalylst, the conversion was roughly the same, but peroxide formation was not detected.

Milder conditions are necessary when using peroxides as oxidants; silver-ion exchanged γ-ZrP (Table 2-2, entry 9) catalyzed cyclohexene oxidation with TBHP in acetonitrile to cyclohexanol [125]. Cu-modified mesoporous Nb_2O_5 was used for TBHP-epoxidation of cyclohexene in ACN [126]. Cu-doped Nb_2O_5 was more active (entry 10) than Cu-loaded Nb_2O_5 exhibiting about the same conversion as unmodified Nb_2O_5. However, both Cu catalysts showed a high selectivity to cyclohexenone (70-80 %), the epoxide being only a minor side product (selectity <5 %). Two Cu metal-organic frameworks, Cu-BTC [127] and $Cu(H_2btec)(bipy)]_\infty$ [42] were also used for cyclohexene epoxidation with TBHP. Cu-BTC exhibited only low catalytic activity potentially due to micropore diffusion limitations (entry 11). A relatively high selectivity of 73 % with TOFs up to 80 h^{-1} in 1,2-dichloroethane were obtained with $(H_2btec)(bipy)]_\infty$ (entry 12) though already around half of the conversion obtained with catalyst was obtained in the absence of the catalyst. By using more complex peroxides, allylic oxidation of cyclohexene can afford other products than the alcohol and ketone, respectively. As an example, Cu exchanged Na-HSZ-320 zeolite used with ^{t}butylperbenzoate oxidized cycloalkenes to allylic benzoates (Scheme 2-9) [26].

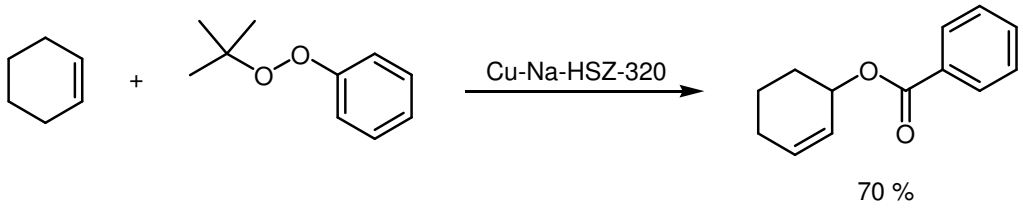

Scheme 2-9: Synthesis Cyclohex-1-enylbenzoate [26].

2.3.2.2 Epoxidation of styrene

Contrary to cyclohexene, no allylic oxidation can occur with styrene as substrate for epoxidation. A dominant side reaction is the C=C bond cleavage affording the corresponding carbonyl compounds. The formation of benzaldehyde can complicate the mechanistic investigation of aerobic epoxidations, as aldehydes in connection with O_2 can form carboxylperoxo radicals being the actual epoxidizing species (*cf*. Scheme 2-7). The most often studied substrate styrene can additionally undergo oligomerization, especially in the presence of radicals. Oligomers are not detectable *via* GC analysis and so the use of an internal standard is mandatory in order to obtain reliable results. As for cyclohexene, Au catalysts were also described to epoxidize styrene with molecular oxygen as the sole oxidant. While in the studies by Hutching's group for cyclohexene [97] a small amount of radical initiator was necessary, gold clusters consisting of 55 atoms deposited on TiO_2 oxidized styrene to benzaldehyde, acetophenone and styrene epoxide at 100 °C without any radical initiators (Table 2-3, entry 1) [129]. Benzoic acid was not observed ruling out that epoxidation occurs *via* a peroxocarboxylic acid intermediate. Hence, epoxidation is assumed to occur directly on the Au surface of nanoparticles smaller than 3.5 nm. Further mechanistic studies (e.g. by attenuated total reflection-infra red spectroscopy [ATR-IR]) are necessary to test this assumption. Note that in the previously described paper by the group of Hutchings styrene oxide selectivities of up to 97 % were reported. Lignier *et al.* investigated the epoxidation of (*E*)-stilbene with Au/TiO_2 and other gold catalysts where methylcyclohexane was mandatory as a solvent (Table 2-3, entry 2) [130-133]. 1,3-Dimethylcyclohexane served as an activator of molecular oxygen by forming peroxo radicals thereby of course being consumed, rendering the reaction less attractive compared to the previous reports. Epoxidation is facilitated not directly by the metal but by a free radical autoxidation mechanism as it is mostly the case when organic sacrificial reductants are involved and is exemplary shown in Scheme 2-10. The radical mechanism is initiated by $^{t}BuOO\cdot$ radicals (step 1). Abstraction of H· (step 2) and addition of O_2 (step 3) to the solvent molecules affords a peroxy radical capable of epoxidizing the olefin (step 3 and 4). The alkoxy radical activates another solvent molecule (step 5). The exact role of the catalyst was not elucidated.

Two examples of Cu catalyzing aerobic epoxidation of styrene are the previously described low-surface area phosphates $Cu_2(OH)PO_4$ and $Cu_4O(PO_4)_2$ [60, 128]. Selectivities to the epoxide reached 20 % for styrene (TOF 0.25 h^{-1} at 80 °C); the use of a standard was not reported.

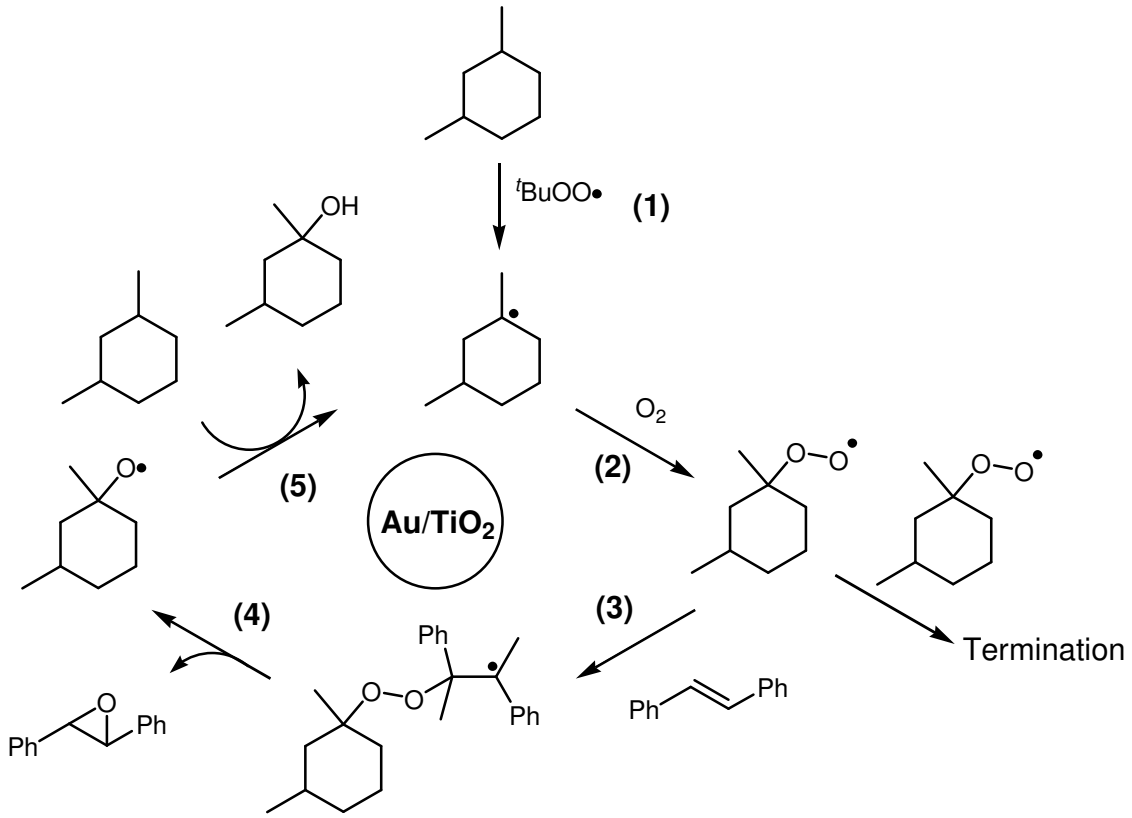

Scheme 2-10: Epoxidation of (*E*)-stilbene initiated by TBHP in the presence of Au/TiO_2 with 1,3-dimethylcyclohexane as solvent and sacrificial reductant [132].

In most epoxidation studies with coinage metals as catalysts, peroxides were used as oxidants, i.e. either H_2O_2 or TBHP. The epoxidation of styrene with TBHP was extensively studied by the group of Choudhary using nano-sized gold supported on numerous oxides with either benzene or water as solvent [134-137]. As an example, with Au/MgO an epoxide selectivity of up to 66 % at 67 % conversion (TOF 60 h^{-1}, entry 4) was achieved [138], though no standard was used, so styrene oligomerization might not have been accounted for. The same group also studied and compared CuO nanoparticles supported on various oxides with gold catalysts under identical conditions [48]. CuO/Ga_2O_3 was found to be the most active and selective Cu catalyst reaching higher TOFs as the previously investigated Au catalysts (Table 2-3, entry 5), though, again, no internal standard was used. Interestingly, bulk CuO particles also exhibited considerable catalytic activity. CuO particles used in other oxidation reactions often tend to leach severely which was not investigated in the cited study. Using Cu-containing sol-gel synthesized hexagonal mesoporous silicas for styrene epoxidation with TBHP, leaching was

Table 2-3: Epoxidation of styrene.

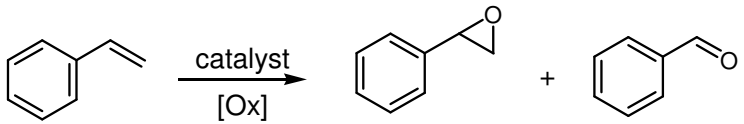

Entry	Catalyst	Oxidant	Solvent	T (°C)	Rct. time (h)	Conversion	Selectivity		TOF (h^{-1})	Ref.
							SO[a]	BA[b]		
1	Au_{55}/SiO_2	O_2	toluene	100	15	26%	12%	82%	61	[129]
2	Au/TiO_2	O_2	methylcyclo-hexane	80	24	64%[c]	69%	n.a.	13	[133]
3*	$Cu_2(OH)PO_4$	O_2	-	80	24	29%	17%	60%	0.3	[60]
4*	Au/MgO	TBHP	benzene	80	3	67%	66%	0.1%	60	[138]
5*	CuO/Ga_2O_3	TBHP	-	107	3	74%	78%	1.2%	12	[48]
6	Cu-HMS[d]	TBHP	ACN/DMF	80	12	99%	84%	6.9%	37	[139]
7*	$[Cu(H_2btec)(bipy)]_\infty$	TBHP	DCE	75	24	24%	71%	29%	40	[42]
8	Ag/VSB-5	H_2O_2	acetone	70	10	37%[e]	-	-	-	[140]
9*	Ag-*γ*-ZrP	TBHP	ACN	82	8	43%	93%	4.7%	30	[141]
10*	Ag-VPO	TBHP	ACN	82	3	98%	0.9%	89%	~100	[85]
11*	Ag nanocubes	TBHP	none	Reflux	12	82%	19%	81%	1-2	[62]
12*	Silver nanolithes	TBHP	toluene	~ 110	3	29%	41%	59%	0.6	[66]
13*	Ag/SBA-12	H_2O_2	water	100-150 (MW[g])	0.5	90%	85%	-	880	[142]
14	$1\%Ag/TiO_2\text{-}SiO_2\text{-}f$[h]	H_2O_2	water	176 (MW[f,g])	0.25	99%	87%	-	1700	[79]
15	$0.5\%Ag/TiO_2\text{-}SiO_2\text{-}f$[h]	H_2O_2	water	96 (MW[f,g])	0.25	60%	99%	-	570	[79]

*No standard use reported. [a]Styrene oxide. [b]Benzaldehyde. [c](*E*)-stilbene as substrate. [d]Hexagonal mesoporous silica. [e]Oligomer formed. [f]Maximum temperature. [g]Microwave irradiation. [h]Organo-functionalized.

observed in DMF or acetonitrile as a solvent [139]. Depending on the weight loading and preparation method, two different kinds of Cu-HMS catalysts were synthesized, i.e. catalysts containing Cu_xO particles and catalysts with highly dispersed Cu moieties. Cu_xO particles containing catalysts were less active than catalysts featuring high Cu dispersion and tended to leach and deactivate significantly while in the other case leaching was only detected in the first run. Full conversion was obtained in a DMF/ACN mixture with a high epoxide selectivity of 84 % (TOF 37 h^{-1}, entry 6). Highly dispersed Cu is also present in metal-organic frameworks; $Cu(H_2btec)(bipy)]_\infty$ [42] epoxidized styrene with TOF of up to 28 h^{-1} at 75 °C with 71 % selectivity (entry 7). The authors suggest the epoxidation to occur directly at the Cu centers, thus not as an autoxidation. Bimetallic MCM-41 incorporated RuCu catalysts were also studied yielding only low styrene conversions while they acted as highly active benzene hydroxylation catalysts [143].

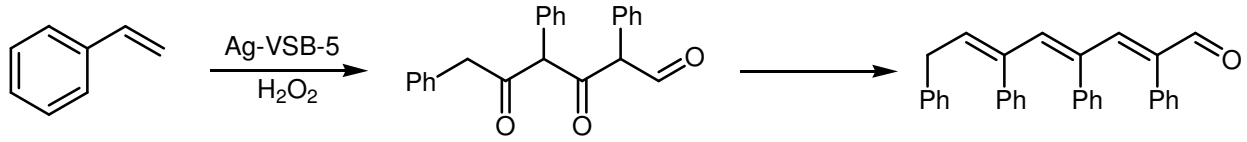

Scheme 2-11: Oligomerization of styrene with H_2O_2 and Ag-VSB-5 [14].

Studies with silver catalysts focus on styrene as a substrate. The study by Chen et al. [140] used 1.1 nm Ag-arrays incorporated in nanoporous VSB-5, a nickel phosphate molecular sieve, in order oxidize styrene. Liquid chromatography analysis showed that mainly oligomers were formed from successive oxidation and aldol condensation (Table 2-3, entry 8) demonstrating that GC analysis is not generally capable of giving a thorough description of the products formed in styrene oxidation (Scheme 2-11). Other metal phosphates were also tested in combination with silver. Silver-ion exchanged *γ*-ZrP (entry 9) catalyzed styrene epoxidation with high selectivity [141]; interestingly, the epoxidation with TBHP had to be carried out under Argon atmosphere for optimal performance. Using air as the primary oxidant, some conversion to the epoxide (TOF ~1h^{-1}) was also observed with a high selectivity (75%) compared to other oxygen-based epoxidations. The reaction was strongly dependent on the choice of solvent, acetonitrile and dichloromethane giving the best results. The same group also tested the combination of vanadium phosphates modified with silver [85]. Again, argon atmosphere was mandatory. The combination of V and Ag with phosphate was more active than the silver-zirconium phosphate combination achieving TOFs around 100 h^{-1} (Table 2-3, entry 10). In a more fundamental study, silver nanoparticles with different morphologies were investigated for different activities of the silver facets [62]. The activity was sorted as *γ*(110) > *γ*(100) > *γ*(111); however, no internal standard was used under

the quite harsh reaction conditions (refluxing styrene, entry 11). Macroporous nanolithes derived from reduction of $AgNO_3$ with glycerol were also investigated and found to be catalytically active (entry 12) [66]. High selectivities to the epoxide in combination with a high reaction rate can be achieved over silver catalysts by using microwave irradiation where H_2O_2 as an oxidant already gave very good results (entry 6, 7a,b). With silver particles supported on SBA-12, a mesoporous silica, almost full conversion could be obtained after 30 min (entry 13) [142]. Compared to SBA-12 supported gold particles, the silver catalyst was more reactive with a lower selectivity (85 % vs. >99 %). Interestingly, the inverse behavior was observed comparing the two catalysts in benzyl alcohol oxidation. The temperatures reached during microwave irradiation are often significantly higher than 100 °C, so even considering the short reaction times, styrene oligomerization cannot be excluded. By using an internal standard technique Purcar *et al.* demonstrated that indeed very high selectivities can be obtained in a microwave oven [79]. As a catalyst, Ag supported on SiO_2 modified with surface active groups, i.e. methyl- and 3-mercaptopropyl-groups, and additionally Ti^{4+} was used. As often observed for silver catalysts, the particle size distribution was quite broad ranging from a few nms to particles larger than 30 nm, of course also depending on the weight loading. The sulfur containing moiety did not deactivate but stabilized the silver nanoparticles. Where ionic Ag^{I} was still present in the catalyst (due to incomplete reduction) leaching was observed and caused both rapid deactivation and low epoxide selectivities (> 50 %). Catalysts without ionic Ag species deactivated only to a small extent. Under optimized conditions, full conversion could be obtained after 15 min with a selectivity around 90 % (entry 14). Under milder conditions, the exclusive formation of the epoxide as a product was observed (entry 15). The reaction was also investigated under conventional heating resulting in less than 30 % conversion after 12 h demonstrating the advantage of microwave usage. Note that supported silver catalysts and also gold catalysts can catalyze the reverse reaction, i.e. the deoxygenation of epoxides to olefins [144]. With alcohol as a reductant, selectivities of >99 % were obtainable often with quantitative conversion (Scheme 2-12).

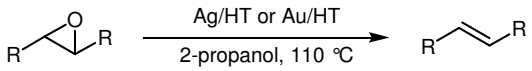

Scheme 2-12: Deoxygenation of epoxides with 2-propanol over Ag and Au catalysts [144].

Finally, an interesting study describes the use of Cu-exchanged zeolite X catalyzing the oxidative cleavage of the double bond in enamines yielding a ketone and an amide [145]. The catalyst required activation

in a chlorinated solvent where a copper-chloro complex was formed as evidenced with X-ray absorption spectroscopy (Scheme 2-13). No leaching was observed, the catalyst being stable during several recycles.

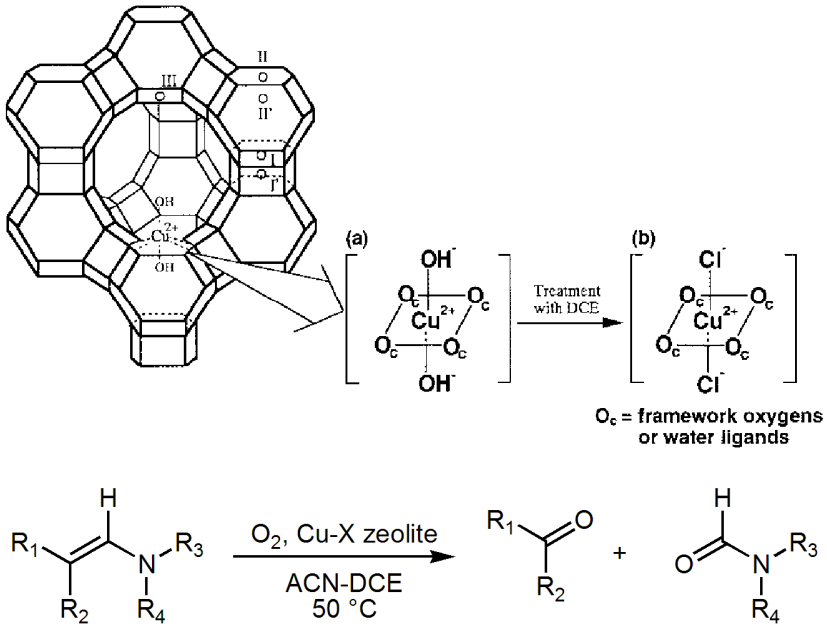

Scheme 2-13: Oxidative cleavage of enamines by *in-situ* formed Cu-Cl complexes [145]. Reprinted with permission from the Royal Society of Chemistry © 2000.

2.3.3 Side-chain oxidation of alkyl aromatic compounds

The side-chain oxidation of alkyl aromatic compounds is of enormous industrial importance: terephthalic acid is produced from *p*-xylene by reaction with molecular oxygen over a very active and effective Co/Mn/Br homogeneous catalyst system in the AMOCO process [146]. Using this catalyst system, many alkyl aromatic compounds can effectively be oxidized, e.g. ethylbenzene, toluene, cumenes, tetralines etc. The oxidation is in general accepted to occur *via* a free radical autoxidation mechanism. However, both the homogeneity of the reaction and the use of acetic acid as a solvent being partly decomposed under the harsh reaction conditions still leave room for improvement.

2.3.3.1 Peroxides as oxidants

The use of Cu catalysts for this reaction is troublesome to some extent as Cu in combination with peroxides – especially H_2O_2 – also catalyzes the ring hydroxylation (Table 2-4, entries 1-3, Figure 2-10) [31, 33, 147]. Thus,

for toluene, cresols as side chain oxidation products were obtained with no dominant selectivity for either reaction pathway. The same was observed for the three xylene isomers. With increasing steric hindrance side-chain oxidation is favored [31]. In the cited studies, acetonitrile (ACN) was used as solvent which is often favoring ring hydroxylation (see the respective section). Whether the choice of solvent can markedly influence the selectivity, was not investigated.

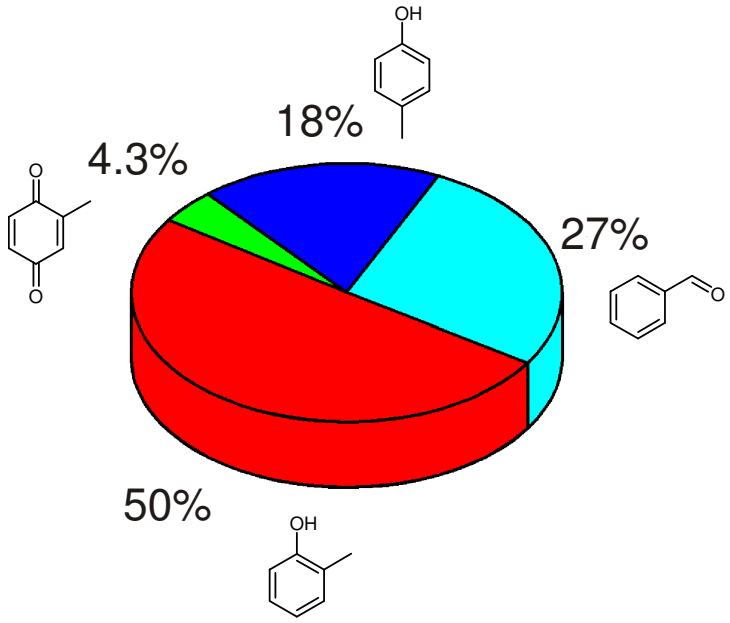

Figure 2-10: Product distribution obtained from Cu-APO-5 catalyzed toluene oxidation with H_2O_2 [31].

The use of TBHP as oxidant for activated alkyl aromatics allows for milder reactions conditions; almost quantitative conversion of diphenylmethane to benzophenone could be obtained with Cu-doped hydrotalcite as the catalyst under mild reaction conditions (60 °C, entry 4) [148]. As often observed, ACN solvent gave the best results by far with a TOF of 2.5 h^{-1} over 24 h. TBHP was also successfully used with the $Cu_3(BTC)_2$ metal-organic framework oxidizing xanthene to xanthone at 70 °C [149]. The very low TOF (0.02 h^{-1}, TON 0.56) might result from the inaccessibility of the MOF micropores to the substrate (Table 2-4, entry 5).

Table 2-4: Side-chain oxidation of alkyl aromatic compounds

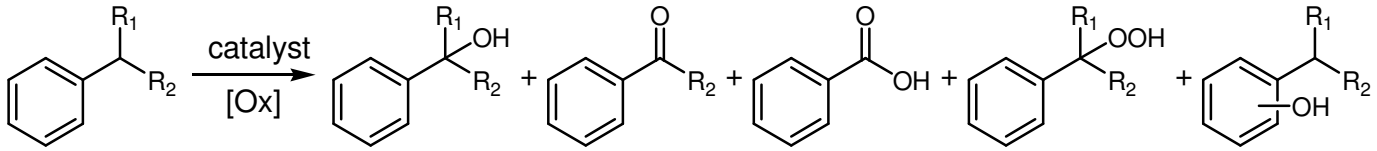

Al On Ac POx Ring

Entry	Catalyst	Substrate	Oxidant	Solvent	T (°C)	Rct. time (h)	Conversion	Selectivity					TOF (h^{-1})	Ref.
								Al[a]	On[b]	Ac[c]	POx[d]	Ring[e]		
1a*	Cu-Al/mont-morellite	toluene	H_2O_2	ACN	92	1	27%	-	29%	-	-	68%	-	[33]
1b*	Cu-Al/mont-morellite	*p*-xylene	H_2O_2	ACN	92	1	24%	-	43%	-	-	53%	-	[33]
2a*	$Zn_{0.9}Cu_{0.1}$/ LDH[f]	toluene	H_2O_2	ACN	60	1	15%	30%				70%	-	[147]
2b*	$Zn_{0.9}Cu_{0.1}$/ LDH[f]	*p*-xylene	H_2O_2	ACN	60	1	19%	48%				52%	-	[147]
3a	Cu-APO-5	toluene	H_2O_2	ACN	60	3	14%	28%				72%	14	[31]
3b	Cu-APO-5	ethyl-benzene	H_2O_2	ACN	60	3	10%	48%				46%	8.3	[31]
4	Cu-HT	diphenyl-methane	TBHP	ACN	60	24	95%	-	100%	-	-	-	2.5	[148]
5	$Cu_3(BTC)_2$	xanthene	TBHP	ACN	70	24	96%	-	85%	-	-	-	0.02	[149]
6a	$CuFe/Al_2O_3$	toluene	O_2	-	190	2	7.4%	24%	46%	27%	-	-	-[g]	[150]
6b	$CuFe/Al_2O_3$	toluene	O_2	-	190	4	25%	1.0%	27%	72%	-	-	-[g]	[150]
7	$Cu_xMn_yO_4$	toluene	O_2	-	190	2	17%	17%	15%	62%	-	-	-[g]	[25]
8	Cu_2O	cumene	O_2	-	80	-	-	-	-	-	-	-	0.15	[151]
9	Ag_2O/ α-Al_2O_3	ethyl-benzene	O_2	-	70	-	-	-	-	-	-	-	8.5	[72]
10	Ag/CeO_2-SiO_2	toluene	O_2	-	170	1	2.6%[h]	42%	38%	19%	-	-	11	[91]
11	Ag/CeO_2-SiO_2	*p*-xylene	O_2	-	135	3	13.4%[h]	22%	19%	58%	n.a.	-	600	[91]
12	Ag/CeO_2-SiO_2	ethyl-benzene	O_2	-	135	3	15%[h]	27%	45%	-	28%	-	670	[91]
13	Ag/CeO_2-SiO_2	cumene	O_2	-	135	3	2.3%[h]	4.3%	70%	-	26%	-	100	[91]

*No standard use reported. [a]Alcohol. [b]Aldehyde/ ketone. [c]Carboxylic acid. [d]Peroxide. [e]Ring hydroxylation. [f]Layered double hydroxide. [g]TOF for catalysts with 2 active metals were not calculated. [h]Yield; selectivities calculated from yields.

2.3.3.2 Aerobic oxidation

Given that the use of molecular oxygen for this type of reaction is long established in industry, the most promising systems also involve the use of this inexpensive oxidant. Side chain oxidation of toluene results mainly in benzyl alcohol, benzaldehyde and benzoic acid, with benzaldehyde as the most valuable reaction product. High benzaldehyde selectivities require low toluene conversions. Two binary metal oxides involving Cu were found to be useful catalysts for toluene to benzaldehyde conversion. $CuFe/Al_2O_3$ was reusable for toluene oxidation with oxygen at elevated pressures and 190 °C (entry 6a) [150]. Under solventless conditions, a benzaldehyde selectivity of 46 % at 7.4 % conversion could be improved to 86 % (at 7.3 % conversion) by addition of pyridine. The authors suggest that pyridine hinders benzaldehyde adsorption to the catalyst surface thereby suppressing the oxidation to benzoic acid. At high conversions (25.4 %), benzoic acid could be synthesized with moderate selectivity (72 %, entry 6b). Interestingly, both Cu/Al_2O_3 and Fe/Al_2O_3 where almost inactive. All the catalysts in this study where synthesized by impregnation which usually leads to formation of metal oxide particles. In the case of Cu, this can lead to excessive leaching which was unfortunately not investigated. The synergistic effect of Fe on Cu might result from a stabilization of CuO particles. $Cu_xMn_{3-x}O_4$ spinels were also investigated under the same conditions [25]. A 1:1 ratio of Cu to Mn gave the best catalyst and the spinel was clearly favored over amorphous mixed CuMn oxides obtained by calcination of the coprecipitate at lower temperatures. With this catalyst, the selectivity to benzaldehyde dropped rapidly. After 3 hours reaction time 75 % selectivity to benzoic acid was obtained at 21.3 % conversion (entry 7).

Already in the 1970s it was shown that Cu_2O initiates the autoxidation of cumene (entry 8) [151], though being highly inferior to Co_3O_4. The oxidation of cumene occurs readily due to the low bond dissociation energy of the tertiary C-H of 351.6 kJ/mol (toluene 375.0 kJ/mol) [152]. Metallic Cu was found to be inactive as a catalyst contrary to bulk metallic silver being a good initiator for the radical autoxidation of cumene [153]. Interestingly, the decomposition of cumene hydroperoxide depended on the gas atmosphere and occurred only in N_2 but not in O_2. Ag/SiO_2 was also found to be a useful catalyst [154]. Alloying of Ag with Au supported on SiO_2 *via* impregnation improved the catalyst performance, Au/SiO_2 being entirely inactive [155]. Ag_2O supported on α- and γ-Al_2O_3 and zeolite 15X oxidized ethylbenzene to 1-phenylethanol, acetophenone and ethylbenzene hydroperoxide (entry 9) [72]. The role of silver was also to initiate a radical autoxidation but while AiBN – also acting as an initiator – afforded mainly the peroxide, this species was decomposed on the silver catalysts. At 70 °C, the reaction proceeded only slowly (initial TOF between 3-8.5 h^{-1} for the three different silver catalysts). At higher reaction temperatures (135 °C), ethylbenzene is oxidized more rapidly in

the presence of oxygen by an impregnated Ag/SiO_2 catalyst [91]. Also *p*-xylene and cumene could be successfully oxidized though for *p*-xylene only one methyl group was activated by this catalyst. CeO_2 and a carboxylic acid as additives increased the *p*-xylene oxidation rate. On the other hand, cumene oxidation was markedly hindered by the presence of CeO_2 nanoparticles. In the absence of a carboxylic acid, CeO_2 completely suppressed the alkyl aromatic oxidation being a radical scavenger. Toluene required higher reaction temperatures (entry 10). Significant silver leaching was observed with the impregnated catalyst which could be circumvented by using flame-spray pyrolysis as a synthesis technique for Ag/SiO_2-CeO_2 catalysts. This way, TOFs of 650 h^{-1} were obtained (Table 2-4, entry 11-13). To the best of the author's knowledge, no studies focus on using heterogenous gold catalysts for this reaction. However, Corma's group demonstrated the usability of gold for this reaction by using the peroxides formed during cumene oxidation by Au/CeO_2 for epoxidation of aliphatic olefins [124].

2.3.4 Oxidation of cyclohexane

The oxidation of cyclohexane is of enormous industrial importance for the production of K/A-oil, a mixture of cyclohexanone (K) and cyclohexanol (A) (preferably with a high ketone fraction) serving as an intermediate in the production of Nylon 6,6 and Nylon 6 [11]. Industrially, K/A-oil is either obtained *via* non-catalytic autoxidation or by using homogeneous Co catalysts in ppm-amounts. A large variety of products is formed. High K/A selectivities are only obtained at low conversions. Harsh conditions are necessary with 10-15 bar of air at temperatures around 150 °C being last but not least a considerable safety concern [11]. Ever since industrial processes where established in the 1940s, considerable research towards more efficient and especially heterogeneous catalysts has been conducted, yet finding better catalysts active under more benign conditions remains a challenge [157]. Even more, the reaction is also complex from an experimental point of view: oxidation of cyclohexane to different gaseous, volatile and products of low solubility partly being thermo-sensitive makes the accurate determination of conversions and selectivities challenging [158]. The formation of around 40 products was reported the most important products besides K/A oil being cyclohexane peroxides, as well as C_5 and C_6 acids (Scheme 2-14) [156]. At least the use of a suitable internal standard is mandatory to obtain K/A yields not being overestimated [156, 159]. The last point has led to considerable discrepancy in the open literature on the catalytic activity of gold catalysts.

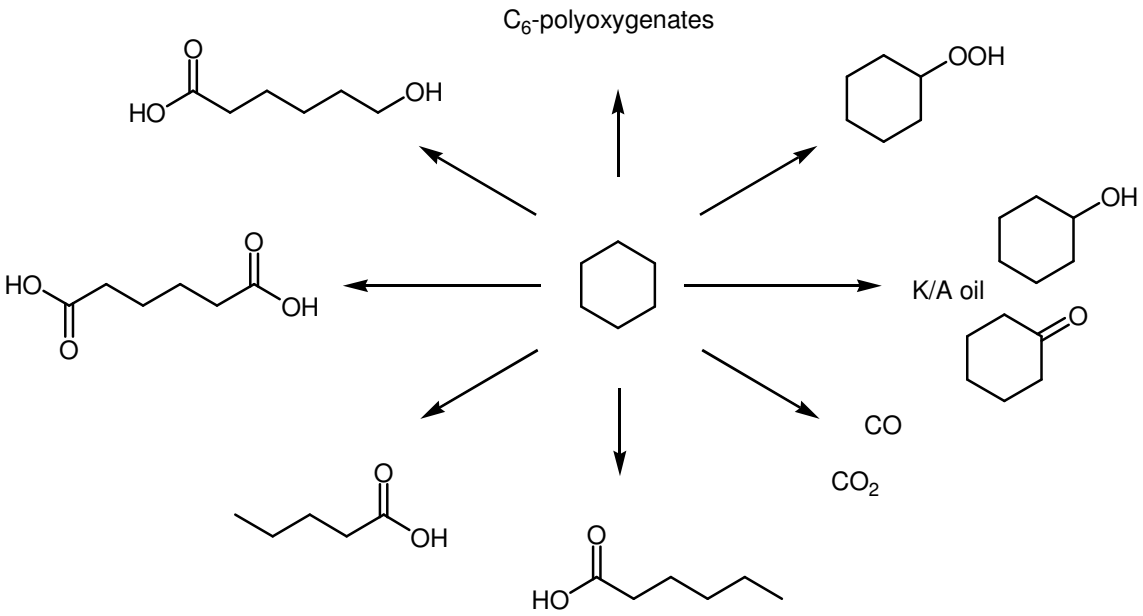

Scheme 2-14: Main products of cyclohexane oxidation [156].

2.3.4.1 Gold catalysts

At conditions comparable to industry, TOFs for the gold catalyzed oxidation of cyclohexane are reported to be in the range of several thousand per hour e.g. with Au/ZSM-5 (Table 2-5, entry 1) [160], Au/SBA-15 (entry 2 and 3) [161, 162], Au/MCM-41 (entry 4) [163], Au/SiO_2 (entry 5) and Au/SiO_2-TiO_2 [164], Au/Al_2O_3 (entry 6) [165] and Au/SiO_2-Al_2O_3 (entry 7) [166]. In the industrial process, high cyclohexane conversion is avoided since the selectivity to K/A oil drops significantly when exceeding 4 %. With the cited Au catalysts overall K/A selectivities higher than in the industrial case at higher conversions are reported. The group of Hutchings investigated the reaction at low temperatures (70 °C) where TBHP was necessary as a radical initiator [159]. As in the industrial case the K/A selectivity was merely a function of conversion, a general conclusion being that gold is not exceptionally active for this reaction (Table 2-5, entry 8). Hereijgers *et al.* [156] investigated various supported Au catalysts finding gold to act only as an initiator for a radical autoxidation of cyclohexene (entry 9). Gold was neither especially selective nor active giving similar conversions as unpassivated autoclave steel (Figure 2-11). The high calculated TOF also found here was mainly a consequence of the nature of a radical reaction at the high temperatures which is only initiated by gold and maintains itself. In combination with homogeneous Co, Au supported on SBA-15 even inhibited the reaction to a certain extend. Contrary to many other cyclohexane

oxidation studies, product analysis was done monitoring both gaseous and liquid products thereby providing very reliable results in terms of the industrially important selectivities.

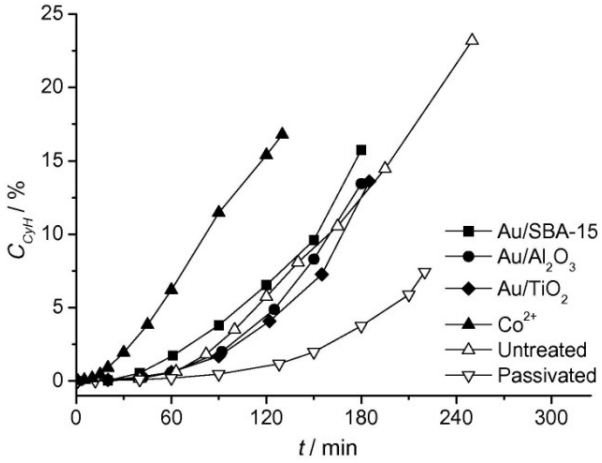

Figure 2-11: Cylohexane conversion *vs.* time on stream during cyclohexane autoxidations (open symbols) and catalyzed oxidation (solid symbols) at 150 °C and 1.2 – 1.5 MPa [156]; reprinted with permission from Elsevier © 2010.

2.3.4.2 Silver catalysts

Silver catalysts were investigated at similarly harsh conditions using molecular oxygen as the oxidant. Ag supported on MCM-41 (entry 10), TS-1 and Al_2O_3 was an effective initiator for the aerobic radical autoxidation reaction [80]. At 140 °C, high amounts of cyclohexylhydroperoxide were formed while at 155 °C, K/A oil was formed in 80 % selectivity with a conversion around 10 %. Compared to examples with gold, an attractive advantage of silver is the relatively high K/A ratio > 1. With respect to the industrial process, these values are high though the promising results must be taken with care when product analysis is not carried out as accurately (i.e. gas and liquid phase) as reported in ref. [156] (*cf.* section 2.3.4.1 previously discussed) though an internal standard was used. Lower K/A selectivities were reported for Ag decamolybdovanadophosphate in pressurized CO_2 in combination with MeOH as a solvent (entry 11) [167]. On the other hand, overall organic oxygenates were formed with high selectivity (96 % at 10 % conversion), i.e. over-oxidation to CO and CO_2 was low even at 180 °C. K/A ratios around 2 were obtained. Interestingly, the polyoxymetallate catalyst was more suitable for this reaction compared to the homogeneous Co/Mn/Br system applied in the AMOCO process [146] giving mainly carbon oxides as products.

2.3.4.3 Copper catalysts

Contrary to silver and gold most studies focusing on copper applied milder reaction conditions at the cost of oxygen being necessary in an activated form as H_2O_2 or TBHP in an additional solvent. Cu is active in its fully oxidized form as Cu(II). The activation of peroxides by copper complexes is intensively studied [168-171] and rather complex and may include intermediate Cu(I) but also Cu(III) [171] species. Hydroxy, alkyloxy and alkyperoxy radicals are generated from TBHP or H_2O_2, respectively, suggesting that the cyclohexane oxidation over Cu(II) follows a radical autoxidation mechanism. Many Cu catalysts are supported on or integrated in silica frameworks where significant leaching is often encountered as a problem and a deactivation pathway. A good example is Cu/MCM-41 [37]. Cu being applied during the synthesis of MCM-41 resulted in low surface areas and an almost inactive catalyst. Cu_xO particles (thus not integrated in the framework) were rapidly washed out under reaction conditions. With 3-aminopropyl-linkers, the stability of the catalyst towards leaching was improved (though not eliminated) and TOFs around 2 h^{-1} with H_2O_2 as oxidant at 100 °C were obtained (Table 2-5, entry 12). Product formation was already found at room temperature. K/A ratios were around 2, K/A ratios > 1 being in general observed with peroxides over Cu catalysts. Leaching was also a problem for Cu(II) on another mesoporous silicate, TUD-1 [172]. With TBHP as oxidizing agent, TOFs around 7 h^{-1} were obtained in the absence of an additional solvent at 70 °C (entry 13). Substantial Cu leaching was also encountered with sol-gel derived Cu/SiO_2 which could be slightly improved by calcination [173, 178]. Also here, no additional solvent was necessary with TBHP as the oxidant (entry 14). TOFs were comparable to TUD-1. Despite the leaching, homogeneous Cu species were not catalytically active. A problem of Cu can be the low efficacy in the use of peroxides due to unselective peroxide decomposition [37, 174]. The other side of the medal is a desirable low selectivity to cyclohexyl peroxides [37, 172-174]. Selectivities of up to 100 % to K/A-oil were reported e.g. with Cu-ZSM-5 in an ionic liquid [174] with moderate TOFs (6 h^{-1}) at 90 °C (entry 15). Of course, these high selectivities are only reliable when obtained by very thorough product quantification [156]. As an exception, Cu supported on magnesium manganese oxide octahedral molecular sieves featured a high selectivity to cyclohexane peroxide and *t*-butyl cyclohexyl perether with TBHP [32] though at higher reaction temperatures cyclohexane peroxide selectivity decreased significantly (Table 2-5, entry 16). Remarkably, no leaching of Cu was found with this material but TOFs were only around 1 h^{-1}. Another mixed oxide, $Cu_{1-x}Zn_xCr_2O_4$ spinel, was found to be catalytically active with TBHP where ACN was required as a solvent (entry 17) [175]. This system was fully recyclable in contrast to many other Cu catalysts where leaching is an issue. Also in ACN but with H_2O_2 as oxidizing agent copper pyrophosphate ($Cu_2P_2O_7$) as a bulk material exhibited considerable catalytic activity [176] already at 65 °C (TOF ~2 h^{-1}, entry 18) and might therefore be interesting as

Table 2-5: Oxidatin of cyclohexane.

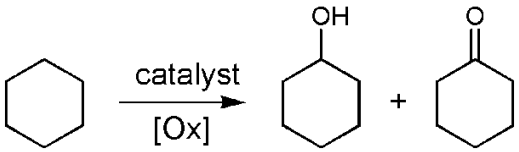

Entry	Catalyst	Oxidant	Solvent	T (°C)	Rct. time (h)	Conversion	Selectivity	TOF	Ref.
1*	Au/ZSM-5	O_2	-	150	3	15%	92%	2,800	[160]
2*	Au/SBA-15-f[a]	O_2	-	150	3	16%	84%	12,000	[161]
3*	Au/SBA-15-f[a]	O_2	-	150	2	17%	92%	6,000	[162]
4*	Au/MCM-41	O_2	-	150	3	12%	97%	11,000	[163]
5*	Au/SiO_2	O_2	-	150	3	9.2%	83%	110,000	[164]
6*	Au/Al_2O_3	O_2	-	150	3	12.6%	85%	16,000	[165]
7*	Au/SiO_2-Al_2O_3	O_2	-	150	3	8.7%	89%	2,700	[166]
8	Au/graphite[b]	O_2	-	70	17	1%	92%	18	[159]
9*	Au/SBA-15	O_2	-	150	1.5	4%	71%	2,000	[156]
10*	Ag/MCM-41	O_2	-	155	3	11%	83%	600	[80]
11	Ag-V-POM	O_2	$scCO_2$/MeOH	180	8	10%	96%[c]	-	[167]
12	Cu-MCM-41-f[a]	H_2O_2	acetone	100	12	4.8%[e]	-	1.7	[37]
13	Cu-TUD-1	TBHP	-	70	24	14%	81%	~7 h^{-1}	[172]
14	Cu-mp-SiO_2[d]	TBHP	-	75	24	4.2%	85%	5.7	[173]
15*	Cu-ZSM-5	TBHP	Ionic liquid [emim]BF_4	90	12	9.5%	100%	6	[174]
16	Cu-OMS-1[f]	TBHP	*tert*.-butanol	80	40	10%	78%	1.7	[32]
17*	Cu-Zn-Cr-spinel	TBHP	ACN	70	10	17%	71%	-	[175]
18	$Cu_2P_2O_7$	H_2O_2	ACN	65	8	59%	100%	1.8	[176]
19a	Cu/TiO_2	O_2	-	120	24	12%	63%	8	[177]
19b	Cu/Al_2O_3	O_2	-	120	24	14%	67%	10	[177]
19c	Cu/Fe_2O_3[g]	O_2	-	120	24	14%	69%	10	[177]
20	Cu-ZSM-5	O_2	-	100	4	6.3%	75%	180	[27]

*No standard use reported. [a]Organo-functionalized. [b]Catalytic amount of TBHP/1,4-difluorobenzene added. [c]Selectivity to partially oxygenated products. [d]Microporous silica. [e]Yield. [f]Octahedral molecular sieve. [g]Strong deactivation.

a supported catalyst. The authors further stated that surface hydrophobicity is a crucial parameter for this material.

There are only few studies investigating cyclohexane oxidation focusing on molecular oxygen with Cu catalysts. By using a sophisticated deposition method (including evaporation of Cu and trapping in acetone) metallic Cu nanoparticles in the size range of 2-6 nm were supported on TiO_2 (entry 19a), Al_2O_3 (entry 19b) and Fe_2O_3 (entry 19c) [177] and used as catalysts. Cu particles likely oxidized at the elevated pressures (20 bar) and temperatures (120 °C), the latter still being significantly lower than those used in the industrial case and in Au catalysis. Copper leaching with TiO_2 and Al_2O_3 was only observed in the first run making these catalysts highly recyclable. Only cyclohexanol and cyclohexanone yields were reported and the reaction times were long (TOF 10 h^{-1} over 24 h) which may be related to the low temperatures. Interestingly, high K/A ratios of up to 11.5 could be obtained at relatively high yields around 10 %. Cu/ZSM-5 catalyzed the oxidation with molecular oxygen already at 100 °C (entry 20) [27]. Calculated TOFs were in the order of 100-200 h^{-1} and thus significantly higher than in the previous case. Lower K/A ratios around 1 were obtained which remained virtually unaffected when adding substoichiometric amounts of TBHP as a radical initiator. The unchanged product distribution at higher conversions suggests that Cu acts as a radical initiator. Calcination of Cu-ZSM-5 decreased its catalytic performance. Co-ZSM-5 studied in the same project was always more active; nevertheless, the activity of Cu-ZSM-5 was promising and it would be interesting to see its performance under industrial conditions. Unfortunately, leaching studies for Cu-ZSM-5 were not performed. As another Cu-modified zeolite NaY was selectively converting cyclohexane to K/A oil under UV light irradiation at room temperature [30]. Finally, a short report emphasizing the importance of reliable procedures and very worth reading within cyclohexane oxidation with Cu catalysts is ref. [179].

2.3.5 Hydroxylation of aromatics

The oxidation of benzene or other aromatics to phenol or hydroxylated aromatics with hydrogen peroxide is a reaction which has experienced considerable attention with heterogeneous Cu catalysts. Apparently, two different classes of Cu catalysts exist: those which require acetonitrile as a solvent and those preferring other reaction media; the former will first be described.

Table 2-6: Ring hydroxylation of aryl compounds.

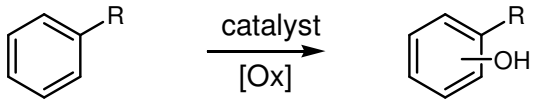

Entry	Catalyst	Substrate	Product	Oxidant	Solvent	T (°C)	Rct. time (h)	Conversion	Selectivity	TOF (h^{-1})	Ref.
1	Cu-SiO_2-f[a]	benzene	phenol	H_2O_2	ACN	60	4	7.1%	21%	2.1	[180]
2	Cu-APO-5	benzene	phenol	H_2O_2	ACN	60	3	28%	100%	33	[31]
3	Cu-Al-MCM-41	TMP[b]	TMBQ[c]	H_2O_2	ACN	60	0.33	64%	73%	230	[38]
4	CuAPO-11	benzene	phenol	H_2O_2	ACN	70	6	11%	100%	8.3	[41]
5	$Cu_2(OH)PO_4$	phenol	HQ[d] + CAT[e]	H_2O_2	H_2O	80	4	28%	99%	2.2	[59]
6	$Cu_2(OH)PO_4$	benzene	phenol	H_2O_2	-	80	8	31%	80%	1.2	[181]
7	Cu/Al-PILCs[f]	benzene	phenol	H_2O_2	ACN	60	3	55%	81%	110	[45]
8	Fe_5VCu/TiO_2	benzene	phenol	O_2/asc. ac[g]	ACN	30	24	6.6%	85%	-	[47]
9	CuO/ MCM-41	benzene	phenol	H_2O_2	HAc	30	1.7	21%	94%	45	[182]
10	Cu_xO/C	benzene	phenol	H_2O_2	acetone	65	5	63%	54%	-	[183]
11	CuCo/HT	phenol	HQ[g] + CAT[h]	H_2O_2	H_2O	65	2	21%	~ 100%	-	[184]
12	Cu-Ni-HT	phenol	HQ[g] + CAT[h]	H_2O_2	H_2O	65	2	24%	~ 100%	-	[185]
13	CuNi/HT	benzene	phenol	H_2O_2	pyridine	65	24	4.8%	-	-	[186]
14	Cu-HX	benzene	phenol	O_2/asc. ac[g]	aq. HAc	30	24	2.3%[h]	-	0.2	[187]
15	Cu-NaY	benzene	phenol	O_2/asc. ac[g]	aq. HAc	30	24	1.7%[h]	-	0.3	[29]
16	Cu/MCM-41	benzene	phenol	O_2/asc. ac[g]	aq. HAc	30	5	1.3%[h]	-	0.9	[50]
17	Cu-Al_2O_3	benzene	phenol	O_2/asc. ac[g]	aq. HAc	30	24	2.5%[h]	-	0.2	[43]
18a	VO_x/Cu-SBA-15	benzene	phenol	O_2/asc. ac[g]	HAc/H_2O	80	5	25%[h]	-	-	[188]
18b	VO_x/Ag-SBA-15	benzene	phenol	O_2/asc. ac[g]	HAc/H_2O	80	5	18%[h]	-	-	[188]

[a]Organo-functionalized. [b]1,2,5-Trimethylphenol. [c]Trimethylbenzoquinone. [d]Hydroquinone. [e]Catechol. [f]Al-pillared interlayer clays. [g]Ascorbic acid. [h]Yield.

2.3.5.1 Hydroxylation in acetonitrile

Acetonitrile is in some cases assumed to participate directly in the catalytic oxidation [180] therefore being consumed. The oxidation of benzene also proceeds in other solvents but often either highly unselectively or with low rates [31, 45, 180]. Reactions are typically carried out at temperatures around 60 °C; higher reaction temperatures cause H_2O_2 decomposition. When comparing Cu with oxidic V and Fe incorporated in SiO_2-based amorphous microporous mixed oxides, the latter two metals gave higher yields [180]. TOFs for Cu were around 2 h^{-1} at 60 °C (Table 2-6, entry 1). Increasing the hydrophobicity of the silica matrix by end-capping with methyl groups had a negative effect though the surface areas were nearly unaffected. Leaching was experienced with every catalyst though doping with Al helped in the case of Fe. The effect of Al-doping on Cu leaching was not investigated. In another study, co-impregnation of Cu and Al indeed had a beneficial effect on the catalytic activity [31]. Cu(II)-doped materials ($AlPO_4$-5 and MCM-41) gave higher phenol yields than impregnated catalysts with TOFs around 30-40 h^{-1} (entry 2). Catalysts featuring isolated Cu sites are often superior to supported Cu_xO particles especially where leaching is a major problem. Interestingly, incorporation of Cu in MCM-41 did not have the often observed negative effect on the silica material when Al was co-doped. Benzene could be hydroxylated to phenol with nearly 100 % selectivity. Alkylated aromatics underwent both ring and side-chain hydroxylation though usually with good to moderate yields to the ring hydroxylation product. The oxidation of 2,3,5-trimethylphenol (TMP) to 2,3,5-trimethylbenzoquinone (TMBQ) also proceeded in benzaldehyde as the solvent using molecular oxygen as the oxidant. These conditions are typical for epoxidation reactions. Consequently, Cu-$AlPO_4$-5 and Cu-Al-MCM-41 might also be active in epoxidation reactions (note however that steel is already capable of activating aldehydes for epoxidation reactions [189]). Detailed studies on TMP oxidation with Cu-Al-MCM-41 were reported in ref. [38] (entry 3). TOFs around 8 h^{-1} were measured for the hydroxylation of benzene with Cu-$AlPO_4$-5 and Cu-$AlPO_4$-11 at slightly higher reaction temperatures (entry 4) [41]. Contrary to the previous paper, however, overoxidation of phenol was observed with Cu-$AlPO_4$-5 having larger pores than Cu-$AlPO_4$-11 with which the phenol selectivity was close to 100%. Comparsion of ref.s [31] and [41] both using Cu-$AlPO_4$ as catalysts shows how much reaction conditions and catalyst preparation can influence the selectivity. Also here, the isomorphous incorporation of Cu into the framework of the aluminophosphate was assumed to be substantial for obtaining catalytic activity. Further Cu-phosphate catalysts, i.e. $Cu_2(OH)PO_4$ and $Cu_4O(PO_4)_2$ also exhibited considerable catalytic activity, though being a bulk material (BET surface areas ~ 1-2 m^2/g), in the hydroxylation of benzene, phenol and 1-naphthol (entry 5 and 6) [59, 181]. Both water and acetonitrile were suitable solvents in combination with H_2O_2 as oxidant. The

importance of isolated Cu species was further underlined by studying Cu-modified Al-pillared interlayer clays [45]. Though the selectivity was somewhat lower than obtainable with Cu-$AlPO_4$ materials, high TOFs of up to 100 h^{-1} (60 °C) were obtained (Table 2-6, entry 7). Leaching was assumed to be responsible for catalyst deactivation. Such Cu-doped pillared clays (montmorillonites, Figure 2-2) were also investigated as catalysts for toluene as well as *o*-, *m*- and *p*-xylene oxidation with hydrogen peroxide in acetonitrile [33]. Both ring and side-chain oxidation was observed to a similar extent rendering the oxidation of alkylaromatics with Cu and H_2O_2 not very selective. The same was observed with Zn,Cu,Al-layered double hydroxides (hydrotalcites like compounds) [147]. By means of EPR, in both studies isolated Cu(II) species and bulk CuO were identified. CuO was connected to H_2O_2 decomposition, thus, giving another example where isolated Cu(II) centers are mandatory for an effective catalyst. Benzene can also be oxidized with H_2O_2 using high amounts of ascorbic acid as a co-reductant [47]. This allows the reaction to be carried out close to room temperature (TOF of ~5 h^{-1} at 30 °C) with Fe/Cu/V mixed oxides supported on TiO_2 (Table 2-6, entry 8).

2.3.5.2 Hydroxylation in other solvents

Cu-MCM-41 is a catalyst which is active both in acetonitrile and in acetic acid [182]. Hence, the role of acetonitrile as either an inert or reactive solvent may be different depending on the type of Cu catalyst. Cu-MCM-41 in acetic acid was active already at 30 °C in acetic acid/H_2O_2 with comparably good TOFs around 45 h^{-1} at phenol selectivities above 90 % (entry 9) [182]. Again it was shown that the appearance of crystalline CuO particles had no beneficial effect on the activity. Cu-MCM-41 was also used for the selective oxidation of 4-methylanisole with H_2O_2 to the corresponding benzoquinone (TOF ~30 h^{-1}) [190]. No leaching was found in acetic acid. With acetonitrile as a solvent, almost no conversion was found. A comparative leaching experiment was unfortunately not reported. In another study [191], Cu-MCM-41 oxidized anthracene to antraquinone by TBHP or H_2O_2 in benzene solvent. Almost no catalyst deactivation was observed indicating that leaching was low. Contrary to homodispersed Cu in MCM-41, Cu_xO particles supported on activated carbon exhibited only low efficacy in benzene hydroxylation [183] lower than that of iron and vanadium oxide particles (entry 10) supporting the assumption that Cu_xO particles are catalytically active, however, not the most efficient catalysts for aromatics hydroxylation. CuO incorporated in a polymer membrane was furthermore used in a more application-oriented study [192]. Dubey *et al*. investigated in several reports the catalytic activity of Cu-containing ternary hydrotalcites in the hydroxylation of phenol [58, 184, 185] affording both catechol and hydroquinone. The reaction studied with CuCoAl (Table 2-6, entry 11) and CuNiAl hydrotalcites (entry 12) gave

the best results and required H_2O_2. TBHP was no suitable oxidant. These hydrotalcites were also capable of oxidizing benzene to phenol with nearly 100 % selectivity when pyridine was used as a solvent though catalyzing the reaction rather slowly (entry 13) [186]. The combination of Cu with Ru in MCM-41 was catalytically active in neat benzene with H_2O_2 at 50 °C [143]. Phenol was the only product observed and TOFs were outstandingly high (above 600 h^{-1}, based on the combined amount of Ru and Cu).

The group of Tsuruya investigated the use of molecular oxygen as oxidizing agent which required the use of ascorbic acid as a sacrificial reductant in aqueous acidic solvents (entries 14-17) [28, 29, 43, 50, 187]. Various Cu catalysts were tested as catalysts, including Cu supported on Al_2O_3, SiO_2 (also MCM-41) and TiO_2 as well as ion exchanged zeolites. Conversions were rather low at 30 °C (TOF < 1 h^{-1}). Higher reaction temperatures had a negative effect on the overall conversion which was ascribed partly to ascorbic acid decomposition. The formation of H_2O_2 was evidenced during the reaction. Thus, it is reasonable to assume H_2O_2 to act as the primary hydroxylating agent. It was found that both framework incorporated Cu(II) species were catalytically active as well as leached Cu(II). Leached species gradually deactivated to Cu_2O making truly heterogeneous catalysts the most effective catalysts. This also explains why heterogeneous Cu-zeolite catalysts are better suited for this type of reaction [28] than different homogeneous Cu catalysts. CuO/Al_2O_3 was additionally more stable against leaching when prepared *via* co-precipitation rather than impregnation [187]. In a more recent publication V-Cu catalysts on various supports were successfully applied with ascorbic acid/O_2 in an acetic medium (entry 18a) [188]. The potential of this dyad was shown by more drastic reaction conditions, i.e. 80 °C as a reaction temperature and oxygen partial pressures of 7 bar. Probably due to decomposition, H_2O_2 was no suitable oxidant. Dissolved Cu was not observed in the reaction mixture (though insoluble Cu_2O may form from leached species, *vide supra*), while V leaching was an issue. This approach resulted in more active catalysts with a TOF of 2 h^{-1} (based on the amount of both V and Cu). To the best of the author's knowledge, this study is also the only example where Ag was found to be active (though also in combination with V, entry 18b). Indeed, the literature provides only few examples of heterogeneous silver or gold catalysts active for this reaction although both metals proved numerous times to be capable of activating hydrogen peroxide. A recent study using Au/TiO_2 and Au/Al_2O_3 as catalysts for the oxidation of phenols with hydrogen peroxide found that the arene is not hydroxylated but biaryls are formed [193]. The authors suggest the reaction to occur *via* coupling of free aromatic radicals. MeOH as a solvent gave the best results suggesting that HO· radicals – which are scavenged by alcohols – play no major role; interestingly, the reaction did not proceed with TBHP which was ascribed to the specific formation of a Au-H_2O_2 intermediate. As another example, Au supported on TiO_2 and different carbons converted 2-methyl-1-naphthol to 2-methyl-1,4-

naphtoquinone with molecular oxygen [194]. While gold catalysts gave high conversions, the selectivity to the quinone was low and thus higher yields were obtained in the absence of any catalyst as gold was promoting the overoxidation.

2.3.6 Oxidation of amines

The oxidation of amines to (mainly) imines or amides over heterogeneous catalysts is a young field of research. Catalysis with gold has evolved quickly after the first reports in 2007 [119]. The oxidation of a broad range of different amines [195] is now well-established. Successfully applied catalysts are Au/graphite (Table 2-7, entry 1 and 2) [195, 196], Au/CeO_2 (entry 3 and 4) [197-199], Au/Al_2O_3 (entry 5a) [200], Au/hydroxylapaptite [195] and Au/TiO_2 (entry 6) [196, 201]; TiO_2 alone is also catalytically active even in the absence of light [201]. The oxidation is usually carried out in non-polar solvents at elevated temperatures (≥100 °C), the TOFs of all cited nano-catalysts are comparable being in the range of 1 h^{-1} to 10 h^{-1} for the oxidation of dibenzylamine. The group of Corma showed that at least for Au/TiO_2 smaller Au nanoparticles afforded a more active catalyst [196]. On the other hand, the oxidation of amines is a rare example where bulk gold also shows considerable catalytic activity (entry 5b) [119, 200]. This might explain why heterogeneous catalysts prepared *in situ* giving rather large Au NPs on CeO_2 were highly active [197] which would, however, limit the scope of the very straightforward *in situ* catalyst synthesis (Figure 2-12) as for many oxidation reactions small nanoparticles are beneficial. The high activity of bulk gold for the oxidation of amines offers an intriguing opportunity for the

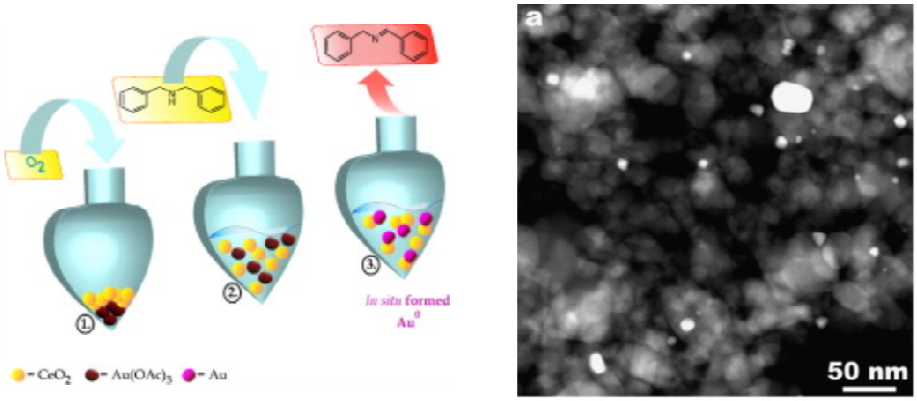

Figure 2-12: *In situ* synthesis of Au/CeO_2 for amine oxidation: CeO_2, $Au(OAc)_3$ and amine solution were mixed simultaneously. Au/CeO_2 formed under reaction conditions with Au particle sizes from a few nm to ca. 30 nm [197]; reprinted with permission from Elsevier © 2009 (no higher image resolution available).

Table 2-7: Aerobic oxidation of amines.

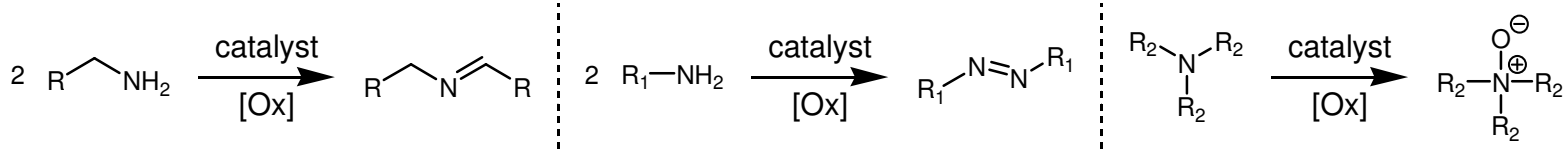

Entry	Catalyst	Substrate	Product	Solvent	T (°C)	Rct. Time (h)	Conversion	Selectivity	TOF (h^{-1})	Ref.
1	Au/graphite	dibenzyl amine	BB[a]	toluene	110	17	100%	95%	1.2	[195]
2	Au/graphite	benzyl amine	BB[a]	toluene	100	1	99%	100%	100	[196]
3	Au/CeO_2	aniline	diazobenzene	toluene	100	6	98%	91%	75	[199]
4	Au/CeO_2[b]	benzyl amine	BB[a]	toluene	108	8	>99%	91%	7.2	[197]
5a	Au/Al_2O_3	benzyl amine	BB[a]	toluene	100	24	92%[c]	-	0.2	[200]
5b	gold powder	benzyl amine	BB[a]	toluene	100	24	92%[c]	-	0.001	[200]
6	Au/TiO_2	*n*-hexylamine	*n*-hexyl caproic amide	-	130	20	60%	91%	15	[201]
7	Au/C	triethyl amine	triethyl amine-*N*-oxide	aq. NaOH	70	2	100%	100%	500	[202]
8	Au/TiO_2	aniline	diazobenzene	toluene	100	9	100%	90%	15	[199]

[a]*N*-benzylidenbenzyl amine. [b]Formed *in situ*. [c]Yield.

design of catalysts chemoselective only for the oxidation of amine groups in multifunctional molecules, a feature rarely found for heterogeneous oxidation catalysts. Tertiary amines can also be oxidized to the corresponding *N*-oxides [202] in aqueous systems with higher TOFs (e.g. 500 h^{-1} for triethylamine with Au/C, entry 7). Primary anilines not bearing an oxidizable α-C-atom can be selectively oxidized with O_2 by Au/TiO_2 and Au/CeO_2 catalysts to the corresponding azo compounds offering a very attractive and environmentally benign alternative to industrial procedures (Table 2-7, entry 8) [199]. This reaction is furthermore catalyzed by dissolved Cu(I)halides in the presence of pyridine [203]. In combination with ascorbic acid, homogeneous Cu(I) compounds also oxidized primary amines to imines with molecular oxygen at significantly lower temperatures (60 °C) than with gold and afforded ketones from primary amines [204]. Dehydroascorbic acid was assumed to be the primary oxidant. These two Cu systems demonstrate the principal feasibility of Cu as an amine oxidation catalyst. Furthermore, supported silver salts can be used as stoichiometric oxidizing agents for aniline oxidation to azo compounds [205]. Once more, however, reports dealing with supported Cu or Ag catalysts (especially heterogeneous catalysts) for amine oxidation are scarce which is not necessarily connected to their catalytic inactivity as the rapid development for gold catalysts has shown. In fact, the activity of gold was indicated already earlier by the successful use of gold-modified electrode materials in the electrocatalytic oxidation of amines [206-210]. Thus, the successful use of silver nanoparticles [83] as well as copper and silver oxides [211] as amine oxidation electrocatalysts might induce further research in this field.

2.3.7 Oxidation of hydroquinones

Quinone and hydroquinone derivatives have found wide-spread use in industrial chemistry [11] e.g. as antioxidants. Quinones can also function as relevant oxidizing agents especially as cofactors in enzymes such as amine oxidase (e.g. [212] and ref. therein) containing copper as the active metal. It is therefore not surprising that many Cu-based catalysts are reported for the regeneration of hydroquinones to quinones for which a high number of especially homogeneous catalysts can be found in the open literature. An early extensive study evaluated various dissolved Cu-salts as catalysts in the aerobic oxidation of hydroquinone to *p*-benzoquinone [213]. As one of the first heterogeneous Cu catalysts $CuSO_4/Al_2O_3$ was used with oxygen for the oxidation of various hydroquinones achieving high selectivities (Table 2-8, entry 1) [46]. This catalyst was capable of also oxidizing less reactive electron-poor hydroquinones but catalyst deactivation, high reaction temperatures

Table 2-8: Oxidation of hydroquinones.

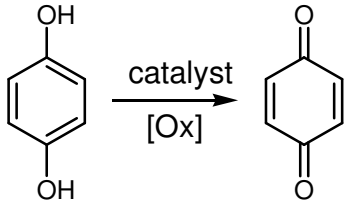

Entry	Catalyst	Substrate	Oxidant	Solvent	T (°C)	Rct. time (h)	Conversion	Selectivity	TOF (h^{-1})	Ref.
1	$CuSO_4/Al_2O_3$	HQ[a]	O_2	propyl acetate	100	8	94%[b]	-	0.6	[46]
2	$Cu_3(BTC)_2$	HQ[a]	O_2	Tris-HCl-buffer	40	-	-	-	100	[214]
3	Cu^{II}-chitosan	HQ[a]	H_2O_2[c]	H_2O	RT	-	-	-	-	[215]
4	Cu-Al(O)OH	HQ	O_2	toluene	25	2	96%[b]	-	11	[216]
5	$Cu(OH)_2/SiO_2$	CAT[d,e]	H_2O_2	aq. NaOH	22	-	-	-	-	[217]
6	Cu_2O nanocubes	TMHQ[f]	O_2	$MeOH/H_2O$	50	-	75%	-	1	[57]
7a	$Cu/Cu_2O/CuO$ nanopowders	TMHQ[f]	O_2	$MeOH/H_2O$	50	-	59%[g]	-	-	[55]
7b	$Cu/Cu_2O/CuO$ nanopowders	TMHQ[d]	O_2	$MeOH/H_2O$	50	-	79%[h]	-	-	[55]
8	Ag_2O	HQ	H_2O_2	MeOH	25	0.5	94%	99%	14	[218]
9	Au-polymer	HQ	O_2	$CHCl_3/H_2O$	RT	3	86%[b]	-	115	[219]

[a]Hydroquinone. [b]Yield. [c]Reaction proceeds also with O_2. [d]Catechol. [e]Reaction product: *α*-hydro-*β*-hydroxymuco-*γ*-lactone.
[f]Trimethylhydroquinone. [g]Without previous magnetization. [h]With previous magnetization.

of 100 °C, low turnovers and long reaction times still leave room for improvement. The metal-organic framework $Cu_3(BTC)_2$ reached TOFs of 100 h^{-1} at 40 °C in an aqueous solvent (Table 2-8, entry 2) exhibiting higher catalytic activity than the analogue Co- and Ni-MOFs [214]. Due to differences in the size of micropores in the studied MOFs, however, this is not necessarily connected to an intrinsic higher activity of Cu. Using H_2O_2 as oxidant the oxidation can be done at room temperature as was shown with Cu(II)-treated chitosan, an amino-polysaccharide (Figure 2-13) [215]. The use of H_2O_2, however, also caused overoxidation and at low pH no catalyst is necessary to achieve hydroquinone oxidation. On the contrary, Kim *et al.* could use

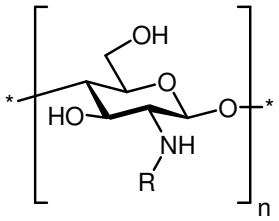

Figure 2-13: Chitosan structure.

oxygen to achieve the oxidation of various hydroquinones at room temperature (entry 4) [216]. The Cu/AlO(OH) catalyst exhibited good activity (TOF 15 h^{-1} for methylhydroquinone) with selectivities always approaching 100 % both for electron-rich and (relatively) electron-poor hydroquinones. Hydroquinones bearing carbonyl-groups were unreactive. Interestingly, Cu/AlO(OH) could further facilitate the 2,5-diamination of benzoquinone allowing the formation of complex products in high yield as was demonstrated by the simple one-step synthesis of an Alzheimer's disease drug candidate (Scheme 2-15). Catechol was not oxidized.

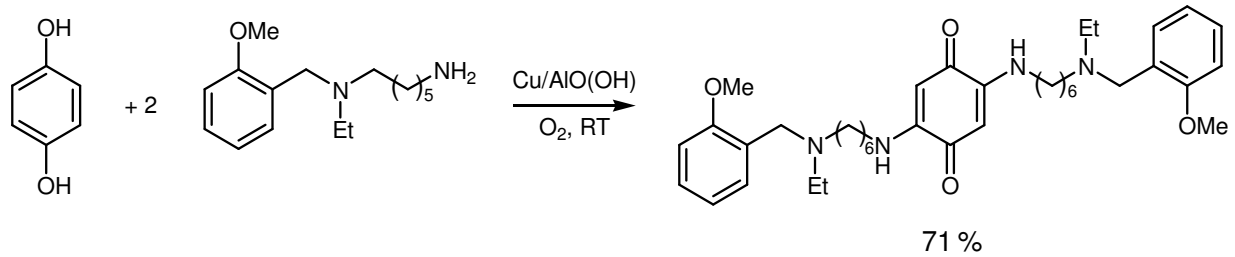

Scheme 2-15: Combined oxidation and amination of hydroquinone for the synthesis of a complex drug candidate [216].

Using H_2O_2 as an oxidant also no catechol reaction was observed on different Cu-MCM-41 catalysts [220] while $Cu(OH)_2/SiO_2$ overoxidized catechol in the presence of a base and H_2O_2 to *α*-hydro-*β*-hydroxymuco-*γ*-lactone also at room temperature (entry 5) [217]. Two publications deal with the state of Cu in (nano)particles oxidizing 2,3,5-trimethyl benzoquinone with molecular oxygen (entry 6 and 7a/b) [55, 57]. It was found that Cu_2O was necessary for catalytic activity. This entails that the catalysts are sensitive to air over a longer period of time where the oxidation of Cu_2O to inactive CuO was observed. Yermakov *et al.* [55] further described a very interesting effect where the initial catalytic activity of $Cu/Cu_2O/CuO$ particles could be enhanced by a preceding treatment in a magnetic field (entry 7a and 7b). Though not catalytically active, CuO was necessary in minor amounts as its paramagnetic properties were necessary for the magnetic response. Too high CuO concentrations prevented the response to the magnetic field.

Contrary to Cu, far less publications deal with heterogeneous Au and Ag catalysts. Gold nanoparticles are often found to be active in the electrooxidation of hydroquinone [221] but the field of electrocatalysis is beyond the scope of this overview. In a recent publication, bulk silver oxide was used as a catalyst at room temperature with H_2O_2 with a TOF of e.g. 14 h^{-1} for hydroquinone (entry 8), which is very reasonable for the activity of a bulk material. No leaching was reported. The catalyst was highly selective (>95 %) both for electron-poor and -rich hydroquinones. Preliminary studies showed that Ag_2O is also effective with oxygen at room temperature the reaction rates being of course slower. It was proposed by the authors that hydroquinone is oxidized by silver(I) oxide. Metallic silver is then reoxidized by the oxidant. Such a redox system would be promising: supported ionic silver can be used as stoichiometric yet expensive oxidant in various organic transformations [222-224]. Compared to the described silver catalyst, gold nanoparticles stabilized in a polystyrene-based matrix [219] exhibited improved performance using oxygen instead of H_2O_2 with TOFs being around an order of magnitude higher (115 h^{-1} [entry 9] compared to 14 h^{-1}). Substoichiometric amounts of base were necessary to oxidize electron-poor hydroquinones. The disadvantage from an environmental point of view compared to the silver catalyst was the necessity of using chlorinated solvents for a high selectivity. An even higher catalytic activity as for gold was observed for Pt particles under very similar conditions by the same group with TOFs for hydroquinone of up to 400 h^{-1} [225].

2.3.8 Oxidation of sulfides

There are only very few examples of heterogeneous coinage metal catalysts oxidizing thioethers to sulfoxides and sulfones yet quite a number of homogeneous catalysts exist. A silver salt of the polyoxometalate $Ag_5PV_2Mo_{10}O_{40}$ frequently used in oxidation catalysis was reported to be active as a heterogeneous catalyst in the oxidation of 2-chloroethyl ethyl sulfide (a model compound for mustard gas) with ambient air at room temperature (Scheme 2-16) [226]. The activity of the truly heterogeneous catalyst was ascribed to an interaction of redox active Ag and V. In this study, also homogeneously dissolved $AgNO_3$ catalyzed the ambient oxidation. The same group published an example for a highly active homogeneous Au(III) catalyst [227] for which further examples exist [228]. Homogeneous Cu complexes were also reported to oxidize thioethers with molecular oxygen (e.g. [229]) or H_2O_2 (potentially enantioselectively [230, 231]). Immobilized analogous Cu complexes were further reported [232, 233], however, examples of "classical" heterogeneous Cu catalysts for sulfide oxidation are rare and limited in scope (e.g. aqueous H_2S with Cu/carbon [234]). This and the high amount of potent homogeneous catalysts leave substantial potential for further research.

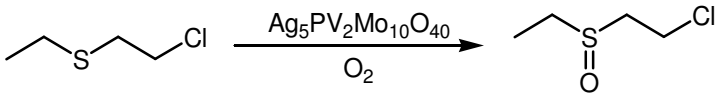

Scheme 2-16: Oxidation of 2-chloroethyl ethylsulfide [226]**.**

2.3.9 Oxidation of silanes

The oxidation of silanes to silanols over supported Ag and Au catalysts has been reported only recently (Table 2-9). Mitsudome *et al.* tested Ag and Au nanoparticles on various supports (e.g. TiO_2, SiO_2 and Al_2O_3) for the oxidation of silanes [87, 235]. Hydroxyapatite turned out to be the best support material both for Ag and Au. The oxidation with water as oxidant and solvent had various advantages also including facile product separation. Both catalysts exhibited selectivities exceeding 99 %, so virtually no disiloxane usually being a common byproduct in silane oxidation could be found. While gold was identified to be the most universal catalyst oxidizing both aliphatic (Table 2-9, entry 1a) and aromatic silanes (Table 2-9, entry 1b), silver was selective only to aromatic silanes (entry 2a, Scheme 2-17). The selectivity was ascribed to the aromatic moiety being necessary for binding of the substrate to the silver particles. Silver was more active than gold catalyzing the reaction already at room temperature (entry 2b) and -40 °C. The maximum TONs of 1600 were superior to other homogeneous and heterogeneous systems. The high activity in the oxidation of aliphatic silanes is not a

Table 2-9: Oxidation of silanes with water.

Entry	Catalyst	Substrate	Product	Solvent	T (°C)	Rct. time (h)	Conversion	Selectivity	TOF (h^{-1})	Reference
1a	Au/HAP	Et_3SiH	Et_3SiOH	H_2O	80	2	>99%	>99%	60	[235]
1b	Au/HAP	Me_2PhSi	$Me_2PhSiOH$	H_2O	80	2	>99%	>99%	40	[235]
2a	Ag/HAP	Me_2PhSiH	$Me_2PhSiOH$	H_2O	80	0.25	99%	>99%	130	[87]
2b	Ag/HAP	Me_2PhSiH	$Me_2PhSiOH$	H_2O	RT	1.5	99%	>99%	22	[87]
3	Pt-nanoclusters	Me_2PhSiH	$Me_2PhSiOH$	THF	RT	5	95%[a]	-	200	[236]

[a]Isolated yield.

feature unique to gold. Though the use of THF was necessary, Pt nanoparticles in PHMS (poly(methylhydro)siloxane) were found to be as universal as gold at significantly higher reaction rates than silver also using water as an oxidant (entry 3a and 3b) and equally high selectivities [236]. Cu is principally also a feasible catalyst material. Dissolved Cu salts catalyzed the aerobic oxidation *via* a Cu(II)/Cu(I) redox cycle [237, 238]. Reoxidation of Cu(I) with molecular oxygen is facilitated by the higher stability of Cu(II) in complexes which would also be an important design parameter for heterogeneous catalysts.

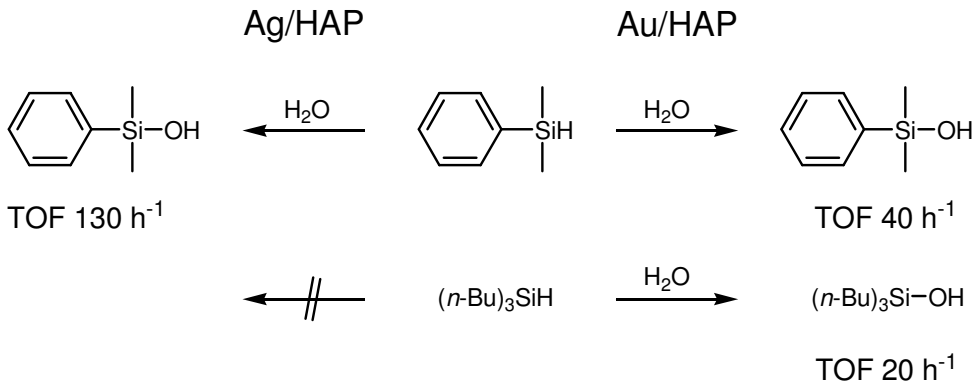

Scheme 2-17: Oxidation of aliphatic and aromatic silanes over Ag/HAP [87] and Au/HAP [235].

2.4 Strengths and opportunities of coinage metals as oxidation catalysts

A great deal of the success of gold is certainly connected to the high effort which was put in this field of research. Simple synthesis methods like impregnation are hardly used and achieve poor dispersions [200]. Hence, newly developed more sophisticated synthesis strategies [24] allow tuning of the Au nanoparticles size [239]. This can also be a disadvantage: in addition to the high raw material costs of Au, more sophisticated methods are also more expensive. On the contrary, Cu combines low cost of the metal with a high efficacy of simple synthesis methods like ion-exchange and coprecipitation. This way also mixed oxides are easily accessible. Due to the often high importance of isolated sites, optimal catalyst loadings can be very low. Silver lies somewhere between these two; though many metallic silver catalysts studied in the open literature were prepared by impregnation, more elaborate techniques usually afforded better catalysts. Potentially due to sintering, calcination times should be chosen with care for silver catalysts [71]. Calcination in air is apparently

Table 2-10: Oxidation reactions catalyzed by different catalyst types (*cf.* Figure 2-1) prepared from the coinage metals. Note that the classification of catalysts described by the reviewed literature was not unambiguously possible in some cases.

	metallic (nano)particles	oxidic (nano)particles	subsurface-mod. metals	(homo)disperse ions	mixed oxides	MOFs
Anaerobic alcohol oxidation	**Cu** **Ag**		**Ag**			
Aerobic alcohol oxidation	**Ag** **Au**	**Cu**	**Ag**	**Ag**	**Cu**	
Epoxidation	**Ag** **Au**	**Cu**		**Cu** **Ag**	(**Cu**)	**Cu**
Allylic oxidation	**Au** **Ag**	**Cu**		**Cu** **Ag**	(**Cu**)	**Cu**
Side-chain oxidation of alkyl aromatic compounds	**Ag** (**Au**)	**Cu** **Ag**		**Cu**	**Cu**	**Cu**
Cyclohexane oxidation	**Ag** **Au**	**Cu**		**Cu** **Ag**	**Cu**	
Hydroxylation of aromatics		**Cu**		**Cu** (**Ag**)		
Amine oxidation	**Au**					
Hydroquinone oxidation	**Au**	**Cu** **Ag**		(**Cu**)		**Cu**
Sulfide oxidation				**Ag**		
Silane oxidation	**Ag** **Au**					

an important activation step as silver-oxygen species are formed [73, 74]. As outlined in section 2.2, different catalyst types exist depending e.g. on the oxidation state of the metal. Table 2-10 gives an overview over the reactivities of the different catalyst types emphasizing that – except for alcohol oxidation – the structural difference between gold and copper is big, gold being metallic and copper in the most cases ionic during the oxidation reaction. This causes a significant difference in reactivity. Both Cu and Au catalysts apparently feature areas where they are dominating. For gold, this would e.g. be the aerobic oxidation of alcohols offering high selectivity and often good reusability while the capability of Cu to generate hydroxyl radicals [170] make it a preferred catalyst material for benzene hydroxylation. Also the other oxidation reactions described here appear to be dominated by either of the two metals. Silver is less often considered and shows its potential only occasionally but often with respectable results; e.g. in the aerobic oxidation of alcohols, similar activities compared to Au reference catalysts were obtained [71, 86].

2.4.1 Catalysis by gold

In selected cases, impressive results were reported with Au catalysts. High selectivities with Au catalysts were obtained, i.e. especially overoxidation products like carboxylic acids and esters in alcohol oxidation were formed in low amounts and often gold catalysts provide excellent reusability. A noteworthy feature of gold is also its capability to oxidize polyols [5] which to the best of the author's knowledge has not yet been achieved over Cu and Ag catalysts in the liquid phase. Similar to alcohol oxidation, amine oxidation is dominated by gold catalysts though – especially in contrast to alcohols – still rather high reaction temperatures and low TOFs were obtained for benzylic amines leaving substantial potential for this rather young field of research – also for Cu and Ag catalysts. Gold plays an outstanding role for epoxidation reactions where employing oxygen is difficult: few examples of gold catalysts were reported being intriguing from an academic point of view but exhibiting only low selectivities in styrene epoxidation [129]. Cyclohexene epoxidation was conducted with great success in two studies from the group of Hutchings [120, 121] while other groups mainly reported the formation of allylic oxidation products [122]. The reasons for this difference are poorly understood and more fundamental studies are required to exploit the potential of the aerobic epoxidation over gold.

Styrene epoxidations with TBHP were also intensively investigated by the group of Choudhary [134-138, 240] giving solid but not overly impressive results in terms of activity and selectivity. It should also be added that styrene oligomerization was not taken into account and therefore these studies need

to be taken with care. Au catalysts are also effective in hydroquinone and silane oxidation where Au acts as a universal catalyst in contrast to silver. In these oxidation reactions, benzyl alcohol, cyclohexene, styrene etc. are used as model substrates demonstrating the general applicability of the investigated catalysts for the synthesis of potentially more complex fine chemicals. The oxidation of a number of hydrocarbons, on the contrary, is of immediate industrial importance for the production of oxygenated commodity chemicals. Due to its high price, the use of gold is only justifiable when outstanding selectivities and activities are obtained – considering especially that hydrocarbon functionalization is a domain of inexpensive Co catalysts [241]. Partly implied by the small amount of reports, gold features only low efficacy for a number of relevant reactions, i.e. benzene hydroxylation with H_2O_2, side-chain oxidation of alkyl aromatic compounds (Au/SiO_2 was found to be catalytically inactive [155]) and potentially also cyclohexane oxidation. In the latter case, TOFs exceeding 100,000 h^{-1} (blind test resulting in 0 % conversion at 150 °C!) [164-166] need to be seen alongside with the fact that unpassivated autoclave steel can afford similar conversions [156]. Furthermore at low reaction temperatures, only low activities of Au were observed and additionally a radical initiator was necessary, the reaction clearly following a radical autoxidation mechanism [159]. Further studies with accurate product determination are necessary to clarify this point.

2.4.2 Catalysis by copper

In contrast to gold, the use of copper catalyst for the synthesis of commodity chemicals appears more reasonable from an economic point of view and thus many Cu catalysts exist for benzene hydroxylation with H_2O_2. In many cases, isolated Cu species appear to be the species resulting in the highest catalytic activity for this reaction. EPR investigations on copper complexes suggest that this is due to the specific interaction of ionic copper with peroxides generating oxygen centered radical species [168-171]. TOFs obtained for hydroxylation differ greatly being in the one-digit area and up to around 100 h^{-1}. Strong solvent effects were observed in many cases which might be connected to an unfavorable side-oxidation of the ACN solvent [180]. Interesting from an academic point of view is the possibility to use oxygen in combination with ascorbic acid [28, 29, 50, 187]. Hydroxyl radicals are suggested to be the hydroxylating species indirectly generated from reaction of Cu(I) with molecular oxygen. Though reaction rates were very low compared to other examples, it is remarkable that Cu mediates benzene hydroxylation even at room temperature. Indeed in combination with V, quite impressive conversions were obtained with this approach [188]. There are also Cu catalysts which were investigated for cyclohexane oxidation under aerobic conditions and especially Cu-ZSM-5 [27] showed good activity. Still, these studies should be

extended to industrial conditions and compared to Au catalysts and dissolved Co. This catalyst might also be suitable for the aerobic oxidation of alkyl aromatic compounds and *vice versa*. Especially $CuFe/Al_2O_3$ gave promising results for toluene oxidation though under harsh reaction conditions [150]. Most other Cu catalysts for the oxidation of cyclohexane and alkylaromatic compounds used H_2O_2 and TBHP, respectively. Due to the ring hydroxylation activity of Cu this can be problematic (as described previously) but also high cost for the oxidant for the production of commodity chemicals – given that these reaction can be carried out with oxygen – make the use of H_2O_2 and TBHP unattractive. Additionally, the employment of peroxides limits the maximal applicable temperature due to unselective decomposition above ~ 80 °C making breakage of rather inert C-H bonds difficult. It is therefore not surprising that TOFs are low with peroxides. Still, the ability of these Cu catalysts to interact with TBHP or H_2O_2 might make them suitable candidates for epoxidation reactions. Though mostly catalysts with CuO particles were used, isolated Cu centers (as used for many other oxidation reactions) also appear to be suitable catalysts for epoxidation reactions as they appear in MOFs [42, 127]. CuO/Ga_2O_3 [48] was also found to be an effective catalyst for styrene epoxidation with TBHP (even better than Au catalysts) but leaching studies were unfortunately not reported. Since styrene oligomerization was not taken into account, however, a final conclusion cannot be drawn. $Cu_2(OH)PO_4$ as an example for Cu phosphates also oxidized styrene under aerobic conditions [60] though the selectivity was low. Cu phosphates are in general good oxidation catalysts (useful e.g. also in benzene hydroxylation [59]) which might be due to isolation of the Cu ions by interjacent phosphate groups. Cu catalysts are also suitable for hydroquinone oxidation with oxygen; a good example being Cu/Al(OH) giving full conversion under mild conditions already at room temperature [216]. $Cu_3(BTC)_2$ also exhibited high TOFs [214]. Though for hydroquinone oxidation a gold catalyst gave the highest TOFs [219], the necessity of chloroform makes this approach less attractive favoring Cu catalysts especially when taking – once more – the difference in price into account. As outlined before, alcohol oxidation is certainly a reaction where gold is highly suitable – under aerobic conditions. Cu affects alcohol oxidation under anaerobic conditions and among the oxidation reaction this also the only reaction where metallic copper is the active phase. Therefore, alcohol oxidation is in principal the reaction where the three metals are most comparable. This reaction requires high temperatures and the reaction rates are usually significantly lower than in aerobic alcohol oxidation. Cu (and also Ag, *vide infra*) should thus not be seen as competitors but rather as a complementary tool to aerobic alcohol oxidation catalyzed by Au (or Pt-group metals): oxygen-free conditions are safer to handle, aldehydes which are highly prone to overoxidation can be synthesized with high selectivities (e.g. octanal [51]) and most importantely

different chemoselectivities can be obtained with Cu catalysts [52, 100]. Also Pd catalysts catalyze the anaerobic oxidation of alcohols but both rapid poisoning by CO [114] and the hydrogenation activity of Pd (giving e.g. toluene from benzyl alcohol) were observed as a problem. The hydrogen remaining in the system also offers opportunities – thus, Cu catalysts can also catalyze isomerization reactions under anaerobic, acceptor-free conditions [101]. On a mechanistic level (Scheme 2-18), alcohol oxidation on e.g. palladium catalysts [114] is assumed to occur *via* a dehydrogenation mechanism [7] where the O-H bond is broken upon adsorption followed by *β*-C-H bond scission affording the carbonyl compound. Oxygen (or another hydrogen acceptor) regenerates the metallic surface either by removal of hydrogen or oxidative cleansing of the metal surface from adsorpt catalyst poisons like CO. Pre-adsorpt oxygen may facilitate breaking of O-H bonds [242, 243] which can also be supported by bases as often necessary for the Au catalyzed alcohol oxidation [7]. This may be the reason why anaerobic alcohol oxidation has not been described over gold catalysts so far. Both for Au [244] and for Ag [67] a positively polarized transition state was proposed. Since alcohol oxidation proceeds over Cu (and Ag) in the absence of an oxidant, this also makes the dehydrogenation mechanism likely. From high-vacuum experiments it is known that alcohol oxidation proceeds both on clean Cu and Ag surfaces without pre-adsorbed oxygen though in the case of Ag with a higher activation energy [10, 245].

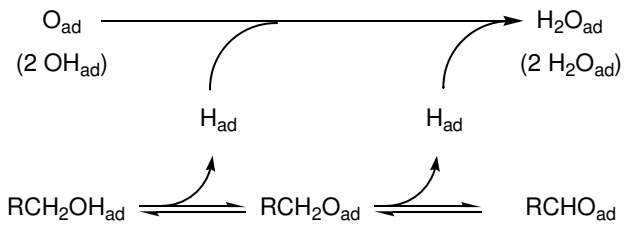

Scheme 2-18: Schematic alcohol dehydrogenation mechanism [7], reproduced with permission from the American Chemical Society © 2004.

2.4.3 Catalysis by silver

Ag is also active under anaerobic conditions [86]. In contrast to Cu, no hydrogenation activity was observed thus double bonds in alcohols remained untouched: only the C-O bond was oxidized in cinnamic alcohol. An important design parameter for active Ag catalysts appears to be the abundance of both acidic and basic sites on the support [67] but in general studies shedding light into reaction mechanisms are still scarce both for Cu and Ag catalysts. Contrary to Cu, supported Ag particles are also active in aerobic alcohol oxidation. Given that there are only few studies with Ag, the activity of Ag/SiO_2

prepared by both impregnation [71] and flame-spray pyrolysis [90] comparable to Au reference catalysts is promising. Also aliphatic alcohols were oxidized with high activity, and TOFs as a high as 6000 h^{-1} were reported with Ag/HT for benzyl alcohol oxidation (though this may be overestimated given the very low reported silver loading) [86]. *γ*-O species may be important during alcohol oxidation [67-69, 71] though the Ag/HT catalyst was prepared under conditions were *γ*-O was not formed. When used for silane oxidation, silver exhibited a high chemoselectivity to aromatic silanes. The aryl moiety was necessary for adsorption of the substrate and therefore it would be interesting to see whether the high chemoselectivity prevails for molecules bearing both aromatic and aliphatic silane groups. Silver in combination with peroxides is useful for styrene epoxidation but as previously described, many publications did not consider styrene oligomerization. Noticeably, argon atmosphere is required in some cases as oxygen can inhibit product formation. Two epoxidation catalysts in connection with Ag are especially noteworthy; one example employing metallic silver particles can epoxidize cyclohexene with (considering aerobic conditions) remarkable selectivities of 50 % to the epoxide [92] but harsh reaction conditions and rapid catalyst deactivation also limit the scope of this reaction. By making the concession of using activated oxygen in the form of H_2O_2 very attractive results were obtained: silver supported on TiO_2-SiO_2 was reactive in water as a solvent with very high selectivities (90 % and more) at the price of using microwave irradiation [79]. This underlines the great potential of silver in selected cases. Note that the support alone gave considerably lower conversions at high selectivity so there might be a specific synergistic interaction between Ag particles and Ti sites though this was not investigated. Note additionally that other catalysts required more expensive TBHP as epoxidizing agent. Silver catalysts are also useful in the aerobic oxidation of cyclohexane and alkyl aromatic compounds; especially in the latter case high TOFs were obtained for *p*-xylene and ethylbenzene oxidation with Ag supported on CeO_2-SiO_2 [91] though the catalyst activity was still no-where near the industrial catalyst. Massive leaching was encountered with impregnated catalysts; flame-spray pyrolysis as an alternative synthesis technique gave more stable catalysts [91]. The capability of Ag to form peroxides from alkyl aromatic compounds would also allow epoxidation reactions as proposed by ref. [124]. Within silver catalysis, special attention has to be drawn to Ag-V materials which are very universal catalysts catalyzing alcohol oxidation [94], sulfide oxidation [226], epoxidation [92], benzene hydroxylation [188] and cyclohexane oxidation [167], the latter with high selectivity to oxygenated products even under harsh reaction conditions. For comparison, the prominently used Co/Mn/Br oxidation system afforded mainly carbon oxides. Both catalysts with metallic and oxidic silver can be synthesized (though the oxidation state under reaction conditions has not yet been investigated). Silver has recently found an application as

hydroquinone oxidation catalyst with H_2O_2 [218] (while other catalysts can employ oxygen) demonstrating its principal suitability for this reaction. Amine oxidation certainly is also a field of interest for silver catalysts though silver appears to be especially promising in alcohol oxidation and epoxidation reactions.

2.4.4 Cascade reactions

Combining two reaction steps (or more) to one step simplifies the production of target compounds, can potentially result in higher yields and is therefore a field of research which has started to attract attention resulting in an increasing amount of literature [246-249]. Therefore, materials catalyzing multistep cascade reactions need to be multifunctional. Bifunctionality is e.g. given where a redox active noble metal is combined with a basic [249] or acidic [250] support. Additionally (and probably more problematic), the reaction conditions need to be adjusted to suit both reactions. This compromise may prevent the combination of the two most reactive catalysts for one reaction and is therefore a true chance for catalysts with apparently lower efficacy active under different reaction conditions. Examples for cascade reactions can also be found for the coinage metals. An example for gold was reported for epoxidation [124] where in a first step cumene was oxidized by Au/CeO_2 to cumene hydroperoxide which epoxidized olefins over Ti-MCM-41 also present in the reaction system (thus combining two catalysts rather than having a bifunctional catalyst). For the first step, the activation of cumene is crucial which can also be facilitated by copper [150] and silver [91] catalysts. Also other alkyl aromatic compounds might be applicable resulting in more useful byproducts compared to α,α-dimethylbenzyl alcohol obtained from cumene. Since additionally silver supported on SiO_2 is a suitable catalyst [91], an $Ag/Ti\text{-}SiO_2$ catalyst could provide true bifunctionality for both reaction steps. Cu catalysts for the anaerobic alcohol oxidation can conduct two reaction steps concomitantly as was shown for carveol [100] being principally an isomerization reaction. Based on this principle, the amination of alcohols over CuAl-HT also gave good results, running through the steps alcohol dehydrogenation – imine formation – imine hydrogenation [102]. Due to the lack of hydrogenation activity [86] similar reactions on silver catalysts under anaerobic conditions seem unlikely. (Di)amination was also successfully achieved during hydroquinone oxidation [216] resulting in highly functionalized reaction products. Memoquin (a drug candidate) could be synthesized in 71 % yield compared to 17 % from the conventional synthesis. A prerequisite for this reaction is a good chemoselectivity of the catalyst for hydroquinone oxidation leaving the amine group untouched.

2.4.5 Catalyst deactivation

During oxidation of organic substrates, suitable ligands like carboxylic acids are formed. Leaching of the active species is therefore a common deactivation pathway for copper catalysts, especially where Cu_xO particles are present (Scheme 2-19) [37, 172, 173, 178]. Since these species are often not necessary from a catalytic point of view, an optimized catalyst synthesis offers a good opportunity for circumventing at least strong leaching. Catalysts with both isolated Cu species and Cu_xO particles may exhibit significant leaching problems only during the first catalytic run after which the catalyst is stable [139, 177]. Therefore, undesired Cu_xO could be removed by a suitable pretreatment procedure preceding the first use as catalyst. In some cases Al [38] and potentially also Fe [150] may stabilize the Cu species against leaching. Leaching studies may be further complicated since leached Cu can precipitate again as Cu_2O resulting in an apparently underestimated leaching [43]. On the other hand, reduced copper catalysts used in anaerobic oxidation often show good reusability indicating low leaching.

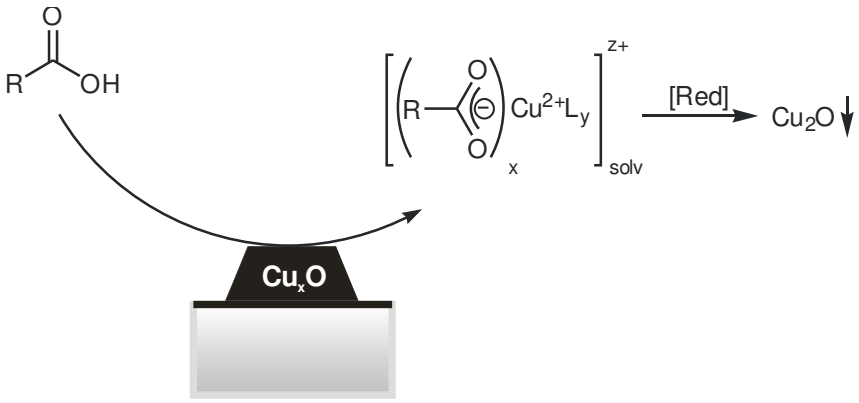

Scheme 2-19: Simplified leaching process of oxidized copper particles.

Also ionic silver has been observed to be prone to strong leaching and catalyst deactivation [79]. On the contrary, catalysts with reduced silver were highly reusable in some cases [86, 87, 144]. For other catalysts with metallic silver, *γ*-O species appear to be connected to the catalytic activity [69]. (Partial) Reactivation of the catalysts could be achieved *via* calcination in air (known to generate these species) which may indicate that removal of *γ*-O is a deactivation pathway for silver [67, 71]. Of course, calcination affects the catalyst in many ways and therefore a straightforward connection to *γ*-O is not given. Strongly adsorbed species may also be removed. Additionally, some silver catalysts were highly active without a *γ*-O forming treatment. Benzaldehyde and water were shown to deactivate silver catalysts during aerobic alcohol oxidation [71] though in other cases water was also successfully used as a solvent [107]. Little is known about other adsorbing species; typical adsorbates causing deactivation

on Au catalysts are (bi)carbonates and formates [251-253] (observed during CO oxidation) and especially sulfur containing compounds in liquid phase oxidations [254, 255]. With respect to the widely discussed use of pressurized CO_2 as "green" solvent, the strong adsorption of carbonates on silver surfaces obtained from reaction of CO_2 with an oxygen pre-covered metallic silver surface [256] might hamper future applications in this field. The carbonates require a temperature of ca. 200 °C to decompose. Sintering is usually not considered in liquid phase reactions due to the low reaction temperatures. Given the low melting point of small silver nanoparticles [78], this might however also be a potential deactivation pathway. In general, however, good reusabilites are often reported so that a strongly deactivating catalyst will rather be replaced by a more robust material than improved for a higher stability. Also for this reason studies concerning deactivation mechanisms are rare.

2.4.6 (Some) opportunities for further research

This overview concentrated on summarizing the catalytic activities obtained with coinage metal catalysts. In many cases the underlying mechanisms are poorly understood and there is a need for more e.g. *in situ* studies. The catalysis chemistry of ionic copper in combination with peroxides (and also oxygen) is generally accepted to be based on oxygen centered radicals [169-171] and therefore appears to be limited to radical-mediated oxidation reactions. As an example, H_2O_2 in combination with Cu liberates ·OH radicals which can oxidize benzene and cyclohexane but are undesirable in epoxidation reactions where peroxy radicals may be necessary. Systems consisting of oxidized Cu catalysts and molecular oxygen also activated C-H bonds which can be useful in e.g. epoxidation (*cf.* Scheme 2-10) still being a very challenging oxidation reaction. While ionic copper is usually most active as isolated species, metallic copper behaves very different. The finding that this species catalyzes the alcohol dehydrogenation apparently without being poisoned (unlike Pd [7]) is promising and may be further investigated by optimizing catalyst synthesis techniques. The simultaneous hydrogenation activity may be exploited to plan the synthesis of more complex substrates. Metallic Cu might furthermore be applicable in (anaerobic) amine oxidation and also the oxidation of silanes with water generating hydrogen as a byproduct is a worthwhile investigation. The limitation of metallic copper is its strong susceptibility to oxidation with oxygen. Metallic silver is more stable towards oxidation and can also catalyze the anaerobic alcohol oxidation though without exhibiting hydrogenation activity. Understanding the influence of subsurface oxygen species on the activity in liquid phase oxidations might lead to more active and/or more stable catalysts. Considering that there are only a handful of

publications on alcohol oxidation with silver catalysts, similar outstanding results as with gold catalysts might be seen, potentially also for e.g. amine oxidation where silver catalysts – to the best of the author's knowledge – are not yet investigated. Silver catalysts also performed well in the epoxidation of styrene with H_2O_2 [79] and thus featured an interesting synergism with Ti-doped SiO_2 used as the support, which needs to be further exploited. Such a material should also catalyze the epoxidation as proposed by Aprile *et al.* [124] with an alkyl aromatic compound being simultaneously oxidized. The wealth of knowledge on dopants for silver catalysts from gas phase catalysis might additionally be helpful for improving the performance of silver catalysts. From the viewpoint of "Green Chemistry", the capability of gold to catalyze the epoxidation with molecular oxygen only is certainly intriguing and may have enormous potential. Since the epoxidation activity of gold is apparently no intrinsic feature, more fundamental understanding is necessary in order to exploit this epoxidation strategy. Alvaro *et al.* made an interesting start in this field showing that organo-gold species form upon trapping of azobis(isobutyrnitrile) derived radicals [257]. Note that silver also exhibited epoxidation activity with oxygen only [92], though the strong deactivation of the catalyst might hinder further research.

2.5 Conclusions and outlook

Among the coinage metals gold catalysts are without a doubt dominating within many oxidation reactions, especially concerning fine chemicals e.g. in alcohol or amine oxidation. Still, silver and copper showed in this chapter that they are capable of catalyzing the same reactions: both for alcohol oxidation and for epoxidation reactions good results were achieved. More research for better Ag and Cu catalysts will certainly be fruitful in the future. Hydroquinone, silane and amine oxidations (and also sulfide oxidation) are not yet excessively investigated. Good activity was obtained with gold catalysts but Cu and Ag catalysts also showed promising results but there is still great potential for new discoveries. When it comes to oxidation reactions where the primary role of the heterogeneous catalyst is likely that of a radical initiator, i.e. cyclohexane, alkyl aromatics and benzene oxidation, gold catalysts were rarely used with great success; especially the high TOFs reported in some papers need to be evaluated with care as the product analysis is very challenging and gold simply acts as a radical initiator. For these reactions, a higher number of Cu and Ag catalysts exist though (except for benzene hydroxylation) Co catalysts in general give the best results. The strength of the two lighter coinage metals as a catalyst material is – apart from the low price compared to other noble metals used for oxidation reactions – the specific (chemo)selectivity which was reported e.g. for the anaerobic alcohol oxidation with copper or

the epoxidation of styrene with H_2O_2 and the silane oxidation over silver catalysts. A prerequisite for obtaining good catalytic activity is of course a target-oriented synthesis of a catalyst for which some guidelines were compiled. It was the intention of this overview to show where potential is hidden for the development of new catalyst materials and processes. More fundamental mechanistic studies are needed in order to further understand the catalytic processes, limitations and deactivation pathways as was briefly discussed; as an example, one deactivation pathway investigated intensively for Cu is leaching. Moreover, examples for the use of supercritical solvents, especially CO_2, and alloying of the coinage metals with focus on Ag und Cu has not yet been approached intensively and will offer further opportunities. There is still much potential and therefore the coinage metals are certainly a valuable tool in oxidation catalysis and will contribute to establishing greener and sustainable catalytic processes.

2.6 References

[1] M. Haruta, T. Kobayashi, H. Sano, N. Yamada, Chem. Lett. (1987) 405.

[2] M. Haruta, N. Yamada, T. Kobayashi, S. Iijima, J. Catal. 115 (1989) 301.

[3] M. Haruta, S. Tsubota, T. Kobayashi, H. Kageyama, M.J. Genet, B. Delmon, J. Catal. 144 (1993) 175.

[4] Z. Li, S.G. Divakara, R.M. Richards, "Advanced nanomaterials", Wiley-VCH , Weinheim 2010, 333.

[5] A. Corma, H. Garcia, Chem. Soc. Rev. 37 (2008) 2096.

[6] C. Della Pina, E. Falletta, L. Prati, M. Rossi, Chem. Soc. Rev. 37 (2008) 2077.

[7] T. Mallat, A. Baiker, Chem. Rev. 104 (2004) 3037.

[8] T. Punniyamurthy, S. Velusamy, J. Iqbal, Chem. Rev. 105 (2005) 2329.

[9] R. Skouta, C. Li, Tetrahedron 64 (2008) 4917.

[10] X. Liu, R.J. Madix, C.M. Friend, Chem. Soc. Rev. 37 (2008) 2243.

[11] F. Ullmann, "Ullmann's encyclopedia of industrial chemistry", Wiley-VCH, Weinheim, 2003.

[12] Z.P. Qu, M.J. Cheng, W.X. Huang, X.H. Bao, J. Catal. 229 (2005) 446.

[13] Z.P. Qu, W.X. Huang, M.J. Cheng, X.H. Bao, J. Phys. Chem. B 109 (2005) 15842.

[14] L. Chen, D. Ma, X. Bao, J. Phys. Chem. C 111 (2007) 2229.

[15] H. Liu, D. Ma, R.A. Blackley, W. Zhou, X. Bao, Chem. Commun. (2008) 2677.

[16] A.W. Smith, J. Catal. 4 (1965) 172.

[17] G. Sedmak, S. Hocevar, J. Levec, J. Catal. 222 (2004) 87.

[18] C.S. Polster, H. Nair, C.D. Baertsch, J. Catal. 266 (2009) 308.

[19] A. Martinez-Arias, M. Fernandez-Garcia, O. Galvez, J.M. Coronado, J.A. Anderson, J.C. Conesa, J. Soria, G. Munuera, J. Catal. 195 (2000) 207.

[20] G. Doreau, E. Chornet, Water Pollut. Res. Can. 13 (1978) 21.

[21] X. Zhao, B. Zhang, K. Ai, G. Zhang, L. Cao, X. Liu, H. Sun, H. Wang, L. Lu, J. Mater. Chem. 19 (2009) 5547.

[22] H. Fei, D.L. Rogow, S.R.J. Oliver, J. Am. Chem. Soc. 132 (2010) 7202.

[23] L. Shang, B. Li, W. Dong, B. Chen, C. Li, W. Tang, G. Wang, J. Wu, Y. Ying, J. Hazard. Mater. 178 (2010) 1109.

[24] M. Haruta, Gold Bull. 37 (2004) 27.

[25] X. Li, J. Xu, L. Zhou, F. Wang, J. Gao, C. Chen, J. Ning, H. Ma, Catal. Lett. 110 (2006) 149.

[26] S. Carloni, B. Frullanti, R. Maggi, A. Mazzacani, F. Bigi, G. Sartori, Tetrahedron Lett. 41 (2000) 8947.

[27] H.X. Yuan, Q.H. Xia, H.J. Zhan, X.H. Lu, K.X. Su, Appl. Catal. A 304 (2006) 178.

[28] T. Ohtani, S. Nishiyama, S. Tsuruya, M. Masai, Stud. Surf. Sci. Catal. 75 (1993) 1999.

[29] T. Ohtani, S. Nishiyama, S. Tsuruya, M. Masai, J. Catal. 155 (1995) 158.

[30] K. Sokmen, F. Sevin, J. Colloid Interface Sci. 264 (2003) 208.

[31] B.Y. Chou, J.L. Tsai, S.F. Cheng, Microporous Mesoporous Mat. 48 (2001) 309.

[32] J. Wang, G. Xia, Y. Yin, S.L. Suib, C.L.O. O'Young, J. Catal. 176 (1998) 275.

[33] K. Bahranowski, M. Gasior, A. Kielski, J. Podobinski, E.M. Serwicka, L.A. Vartikian, K. Wodnicka, Clay Miner. 34 (1999) 79.

[34] N.S. Figoli, H.R. Keselman, P.C. Largentiere, C.L. Lazzaroni, J. Catal. 77 (1982) 64.

[35] I.C. Chisem, J.S. Rafelt, J.H. Clark, Chem. Commun. (1997) 2203.

[36] A.N. Zakharov, N.S. Zefirov, Mendeleev Commun. (2005) 111.

[37] W.A. Carvalho, M. Wallau, U. Schuchardt, J. Mol. Catal. A 144 (1999) 91.

[38] C.L. Tsai, B. Chou, S. Cheng, J.F. Lee, Appl. Catal. A 208 (2001) 279.

[39] A. Gervasini, M. Manzoli, G. Martra, A. Ponti, N. Ravasio, L. Sordelli, F. Zaccheria, J. Phys. Chem. B 110 (2006) 7851.

[40] S. Hocevar, U.O. Krasovec, B. Orel, A.S. Arico, H. Kim, Appl. Catal. B 28 (2000) 113.

[41] X. Qi, J. Li, T. Ji, Y. Wang, L. Feng, Y. Zhu, X. Fan, C. Zhang, Micropor. Mesopor. Mater. 122 (2009) 36.

[42] K. Brown, S. Zolezzi, P. Aguirre, D. Venegas-Yazigi, V. Paredes-Garcia, R. Baggio, M.A. Novak, E. Spodine, Dalton Trans. (2009) 1422.

[43] H. Kanzaki, T. Kitamura, R. Hamada, S. Nishiyama, S. Tsuruya, J. Mol. Catal. A 208 (2004) 203.

[44] E. Jobson, A. Baiker, A. Wokaun, J. Chem. Soc. Faraday 86 (1990) 1131.

[45] J. Pan, C. Wang, S. Guo, J. Li, Z. Yang, Catal. Commun. 9 (2008) 176.

[46] T. Sakamoto, H. Yonehara, C. Pac, J. Org. Chem. 62 (1997) 3194.

[47] G. Tanarungsun, W. Kiatkittipong, P. Praserthdam, H. Yamada, T. Tagawa, S. Assabumrungrat, J. Ind. Eng. Chem. 14 (2008) 596.

[48] V.R. Choudhary, R. Jha, N.K. Chaudhari, P. Jana, Catal. Commun. 8 (2007) 1556.

[49] Q. Zhang, Q. Xia, X. Lu, H. Zhan, G. Xu, Ind. J. Chem. A 46 (2007) 909.

[50] J. Okamura, S. Nishiyama, S. Tsuruya, M. Masai, J. Mol. Catal. A 135 (1998) 133.

[51] R. Shi, F. Wang, X. Mu, Y. Li, X. Huang, W. Shen, Catal. Commun. 11 (2009) 306.

[52] T. Mitsudome, Y. Mikami, K. Ebata, T. Mizugaki, K. Jitsukawa, K. Kaneda, Chem. Commun. (2008) 4804.

[53] R. Shi, F. Wang, Tana, Y. Li, X. Huang, W. Shen, Green Chem. 12 (2010) 108.

[54] S. Vukojevic, O. Trapp, J.-D. Grunwaldt, C. Kiener, F. Schuth, Angew. Chem. Int. Ed. 44 (2005) 7978.

[55] A.Y. Yermakov, T.A. Feduschak, M.A. Uimin, A.A. Mysik, V.S. Gaviko, O.N. Chupakhin, A.B. Shishmakov, V.G. Kharchuk, L.A. Petrov, Y.A. Kotov, A.V. Vosmerikov, A.V. Korolyov, Solid State Ionics 172 (2004) 317.

[56] H. Tumma, N. Nagaraju, K.V. Reddy, J. Mol. Catal. A 310 (2009) 121.

[57] Y.R. Uhm, J.H. Park, W.W. Kim, M.K. Lee, C.K. Rhee, Mater. Sci. Eng. A A449-A451 (2007) 817.

[58] A. Dubey, S. Kannan, S. Velu, K. Suzuki, Appl. Catal. A 238 (2003) 319.

[59] F.S. Xiao, J.M. Sun, X.J. Meng, R.B. Yu, H.M. Yuan, J.N. Xu, T.Y. Song, D.Z. Jiang, R.R. Xu, J. Catal. 199 (2001) 273.

[60] X.J. Meng, K.F. Lin, X.Y. Yang, Z.H. Sun, D.Z. Jiang, F.S. Xiao, J. Catal. 218 (2003) 460.

[61] Q. Tang, X. Gong, P. Zhao, Y. Chen, Y. Yang, Appl. Catal. A 389 (2010) 101.

[62] R. Xu, D. Wang, J. Zhang, Y. Li, Chem. Asian. J. 1 (2006) 888.

[63] R. Jose Chimentao, F. Medina, J. Eduardo Sueiras, J.L. Garcia Fierro, Y. Cesteros, P. Salagre, J. Mater. Sci. 42 (2007) 3307.

[64] J.M. Campelo, D. Luna, R. Luque, J.M. Marinas, A.A. Romero, ChemSusChem 2 (2009) 18.

[65] W. Zhang, X. Qiao, J. Chen, Mater. Sci. Eng. B 142 (2007) 1.

[66] J. Du, D.J. Kang, Mater. Lett. 62 (2008) 3185.

[67] K. Shimizu, K. Sugino, K. Sawabe, A. Satsuma, Chem. Eur. J. 15 (2009) 2341.

[68] K. Shimizu, K. Ohshima, A. Satsuma, Chem. Eur. J. 15 (2009) 9977.

[69] L.F. Liotta, A.M. Venezia, G. Deganello, A. Longo, A. Martorana, Z. Schay, L. Guczi, Catal. Today 66 (2001) 271.

[70] S. Karski, I. Witonska, J. Rogowski, J. Goluchowska, J. Mol. Catal. A 240 (2005) 155.

[71] M.J. Beier, T.W. Hansen, J.-D. Grunwaldt, J. Catal. 266 (2009) 320.

[72] S. Bociorishvili, I. Manenti, F. Trifiro, Oxid. Commun. 4 (1983) 471.

[73] X. Bao, M. Muhler, B. Pettinger, R. Schlögl, G. Ertl, Catal. Lett. 22 (1993) 215.

[74] C. Rehren, M. Muhler, X. Bao, R. Schlögl, G. Ertl, Z. Phys. Chem. 174 (1991) 11.

[75] H. Schubert, U. Tegtmeyer, D. Herein, X. Bao, M. Muhler, R. Schlogl, Catal. Lett. 33 (1995) 305.

[76] D.S. Su, T. Jacob, T. Hansen, D. Wang, R. Schlögl, B. Freitag, S. Kujawa, Angew. Chem. Int. Ed. 47 (2008) 5005.

[77] A.J. Nagy, G. Mestl, D. Herein, G. Weinberg, E. Kitzelmann, F. Schlogl, J. Catal. 182 (1999) 417.

[78] O.A. Yeshchenko, I.M. Dmitruk, A.A. Alexeenko, A.V. Kotko, Nanotechnology 21 (2010) 045203/1.

[79] V. Purcar, D. Donescu, C. Petcu, R. Luque, D.J. Macquarrie, App. Catal. A 363 (2009) 122.

[80] H. Zhao, J.C. Zhou, H. Luo, C.Y. Zeng, D.H. Li, Y.J. Liu, Catal. Lett. 108 (2006) 49.

[81] R.J. Chimentao, I. Kirm, F. Medina, X. Rodriguez, Y. Cesteros, P. Salagre, J.E. Sueiras, J.L.G. Fierro, Appl. Surf. Sci. 252 (2005) 793.

[82] H. Tada, K. Suzuki, H. Kobayashi, Recent Res. Dev. Mater. Sci. 6 (2005) 1.

[83] G. Gao, D. Guo, C. Wang, H. Li, Electrochem. Commun. 9 (2007) 1582.

[84] S. Rakovsky, S. Nikolova, L. Dimitrov, L. Minchev, J. Ilkova, Oxidation Commun. 18 (1995) 407.

[85] J. Liu, F. Wang, Z. Gu, X. Xu, Chem. Eng. J. 151 (2009) 319.

[86] T. Mitsudome, Y. Mikami, H. Funai, T. Mizugaki, K. Jitsukawa, K. Kaneda, Angew. Chem. Int. Ed. 47 (2008) 138.

[87] T. Mitsudome, S. Arita, H. Mori, T. Mizugaki, K. Jitsukawa, K. Kaneda, Angew. Chem. Int. Ed. 47 (2008) 7938.

[88] G.A. Sotiriou, S.E. Pratsinis, Environ. Sci. Technol. 44 (2010) 5649.

[89] S. Hannemann, J.-D. Grunwaldt, F. Krumeich, P. Kappen, A. Baiker, Appl. Surf. Sci. 252 (2006) 7862.

[90] S. Mikkelsen, Bachelor Thesis, Technical University of Denmark 2009.

[91] M.J. Beier, B. Schimmoeller, T.W. Hansen, J.E.T. Andersen, S.E. Pratsinis, J.-D. Grunwaldt, J. Mol. Catal. A 331 (2010) 40.

[92] G. Maayan, R. Neumann, Chem. Commun. (2005) 4595.

[93] L. Pettersson, I. Andersson, A. Selling, J.H. Grate, Inorg. Chem. 33 (1994) 982.

[94] P. Nagaraju, M. Balaraju, K.M. Reddy, P.S. Sai Prasad, N. Lingaiah, Catal. Commun. 9 (2008) 1389.

[95] A.S.K. Hashmi, G.J. Hutchings, Angew. Chem. Int. Ed. 45 (2006) 7896.

[96] A. Abad, P. Concepcion, A. Corma, H. Garcia, Angew. Chem. Int. Edit. 44 (2005) 4066.

[97] D.I. Enache, D.W. Knight, G.J. Hutchings, Catal. Lett. 103 (2005) 43.

[98] P. Haider, A. Baiker, J. Catal. 248 (2007) 175.

[99] L.E. Schniepp, H.H. Geller, J. Am. Chem. Soc. 69 (1947) 1545.

[100] F. Zaccheria, N. Ravasio, R. Psaro, A. Fusi, Chem. Eur. J. 12 (2006) 6426.

[101] F. Zaccheria, N. Ravasio, R. Psaro, A. Fusi, Chem. Commun. (2005) 253.

[102] P.R. Likhar, R. Arundhathi, M.L. Kantam, P.S. Prathima, Eur. J. Org. Chem. (2009) 5383.

[103] S. Vijaikumar, T. Subramanian, K. Pitchumani, J. Nanomater. (2008) 257691.

[104] P.P. Hankare, P.D. Kamble, S.P. Maradur, M.R. Kadam, U.B. Sankpal, R.P. Patil, R.K. Nimat, P.D. Lokhande, J. Alloys Compd. 487 (2009) 730.

[105] V.R. Choudhary, D.K. Dumbre, B.S. Uphade, V.S. Narkhede, J. Mol. Catal. A 215 (2004) 129.

[106] M.L. Kantam, R. Arundhathi, P.R. Likhar, D. Damodara, Adv. Synth. Catal. 351 (2009) 2633.

[107] H. Kochkar, L. Lassalle, M. Morawietz, W.F. Holderich, J. Catal. 194 (2000) 343.

[108] A. Chrobok, S. Baj, W. Pudło, A. Jarzębski, Appl. Catal. A 389 (2010) 179.

[109] W. Fang, Q. Zhang, J. Chen, W. Deng, Y. Wang, Chem. Commun. 46 (2010) 1547.

[110] T. Mitsudome, A. Noujima, T. Mizugaki, K. Jitsukawa, K. Kaneda, Adv. Synth. Catal. 351 (2009) 1890.

[111] Y. Mikami, K. Ebata, T. Mitsudome, T. Mizugaki, K. Jitsukawa, K. Kaneda, Heterocycles 80 (2010) 855.

[112] R.L. Narayan, T.S. King, Thermochim. Acta 312 (1998) 105.

[113] C. Keresszegi, T. Burgi, T. Mallat, A. Baiker, J. Catal. 211 (2002) 244.

[114] C. Keresszegi, D. Ferri, T. Mallat, A. Baiker, J. Phys. Chem. B 109 (2005) 958.

[115] C. Rehren, G. Isaac, R. Schlögl, G. Ertl, Catal. Lett. 11 (1991) 253.

[116] B. Pettinger, X. Bao, I. Wilcock, M. Muhler, R. Schlögl, G. Ertl, Angew. Chem. Int. Edit. 33 (1994) 85.

[117] T. Ishida, M. Haruta, ChemSusChem 2 (2009) 538.

[118] L. Zhou, C.G. Freyschlag, B. Xu, C.M. Friend, R.J. Madix, Chem. Commun. 46 (2010) 704.

[119] B. Zhu, R.J. Angelici, Chem. Commun. (2007) 2157.

[120] S. Bawaked, N.F. Dummer, N. Dimitratos, D. Bethell, Q. He, C.J. Kiely, G.J. Hutchings, Green Chem. 11 (2009) 1037.

[121] M.D. Hughes, Y.J. Xu, P. Jenkins, P. McMorn, P. Landon, D.I. Enache, A.F. Carley, G.A. Attard, G.J. Hutchings, F. King, E.H. Stitt, P. Johnston, K. Griffin, C.J. Kiely, Nature 437 (2005) 1132.

[122] Z. Cai, M. Zhu, J. Chen, Y. Shen, J. Zhao, Y. Tang, X. Chen, Catal. Commun.12 (2010) 197.

[123] C.H.A. Tsang, Y. Liu, Z. Kang, D.D.D. Ma, N. Wong, S. Lee, Chem. Commun. (2009) 5829.

[124] C. Aprile, A. Corma, M.E. Domine, H. Garcia, C. Mitchell, J. Catal. 264 (2009) 44.

[125] J. Liu, F. Wang, X. Xu, Catal. Lett. 120 (2008) 106.

[126] T. Yamashita, D.L. Lu, J.N. Kondo, M. Hara, K. Domen, Chem. Lett. 32 (2003) 1034.

[127] C. Sposato, E. Janiszewska, A. Macario, S. Kowalak, G. Braccio, G. Giordano, Stud. Surf. Sci. Catal. 174B (2008) 1275.

[128] X. Meng, Z. Sun, R. Wang, S. Lin, J. Sun, M. Yang, K. Lin, D. Jiang, F. Xiao, Catal. Lett. 76 (2001) 105.

[129] M. Turner, V.B. Golovko, O.P.H. Vaughan, P. Abdulkin, A. Berenguer-Murcia, M.S. Tikhov, B.F.G. Johnson, R.M. Lambert, Nature 454 (2008) 981.

[130] P. Lignier, F. Morfin, L. Piccolo, J. Rousset, V. Caps, Catal. Today 122 (2007) 284.

[131] P. Lignier, F. Morfin, S. Mangematin, L. Massin, J. Rousset, V. Caps, Chem. Commun. (2007) 186.

[132] P. Lignier, S. Mangematin, F. Morfin, J. Rousset, V. Caps, Catal. Today 138 (2008) 50.

[133] P. Lignier, M. Comotti, F. Schueth, J. Rousset, V. Caps, Catal. Today 141 (2009) 355.

[134] N.S. Patil, B.S. Uphade, D.G. McCulloh, S.K. Bhargava, V.R. Choudhary, Catal. Commun. 5 (2004) 681.

[135] N.S. Patil, B.S. Uphade, P. Jana, R.S. Sonawane, S.K. Bhargava, V.R. Choudhary, Catal. Lett. 94 (2004) 89.

[136] N.S. Patil, B.S. Uphade, P. Jana, S.K. Bhargava, V.R. Choudhary, Chem. Lett. 33 (2004) 400.

[137] N.S. Patil, R. Jha, B.S. Uphade, S.K. Bhargava, V.R. Choudhary, Appl. Catal. A 275 (2004) 87.

[138] N.S. Patil, B.S. Uphade, P. Jana, S.K. Bharagava, V.R. Choudhary, J. Catal. 223 (2004) 236.

[139] X. Lu, Y. Yuan, Appl. Catal. A365 (2009) 180.

[140] Z. Chen, Q.M. Gao, D.M. Gao, Q.Y. Wei, M.L. Ruan, Mater. Lett. 60 (2006) 1816.

[141] J. Liu, F. Wang, Z. Gu, X. Xu, Catal. Commun. 10 (2009) 868.

[142] J.M. Campelo, T.D. Conesa, M.J. Gracia, M.J. Jurado, R. Luque, J.M. Marinas, A.A. Romero, Green Chem. 10 (2008) 853.

[143] V. Parvulescu, C. Anastasescu, B.L. Su, J. Mol. Catal. A 211 (2004) 143.

[144] T. Mitsudome, A. Noujima, Y. Mikami, T. Mizugaki, K. Jitsukawa, K. Kaneda, Angew. Chem. Int. Ed. 49 (2010) 5545.

[145] K. Ebitani, K. Nagashima, T. Mizugaki, K. Kaneda, Chem. Commun. (2000) 869.

[146] W. Partenheimer, Catal. Today 23 (1995) 69.

[147] K. Bahranowski, R. Dula, M. Gasior, M. Labanowska, A. Michalik, L.A. Vartikian, E.M. Serwicka, Appl. Clay. Sci. 18 (2001) 93.

[148] D. Kishore, A.E. Rodrigues, Catal. Commun. 10 (2009) 1212.

[149] A. Dhakshinamoorthy, M. Alvaro, H. Garcia, J. Catal. 267 (2009) 1.

[150] F. Wang, J. Xu, X.Q. Li, J. Gao, L.P. Zhou, R. Ohnishi, Adv. Synth. Catal. 347 (2005) 1987.

[151] G.R. Varma, W.F. Graydon, J. Catal. 28 (1973) 236.

[152] E.T. Denisov, E.V. Tumanov, Usp. Khim. 74 (2005) 905.

[153] J.H. Casemier, B.E. Nieuwenh, W.M. Sachtler, J. Catal. 29 (1973) 367.

[154] A.D. Vreugdenhil, J. Catal. 28 (1973) 493.

[155] N.H.A. Vanham, B.E. Nieuwenh, W.M. Sachtler, J. Catal. 20 (1971) 408.

[156] B.P.C. Hereijgers, B.M. Weckhuysen, J. Catal. 270 (2010) 16.

[157] U. Schuchardt, D. Cardoso, R. Sercheli, R. Pereira, R.S. de Cruz, M.C. Guerreiro, D. Mandelli, E.V. Spinace, E.L. Fires, Appl. Catal. A 211 (2001) 1.

[158] X. Quek, Q. Tang, S. Hu, Y. Yang, Appl. Catal. A 361 (2009) 130.

[159] Y.J. Xu, P. Landon, D. Enache, A. Carley, M. Roberts, G. Hutchings, Catal. Lett. 101 (2005) 175.

[160] R. Zhao, D. Ji, G.M. Lv, G. Qian, L. Yan, X.L. Wang, J.S. Suo, Chem. Commun. (2004) 904.

[161] L. Li, C. Jin, X. Wang, W. Ji, Y. Pan, T. van der Knaap, R. van der Stoel, C.T. Au, Catal. Lett. 129 (2009) 303.

[162] P. Wu, P. Bai, K.P. Loh, X.S. Zhao, Catal. Today 158 (2010) 220.

[163] G.M. Lu, R. Zhao, G. Qian, Y.X. Qi, X.L. Wang, J.S. Suo, Catal. Lett. 97 (2004) 115.

[164] L. Xu, C. He, M. Zhu, K. Wu, Y. Lai, Catal. Lett. 118 (2007) 248.

[165] L. Xu, C. He, M. Zhu, S. Fang, Catal. Lett. 114 (2007) 202.

[166] L. Xu, C. He, M. Zhu, K. Wu, Y. Lai, Catal. Commun. 9 (2008) 816.

[167] K.M.K. Yu, A. Abutaki, Y. Zhou, B. Yue, H.Y. He, S.C. Tsang, Catal. Lett. 113 (2007) 115.

[168] B.C. Gilbert, S. Silvester, P.H. Walton, J. Chem. Soc. Perkin 2 (1999) 1115.

[169] Q. Zhu, Y. Lian, S. Thyagarajan, S.E. Rokita, K.D. Karlin, N.V. Blough, J. Am. Chem. Soc. 130 (2008) 6304.

[170] T. Osako, S. Nagatomo, T. Kitagawa, C.J. Cramer, S. Itoh, J. Biol. Inorg. Chem. 10 (2005) 581.

[171] C.M. Jones, M.J. Burkitt, J. Am. Chem. Soc. 125 (2003) 6946.

[172] M.S. Hamdy, G. Mul, W. Wei, R. Anand, U. Hanefeld, J.C. Jansen, J.A. Moulijn, Catal. Today 110 (2005) 264.

[173] U. Arnold, R. Serpa da Cruz, D. Mandell, U. Schuchardt, Stud. Surf. Sci. Catal. 135 (2001) 4415.

[174] H. Wang, F. Zhao, R. Liu, Y. Hu, J. Mol. Catal. A 279 (2008) 153.

[175] K. George, S. Sugunan, React. Kinet. Catal. L. 94 (2008) 253.

[176] Y. Du, Y. Xiong, J. Li, X. Yang, J. Mol. Catal. A 298 (2009) 12.

[177] C. Evangelisti, G. Vitulli, E. Schiavi, M. Vitulli, S. Bertozzi, P. Salvadori, L. Bertinetti, G. Martra, Catal. Lett. 116 (2007) 57.

[178] R.S. da Cruz, J.M.D.E. Silva, U. Arnold, M.S. Sercheli, U. Schuchardt, J. Brazil. Chem. Soc. 13 (2002) 170.

[179] M. Studer, J. Hazard. Mater. 169 (2009) 1184.

[180] M. Stockmann, F. Konietzni, J.U. Notheis, J. Voss, W. Keune, W.F. Maier, Appl. Catal. A 208 (2001) 343.

[181] F.S. Xiao, J.M. Sun, X.J. Meng, R.B. Yu, H.M. Yuan, D.Z. Jiang, S.L. Qiu, R.R. Xu, Appl. Catal. A 207 (2001) 267.

[182] K.M. Parida, D. Rath, Appl. Catal. A 321 (2007) 101.

[183] J.S. Choi, T.H. Kim, K.Y. Choo, J.S. Sung, M.B. Saidutta, S.D. Song, Y.W. Rhee, J. Porous Mat. 12 (2005) 301.

[184] V. Rives, A. Dubey, S. Kannan, Phys. Chem. Chem. Phys. 3 (2001) 4826.

[185] A. Dubey, V. Rives, S. Kannan, J. Mol. Catal. A 181 (2002) 151.

[186] A. Dubey, S. Kannan, Catal. Commun.6 (2005) 394.

[187] T. Miyahara, H. Kanzaki, R. Hamada, S. Kuroiwa, S. Nishiyama, S. Tsuruya, J. Mol. Catal. A 176 (2001) 141.

[188] Y. Gu, X. Zhao, G. Zhang, H. Ding, Y. Shan, Appl. Catal. A 328 (2007) 150.

[189] F. Loeker, W. Leitner, Chem. Eur. J. 6 (2000) 2011.

[190] B. Li, J. Wang, J. Li, Y. Xu, J. Fu, W. Yao, G. Zi, W. Wang, J. Wang, Catal. Commun. 10 (2009) 1599.

[191] N. Srinivas, V.R. Rani, S.J. Kulkarni, K.V. Raghavan, J. Mol. Catal. A 179 (2002) 221.

[192] R. Molinari, T. Poerio, Appl. Catal. A 358 (2009) 119.

[193] Y. Cheneviere, V. Caps, A. Tuel, Appl. Catal. A 387 (2010) 129.

[194] O.A. Kholdeeva, O.V. Zalomaeva, A.B. Sorokin, I.D. Ivanchikova, C. Della Pina, M. Rossi, Catal. Today 121 (2007) 58.

[195] M. So, Y. Liu, C. Ho, C. Che, Chem. Asian J. 4 (2009) 1551.

[196] A. Grirrane, A. Corma, H. Garcia, J. Catal. 264 (2009) 138.

[197] L. Aschwanden, T. Mallat, F. Krumeich, A. Baiker, J. Mol. Catal. A 309 (2009) 57.

[198] L. Aschwanden, T. Mallat, M. Maciejewski, F. Krumeich, A. Baiker, ChemCatChem 2 (2010) 666.

[199] A. Grirrane, A. Corma, H. Garcia, Science 322 (2008) 1661.

[200] B. Zhu, M. Lazar, B.G. Trewyn, R.J. Angelici, J. Catal. 260 (2008) 1.

[201] S.K. Klitgaard, K. Egeblad, U.V. Mentzel, A.G. Popov, T. Jensen, E. Taarning, I.S. Nielsen, C.H. Christensen, Green Chem. 10 (2008) 419.

[202] C. Della Pina, E. Falletta, M. Rossi, Top. Catal. 44 (2007) 325.

[203] C. Zhang, N. Jiao, Angew. Chem. Int. Edit. 49 (2010) 6174.

[204] J. Srogl, S. Voltrova, Org. Lett. 11 (2009) 843.

[205] R. Miranda, E. Trejo, A. Cano, Rev. Latinoam. Quim. 23 (1992) 13.

[206] W.A. Jackson, W.R. LaCourse, D.A. Dobberpuhl, D.C. Johnson, Electroanalysis 3 (1991) 607.

[207] C.R. Raj, T. Okajima, T. Ohsaka, J. Electroanal. Chem. 543 (2003) 127.

[208] A. Adenier, M.M. Chehimi, I. Gallardo, J. Pinson, N. Vila, Langmuir 20 (2004) 8243.

[209] T. Luczak, J. Appl. Electrochem. 37 (2007) 653.

[210] T. Luczak, J. Appl. Electrochem. 37 (2007) 269.

[211] M. Fleischmann, K. Korinek, D. Pletcher, J. Chem. Soc. Perkin 2 (1972) 1396.

[212] C.M. Wilmot, J.M. Murray, G. Alton, M.R. Parsons, M.A. Convery, V. Blakeley, A.S. Corner, M.M. Palcic, P.F. Knowles, M.J. McPherson, S.E.V. Phillips, Biochemistry 36 (1997) 1608.

[213] R.J. Radel, J.M. Sullivan, J.D. Hatfield, Ind. Eng. Chem. Prod. Res. Dev. 21 (1982) 566.

[214] Y. Wu, L. Qiu, W. Wang, Z. Li, T. Xu, Z. Wu, X. Jiang, Transition Met. Chem. 34 (2009) 263.

[215] E. Guibal, T. Vincent, E. Touraud, S. Colombo, A. Ferguson, J. Appl. Polym. Sci. 100 (2006) 3034.

[216] S. Kim, D. Kim, J. Park, Adv. Synth. Catal. 351 (2009) 2573.

[217] G.L. Elizarova, L.G. Matvienko, A.O. Kuzmin, E.R. Savinova, V.N. Parmon, Mendeleev Commun. (2001) 15.

[218] F. Derikvand, F. Bigi, R. Maggi, C.G. Piscopo, G. Sartori, J. Catal. 271 (2010) 99.

[219] H. Miyamura, M. Shiramizu, R. Matsubara, S. Kobayashi, Chem. Lett. 37 (2008) 360.

[220] L. Norena-Franco, I. Hernandez-Perez, P. Aguilar, A. Maubert-Franco, Catal. Today 75 (2002) 189.

[221] S.A. Miscoria, G.D. Barrera, G.A. Rivas, Electroanalysis 17 (2005) 1578.

[222] F.J. Kakis, M. Fetizon, Douchkin.N, M. Golfier, P. Mourgues, T. Prange, J. Org. Chem. 39 (1974) 523.

[223] M. Fetizon, M. Golfier, Acad. Sci. Ser. C 267 (1968) 900.

[224] T. Nishiguchi, F. Asano, J. Org. Chem. 54 (1989) 1531.

[225] H. Miyamura, M. Shiramizu, R. Matsubara, S. Kobayashi, Angew. Chem. Int. Ed. 47 (2008) 8093.

[226] J.T. Rhule, W.A. Neiwert, K.I. Hardcastle, B.T. Do, C.L. Hill, J. Am. Chem. Soc. 123 (2001) 12101.

[227] E. Boring, Y.V. Geletii, C.L. Hill, J. Am. Chem. Soc. 123 (2001) 1625.

[228] F. Gasparrini, M. Giovannoli, D. Misiti, G. Natile, G. Palmieri, Tetrahedron 39 (1983) 3181.

[229] H. Firouzabadi, N. Iranpoor, M.A. Zolfigol, Synth. Commun. 28 (1998) 1179.

[230] P. Kelly, S.E. Lawrence, A.R. Maguire, Synlett (2007) 1501.

[231] H. Sakuraba, H. Maekawa, J. Inclusion Phenom. Macrocyclic Chem. 54 (2006) 41.

[232] V. Ayala, A. Corma, M. Iglesias, F. Sanchez, J. Mol. Catal. A 221 (2004) 201.

[233] M.J. Alcon, A. Corma, M. Iglesias, F. Sanchez, J. Mol. Catal. A 178 (2002) 253.

[234] S.S. Stavitskaya, I.A. Tarkovskaya, T.P. Petrenko, N.T. Kartel, Carbon (2001) 421.

[235] T. Mitsudome, A. Noujima, T. Mizugaki, K. Jitsukawa, K. Kaneda, Chem. Commun. (2009) 5302.

[236] B.P.S. Chauhan, A. Sarkar, M. Chauhan, A. Roka, Appl. Organomet. Chem. 23 (2009) 385.

[237] B. Marciniec, Rocz. Chem. 48 (1974) 163.

[238] B. Marciniec, Rocz. Chem. 49 (1975) 1565.

[239] P. Haider, B. Kimmerle, F. Krumeich, W. Kleist, J.-D. Grunwaldt, A. Baiker, Catal. Lett. 125 (2008) 169.

[240] V.R. Choudhary, D.K. Dumbre, Top. Catal. 52 (2009) 1677.

[241] W. Partenheimer, Adv. Synth. Catal. 351 (2009) 456.

[242] D.A. Outka, R.J. Madix, Surf. Sci. 179 (1987) 361.

[243] I.E. Wachs, R.J. Madix, Surf. Sci. 76 (1978) 531.

[244] P. Fristrup, L.B. Johansen, C.H. Christensen, Catal. Lett. 120 (2008) 184.

[245] W.F. Hoelderich, Catal. Today 62 (2000) 115.

[246] A. Corma, S.B.A. Hamid, S. Iborra, A. Velty, ChemSusChem 1 (2008) 85.

[247] M.J. Climent, A. Corma, S. Iborra, ChemSusChem 2 (2009) 500.

[248] L.L. Santos, P. Serna, A. Corma, Chem. Eur. J. 15 (2009) 8196.

[249] A. Corma, T. Rodenas, M.J. Sabater, Chem. Eur. J. 16 (2010) 254.

[250] T. Seki, J.-D. Grunwaldt, N. van Vegten, A. Baiker, Adv. Synth. Catal. 350 (2008) 691.

[251] T.A. Nijhuis, T.Q. Gardner, B.M. Weckhuysen, J. Catal. 236 (2005) 153.

[252] Y. Hao, M. Mihaylov, E. Ivanova, K. Hadjiivanov, H. Knoezinger, B.C. Gates, J. Catal. 261 (2009) 137.

[253] M.C. Raphulu, J. McPherson, E. van der Lingen, J.A. Anderson, M.S. Scurrell, Gold Bull. 43 (2010) 21.

[254] C. Della Pina, E. Falletta, M. Rossi, A. Sacco, J. Catal. 263 (2009) 92.

[255] P. Haider, A. Urakawa, E. Schmidt, A. Baiker, J. Mol. Catal. A 305 (2009) 161.

[256] F. Solymosi, J. Mol. Catal. 65 (1991) 337.

[257] C. Aprile, M. Boronat, B. Ferrer, A. Corma, H. Garcia, J. Am. Chem. Soc. 128 (2006) 8388.

Chapter 3

Selective Liquid-Phase Oxidation of Alcohols Catalyzed by a Silver-Based Catalyst Promoted by the Presence of Ceria

Abstract

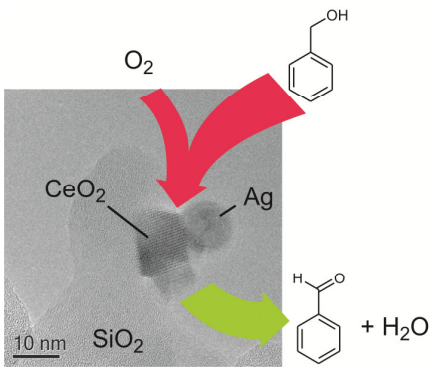

Alcohol oxidation by $Ag/SiO_2 – CeO_2$.

A number of impregnated silver catalysts supported on SiO_2, Al_2O_3, celite, CeO_2, kaolin, MgO and activated carbon were screened for their catalytic activity in the selective liquid phase oxidation of benzyl alcohol using a special screening approach. For this purpose 5-6 catalyst samples were mixed and tested simultaneously. When a high catalytic conversion (> 30 % over 2 h) was found the number of catalyst components was reduced in the following tests. Thereby, a collaborative effect between a physical mixture of ceria nanoparticles and silver-impregnated silica (10 wt.-% Ag/SiO_2) was found. The catalytic activity was highly dependent on the silver loading, the amount of ceria and especially the calcination procedure. Transmission electron microscopy (TEM), X-ray diffraction (XRD) and X-ray absorption spectroscopy (XANES, EXAFS) demonstrate that silver is mainly present as metallic particles. This is also supported by *in situ* XAS experiments. Silver-oxygen species appear to be important for the catalytic oxidation of the alcohol for which a preliminary mechanism is presented. The application of the catalyst was extended to the oxidation of a wide range of primary and secondary alcohols. Compared to Pd and Au catalysts, the new Ag catalyst performed similarly or even superior if CeO_2 was present. In addition, the presence of ceria increased the catalytic activity of all investigated catalysts.

3.1 Introduction

Selective oxidation reactions comprise one of the most important classes of transformations in organic chemistry. The catalytic oxidation of alcohols is especially interesting [1-7] since this reaction can be utilized in the production of aldehydes e.g. useful in the food processing or cosmetics industry. In addition, it has found great interest as one of the key reactions for processing biomass [8-10]. Acknowledging the importance of the oxidation of alcohols under benign conditions, a number of groups have focused on developing economical and ecological reasonable alternatives to the use of toxic chromium(VI) species or specially designed oxidants. Homogeneous catalysts [3, 8, 11], often utilizing nitroxyl radicals and heterogeneous catalytic systems [12, 13] are available for the selective oxidation of a variety of different alcohols to the corresponding carbonyl compounds using preferentially oxygen as oxidant. Heterogeneous catalysts are often based on noble metals like Pt [14], Ru [15], Pd [16] and Au [17-19] or combinations thereof [20-22] when reactions are performed in liquid or liquid-like phases. While especially the Pt group metals afford high catalytic activities under mild conditions, gold catalysts have attained wide interest mainly due to their high selectivity towards aldehydes [23]. On the other hand, catalytic activities are often only moderate. Gold catalysts were also used successfully for upgrading e.g. ethanol as a typical “renewable” into the corresponding acid or ester and proved to be superior when compared to Pt or Pd catalysts [24, 25].

However, there are only very few publications reporting silver being catalytically active in the liquid-phase alcohol oxidation [26-30]. This is surprising since silver catalysts are used in many gas phase oxidations with the most prominent examples being ethylene [31] and methanol oxidation [32]. Early studies report silver salts supported on e.g. silica [33] or celite [34, 35] can be used as stoichiometrical and mild oxidizing agents for the selective liquid phase-oxidation of alcohols. Mitsudome and coworkers [29] described a silver-ion exchanged hydrotalcite which turned out to be catalytically active in the selective oxidation of primary and secondary alcohols. Interestingly, experiments were performed under anaerobic conditions affording very good selectivities. This demonstrates that silver has a high potential for catalytic oxidation reactions also in the liquid phase.

This chapter will asset the potential of silver as a catalyst material for the selective oxidation of alcohols using benzyl alcohol as a model compound. Starting with a screening approach of various silver-impregnated supports, XRD, XAS and TEM as well as catalytic studies on various substrates were used in order to gain a more fundamental understanding of the catalyst structure and a first insight into the reaction mechanism.

3.2 Experimental

3.2.1 Catalyst preparation

For screening different silver catalysts, a number of materials were synthesized by impregnation of TiO_2 (Aeroxide P25, Degussa, 50 m^2/g), Al_2O_3 (MCO-239U, Haldor Topsøe A/S), SiO_2 (Aerosil 200, Degussa, 200 m^2/g), MgO (Sigma Aldrich, 30 mesh), activated carbon (CAP super, SX plus, CA 1, Darco S-51, all NORIT Nederland B. V.), CeO_2 (Aldrich, < 25 nm) and celite (celite 500 fine, Fluka) with an aqueous $AgNO_3$ (Sigma-Aldrich, 99.5 %) solution containing the appropriate silver amount to obtain the targeted weight-loading. The mixtures were protected from light and left at room temperature. Typically after 24 h impregnation time, the catalysts were dried at 90 °C for 24 h followed by calcination for 2 h at a temperature between 300 and 700 °C.

For Ag/SiO_2 the preparation conditions were varied leading to the following synthesis protocol: 5.00 g silica (Aerosil 200, Degussa, 200 m^2/g) were impregnated with 25 mL of an aqueous solution containing 785 mg $AgNO_3$ (Sigma-Aldrich, 99.5 %). After 72 h impregnation time protected from light at room temperature (allowing evaporation of water) the catalyst samples were dried in air at 90 °C for 24 h. The catalyst was calcined at 500 °C for 30 min in a muffle oven controlled by a Eurotherm 904 controller. After grinding, a beige powder was obtained. The catalyst is denoted as $10\%Ag/SiO_2$. Variations to this protocol are described in the corresponding results section.

3.2.2 Catalyst testing

The catalytic tests were typically carried out by pouring a mixture of 40 mL xylene (mixture of isomers, Aldrich), 2.1 g (2.0 mL, 19 mmol) benzyl alcohol (SAFC, 99 %), and 0.10 g biphenyl (Sigma-Aldrich, 99.5 %) as internal standard in a three-necked flask equipped with a reflux condenser, a gas inlet and a magnetic stir bar. The conditions are similar to ref. [29]. The reaction mixture was heated up to reflux and equilibrated for 15 min. After adding 100 mg Ag/SiO_2 and 50 mg CeO_2 (Aldrich, < 25 nm), the solution was continuously saturated with flowing oxygen (Linde, 99.95 %). Samples were taken in regular intervals for GC analysis. GC analysis was performed on an Agilent 6890 N gas chromatograph equipped with a 7683 B series autosampler, a flame ionization detector and a HP Innowax column (30 m x 0.25 mm x 0.25 µm) using biphenyl as an internal standard. Screening experiments were carried out under the same conditions with a grinded mixture of the catalysts. Test reactions with other alcohols were carried out using 1-octanol (Fluka, 99.5 %), 2-octanol (Sigma-Aldrich, 97 %), 2-methoxybenzyl alcohol (Fluka, 97 %), 3-methoxybenzyl alcohol (Aldrich, 98 %), 4-methoxybenzyl alcohol (Aldrich, 98 %), 1-phenylethanol (Aldrich, 98 %), 1-naphthalenemethanol (Aldrich, 98 %), cinnamyl alcohol (Fluka, 97 %)

and cyclohexanol (Fluka, 99 %). In addition, competitive experiments were carried out in a mixture of 20 mL xylene, 2.0 mmol of benzyl alcohol, 2.0 mmol of a *p*-substituted benzyl alcohol (4-methoxybenzyl alcohol, 98 %; 4-chlorobenzyl alcohol, 99 %; 4-trifluoromethylbenzyl alcohol, 98 %; all Aldrich) and 0.10 g biphenyl (Sigma-Aldrich, 99.5 %) under an oxygen atmosphere using 100 mg of 10%Ag/SiO_2 and 50 mg CeO_2. Evaluation was done according to ref. [24] within the first 60 min of the experiments to minimize deactivating influences of the products.

3.2.3 Inductively-coupled plasma mass spectrometry (ICP-MS)

A hot solution obtained after 3 h reaction time was filtered through celite. 5.00 mL of this solution were used for further analysis. After evaporating the organic solvent in vacuo over night the residual was dissolved in concentrated HNO_3 and diluted with double distilled water to 10.0 mL. The measurements were performed with an ICP-MS instrument (Perkin-Elmer Elan 5000) equipped with a cross-flow nebulizer. The plasma Ar flow was set to 13 L/min at 800 W RF power and the nebulizer Ar flow was set to 0.80 L/min. The sample solution was injected with 1.4 mL/min. Quantification of Ce and Ag was done using multielement ICP-MS standard solutions (Fluka).

3.2.4 Characterization

The specific surface area was determined by nitrogen adsorption on an ASAP 2010 (Micromeretics) at liquid nitrogen temperature applying the BET theory. The sample was dried under vacuum at 200 °C for 48 h prior to the measurement.

X-ray diffraction (XRD) was measured with an X'Pert PRO Diffractometer (PANalytical) with a Cu-K_α X-ray source operated at 45 kV and 40 mA equipped with a Ni filter and a slit. Diffractograms were recorded between 2θ (Cu-K_α) = 20° to 90° with a step width of 0.00164°. The crystallite size was measured from the FWHM of the Ag(111) reflection using the Debye-Scherrer equation after correction for the instrument broadening.

X-ray absorption spectroscopy (XAS) was measured at the SuperXAS beamline at the Swiss Light Source (SLS, Villigen) and at the X1 beamline at the Hamburger Synchrotronstrahlungslabor (HASYLAB) at the Deutsche Elektronen-Synchrotron (DESY, Hamburg). XAS Spectra were recorded in step-scanning mode around the Ag-K edge (E = 25.514 keV) with a Si(311) double crystal monochromator in transmission mode by measuring the beam intensity before and after the sample and after the Ag reference foil by ionization chambers. *In situ* studies were performed with the powdered catalyst precursor placed in a glass capillary and heated with an oven as described elsewhere [36]. The glass capillary was open to the environment. The oven was heated from room temperature to 500 °C with

50 °C/min. XANES spectra were processed by energy-calibration, background subtraction and normalization using the WinXAS 3.1 software [37]. EXAFS spectra were extracted from the XAS spectra after analogous treatment and Fourier-transformation between k = 3 $Å^{-1}$-13 $Å^{-1}$. EXAFS fitting was performed in R-space up to 5.5 Å based on the silver lattice structure. The first, second and third silver shell were fitted assuming a constant damping factor of 0.8. Scattering amplitudes and phase shifts were calculated with the FEFF 7.0 code [38]. Particle sizes were calculated from the fitted first shell coordination number as described in [39] assuming spherical particles. The residual was between 7 and 9.

Transmission electron microscopy data was acquired using an FEI Titan 80-300 image corrected microscope operated at 300 kV and an FEI Tecnai T20 G2 operated at 200 kV. Both microscopes are equipped with Oxford Instruments INCA EDX spectrometers for elemental analysis. Ceria and silver particles were distinguished by measuring lattice spacings and angles between lattice fringes. The particle size distribution was automatically calculated using the ImageJ 1.40g software package after enhancing the contrast manually. In order to compare with particle sizes derived from the other characterization methods, the contribution of the particles to the XRD and EXAFS by their volume must be taken into account. Thus, the average particle size was calculated from the particle size distribution by weighting with the individual particle volume according to Equation 1.

$$d_{average} = \sum_{1}^{n} \frac{N_j V_j d_j}{\sum_{1}^{n} N_i V_i} \qquad \text{(Eq. 3-1)}$$

$d_{average}$ Average volume-weighted particle size

$N_{i,j}$ Number of particles with the same diameter

$V_{i,j}$ Volume of particle with diameter d assuming spherical particles

d_j Particle diameter

3.3 Results

3.3.1 Synthesis of silver catalysts and catalyst screening

In order to identify catalysts for alcohol oxidation, a series of silver containing catalysts was synthesized by impregnation of SiO_2, Al_2O_3, TiO_2, CeO_2, kaolin, MgO, celite and activated carbon with 1-10 wt.-% silver loading. The catalysts were calcined in air at temperatures between 300 °C and 700 °C and tested for catalytic activity in the oxidation of benzyl alcohol to benzaldehyde. The reaction was performed

under reflux in an oxygen atmosphere using xylene as a solvent. Since during the screening phase of the catalysts only a simple classification into catalytically active/ inactive was necessary, 5-6 different catalysts were tested simultaneously in one batch. At this early stage only the conversion of benzyl alcohol was considered since the selectivity to benzaldehyde might be influenced by the various materials in the mixture. Selected mixtures to demonstrate the principle are given in Table 3-1. Most catalyst mixtures only resulted in conversions lower than 10%. However, especially one mixture of catalysts exhibited significantly higher catalytic activity (entry 4; 41% conversion). By reducing the number of catalysts tested in each experiment Ag/SiO_2 and Ag/CeO_2 were identified to be required for obtaining catalytic activity (entry 7). Testing the two catalysts separately gave only small conversions

Table 3-1: Selected catalyst mixtures screened for catalytic oxidation of benzyl alcohol. Reaction Conditions: 40 ml xylene, 2.00 mL benzyl alcohol, 0.10 mL ^{t}butyl benzene, 50 mg of each catalyst (Ag/SiO_2: 100 mg), O_2 atmosphere, reaction time 3 h.

Entry	T_{calc} (°C)	Catalyst supports and Ag loading (wt.-%)							Conversion of BzOH (%)
		SiO_2	TiO_2	Al_2O_3	celite	kaolin	CeO_2	MgO	
1	400	3	3		3		3	3	**6**
2	500	3	3		3	5	3	3	**16**
3	600	3	3		3		3	3	**2**
4	500	10	10	10	10		10		**41**
5	Uncalc.	10	10	10	10		10		**6**
6	500		10		10		10		**4**
7	500	10					10		**37**

below 5%. In addition, silver impregnation was not necessary on CeO_2 and thus nanostructured CeO_2 (average particle size 25 nm) and 10 wt.-% Ag/SiO_2, calcined for 2 h at 500 °C, were ascertained as the key components. Interestingly, catalyst mixtures containing CeO_2 and Ag/SiO_2 calcined at 300 °C, 400 °C, 600 °C or 700 °C performed distinctively worse. Silver in Ag/SiO_2 calcined at 500 °C was found to be mainly in metallic state as evidenced by XANES/ EXAFS (Figure 3-1) and XRD (not shown). The near edge structure in the XANES region is similar to silver foil. The Fourier transformed EXAFS spectrum showed mainly the Ag-Ag backscattering typical for metallic silver (*vide infra*). XRD reflections exhibited the typical features of metallic Ag with potentially a small contribution corresponding to Ag_2O. The specific surface area measured by BET was 180 m^2/g.

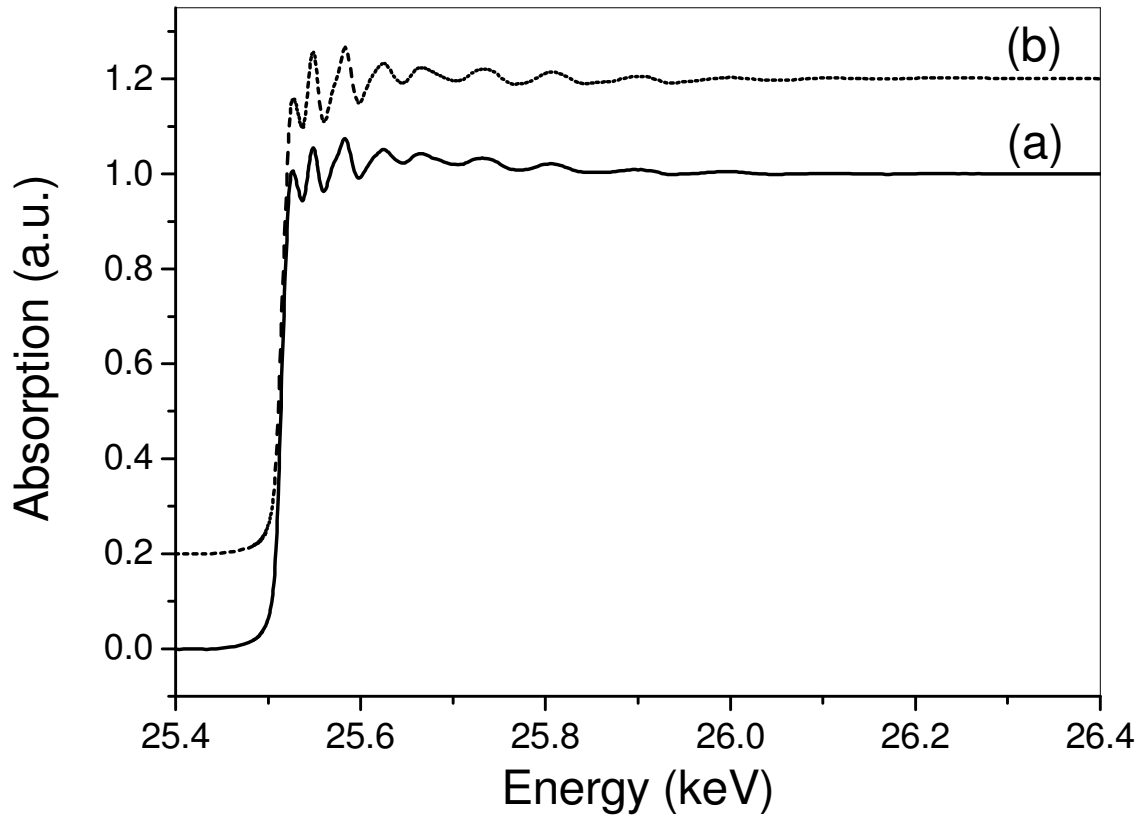

Figure 3-1: EXAFS spectrum recorded at the Ag K-edge of a freshly prepared 10%Ag/SiO_2 catalyst calcined for 2 h at 500 °C (a) compared to silver foil (b).

3.3.2 Investigation of the collaborative behavior of the Ag/SiO_2 – CeO_2 system

Since Ag/SiO_2 and CeO_2 tested alone did not exhibit catalytic activity (conversion < 10 %), the origin of the collaborative behavior and the preparation procedures for Ag/SiO_2 and CeO_2 were studied in more detail. At first, the influence of the silver loading of Ag/SiO_2 catalysts was studied. A series containing 1-20 wt.-% was synthesized by calcination at 500 °C for 2 h and investigated in a mixture with CeO_2. As can be seen in Figure 3-2, a silver loading of 10 wt.-% gave the highest conversion, while a higher loading resulted in a more selective catalyst. Catalysts with a loading of 1 wt.-% did not achieve a significantly higher conversion than a mixture of SiO_2 and CeO_2. The selectivity increased with higher silver loading. As the selectivity is only slightly worse compared to the 20 wt.-% sample, further studies were conducted using silica with 10 wt.-% silver.

The influence of the ratio of Ag/SiO_2 to CeO_2 on the catalytic activity was investigated keeping the amount of silver constant (Figure 3-3). At low CeO_2 contents both catalyst activity and selectivity

increased with increasing amount of CeO_2. The optimum ratio of was found to be 2:1 (Ag/SiO_2 – CeO_2). A ratio of 1:1 (Ag/SiO_2 – CeO_2) led to a decreased catalytic activity. Both the highest conversion and the highest selectivity were obtained with a mixture of 1:3 (Ag/SiO_2 – CeO_2) which, however, seems not preferable as it would refer to 400 mg of catalyst material compared to 150 mg for a 2:1 (Ag/SiO_2 – CeO_2) ratio. A reason for the increased catalytic activity with a higher CeO_2 amount might be that water and benzaldehyde are partly adsorbed thereby preventing catalyst deactivation caused by the reaction products (*vide infra*). Intensive mixing of Ag/SiO_2 and CeO_2 by e.g. grinding was not required prior to reaction so both compounds were added separately to the reaction mixture. Nevertheless, a close proximity of Ag/SiO_2 and CeO_2 was necessary. This is indicated by the observation that when CeO_2 and Ag/SiO_2 were packed in separated filter paper containers the catalytic activity was not higher than Ag/SiO_2 packed in a filter container alone. Additionally, the reaction did not proceed significantly after

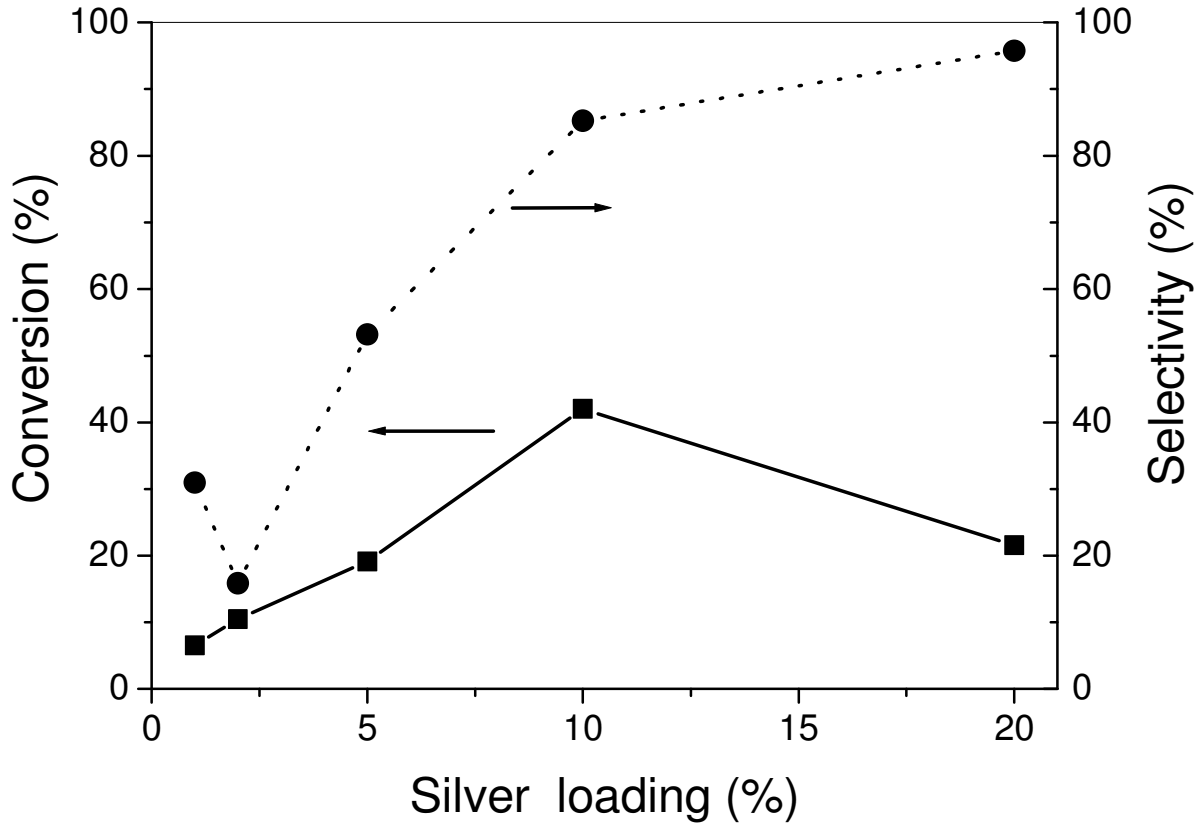

Figure 3-2: Conversion (■) and selectivity (●) obtained from Ag/SiO_2 (calcined in air at 500 °C for 2 h) with different silver loadings. Reaction conditions: 40.0 mL xylene, 19.3 mmol benzyl alcohol, 0.20 g biphenyl, 100 mg Ag/SiO_2, 50 mg CeO_2, reflux, O_2 atmosphere, 3 h reaction time. The lines are for the guide of the eye.

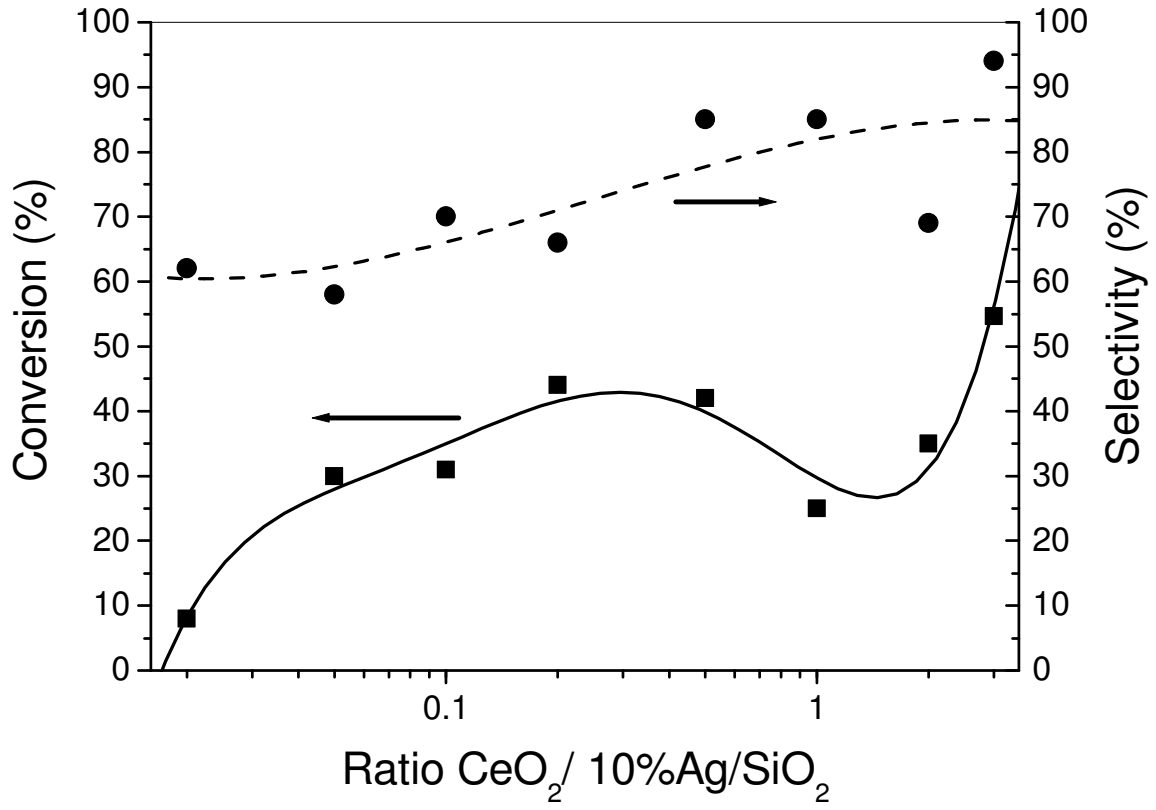

Figure 3-3: Conversion (■) and selectivity (●) obtained from Ag/SiO_2 with different CeO_2 to $10\%Ag/SiO_2$ ratios. Reaction conditions: 40.0 mL xylene, 19.3 mmol benzyl alcohol, 0.20 g biphenyl, 100 mg $10\%Ag/SiO_2$ (calcined in air at 500 °C for 2 h) with the indicated CeO_2 content, reflux, O_2 atmosphere, 3 h reaction time. Note that the abscissa is logarithmic. The lines are for the guide of the eye.

filtering the hot reaction mixture and adding either Ag/SiO_2 or CeO_2. Leaching of silver and cerium was low, i.e. concentrations determined with ICP-MS were 0.10 mg/L (± 0.01 mg/L) for silver and 11 µg/L (± 2 µg/L) for cerium. Addition of Ce(III) 2-ethylhexanoate to Ag/SiO_2 as a soluble cerium source with a nine times higher cerium concentration of 0.1 mg/L did not result in a markedly enhanced benzyl alcohol conversion. However, oxidation of the solvent was observed (*cf.* Chapter 4). In accordance, TEM images of *ex situ* samples reacted for 15 min and 300 min, respectively, showed a high dispersion of the CeO_2 nanoparticles on the silica support (Figure 3-4). Thus, dissolved Ce or Ag species are not the main reason for the enhanced catalytic activity.

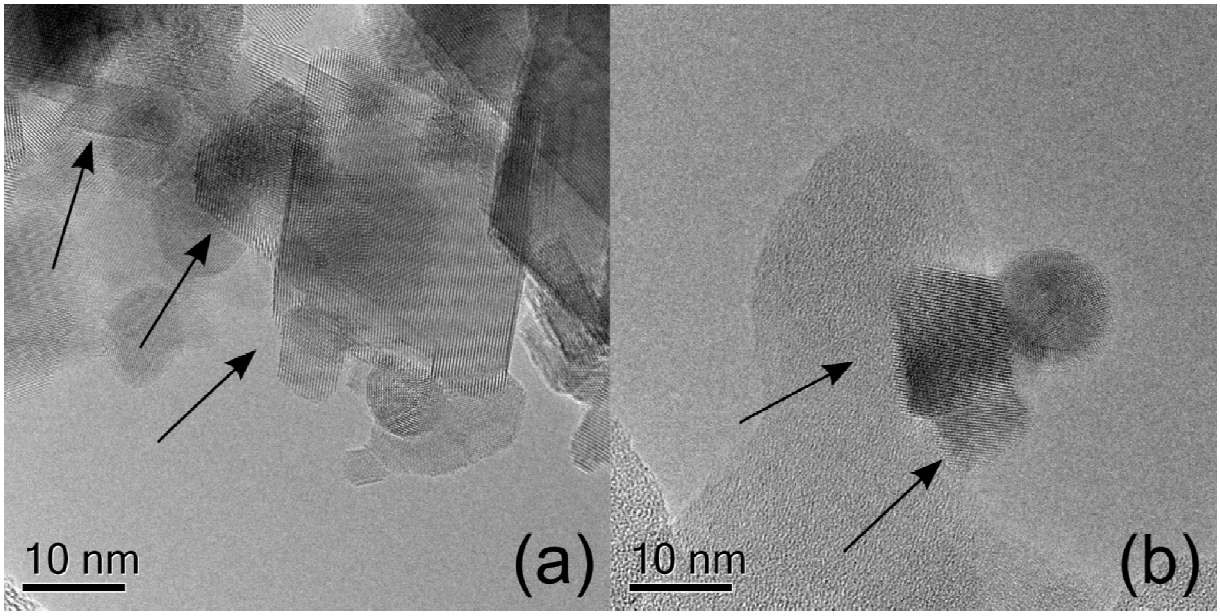

Figure 3-4: TEM images of catalyst mixtures of 10%Ag/SiO_2 and CeO_2 after 15 min (a) and 300 min (b) reaction time. Arrows indicate CeO_2 nanoparticles. Dark circles are silver particles on the silica support (verified with EDX).

3.3.3 Influence of the catalyst synthesis and calcination procedure

The catalyst exhibited higher selectivity by increasing the impregnation time prior to drying from 24 h to 72 h. XRD analysis showed a decrease in the mean particle size from 26 nm to 11 nm with longer impregnation time (measured after calcinations at 500 °C). Further screening experiments (*vide supra*) proposed a calcination temperature of 500 °C resulting in a far superior catalyst compared to 400 °C and 600 °C. In order to trace the changes during calcination, the calcination process was studied *in situ* in a glass capillary (Figure 3-5). The catalyst precursor was heated up rapidly at about 50 °C/min from room temperature to 500 °C with the capillary being open to the environment. The first spectrum corresponds to silver in the state of $AgNO_3$ which is transformed to an intermediate silver species between 300 and 450 °C correlating with the observation of only low conversion (< 10%) by the Ag/SiO_2 obtained from calcination at 400 °C. While pure $AgNO_3$ decomposes to metallic silver above 440 °C, metallic silver was only observed after ca. 20 min at 500 °C. The intermediate species has a similar edge position as the freshly impregnated catalyst precursor, thus silver was mainly in the oxidized state. Note, that the reduction was only observed when the capillary was open to air and not with a flow of 21 vol.-% O_2/He. In a flow of pure He the reduction occurred rapidly at 500 °C.

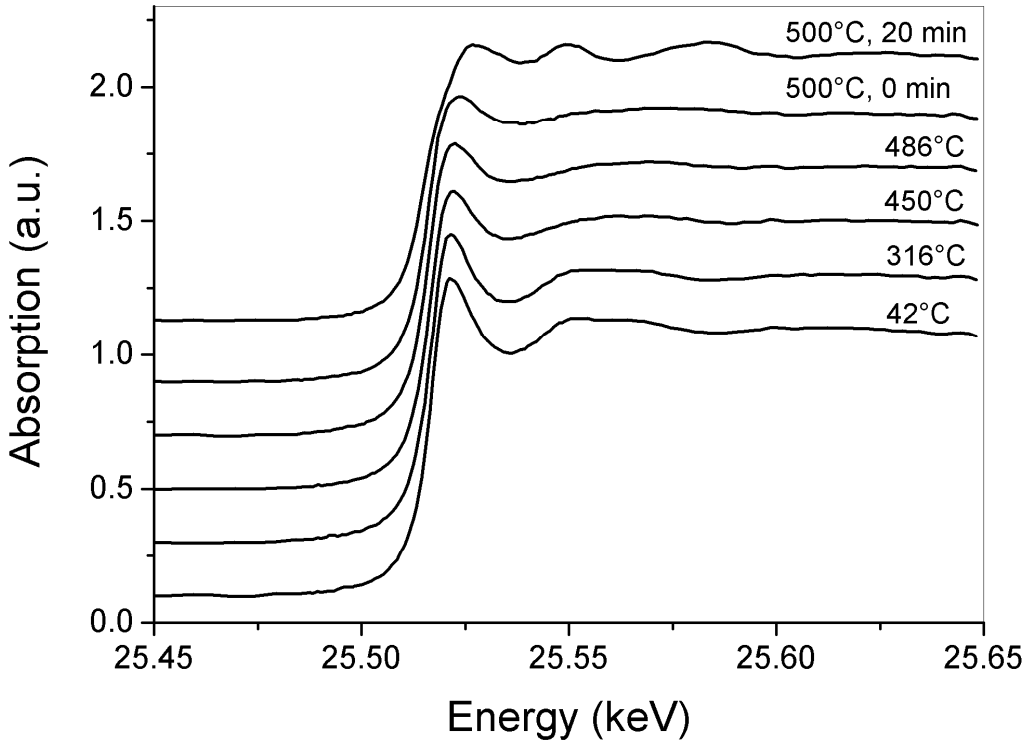

Figure 3-5: *In situ* XANES spectra recorded at the Ag K-edge during calcination of 10%Ag/SiO_2 in air in an open quartz capillary without gas flow.

The XAS studies indicate that calcination time plays an important role. Figure 3-6 shows the performance of catalysts calcined between 15 min and 8 h. The catalyst activity increased with calcination time reaching a maximum after 1 h exhibiting, however, the poorest selectivity. Longer calcination times enhanced the selectivity but had an overall negative effect on the observed conversion suggesting that sintering of Ag particles influences catalyst activity. A calcination time of 30 min gave the most effective catalyst. The particle size obtained from XRD did not show any trend and was varying between 11 and 16 nm. Furthermore, posttreating the calcined catalyst in hydrogen atmosphere at low temperature (150 °C) did not affect the catalyst activity in any way.

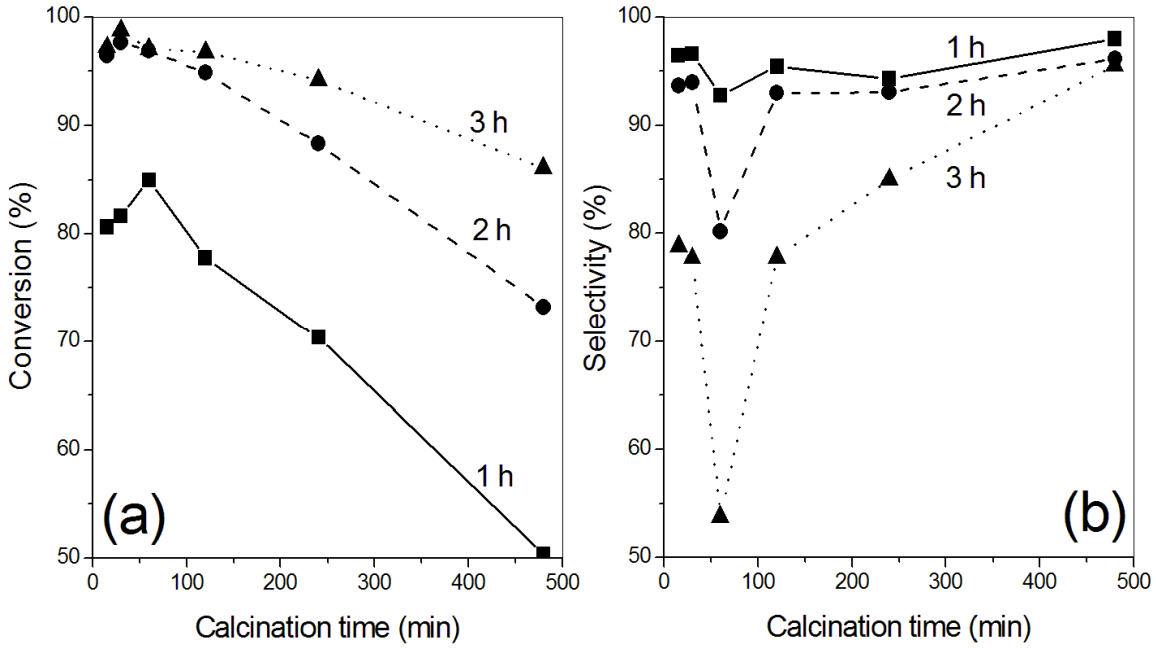

Figure 3-6: Conversion (a) and selectivity (b) depending on the calcination time after 1 h, 2 h and 3 h reaction time. Reaction conditions: 20.0 mL xylene, 2.0 mmol benzyl alcohol, 0.10 g biphenyl, 50 mg 10%Ag/SiO_2, 25 mg CeO_2, reflux, O_2 atmosphere, reaction time as indicated.

3.3.4 Effects of reaction conditions and reaction time

In order to study the influence of the reaction atmosphere, experiments were performed in flowing oxygen, air and inert atmosphere (Table 3-2). The reaction rate is highest in pure oxygen. Decreasing the amount of oxygen led to a lower reaction rate. Anaerobic conditions prevented the formation of any products.

Table 3-2: Conversion and selectivity over 10%Ag/SiO_2 promoted with CeO_2 under different reaction atmospheres. Reaction Conditions: 20.0 mL xylene, 0.10 g biphenyl, 2.00 mmol alcohol, 50 mg 10%Ag/SiO_2, 25 mg CeO_2, 2 h reflux in atmosphere as indicated.

	Flowing O_2	Air	Flowing N_2[a]
Conversion (%)	98	15	< 1
Selectivity (%)	95	94	traces

[a]Reaction mixture purged for 30 min prior to reaction.

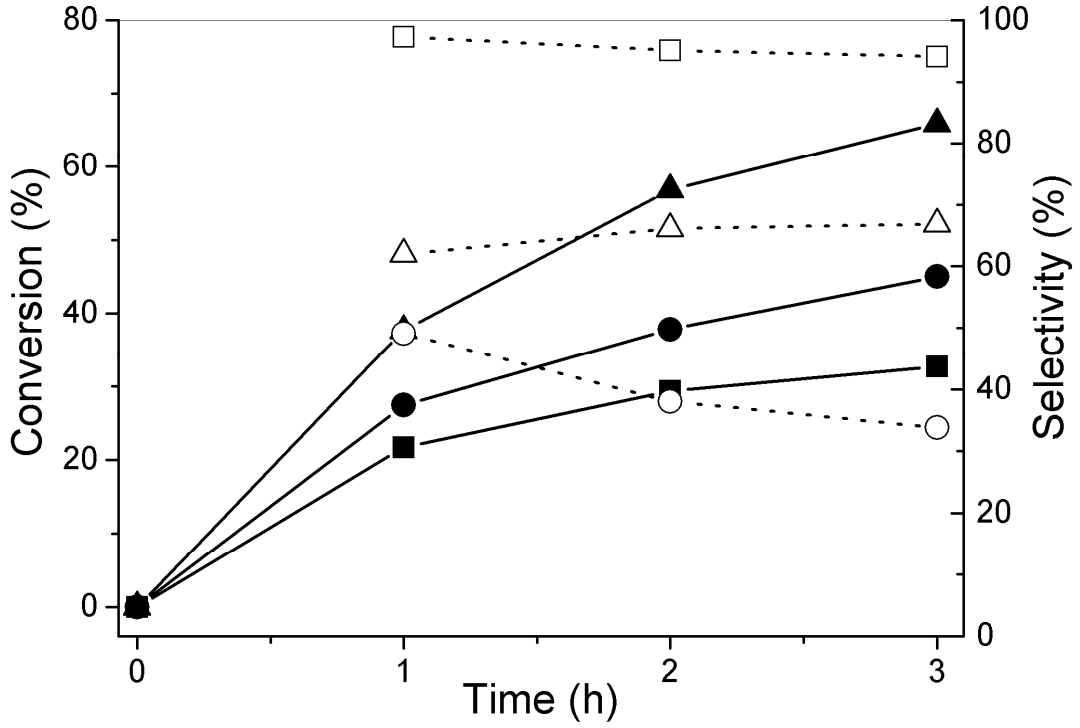

Figure 3-7: Conversion (solid symbols) and selectivity depending on the addition of a drying agent: conversion and selectivity without addition of drying agent (■, □), with molecular sieves 3 Å (▲, Δ) and $MgSO_4$ (●, ○). Reactions conditions: 40.0 mL xylene, 19.3 mmol benzyl alcohol, 0.20 g biphenyl, 100 mg 10%Ag/SiO_2, 50 mg CeO_2, reflux in O_2 atmosphere.

During the course of the reaction, the catalyst deactivated gradually. Since benzaldehyde added to the starting mixture decreased the reactant conversion significantly, competitive adsorption on the reaction sites between reactant and product may hinder the product formation. Furthermore, water has an undesired effect on the catalyst performance since both a catalyst treated with water prior to the reaction considerably lost catalytic activity (conversion < 2 %) and water added during the reaction stopped the product formation. Using a drying agent suitable for high temperatures as in refluxing xylene, i.e. anhydrous $MgSO_4$ and molecular sieves 3 Å, respectively, a significantly higher degree of conversion was found together with an increased amount of overoxidation products (Figure 3-7). The observed lower selectivity which does not originate from the drying agent alone suggests that water also plays a moderating role by e.g. blocking highly active sites. Both deactivation by water [40, 41] and an increase of selectivity by blocking highly active sites [14, 42, 43] are not uncommon in alcohol oxidation. After use, the catalyst was significantly less active (conversion 16 %, Table 3-3). Hence, the catalyst deactivation was not reversible. Reactivation of the used catalyst was only observed after addition of

fresh Ag/SiO_2 while addition of CeO_2 had virtually no influence, so the deactivation is related to Ag/SiO_2. Calcination of used catalyst at 500 °C for 30 min partly reactivated the catalyst leading to a conversion of 45 % after 2 h (Table 3-3).

Table 3-3: Conversion and selectivity of a fresh, used and recalcined CeO_2 promoted 10%Ag/SiO2 catalyst (500 °C, 30 min in air). Reaction Conditions: 20.0 mL xylene, 0.10 g biphenyl, 2.00 mmol alcohol, 50 mg 10%Ag/SiO_2, 25 mg CeO_2, 2 h reflux in oxygen atmosphere.

	Fresh catalyst	Used catalyst	Re-calcined catalyst
Conversion (%)	98	16	45
Selectivity (%)	95	> 99	93

Table 3-4: Structural parameters obtained from EXAFS data fitting.

Sample	Ag-Ag Shell no.	N	R (Å)	σ^2 ($Å^{-2}$)
Ag foil	1	12	2.86[a]	0.009
	2	6	4.03	0.011
	3	24	5.03	0.015
10%Ag/SiO_2	1	7.9	2.86[a]	0.009
	2	6.0[b]	4.01	0.014
	3	4.2	5.04	0.007
10%Ag/SiO_2 – CeO_2 after 15 min	1	10	2.86[a]	0.009
	2	6.0[b]	4.01	0.013
	3	5.0	5.03	0.006

[a]Note that the Ag-Ag distance found is by 0.03 Å too small which is in analogy to examples found in the literature [68]. [b]Coordination number was constrained to 6.0.

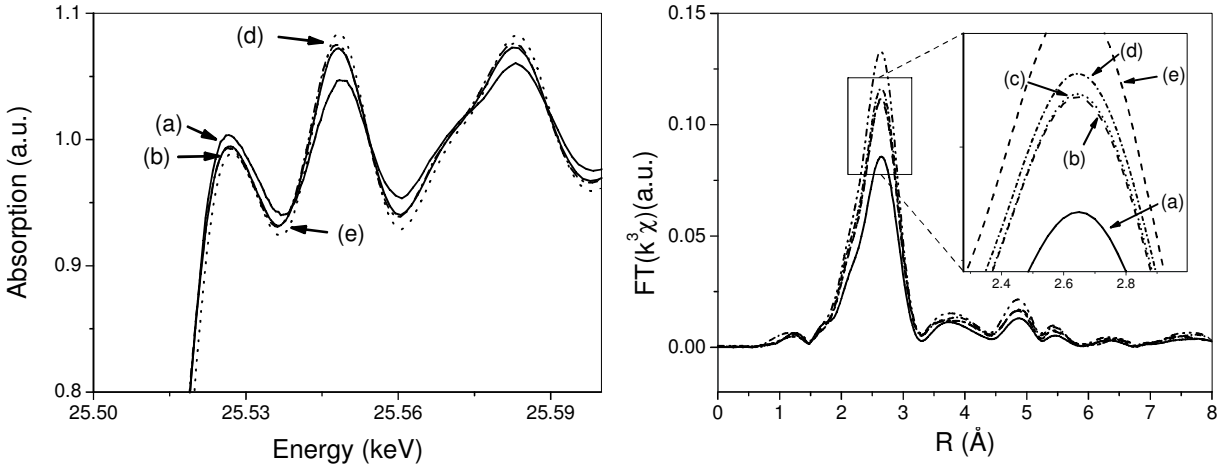

Figure 3-8: XANES (left) and Fourier transformed EXAFS (right) spectra of ex-situ 10%Ag/SiO_2 – CeO_2 (2:1) catalyst samples before reaction (a), after 15 min (b), 90 min (c) and 5 h (d) reaction time; (e) silver foil.

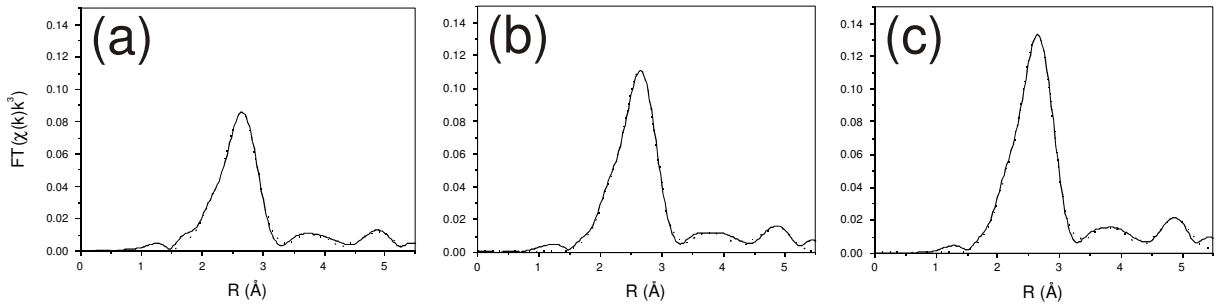

Figure 3-9: Experimental (solid line) and fitted (dashed line) radial distribution function of fresh 10%Ag/SiO_2 catalyst (a), 10%Ag/SiO_2 catalyst after 15 min reaction time (b) and silver foil (c). EXAFS data fits were made up to 5.5 Å for the first three Ag shells.

In order to gain insight into the changes during the reaction, a number of spent catalyst samples reacted between 15 min and 5 h were prepared and investigated using *ex situ* XAS (Figure 3-8). Comparing the XANES region of these samples only a slight change of the catalyst during reaction was found. The Fourier-transformed EXAFS spectra showed a pronounced increase in the magnitude of the peak corresponding to the 1st shell Ag-Ag backscattering between fresh and used catalysts. The difference in magnitude is largest within the first 15 min and increased slightly with higher reaction times but does not reach that of silver foil. The coordination number of the first shell obtained from EXAFS data fitting increased from fresh catalyst to used catalyst to silver foil (Table 3-4 and Figure 3-9). Estimation of the particle size from EXAFS resulted in a cluster size of ca. 1.5 nm for the fresh catalyst and 3 nm for the catalyst after 15 min reaction time which are both significantly lower than the particle size obtained from XRD (29 nm). TEM evaluation proved that most particles were in the range of 2-3 nm, which might be X-ray amorphous (Figure 3-10). However, TEM also showed significantly larger particles

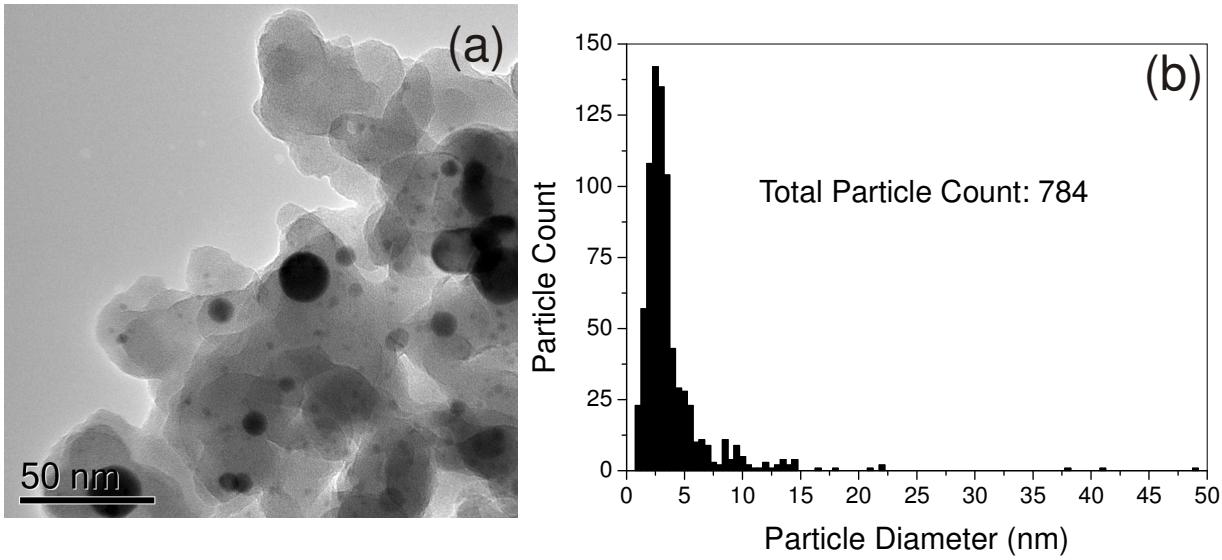

Figure 3-10: TEM images of freshly calcined (2 h, 500 °C) 10%Ag/SiO_2 prior to mixing with CeO_2 (a) and corresponding particle size distribution of freshly calcined 10%Ag/SiO_2 (b).

with some particles even in the range of 50 nm. Since both XRD and EXAFS give a volume- and surface weighted particle size, respectively, large particles have a significantly higher influence on the average particle size. A volume weighted particle size of 33 nm was calculated from the TEM data which is in good agreement with XRD results. Note however, that the influence of large particles on the average volume-based particle size is high. Table 3-5 summarizes particle sizes obtained from XRD, EXAFS and TEM. Obviously, the particle size from EXAFS appears to be significantly underestimated. It can be excluded that very small clusters or isolated silver atoms not observable with TEM contribute significantly to the EXAFS function since these would give different backscattering contributions. An explanation for this discrepancy in the EXAFS results is either imperfections in the lattice or the involvement of silver oxygen species. Oxygen dissolved in silver (β-oxygen) is known to cause disorder in the silver lattice [44]. If an intercalated species does not lie on the axis between absorber atom and reflecting atom [45, 46] it will have a decreasing effect on the inelastic electron mean free path length thereby attenuating the EXAFS amplitude significantly even at low dopant concentrations [47, 48] which might be the case in this study. Note that the oxygen content is presumably too low to be observable directly *via* Ag-O backscattering.

Table 3-5: Overview over the average diameter of silver particles of 10%Ag/SiO_2 (calcined at 500 °C for 2 h) obtained from XRD, EXAFS and TEM.

Characterization method	XRD	EXAFS	TEM	
Particle size (nm)	29	1.5	2.5[a]	33[b]

[a]Most abundant particle size. [b]Average particle size calculated from Eq. 3-1.

3.3.5 Extension to further alcohols and comparison to other noble metal catalysts

In order to broaden the application of the novel silver-based catalyst system, the alcohol oxidation reaction was extended to a number of primary and secondary alcohols (Table 3-6) and compared to other well-described catalyst systems. 10%Ag/SiO_2 calcined for 30 min at 500 °C mixed with CeO_2 in a 2:1 ratio was used as an optimized catalyst for this purpose. Secondary alcohols were oxidized to the corresponding ketones with high selectivity and high conversion for the oxidation of 1-phenylethanol within just 45 min, while the oxidation of 2-octanol afforded moderate yields after 3 h reaction time. The oxidation of cyclohexanol produced a considerable amount of a not identified side product. Primary alcohols were in general also oxidized with high selectivity to the aldehyde while the conversions depended to a high extent on the reactants. The oxidation of 1-octanol commenced with a high initial rate. With reaction times longer than 1 h, the selectivity to octanal decreased significantly favoring the formation of octanoic acid. The silver-based catalyst was compared with three impregnated gold catalysts and one Pd catalyst based on the same catalyst weight for the oxidation of benzyl alcohol (Table 3-7) both with and without the addition of CeO_2 in the absence of a base. Without CeO_2, Ag/SiO_2 is highly selective but gives only very low conversions. Remarkably, the observed conversions for all catalysts increased with addition of CeO_2. Thus, Pd/Al_2O_3 afforded almost full conversion already after 30 min, with, however, only low selectivity while combination with CeO_2 was crucial for the activity of the silver catalyst achieving both a high selectivity and conversion after 2 h (*cf.* Table 3-7). The gold catalysts underwent deactivation during the course of the reaction, i.e. longer reaction times resulted in only slightly higher conversions at the cost of selectivity. Note however, that here reaction conditions optimized for the silver catalyst were used.

Alcohol oxidation on Pt group metals [12] and on Au [24] is believed to occur *via* hydride abstraction thus involving an intermediate cationic species. Comparing the conversion of benzyl alcohol with *para*-substituted benzyl alcohols in a competitive experiment [24], electron withdrawing substituents were found to decrease the reaction rate while electron donating substituents had a beneficial effect (Table 3-8). This supports that also in this case the rate limiting step involves the formation of a cationic species.

Table 3-6 Oxidation of various primary and secondary alcohols catalyzed by 10%Ag/SiO_2 and CeO_2. Reaction conditions: 20.0 mL xylene, 0.10 g biphenyl, 2.00 mmol alcohol, 50 mg Ag/SiO_2, 25 mg CeO_2,, reflux in O_2 atmosphere.

Entry	Substrate	Product	Time (h)	Conv. (%)	Sel. (%)
1	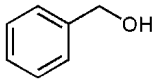	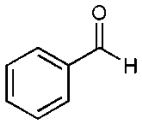	2	98	95
2	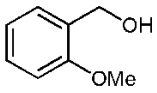	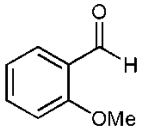	3	90	> 99
3	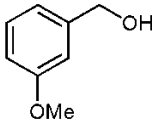	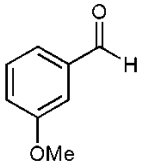	3	92	> 99
4	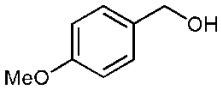	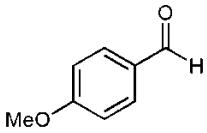	3	83	> 99
5	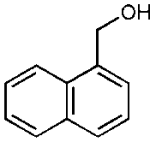	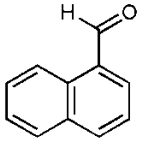	3	39	99
6	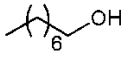	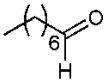	0.75[a]	29	90
7	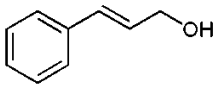	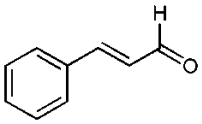	3	83	97
8	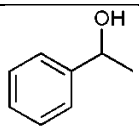	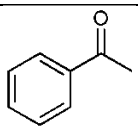	0.75	> 99	> 99
9	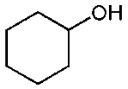	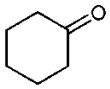	2	22	71
10	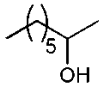	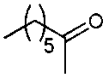	2	63	> 99

[a] Longer reaction times decreased the selectivity considerably.

Table 3-7: Comparison of the optimized Ag catalyst with Pd and Au catalysts. Conditions: 20 mL xylene, 0.10 g biphenyl, 2.00 mmol benzyl alcohol, 50 mg catalyst, 2 h reflux in O_2 atmosphere.

	10%Ag/SiO_2	1%Au/ZnO	1%Au/Al_2O_3	1%Au/TiO_2	0.5%Pd/Al_2O_3
Conv. (%)	6	45	72	24	81
Sel. (%)	> 99	90	90	91	67
Catalyst with CeO_2 (25 mg)					
Conv. (%)	98	75	77	39	94[a]
Sel. (%)	95	93	93	99	58[a]

[a] Reaction time: 30 min.

Table 3-8: Comparison of reaction rate constants based on the conversion of *para*-substituted benzyl alcohols with respect to benzyl alcohol. Reaction conditions: xylene 20.0 mL, 2.00 mmol benzyl alcohol, 2.00 mmol *p*-substituted benzyl alcohol, biphenyl 0.10 g, 100 mg 10%Ag/SiO_2, 50 mg CeO_2, reflux in oxygen atmosphere.

para-substituent	-CF_3	-Cl	-OMe
k_X/k_H[a]	0.18	0.24	1.6

[a] Ratio of 1st-order rate constants based on the conversion of *p*-substituted benzyl alcohol (k_X) and benzyl alcohol (k_H).

3.4 Discussion

In this study focus was laid on silver-based catalysts to investigate whether they can be used as alternatives for other noble metal catalysts such as the recently widely reported gold-based catalysts. By screening several catalysts simultaneously in one batch, a Ag/SiO_2 catalyst was identified that acts as an efficient catalyst but only in the presence of ceria. Often such screening of catalysts is performed by parallel and even robot-controlled high-throughput units requiring sophisticated equipment [49, 50]. For the identification of new catalyst materials, however, qualitative results are often sufficient in preliminary studies which allows for a highly simplified test strategy. This simple test strategy can be regarded as an alternative to single catalyst testing requiring no special instrumentation. A similar approach is used in the split-pool method [51, 52]. However, inhibition or synergetic interactions between the catalyst materials cannot be excluded. In fact, a synergism between Ag/CeO_2 and Ag/SiO_2 calcined at 500 °C was found by using this screening strategy. This combination of catalysts led to a much higher conversion (> 35%, Table 3-1) than all the other supported silver catalysts which exhibited

only poor catalytic activity. A more detailed investigation showed that the use of CeO_2 instead of Ag/CeO_2 was sufficient.

The most effective catalyst was identified to be a 1:2 mixture of CeO_2 nanoparticles and 10 wt.-% Ag/SiO_2 calcined for 30 min at 500 °C. Ag/SiO_2 without CeO_2 reacted considerably slower (Table 3-7) and required harsher conditions to facilitate benzyl alcohol oxidation at which only poor selectivities are obtained [30]. Since the reaction products deactivated the catalyst, the substrate/catalyst ratio had to be adapted to achieve full conversion. Comparison of the optimized silver catalyst reported herein to standard gold and palladium catalysts showed that all catalysts became more active by addition of CeO_2 under the chosen reaction conditions (Table 3-7). Silver and palladium benefited more from the addition than the corresponding gold catalysts. Palladium became highly reactive with a low selectivity, the silver catalyst maintained its high selectivity at almost full conversion. In contrast, the latter gave hardly any conversion in the absence of CeO_2. In light of these studies, silver offers a worthy alternative to well-established noble metals especially when considering that silver is less expensive.

Unlike gold, which is catalytically active on many different supports [23] our screening experiments found a large number of silver catalysts to be virtually inactive under the chosen reaction conditions. This reflects the present status of the literature since there are significantly less reports on silver catalysts than for gold-based catalysts in selective oxidation reactions in liquid phase. It can be expected that silver was in metallic state on all supports after calcination above 600 °C. Since most catalysts gave conversions < 5% (Table 3-1) metallic silver alone cannot be the active phase. There are several points suggesting silver-oxygen species in mostly metallic silver particles play an important role. Silver strongly interacts with oxygen. The formation of different silver-oxygen species highly depends on the pretreatment conditions [44, 53-56] which play a key role in the gas phase oxidation of methanol [57, 58]. Silver oxygen species are classified corresponding to their thermal desorption behavior into α-oxygen (surface adsorbed), β-oxygen (bulk oxygen) and γ-oxygen (subsurface oxygen). On metallic silver the latter two species are formed at temperatures above 500 °C upon exposure with oxygen [55]. In a CO oxidation study [59, 60] Ag/SiO_2 exhibited higher Ag dispersion and therefore increased catalytic activity after low temperature hydrogen treatment. Under these reducing conditions, only γ-oxygen was stable. Since in the present study H_2 treatment neither had a negative nor positive effect on the catalyst activity, α- and β-oxygen species might not be required for catalytic activity leaving γ-oxygen as potentially necessary modifier of the silver surface. The general involvement of oxygen species is indicated by the virtual disagreement in particle size obtained from XRD, EXAFS and TEM. XRD and TEM

suggested an average volume-based particle size in the range of 30 nm making the particle size of less than 2 nm obtained from EXAFS data obviously highly underestimated. Intercalated oxygen species fitting well in the octahedral gaps of the fcc metal [56] could serve as an explanation. The increase in the Ag-Ag backscattering amplitude in EXAFS observed with increasing reaction time (and hence deactivation) indicates additionally that removal of Ag-O species might be at least one deactivation pathway.

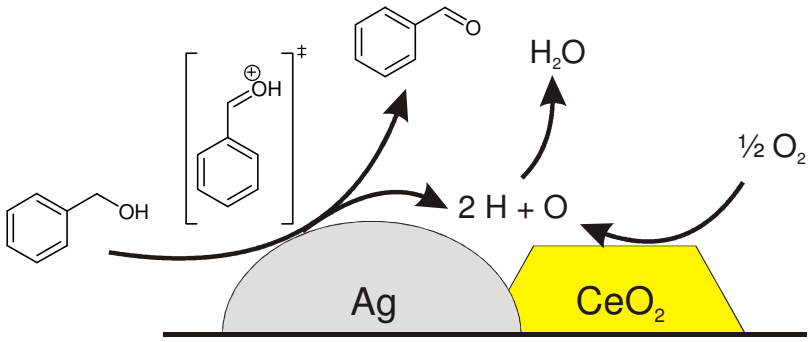

Figure 3-11: Schematic and simplified reaction mechanism. Benzyl alcohol oxidation occurs *via* adsorption of benzyl alcohol on silver, dehydrogenation at the silver surface followed by desorption of benzaldehyde. Hydrogen is removed from the silver surface by means of atomic oxygen provided by the CeO_2-silver interface.

An important finding is that the oxidation pathway did not involve homogeneous catalysis by dissolved cerium or silver species. The concentrations of both components as found with ICP-MS were low and a hot filtered solution did not continue reacting significantly, even when either CeO_2 or Ag/SiO_2 was added. In addition, only low conversions below 10 % were observed, when both CeO_2 and Ag/SiO_2 were separated from each other (and not well mixed). Finally, higher amounts of CeO_2 had a positive effect on the catalytic performance. Hence, like for other noble metals [61-64] alcohol oxidation occurs on the heterogeneous catalyst probably on the silver particles. As for gold [65] the higher reactivity of electron-rich benzyl alcohols suggests a positively charged reaction intermediate formed by hydride abstraction. Unlike silver-modified hydrotalcite [29], the presented catalyst requires oxygen to be catalytically active which emphasizes the role of CeO_2. A beneficial effect of ceria as a support material has been found before [20, 66-71]. The role of CeO_2 may be to act as an oxygen pool as it is capable of reversibly storing oxygen [72]. Figure 3-11 gives a schematic overview over the reactions occurring on the catalyst: after adsorption of benzyl alcohol on the silver surface the alcohol is dehydrogenated forming a cationic intermediate reacting further to benzaldehyde. CeO_2 activates molecular oxygen which reacts with hydrogen from benzyl alcohol thereby regenerating the silver surface. Thus, analogies between the liquid phase alcohol oxidation on silver and the extensively investigated oxidation on

palladium and gold catalysts appear reasonable. In future, further studies e.g. by ATR-IR as known for palladium catalysts [73-75] should be performed to corroborate the suggested mechanism, to understand the collaborative effect between silver and ceria in detail and to shed more light on the deactivation mechanism.

3.5 Conclusions

A variety of silver catalysts could be effectively screened for the selective oxidation of alcohols by a simple one batch approach for which different catalyst materials were mixed and tested together. In this way, a physical mixture of ceria nanoparticles and silver-impregnated silica was found to be catalytically active due to cooperative effects occurring during this screening approach. 10 wt.-% Ag/SiO_2 mixed with ceria nanoparticles in a ratio of 2:1 gave the best catalytic performance. An important parameter was the calcination temperature being optimal at 500 °C. This is probably due to the temperature dependency of the formation of metallic silver oxygen species which are likely to be involved in the catalytic process as indicated by EXAFS, XRD and TEM. At too high temperatures sintering of Ag particles may occur whereas at too low calcination temperatures mainly catalytically inactive oxidized silver species were obtained. The negative effect of electron withdrawing groups in the benzyl alcohol oxidation suggests a mechanism where metallic silver (as other noble metals) acts as main component for the dehydrogenation *via* a cationic intermediate. Dissolved cerium species as the origin of the promoting effect can be excluded. Its role can rather be ascribed to the activation of molecular oxygen. Comparing CeO_2 modified Ag/SiO_2 with Au and Pd catalysts, silver serves as a promising alternative being less expensive and both applicable to a wide variety of alcohols. Interestingly, a positive effect of CeO_2 was also found for Au and Pd catalysts. Therefore, further studies should be devoted to unraveling the promoting effect of ceria in the future.

3.6 References

[1] T. Mallat, A. Baiker, Catal. Today 19 (1994) 247.

[2] M. Besson, P. Gallezot, Catal. Today 57 (2000) 127.

[3] J. Muzart, Tetrahedron 59 (2003) 5789.

[4] K. Kaneda, K. Ebitani, T. Mizugaki, K. Mori, Bull. Chem. Soc. Jpn. 79 (2006) 981.

[5] A.S.K. Hashmi, G.J. Hutchings, Angew. Chem. Int. Ed. 45 (2006) 7896.

[6] A. Corma, H. Garcia, Chem. Soc. Rev. 37 (2008) 2096.

[7] G.J. Hutchings, Chem. Commun. (2008) 1148.

[8] P.L. Bragd, H. van Bekkum, A.C. Besemer, Top. Catal. 27 (2004) 49.

[9] M. Comotti, C. Della Pina, E. Falletta, M. Rossi, J. Catal. 244 (2006) 122.

[10] J.N. Chheda, G.W. Huber, J.A. Dumesic, Angew. Chem. Int. Ed. 46 (2007) 7164.

[11] R.A. Sheldon, I.W.C.E. Arends, Adv. Synth. Catal. 346 (2004) 1051.

[12] T. Mallat, A. Baiker, Chem. Rev. 104 (2004) 3037.

[13] T. Matsumoto, M. Ueno, N. Wang, S. Kobayashi, Chem. Asian J. 3 (2008) 196.

[14] T. Mallat, Z. Bodnar, A. Baiker, O. Greis, H. Strubig, A. Reller, J. Catal. 142 (1993) 237.

[15] Z. Opre, J.-D. Grunwaldt, M. Maciejewski, D. Ferri, T. Mallat, A. Baiker, J. Catal. 230 (2005) 406.

[16] M. Caravati, J.-D. Grunwaldt, A. Baiker, Catal. Today 91-92 (2004) 1.

[17] D.I. Enache, J.K. Edwards, P. Landon, B. Solsona-Espriu, A.F. Carley, A.A. Herzing, M. Watanabe, C.J. Kiely, D.W. Knight, G.J. Hutchings, Science 311 (2006) 362.

[18] H. Miyamura, R. Matsubara, Y. Miyazaki, S. Kobayashi, Angew. Chem. Int. Ed. 46 (2007) 4151.

[19] P. Haider, B. Kimmerle, F. Krumeich, W. Kleist, J.-D. Grunwaldt, A. Baiker, Catal. Lett. 125 (2008) 169.

[20] A. Abad, P. Concepcion, A. Corma, H. Garcia, Angew. Chem. Int. Ed. 44 (2005) 4066.

[21] S. Marx, A. Baiker, J. Phys. Chem. C 113 (2009) 6191.

[22] N. Dimitratos, J.A. Lopez-Sanchez, D. Morgan, A.F. Carley, R. Tiruvalam, C.J. Kiely, D. Bethell, G.J. Hutchings, Phys. Chem. Chem. Phys. 11 (2009) 5142.

[23] C. Della Pina, E. Falletta, L. Prati, M. Rossi, Chem. Soc. Rev. 37 (2008) 2077.

[24] C.H. Christensen, B. Jorgensen, J. Rass-Hansen, K. Egeblad, R. Madsen, S.K. Klitgaard, S.M. Hansen, M.R. Hansen, H.C. Andersen, A. Riisager, Angew. Chem. Int. Ed. 45 (2006) 4648.

[25] B. Jorgensen, S.E. Christiansen, M.L.D. Thomsen, C.H. Christensen, J. Catal. 251 (2007) 332.

[26] L.F. Liotta, A.M. Venezia, G. Deganello, A. Longo, A. Martorana, Z. Schay, L. Guczi, Catal. Today 66 (2001) 271.

[27] P. Nagaraju, M. Balaraju, K.M. Reddy, P.S. Sai Prasad, N. Lingaiah, Catal. Commun. 9 (2008) 1389.

[28] S. Rakovsky, S. Nikolova, L. Dimitrov, L. Minchev, J. Ilkova, Oxidation Commun. 18 (1995) 407.

[29] T. Mitsudome, Y. Mikami, H. Funai, T. Mizugaki, K. Jitsukawa, K. Kaneda, Angew. Chem. Int. Ed. 47 (2008) 138.

[30] F. Adam, A.E. Ahmed, S.L. Min, J. Porous Mat. 15 (2008) 433.

[31] X.E. Verykios, F.P. Stein, R.W. Coughlin, Cat. Rev. Sci. Eng. 22 (1980) 197.

[32] H. Sperber, Chem. Ing. Tech. 41 (1969) 962.

[33] T. Nishiguchi, F. Asano, J. Org. Chem. 54 (1989) 1531.

[34] M. Fetizon, M. Golfier, Acad. Sci. Ser. C 267 (1968) 900.

[35] F.J. Kakis, M. Fetizon, Douchkin.N, M. Golfier, P. Mourgues, T. Prange, J. Org. Chem. 39 (1974) 523.

[36] J.-D. Grunwaldt, M. Caravati, S. Hannemann, A. Baiker, Phys. Chem. Chem. Phys. 6 (2004) 3037.

[37] T. Ressler, J. Synchrotron Radiat. 5 (1998) 118.

[38] S.I. Zabinsky, J.J. Rehr, A. Ankudinov, R.C. Albers, M.J. Eller, Phys. Rev. B 52 (1995) 2995.

[39] A. Jentys, Phys. Chem. Chem. Phys. 1 (1999) 4059.

[40] M. Burgener, T. Tyszewski, D. Ferri, T. Mallat, A. Baiker, Appl. Catal. A 299 (2006) 66.

[41] B. Kimmerle, J.-D. Grunwaldt, A. Baiker, Top. Catal. 44 (2007) 285.

[42] H. Kimura, K. Tsuto, T. Wakisaka, Y. Kazumi, Y. Inaya, Appl. Catal. A 96 (1993) 217.

[43] M. Wenkin, P. Ruiz, B. Delmon, M. Devillers, J. Mol. Catal. A 180 (2002) 141.

[44] B. Pettinger, X. Bao, I. Wilcock, M. Muhler, R. Schlögl, G. Ertl, Angew. Chem. Int. Ed. 33 (1994) 85.

[45] B. Lengeler, Solid State Commun. 55 (1985) 679.

[46] B. Lengeler, Phys. Rev. Lett. 53 (1984) 74.

[47] S. Emura, K. Koto, A. Yoshiasa, H. Ito, S. Gonda, S. Mukai, J. Mater. Sci. Lett. 8 (1989) 1236.

[48] E.A. Stern, B.A. Bunker, S.M. Heald, Phys. Rev. B 21 (1980) 5521.

[49] T. Zech, G. Bohner, O. Laus, J. Klein, M. Fischer, Rev. Sci. Instrum. 76 (2005) 062215.

[50] D. Farrusseng, Surf. Sci. Rep. 63 (2008) 487.

[51] M.A. Aramendía, V. Borau, C. Jiménez, J.M. Marinas, F.J. Romero, F.J. Urbano, J. Catal. 209 (2002) 413.

[52] Y.P. Sun, B.C. Chan, R. Ramnarayanan, W.M. Leventry, T.E. Mallouk, S.R. Bare, R.R. Willis, J. Comb. Chem. 4 (2002) 569.

[53] C. Rehren, G. Isaac, R. Schlögl, G. Ertl, Catal. Lett. 11 (1991) 253.

[54] C. Rehren, M. Muhler, X. Bao, R. Schlögl, G. Ertl, Z. Phys. Chem. 174 (1991) 11.

[55] X. Bao, M. Muhler, B. Pettinger, R. Schlögl, G. Ertl, Catal. Lett. 22 (1993) 215.

[56] A.J. Nagy, G. Mestl, D. Herein, G. Weinberg, E. Kitzelmann, F. Schlogl, J. Catal. 182 (1999) 417.

[57] H. Schubert, U. Tegtmeyer, D. Herein, X. Bao, M. Muhler, R. Schlogl, Catal. Lett. 33 (1995) 305.

[58] X. Bao, M. Muhler, R. Schlögl, G. Ertl, Catal. Lett. 32 (1995) 185.

[59] Z.P. Qu, W.X. Huang, M.J. Cheng, X.H. Bao, J. Phys. Chem. B 109 (2005) 15842.

[60] Z.P. Qu, M.J. Cheng, W.X. Huang, X.H. Bao, J. Catal. 229 (2005) 446.

[61] M. Caravati, J.-D. Grunwaldt, A. Baiker, Phys. Chem. Chem. Phys. 7 (2005) 278.

[62] C. Keresszegi, T. Burgi, T. Mallat, A. Baiker, J. Catal. 211 (2002) 244.

[63] A. Abad, A. Corma, H. Garcia, Chem. Eur. J. 14 (2008) 212.

[64] J.-D. Grunwaldt, M. Caravati, A. Baiker, J. Phys. Chem. B 110 (2006) 25586.

[65] P. Fristrup, L.B. Johansen, C.H. Christensen, Catal. Lett. 120 (2008) 184.

[66] A.N. Pestryakov, Catal. Lett. 28 (1996) 239.

[67] A.N. Pestryakov, N.E. Bogdanchikova, A. Knop-Gericke, Catal. Today 91-92 (2004) 49.

[68] P.R. Sarode, K.R. Priolkar, P. Bera, M.S. Hegde, S. Emura, R. Kumashiro, Mater. Res. Bull. 37 (2002) 1679.

[69] S. Imamura, H. Yamada, K. Utani, Appl. Catal. A 192 (2000) 221.

[70] K. Ebitani, H.-B. Ji, T. Mizugaki, K. Kaneda, J. Mol. Catal. A 212 (2004) 161.

[71] L. Kundakovic, M. Flytzani-Stephanopoulos, J. Catal. 179 (1998) 203.

[72] A. Trovarelli, G.J. Hutchings (Ed.), “Catalysis by ceria and related materials”, Imperial College Press, London, 2002.

[73] T. Burgi, M. Bieri, J. Phys. Chem. B 108 (2004) 13364.

[74] C. Keresszegi, D. Ferri, T. Mallat, A. Baiker, J. Phys. Chem. B 109 (2005) 958.

[75] C. Mondelli, D. Ferri, J.-D. Grunwaldt, F. Krumeich, S. Mangold, R. Psaro, A. Baiker, J. Catal. 252 (2007) 77.

Chapter 4

Selective Side-Chain Oxidation of Alkyl Aromatic Compounds Catalyzed by Cerium Modified Silver Catalysts

Abstract

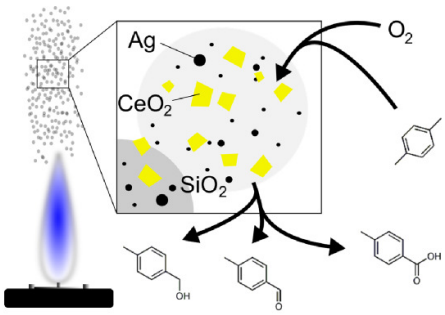

Flame made silver catalysts.

Silver supported on silica was found to effectively catalyze the aerobic side-chain oxidation of alkyl aromatic compounds under solvent-free conditions. Toluene, *p*-xylene, ethylbenzene and cumene were investigated as model substrates. Typically, the reaction was performed at ambient pressure; only for toluene an elevated pressure was required. Carboxylic acids, such as benzoic acid or *p*-toluic acid, additionally increased the reaction rate while CeO_2 could act both as a promoter and an inhibitor depending on the substrate and the reaction conditions. Silver catalysts were prepared both by standard impregnation and flame spray pyrolysis. Addition of a Ce precursor to the FSP catalyst resulted in significantly smaller silver particles. Ce-doped FSP catalysts in general exhibited higher catalytic performance with TONs up to 2000 except for cumene oxidation that appeared to proceed mainly by homogeneous catalysis. In addition, flame-made catalysts were more stable against silver leaching compared to the impregnated catalysts. The structure of the silver catalysts was studied in detail both by X-ray absorption spectroscopy and transmission electron microscopy suggesting metallic silver to be required for catalytic activity. Catalytic studies point to a radical mechanism which differs depending on the type of substrate.

4.1 Introduction

Selective catalytic oxidation by inexpensive reagents such as oxygen, hydrogen peroxide or *t*-butyl hydroperoxide is a viable way of introducing functional groups and thereby upgrading saturated and unsaturated hydrocarbons [1-3]. Finding catalytic systems for these oxidation reactions is of significant industrial importance [4], e.g. for *p*-xylene and cyclohexane oxidation to terephthalic acid and adipinic acid, respectively, which are monomers for commodity polymers [5]. The high industrial impact is also reflected by the large amount of related patent literature [e.g. 6-8]. Nevertheless, these catalytic oxidation reactions still require harsh conditions in industry [4]. As an example, a very effective but highly corrosive and environmentally harmful homogeneous Co/Mn/Br system is employed for *p*-xylene oxidation [9] in liquid phase using acetic acid as solvent which is partly decomposed during reaction. The oxidation follows a radical chain mechanism with the transition metal promoting the chain initiation and the decomposition of peroxo-species [4, 9].

Active catalysts for the selective side-chain oxidation of alkyl aromatic compounds are reported mainly for liquid phase oxidations. Only a few examples are reported in the gas phase [10-12] or in supercritical media [13, 14]. The selective liquid phase oxidation can be conducted both homogeneously and heterogeneously involving mostly metals with two or more stable oxidation states typically under acidic conditions. Most catalytic systems are based on Co often modified with Mn and a Br source [9, 15, 16] but other examples based on e.g. Pt [17] and Cu [18, 19] are also known. Typical oxidizing agents are organic peroxides, hydrogen peroxide, and oxygen offering a cost-effective route to important industrial intermediates such as benzoic acid, acetophenone, benzophenone, toluic acid etc. [5]. Interestingly, ring and side chain oxidation can be controlled by the choice of oxidant [20, 21]. Due to the relative inertness of the corresponding C-H bonds, the reactions are often performed at high pressure and in an additional solvent. Avoiding elevated pressures and working under neat conditions would be the next steps to render the oxidation process more cost-efficient.

Based on the homogeneous Co/Mn/Br system used in the AMOCO process many heterogeneous catalysts employ Co as a catalytically active metal. In the present study, the potential of silver as an active material is further investigated after showing considerable activity as an alcohol oxidation catalyst in previous studies [22] (*cf.* Chapter 3). The impregnation route for catalyst synthesis used previously left considerable potential for improvement as it afforded a broad silver particle size distribution with particles ranging from a few nm up to 50 nm. Flame spray pyrolysis (FSP) has extensively been studied for the preparation of different metal oxide catalysts [23, 24] as well as supported noble metal catalysts often affording high metal dispersions with particle sizes of less than 5 nm on the support [25]. In this

way, a good mixing of the oxide particles can be achieved. Therefore, the Ag/SiO_2-CeO_2 catalyst system was not only prepared by impregnation but also by single-step flame spray pyrolysis and investigated for its potential for the oxidation of aryl aromatic compounds. Comparing Ag/CeO_2-SiO_2 catalysts made by these two routes, the FSP-made catalysts exhibited an improved performance even at significantly lower silver loadings for the oxidation of toluene, *p*-xylene, ethylbenzene and cumene. The structure was further elucidated by X-ray absorption spectroscopy (XAS) and transmission electron microscopy (TEM).

4.2 Experimental

4.2.1 Catalyst synthesis

The impregnated catalyst was prepared by adding 25.0 mL of an aqueous $AgNO_3$ (Fluka, >99.5 %) solution (31 mg/mL) to 5.00 g of SiO_2 (Aerosil 200, Degussa, 200 m^2/g) resulting in a $Ag:SiO_2$ ratio of 1:10. The mixture was stirred with a glass rod and sonicated for 1 h. After drying at 80 °C for 24 h the catalyst was calcined in air at 900 °C for 1 h in a muffle oven controlled by a Eurotherm 904 controller. The catalyst is denoted as $^{imp}10\%Ag/SiO_2$-900.

For catalysts made by flame spray pyrolysis, silver nitrate (Fluka, >99.5 %) dissolved in ethanol (EtOH) and diethyleneglycol-monobutylether (DEGME, Fluka, >98 %; 1:1, Ag 0.5 M), hexamethylsiloxane (HMDSO, Fluka >98 %) and cerium-2-ethylhexanoate (40 % Ce w/v, Strem) were used as silver, silica and ceria precursors, respectively. The appropriate amounts of the above mentioned precursor solutions were mixed with solvents, i.e. DEGME (Fluka, >98 %) and 2-ethylhexanoic acid (Aldrich, >98 %) while keeping the solvent composition constant at 1:1 by volume. The total support metal (Si + Ce) concentration was kept constant at 0.6 M in these solutions. The nominal CeO_2 weight fraction in the product powder ranged from 0 to 50 wt.-%. The silver precursor was added accordingly to reach a nominal 1 wt.-%- Ag loading in the final powder product. The Ag/CeO_2-SiO_2 powders were produced in a laboratory scale FSP reactor as described elsewhere [26]. The liquid and dispersion gas feed rate were kept constant at 5 mL/min and 5 L/min, respectively. The pressure drop above the nozzle was adjusted to 1.7 bar and a sheath gas flow of 5 L/min O_2 was applied through a metal ring (11 mm i.d., 18 mm o.d.) with 32 holes (0.8 mm i.d.) to ensure complete combustion of the precursor. The powders were collected with the aid of a vacuum pump (Busch SV 1025 B) on a glass microfiber filter (Whatman GF/D, 257 mm in diameter). The catalysts are denoted as $^{FSP}1\%Ag/SiO_2$ $^{FSP}1\%Ag/10\%CeO_2$-SiO_2, $^{FSP}1\%Ag/30\%CeO_2$-SiO_2 and $^{FSP}1\%Ag/50\%CeO_2$-SiO_2, respectively. Details are given in Table 4-1. Flame spray pyrolysis was performed by Björn Schimmöller (ETH Zürich).

Table 4-1: Overview over the silver catalysts prepared by flame spray pyrolysis and impregnation.

Catalyst	Ag (wt.-%)	CeO_2 (wt.-%)	SiO_2 (wt.-%)	SSA (m^2/g)[a]	CeO_2 crystal size[b] (nm)	Ag crystal size[b] (nm)	Entry
^{FSP}1%Ag/SiO_2	1	0	100	293	-	n.d.[c]	1
^{FSP}1%Ag/10%CeO_2-SiO_2	1	10	90	273	3.3	n.d.[c]	2
^{FSP}1%Ag/30%CeO_2-SiO_2	1	30	70	194	5.8	n.d.[c]	3
^{FSP}1%Ag/50%CeO_2-SiO_2	1	50	50	152	8.3	n.d.[c]	4
^{imp}10%Ag/SiO_2-900	10	0	100	128	-	43	5

[a]Determined by nitrogen adsorption. [b]Determined by XRD. [c]Not detectable.

4.2.2 Catalyst testing

Catalyst tests were performed in a three-necked flask equipped with a gas inlet and a reflux condenser with *p*-xylene (Sigma-Aldrich >99 %), ethylbenzene (Fluka, >99 %) or cumene (Fluka, 98 %) as substrates with and without CeO_2 nanoparticles (Aldrich, <25 nm), and benzoic acid (Sigma-Aldrich, 99 %) or *p*-toluic acid (Aldrich, 98 %). In a typical experiment the flask was charged with 122 mmol of alkyl aromatic compound and 100 mg biphenyl (Sigma-Aldrich, 99.5 %) as internal standard. Biphenyl was unreactive under the applied reaction conditions, i.e. its presence did not give any additional peaks in the gas chromatogram. The flask was equipped with a magnetic stir bar and placed in an oil bath heated to 140 °C which led to a temperature of the reaction mixture of ca. 135 °C. The mixture was saturated with oxygen (AGA, grade 5.0) via the gas inlet and equilibrated for 1.5 h to ensure a uniform standard and substrate distribution under vigorous stirring (800 rpm). Benzoic acid (0.45 g, 3.7 mmol, 3.0 mol-% with respect to the hydrocarbon; for ethylbenzene and cumene oxidation) and *p*-toluic acid (0.50 g, 3.7 mmol, 3.0 mol-% with respect to the hydrocarbon; for *p*-xylene oxidation), respectively, were added. After 5 min a sample was taken for GC analysis and the reaction was started by adding 100 mg catalyst and optionally 50 mg CeO_2 (Aldrich, < 25 nm) for catalysts not already containing CeO_2.

Analysis was carried out after 1 h, 2 h and 3 h, respectively, by means of an Agilent 6890 N gas chromatograph (GC) equipped with a 7683 B series autosampler, a flame ionization detector and a HP-5 column using biphenyl as internal standard. The following temperature programs were used for product analysis: inlet temperature 250 °C; oven: 110 °C, hold for 10 min; ramp to 120 °C (5 °C/min); ramp to 300 °C (40 °C/min); 300 °C, 2 min; the analysis of hydroperoxides was performed at lower temperatures to ensure minimal decomposition during analysis: inlet temperature 100 °C; oven: 80 °C, hold for 10 min; ramp to 120 °C (5 °C/min); ramp to 300 °C (40 °C/min); 300 °C, 2 min. Products were identified by GC-mass spectrometry (MS). Individual response factors were obtained from commercial compounds,

i.e. cumene hydroperoxide (Aldrich, 80 % in cumene), *p*-methyl benzyl alcohol (Aldrich, 98 %, *p*-methyl benzaldehyde (Aldrich, 97 %), benzaldehyde (Aldrich, >99 %), benzyl alcohol (SAFC, >99 %), 2-phenyl-2-propanol (Aldrich, 97 %), acetophenone (Aldrich, 99 %) and 1-phenyl ethanol (Aldrich, 98 %). Ethylbenzene hydroperoxide was synthesized according to ref. [27] and the response factor determined from a mixture of 1-phenylethanol and ethylbenzene hydroperoxide.

Since starting material was lost during the reaction despite using reflux condensers, yields rather than conversions and selectivities are presented from which TONs are calculated on the basis of the total amount of silver. In general, results were reproducible within an error margin of 5-10 %. Toluene required higher temperatures than its boiling point, thus, toluene oxidation was done in an autoclave view cell (NWA GmbH, Lörrach). The autoclave was charged with 13.0 mL toluene (122 mmol), 100 mg biphenyl, 0.45 g benzoic acid, 50 mg CeO_2 and 100 mg ^{imp}10%Ag/SiO_2-900. A sample for GC analysis was taken, the autoclave was sealed and the 50 mL residual volume charged with air (10 bar, 4.2 mmol O_2). The autoclave was heated up while stirring. After 1 h at the desired temperature the autoclave was cooled and opened after carefully releasing the overpressure followed by sampling for GC analysis.

4.2.3 Catalyst characterization

X-ray absorption near edge structure (XANES) / extended X-ray absorption fine structure (EXAFS): X-ray absorption spectroscopy (XAS) was measured at beamline X1 at the Hamburger Synchrotronstrahlungslabor (HASYLAB) at the Deutsche Elektronen-Synchrotron (DESY, Hamburg). XAS spectra for silver were recorded in step-scanning mode around the Ag-K edge (E = 25.514 keV) with a Si(311) double crystal monochromator in transmission mode and a silver foil for energy calibration. EXAFS spectra were processed by energy-calibration, background subtraction, deglitching, normalization and Fourier-transformed after k^3-weigthing using the WinXAS 3.1 software [28]. EXAFS data fitting was performed in R-space taking only single scattering paths within the first Ag-Ag or Ag-O shells into account. EXAFS data were fitted with a damping factor obtained from silver foil of 0.85. Scattering amplitudes and phase shifts were calculated with the FEFF 7.0 code [29].

X-ray diffraction (XRD): The XRD patterns were collected with an X'Pert PRO Diffractometer (PANalytical) with a Cu-K_α X-ray source operated at 45 kV and 40 mA equipped with a Ni filter and a slit. Diffractograms were recorded between 2θ (Cu-K_α) = 20° to 90° with a step width of 0.00164°. The crystallite size was estimated from Rietveld refinement using a Windows-adapted version of the LHMP program [30].

Inductively-coupled plasma mass spectrometry (ICP-MS): The concentrations of cerium and silver in solution were measured by ICP-MS (Perkin-Elmer Elan 6000) equipped with a cross-flow nebulizer. The plasma Ar flow was set to 13 L/min at 800 W RF power and the nebulizer Ar flow was set to 0.80 L/min. The sample solution was injected at a flow rate of 3.0 mL/min. Quantification of Ce and Ag was performed by using multielement ICP-MS standard solutions (Fluka). Samples for ICP-MS were prepared via filtering of a hot solution obtained after 3 h reaction time through preheated celite. An aliquot of 1.0 mL of the filtrate was taken. Volatile compounds were removed at 120 °C in vacuo overnight. The residual was treated with 3.5 mL concentrated HNO_3 (Merck, *p.a.*), 0.5 mL HCl (Merck, *p.a.*) followed by 2 mL double distilled water and digestion in an Anton Paar Microwave Digestion System Multiwave 3000. The solution was neutralized with ammonium hydroxide solution (Sigma-Aldrich, 28-30 %), filtered, and diluted with distilled water. The overall dilution ratio was 1:500.

Gas adsorption: The specific surface area (SSA) of the catalyst particles were determined by N_2 adsorption at 77K using the BET method (Micromeritics Tristar 3000, 5-point isotherm, $0.05 < p/p_0 < 0.25$).

Transmission electron microscopy (TEM): TEM images were acquired on an FEI Tecnai T20 microscope equipped with a W-filament as electron source operated at 200kV. High resolution (HR)-TEM images were taken on an FEI Titan 80-300 microscope operated at 300kV. Catalyst samples were dispersed in dry form on lacey carbon film supported on Cu grids. Sample agglomerates overlapping the holes in the support film were imaged using a Gatan US1000 CCD camera. Crystal lattice spacings and particle sizes were analyzed using the Digital Micrograph version GMS 1.8 software package from Gatan Inc.

4.3 Results

4.3.1 Catalytic side chain oxidation of *p*-xylene by impregnated Ag/SiO_2

The oxidation of *p*-xylene with an impregnated silica supported Ag catalyst (^{imp}10%Ag/SiO_2-900) in the absence of any solvent resulted in the formation of *p*-methylbenzyl alcohol, *p*-methylbenzaldehyde and *p*-toluic acid at about 3 % yield at 140 °C after 3 h (Scheme 4-1 and Figure 4-1) which corresponds to a TON of 43 based on the overall amount of silver. Note, that at this point TONs only serve as a performance comparison being microscopically seen not relevant as the reaction is presumably based on a radical autoxidation mechanism. The addition of CeO_2 nanoparticles and a carboxylic acid more than doubled the overall catalytic performance resulting in a combined yield of 7 % after 3 h (TON 100).

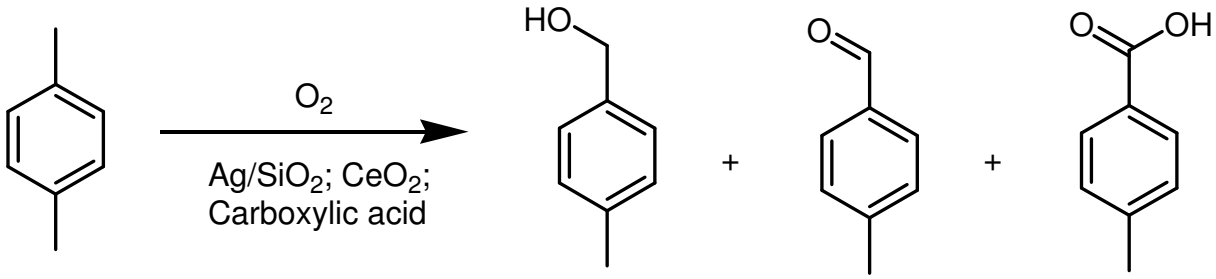

Scheme 4-1: Oxidation of *p*-xylene with molecular oxygen catalyzed by Ag/SiO_2 in the presence of ceria and a carboxylic acid.

Table 4-2: Oxidation of *p*-xylene with silver catalysts in the presence of CeO_2 and carboxylic acid. Reaction conditions: 122 mmol *p*-xylene, 3 mol-% *p*-toluic acid, 100 mg biphenyl, 100 mg catalyst, oxygen atmosphere, 140 °C, 3 h reaction time.

Catalyst	Yields (%)				TON[a]	Entry
	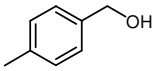	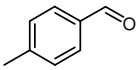	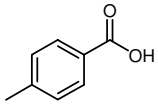	Combined		
$^{imp}10\%Ag/SiO_2$-900[b]	2.1	2.1	2.8	7.0	100	1
$^{imp}10\%Ag/SiO_2$-900[b,c]	2.0	2.0	2.8	6.8	100	2
$^{FSP}1\%Ag/SiO_2$[b]	0.4	0.6	0.2	1.2	160	3
$^{FSP}1\%Ag/10\%CeO_2$-SiO_2	3.0	2.6	7.8	13.4	1800	4
$^{FSP}1\%Ag/10\%CeO_2$-SiO_2[d]	2.3	2.1	3.3	7.7	1000	5
$^{FSP}1\%Ag/30\%CeO_2$-SiO_2	2.8	2.5	5.2	10.5	1400	6
$^{FSP}1\%Ag/50\%CeO_2$-SiO_2	2.4	2.2	3.8	8.4	1100	7
SiO_2[b]	0.2	0.3	0.3	0.8	-	8

[a]Based on the number of product molecules with respect to the total amount of silver during one experiment. [b]50 mg CeO_2 added. [c]3 mol-% benzoic acid used instead of *p*-toluic acid. [d]1st re-use.

No difference between benzoic acid and *p*-toluic acid could be found with respect to the catalytic performance (Table 4-2, entry 1 and 2). As underlined by reaction Scheme 4-1, the second methyl group remained untouched due to the deactivating effect of the electron withdrawing substituent. Some

p-xylene hydroperoxide as an intermediate reaction product was also observed (less than 0.5 %) but no pertoluic acid. Note that the reaction also proceeded in the absence of light in contrast to other examples found in the literature [31, 32]. Figure 4-2 depicts the typical development of the products during the reaction. After a short induction period *p*-methylbenzyl alcohol and *p*-methylbenzaldeyhde were formed at approximately the same rate. Hence, both compounds are presumably formed simultaneously (though not necessarily in the same step) and hardly by successive oxidation. The formation of *p*-toluic acid was first detected after an induction period. Thus, *p*-toluic acid was formed *via* one (or more) of the intermediates, e.g. by reaction between aldehyde and peroxide.

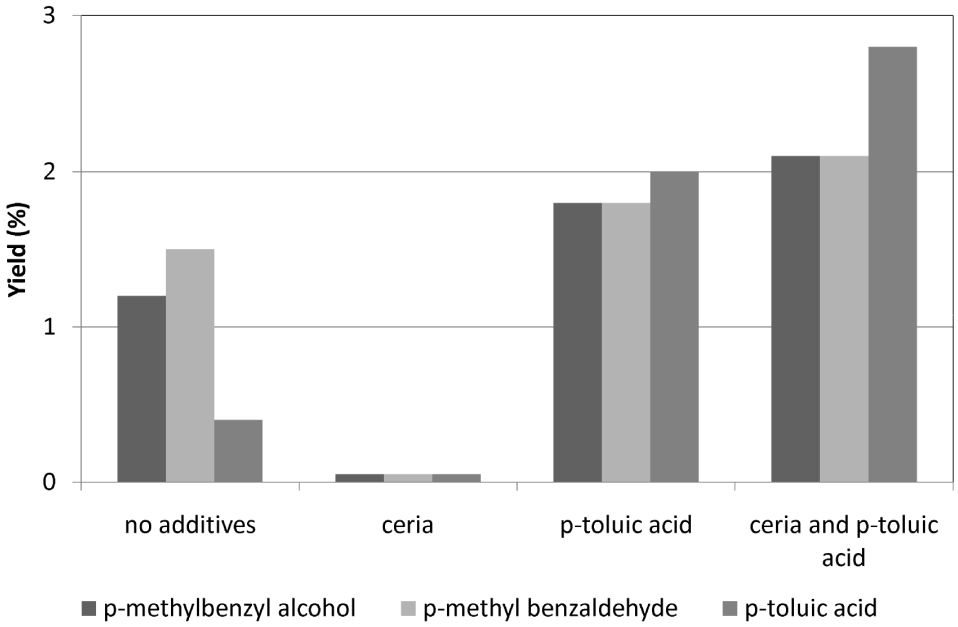

Figure 4-1: Influence of carboxylic acid (*p*-toluic acid) and CeO_2 as additives on the oxidation of *p*-xylene. Reaction conditions: 122 mmol *p*-xylene, optionally 3 mol-% *p*-toluic acid and/or 50 mg CeO_2, 100 mg biphenyl, 100 mg ^{imp}10%Ag/SiO_2-900, oxygen atmosphere, 140 °C, 3 h reaction time.

Silver has a complex interaction with oxygen influencing the catalytic properties [33, 34]. Different silver oxygen species can be formed in an oxygen containing atmosphere depending on the calcination temperature [35, 36]. Therefore, the effect of the calcination temperature on the catalytic performance was studied (Figure 4-3). Within the temperature range investigated, the highest calcination temperature, i.e. 900 °C resulted in the most active silver catalyst with a significant increase in catalytic activity between 600 and 700 °C. After the high temperature treatment rather large silver

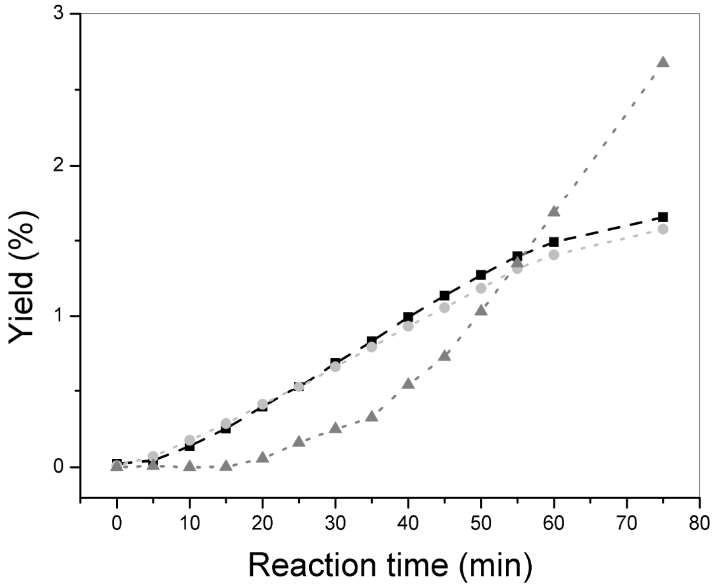

Figure 4-2: Formation of *p*-methylbenzyl alcohol (●), *p*-methylbenzaldehyde (■) and *p*-toluic acid (▲) during the oxidation of *p*-xylene with ^{FSP}1%Ag/10%CeO_2-SiO_2. Reaction conditions: 122 mmol *p*-xylene, 3 mol-% benzoic acid, 100 mg biphenyl, 100 mg ^{FSP}1%Ag/10%CeO_2-SiO_2, oxygen atmosphere, 140 °C.

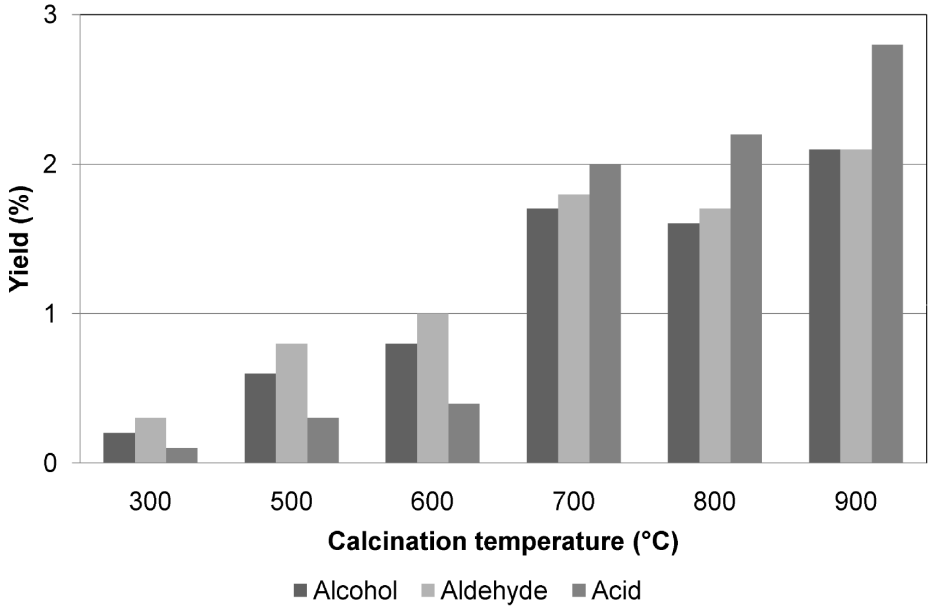

Figure 4-3: Yields of *p*-methylbenzyl alcohol, *p*-methylbenzaldehyde and *p*-toluic acid obtained during the oxidation of *p*-xylene with ^{imp}10%Ag/SiO_2 calcined for 1 h in air at temperatures between 300 °C and 900 °C in the presence of ceria and carboxylic acid. Reaction conditions: 122 mmol *p*-xylene, 3 mol-% *p*-toluenic acid, 100 mg biphenyl, 100 mg ^{imp}10%Ag/SiO_2 calcined in air as indicated, 50 mg CeO_2, oxygen atmosphere, 140 °C, 3 h reaction time.

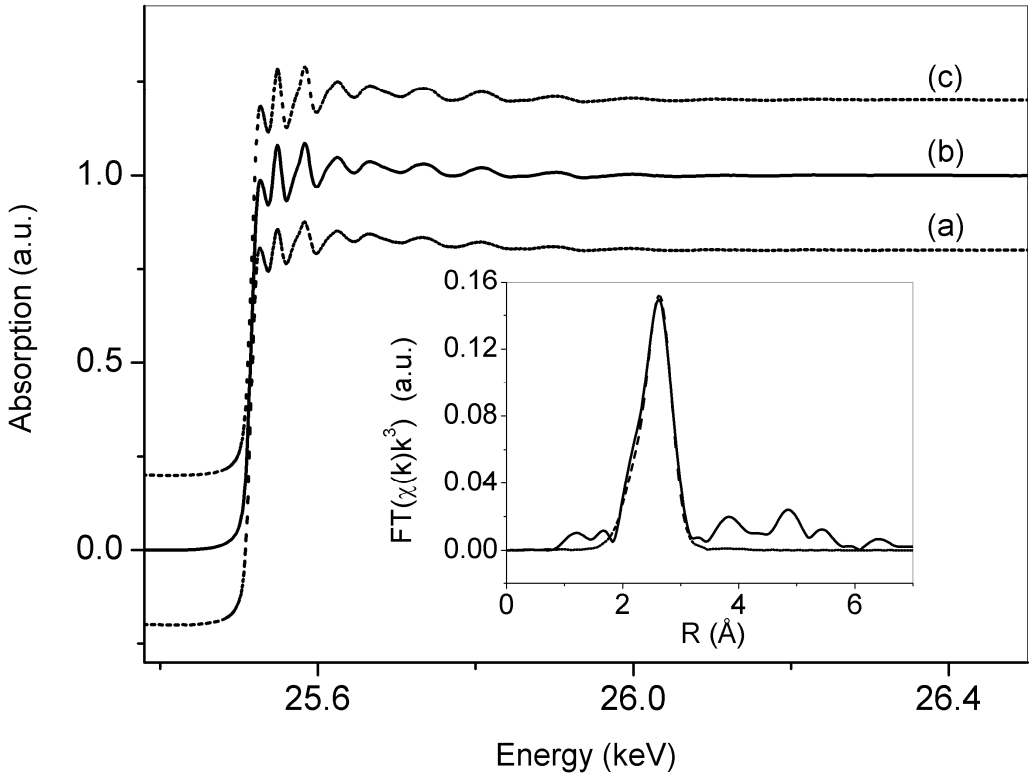

Figure 4-4: EXAFS spectrum of ^{imp}10%Ag/SiO_2 calcined at 500 °C (a), at 900 °C (b) and silver foil (c) recorded at the Ag K-edge. Note the smaller EXAFS oscillation amplitude in (a) compared to (b). Inset: Experimental (solid line) and 1st shell EXAFS data fitted (dashed line) FT EXAFS function of ^{imp}10%Ag/SiO_2-900 from k = 2-15 Å^{-1}.

particles with an average crystal size of 43 nm were observed from XRD analysis (not shown). These most active catalysts were used during further parametric studies. Extended X-ray absorption spectroscopy (EXAFS) revealed that silver was metallic (Figure 4-4) with no indication of oxidized silver suggesting metallic silver to be the active species. The 1st shell silver-silver coordination number of 12 obtained from EXAFS data fitting is in line with metallic silver particles > 5 nm and corroborates the XRD data. Calcination at 500 °C was previously investigated [22] (*cf.* Chapter 3) and resulted in a lower coordination number of 7.9 despite several large silver particles observed.

As described before, CeO_2 nanoparticles and carboxylic acid addition generally had a beneficial effect on the catalytic performance yielding more of the product acid. Also initial addition of the carboxylic acid only had a beneficial effect. Adding, however, CeO_2 nanoparticles alone to ^{imp}10%Ag/SiO_2-900 resulted in the formation of hardly any reaction products (Figure 4-1). This pinpoints to a radical autoxidation mechanism which is suppressed by CeO_2 nanoparticles known to have radical scavenger properties [37, 38]. This is an intriguing feature of ceria since it both promotes non-radical

oxidations [22, 39, 40] and is capable of increasing the selectivity by suppressing reactive radical species. Further evidence for a radical mechanism was found by suppression of *p*-xylene oxidation by either 2,6-di(*tert.*-butyl)phenol or 2,2,6,6-tetramethylpiperodine-1-oxyl (TEMPO) which also can act as a radical scavenger [41]. When investigating the Ag/SiO_2-CeO_2-carboxylic acid system with the impregnated catalyst for leaching, the cerium concentration was below the limit of detection of 0.1 mg/L. In addition, a reaction mixture treated with CeO_2 and carboxylic acid for several hours did not show the promoting effect after filtration of CeO_2 and addition of the silver catalyst. Hence there is no indication for soluble cerium species to be responsible for the promoting effect. It must be added, however, that soluble Ce^{3+} (from Ce(III)ethylhexanoate) indeed promoted the reaction at a high concentration of 10 mg/L also in the absence of a carboxylic acid to result in an overall product yield of 9.5 % or a TON of 140 with respect to silver clearly demonstrating the beneficial effect of Ce. In contrast to the Ce concentration being below the limit of detection, a high silver concentration of 83 mg/L was found and raised the question whether silver promotes the oxidation reaction homogeneously or heterogeneously. Further tests showed that under non-reactive conditions, i.e. in the absence of carboxylic acid but with CeO_2, no silver leaching was observed (Ag concentration <1 mg/L). Hence, leaching is caused by the carboxylic acid and/or the reaction products. Removal of the catalyst by hot filtration almost completely stopped the catalytic reaction. Furthermore, the reaction was performed with silver benzoate as a soluble silver source instead of $^{imp}10\%Ag/SiO_2$-900 (Ag silver concentration of 300 mg/L). Despite the higher silver concentration compared to the leaching experiment, an overall yield of only 1.6 % was obtained compared to 7.0 % with $^{imp}10\%Ag/SiO_2$-900.

4.3.2 Comparison of impregnated catalysts with flame spray pyrolysis (FSP) derived catalysts

Ag/SiO_2 had previously been prepared by FSP resulting in rather large silver particles [42]. A number of CeO_2-SiO_2 supported silver catalysts were prepared without and with 10, 30 and 50 wt.-% CeO_2 (Table 4-1). An increasing fraction of CeO_2 decreased the surface area from 293 m^2/g without CeO_2 to 152 m^2/g with 50 % CeO_2 and additionally the ceria particle size increased with the ceria loading from 3 to 8 nm (obtained from XRD). High silver loadings of 5-10 wt.-% gave silver particles around 10 nm achieving only low overall yields of less than 2 % in the oxidation of *p*-xylene (not shown). No silver diffractions were found in the XRD patterns for CeO_2-SiO_2 materials with 1 wt.-% silver loading due to the low concentration. When tested for catalytic activity in the oxidation of *p*-xylene, FSP catalysts

containing CeO_2 both gave higher TONs and higher product yields than the impregnated catalyst (Table 4-2, *cf.* entries 4, 6, 7 with entry 1), with ^{FSP}1%Ag/10%CeO_2-SiO_2 as the most active catalyst (entry 4). Reusing the catalyst indicated catalyst deactivation (entry 5). ^{FSP}1%Ag/SiO_2 hardly gave higher yields (entry 3) than those obtained in the absence of silver (entry 8). Leaching studies on the mixtures after reaction with fresh ^{FSP}1%Ag/10%CeO_2-SiO_2 showed that the silver concentration was below the limit of detection (<1 mg/L) in contrast to the impregnated catalyst (83 mg/L, *vide supra*) even in the presence of carboxylic acid. The cerium concentration was again below the limit of detection (0.1 mg/L).

TEM analysis of ^{FSP}1%Ag/SiO_2 indicated large silver particles of up to 50 nm which might be a cause for the observed inferior catalytic activity (Figure 4-5a,b). Silica precursors with silver nitrate tend to form bimodal Ag distributions. Large Ag particles are discussed to form by droplet-to-particle

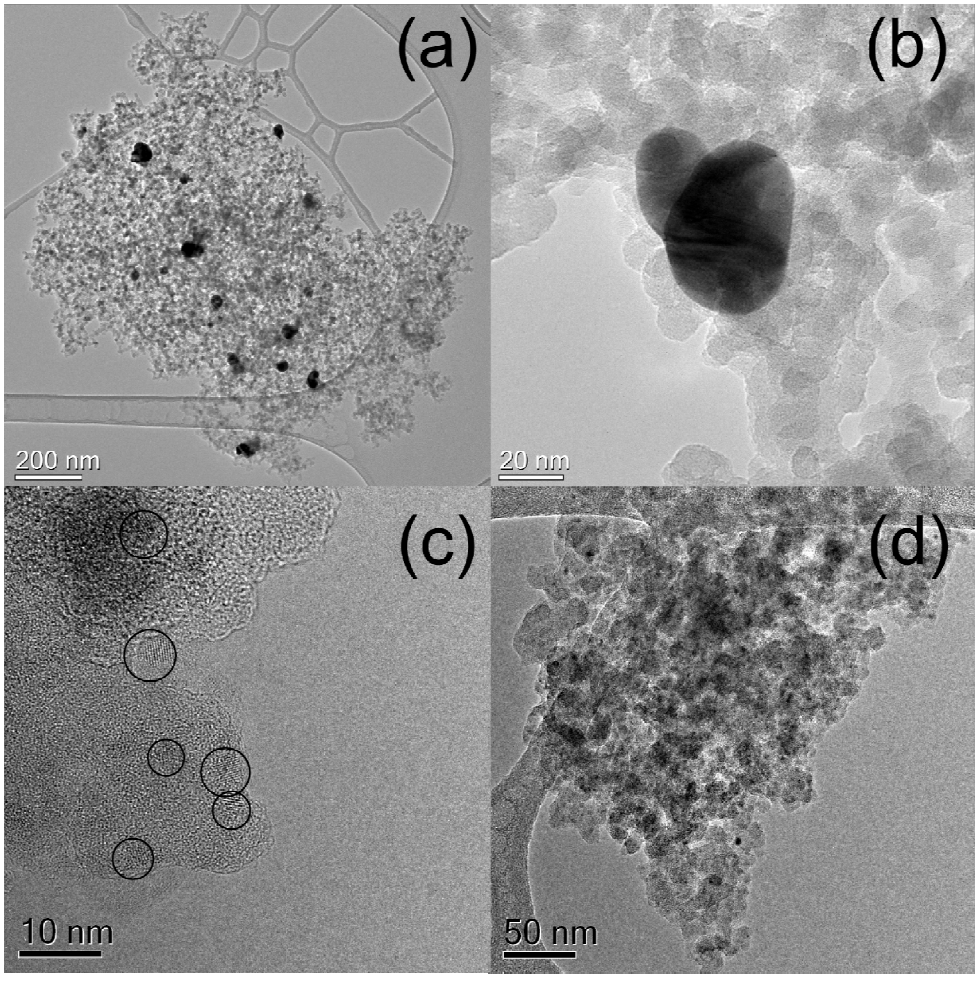

Figure 4-5: TEM images of fresh ^{FSP}1%Ag/SiO_2 (a,b) and fresh 1%Ag/10%CeO_2-SiO_2 (c,d). Dark spots represent silver particles. Circles indicate CeO_2 particles.

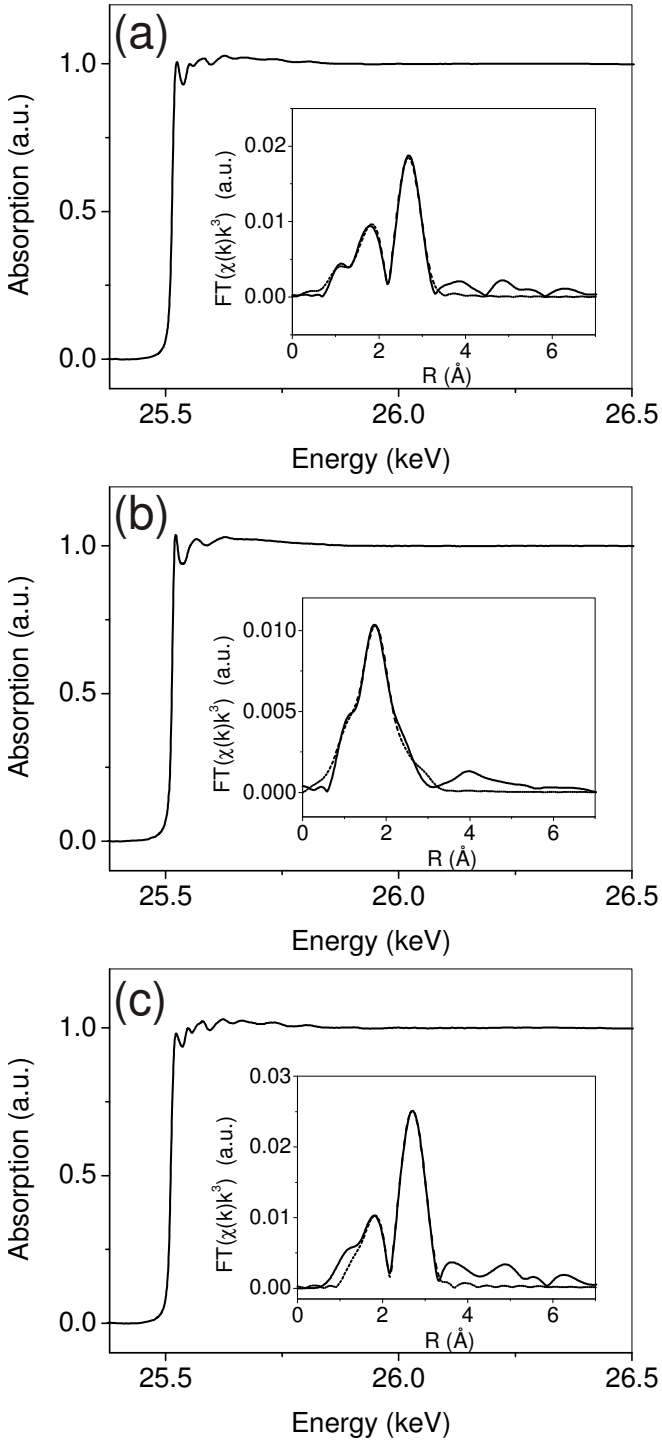

Figure 4-6: EXAFS spectra of flame synthesized ^{FSP}1%Ag/SiO_2 (a), ^{FSP}1%Ag/10%CeO_2-SiO_2 as prepared (b) and after the reaction (c) at the Ag K-edge. Insets: Experimental (solid line) and fitted (dashed line, EXAFS data fitting in R-space) k^3-weighted Fourier transformed EXAFS function.

conversion while fine Ag particles come from gas-to-particle conversion [26]. TEM images of ^{FSP}1%Ag/10%CeO_2-SiO_2 (Figure 4-5c,d) showed distinct CeO_2 nanoparticles with the size in the range as indicated by XRD (3 nm, Table 4-1). Similar morphologies of segregated crystal domains have been observed previously for FSP-made Ta_2O_5/SiO_2 [43] and TiO_2/SiO_2 synthesized in diffusion flames [44]. The presence of ceria allowed no clear determination of the silver particle size by TEM analysis but no large Ag particles with a size even close to that found for ^{FSP}1%Ag/SiO_2 were observed (*cf.* Figures 4-5a and d) indicating that the presence of ceria might have hindered the formation of such large Ag nanoparticles. The stabilizing effect of CeO_2 on the silver nanoparticles during synthesis might also be one cause for the pronounced difference in catalytic activity between doped and undoped catalysts. The Ag K-edge EXAFS spectrum of the impregnated catalyst showed mainly Ag-Ag backscattering contributions due to the metallic state of silver. In addition to a Ag-Ag shell, the FSP catalysts ^{FSP}1%Ag/SiO_2 and ^{FSP}1%Ag/10%CeO_2-SiO_2 also featured a Ag-O shell within the first coordination sphere (Figure 4-6). The as-prepared ^{FSP}1%Ag/SiO_2 catalyst showed both contributions of oxidized and reduced silver. The fitted silver-silver distance of 2.84 Å is close to that for bulk metallic silver (2.89 Å) while the silver-oxygen distance was fitted with 2.29 Å (Table 4-3, entry 2). Similar distances of 2.32 Å (Ag-O) and 2.81 Å (Ag-Ag) were also found for the ceria-doped catalyst ^{FSP}1%Ag/10%CeO_2-SiO_2 (entry 3). The low Ag-Ag distance especially in the latter case might be explained by the lattice contraction of metallic Ag

Table 4-3: Overview over structural parameter obtained from EXAFS data fitting.

Catalyst	Shell	N (±0.5)	R (Å)	σ (Å^{-2})	Residual	Entry
^{imp}10%Ag/SiO_2-900	Ag-Ag	12	2.86	0.010	6.7	1
^{FSP}1%Ag/SiO_2	Ag-O	1.7	2.29	0.016	1.5	2
	Ag-Ag	3.1	2.84	0.016		
^{FSP}1%Ag/10%CeO_2-SiO_2	Ag-O	3.8	2.32	0.022	5.1	3
	Ag-Ag	0.5	2.81	0.013		
^{FSP}1%Ag/10%CeO_2-SiO_2[a]	Ag-O	3.1	2.28	0.030	1.7	4
	Ag-Ag	3.8	2.85	0.010		
Ag_2O	Ag-O	2	2.07	0.003	9.4	5
	Ag-Ag	6	3.37	0.027		
Ag	Ag-Ag	12	2.86	0.009	2.3	6

[a]Used catalyst.

nanoparticles in the low nm-range [45]. The lower Ag-Ag coordination number of ^{FSP}1%Ag/10%CeO_2-SiO_2 compared to ^{FSP}1%Ag/SiO_2 is qualitatively in accordance with the smaller particle size found for the doped catalyst with TEM. However, due to the Ag-O contribution no further quantitative conclusions on the particle size can be drawn. The Ag-O distance in the range of 2.3 Å significantly differs from that found in Ag_2O being 2.047 Å from XRD [46] or 2.07 Å from EXAFS analysis (entry 5). Ag-O bond lengths between 2.2-2.6 Å are typical for silver silicates [47-50]. The high mixing and fast cooling in the flame could facilitate the atomic mixing of Ag and Si and so amorphous silver silicate formed under FSP conditions might indeed account for the observed Ag-O shell. Spent ^{FSP}1%Ag/10%CeO_2-SiO_2 (entry 4) has a lower but still appreciable catalytic activity compared to the fresh catalyst. The Ag-Ag backscattering contribution is higher, pointing to partial reduction of silver under reaction conditions indicating that oxidized silver species are at least partly present on the surface and not in the bulk silica. Possibly also sintering of silver nanoparticles <10 nm might occur as these are already very mobile at temperatures close to those applied in the catalytic reaction [51].

4.3.3 Extension to further alkyl aromatic compounds

Extending the study to other alkyl aromatic compounds, the oxidation of toluene, ethylbenzene and cumene was investigated. None of the catalysts was able to convert toluene to benzyl alcohol, benzaldehyde or benzoic acid under atmospheric pressure which is likely to be connected to the boiling point of toluene being ca. 30 °C lower than that of *p*-xylene and the absence of a second presumably activating methyl group. Thus, toluene oxidation was attempted in an autoclave both at 140 °C and 170 °C with the impregnated catalyst. Hardly any conversion was found at 140 °C but at 170 °C the reaction was completed after 1 h (Table 4-4) the limiting factor here being the amount of oxygen present in the reactor. Note that at this temperature thermal toluene autoxidation becomes relevant but proceeds at lower reaction rates [52].

The oxidation of ethylbenzene gave both 1-phenylethanol and acetophenone and additionally ethylbenzene hydroperoxide (Table 4-5), which are typical products for the radical (aut)oxidation of ethylbenzene [32, 53]. Compared to the oxidation of *p*-xylene, the effect of ceria was different. While for *p*-xylene, the impregnated catalyst was most active in the presence of ceria and carboxylic acid, ceria decreased the catalyst activity in the case of ethylbenzene (Figure 4-7a). Flame synthesized catalysts gave higher TONs of up to 2000 (Table 4-5, entry 2) compared to the impregnated catalyst but lower overall product yields.

Table 4-4: Oxidation of toluene with ^{imp}10%Ag/SiO_2-900 in the presence of ceria and carboxylic acid. Reaction conditions: 122 mmol toluene, 3 mol-% benzoic acid, 100 mg biphenyl, 100 mg ^{imp}10%Ag/SiO_2-900, 10 bar air (4.2 mmol O_2), temperature as indicated, 1 h reaction time.

	Yields (%)				
Reaction temperature	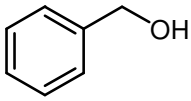	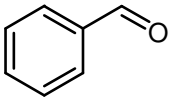	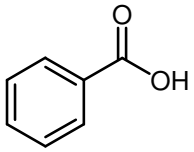	Combined	TON
140 °C	< 0.1	< 0.1	< 0.1	< 0.1	-
170 °C	1.1	1.0	0.5	2.6	34

Table 4-5: Oxidation of ethylbenzene with silver catalysts in the presence of CeO_2 and carboxylic acid. Reaction conditions: 122 mmol ethylbenzene, 3 mol-% benzoic acid, 100 mg biphenyl, 100 mg catalyst, oxygen atmosphere, reflux, 3 h reaction time.

Catalyst	Yields (%)				TON	Entry
	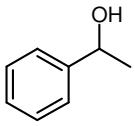	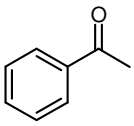	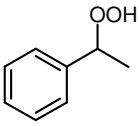	Combined		
^{imp}10%Ag/SiO_2-900	4.4	11.8	4.1	20.3	290	1
^{FSP}1%Ag/10%Ce/SiO_2	4.0	6.8	4.2	15.0	2000	2
^{FSP}1%Ag/30%Ce/SiO_2	2.0	3.8	6.0	11.8	1600	3
^{FSP}1%Ag/50%Ce/SiO_2	1.7	3.2	1.8	6.7	890	4
SiO_2	< 0.1	< 0.1	0.8	0.9	-	5

Cumene oxidation gave mainly cumene hydroperoxide, acetophenone and 2-phenyl-2-propanol (Table 4-6 and Figure 4-7b) with minor side products being benzaldehyde and *α*-methyl styrene. The hydroperoxide exhibited transient behavior, i.e. its yield exhibited a maximum after 1-2 hours in the presence of carboxylic acid and CeO_2. Interestingly, FSP catalysts supported on CeO_2-SiO_2 generally resulted in lower yields (Table 4-6, entries 2-4). Even in the presence of added ceria nanoparticles the obtained yield was higher for ^{imp}10%Ag/SiO_2-900 (entry 1). One of the reasons for this difference might be the close proximity between ceria and silver being the radical initiator for CeO_2-SiO_2 supported FSP catalysts and the smaller CeO_2 particle size (*cf.* Table 4-1, 3-8 nm, compared to 25 nm for the commercial ceria) but also leaching must be considered (*vide infra*). Ceria added to ^{imp}10%Ag/SiO_2-900

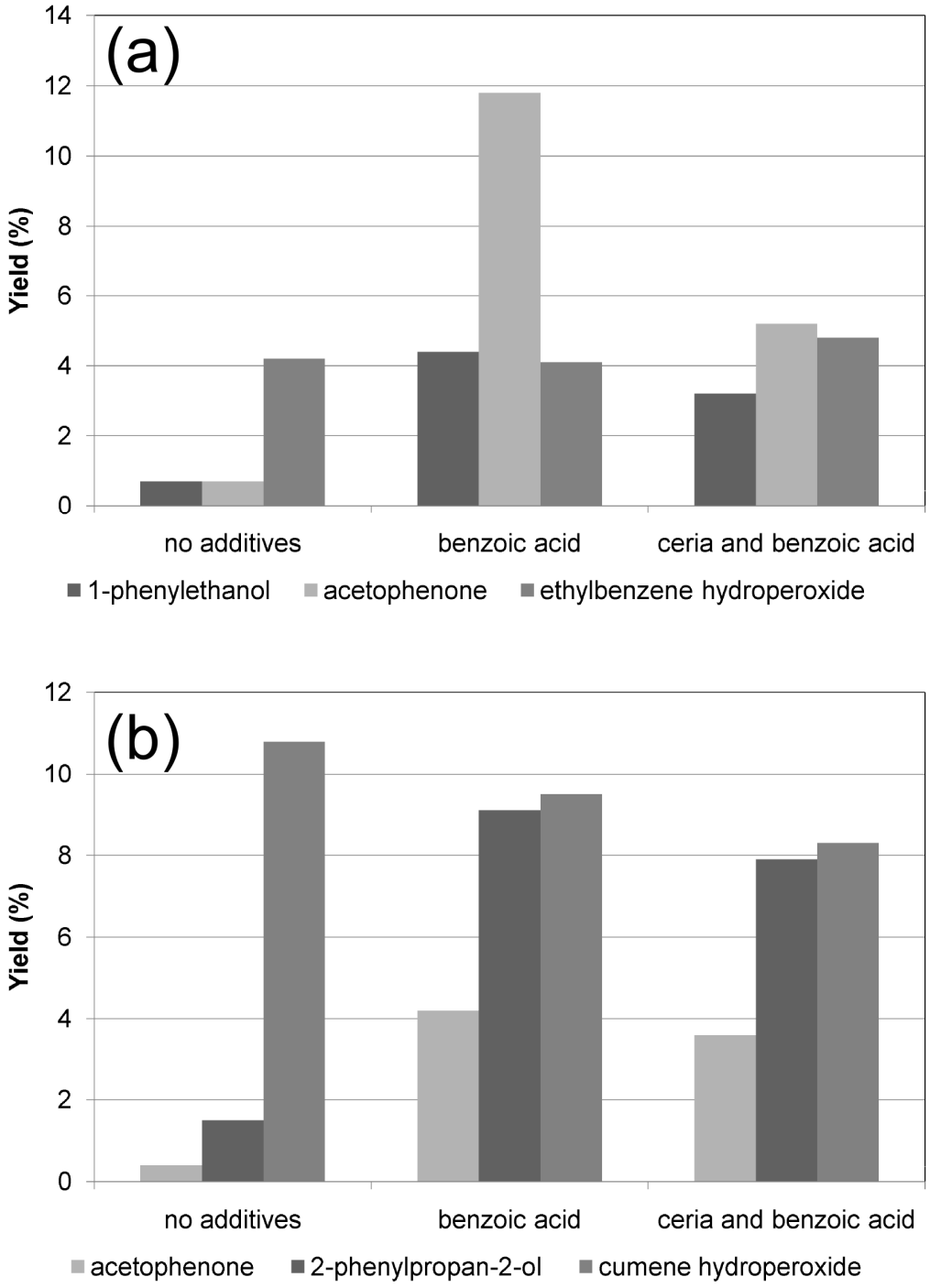

Figure 4-7: Influence of the carboxylic acid and CeO_2 on the oxidation of ethylbenzene (a) and cumene (b). Reaction conditions: 122 mmol ethylbenzene or cumene, optionally 3 mol-% benzoic acid and 50 mg CeO_2, 100 mg biphenyl, 100 mg ^{imp}10%Ag/SiO_2-900, oxygen atmosphere, 140 °C, 3 h reaction time.

had a deactivating effect even in the presence of benzoic acid (Figure 4-7b) as also observed for ethylbenzene oxidation. Interestingly, flame synthesized silver catalysts with SiO_2-CeO_2 support gave not only lower overall yields but also an altered product distribution. Only small amounts of alcohol and peroxide were formed (which are the main products in the reactions with the impregnated Ag catalysts)

Table 4-6: Oxidation of cumene with silver catalysts in the presence of CeO_2 and carboxylic acid. Reaction conditions: 122 mmol cumene, 3 mol-% benzoic acid, 100 mg biphenyl, 100 mg catalyst, 140 °C, 3 h reaction time.

Catalyst	Yields (%)				TON	Entry
	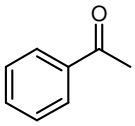	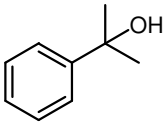	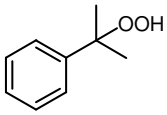	Combined		
^{imp}10%Ag/SiO_2-900	4.2	9.1	9.5	22.8	330	1
^{FSP}1%Ag/10%Ce-SiO_2	1.6	0.1	0.6	2.3	310	2
^{FSP}1%Ag/30%Ce-SiO_2	1.7	0.1	0.5	2.3	310	3
^{FSP}1%Ag/50%Ce-SiO_2	2.4	0.1	0.4	2.9	390	4
SiO_2	< 0.1	0.1	1.7	1.8	-	5

the main product being acetophenone. These alterations indicate a different reaction mechanism and are probably due to a changing ratio of the reaction rates of chain termination *vs.* propagation and the suppression of some radical reaction pathways. When ^{imp}10%Ag/SiO_2-900 was used as a catalyst, the oxidation of ethylbenzene and cumene continued after removal of the solid phase. In case of cumene a silver concentration of 9 mg/L was found by ICP-MS while for ^{FSP}1%Ag/10%CeO_2-SiO_2 the silver concentration was below the detection limit. This indicates a shift from heterogeneous to homogeneous catalysis and explains also the inferior performance and the different product distribution over the FSP-catalysts that tend to leach less. Note that peroxo/peroxide species formed during the presence of the catalyst may also maintain the reaction to a certain extent.

4.4 Discussion and mechanistic considerations

The oxidation of different alkyl aromatic compounds can be promoted by heterogeneous silver catalysts prepared *via* impregnation or flame spray pyrolysis. Yields are similar to other heterogeneous catalyst systems [19] but there is still a large gap in performance compared to the industrial homogeneous

AMOCO process. In the case of *p*-xylene and ethylbenzene the FSP catalysts were considerably more active with respect to the Ag loading. In addition, the FSP catalysts exhibited a significantly lower leaching tendency which might originate from a stronger metal-support interaction established during synthesis by combustion of the liquid precursor. In contrast, the impregnated catalyst performed superior in the cumene oxidation and gave another product distribution than the FSP catalysts thus indicating a different mechanism changing from heterogeneous to homogeneous catalysis.

The suppression of the oxidation reaction by radical scavengers and the formation of hydroperoxides strongly suggest that the investigated *p*-xylene oxidation reaction is based on a radical reaction mechanism, which is supported by many examples from the literature for analogous cases [e.g. 9, 54, 55]. Radical reactions comprise mainly three steps, namely initiation, radical chain reaction and termination (Scheme 4-2). The ratio of rate constants for these steps determines the overall catalytic performance and is dependent on the catalyst. Conversion of starting material was already observed when only the impregnated silver catalyst was used. The addition of peroxides to start the reaction as reported in other cases [56] was not necessary. Hence, silver facilitates the formation of initial radicals (Scheme 4-2, step 1). The chain reaction is likely not to be supported by the silver catalyst, firstly, because the product distribution in the absence of carboxylic acid is typical for uncatalyzed autoxidations [57, 58]. In addition, chain propagation is fast compared to initiation. This would also require a catalyst in the same phase as e.g. in case of the homogeneous Co/Mn/Br catalyst system [9] but a correlation between leaching and catalyst activity could not be established at least for *p*-xylene. Diffusion of the radicals to Ag particles and CeO_2 would be likely to occur in the same time regime so that the rate constants for chain propagation and termination would be similar if chain propagation relies on silver. Silver may, however, play a role in the decomposition of hydroperoxides influencing the radical concentration.

FSP synthesized catalysts featured both metallic silver and Ag-O species which might be reduced under reaction conditions since the used ^{FSP}1%Ag/10%CeO_2-SiO_2 catalyst showed a stronger Ag-Ag backscattering amplitude in the EXAFS spectrum. Silver in the active impregnated catalyst was found to be only metallic. Thus, metallic silver appears to be required for an active catalyst. The ambivalent influence of ceria suggests that ceria is interacting with two parts of the overall radical reaction one of which is obviously the chain termination (Scheme 4-2, step 3), since the reaction is suppressed when only ceria and the silver catalyst is used. Initiation by silver might be influenced by ceria (step 1). Ceria is known to activate oxygen [39], which could then support breaking of C-H bonds in *p*-xylene which are stronger compared to ethylbenzene and cumene. Thus, CeO_2 had no beneficial effect in the latter cases.

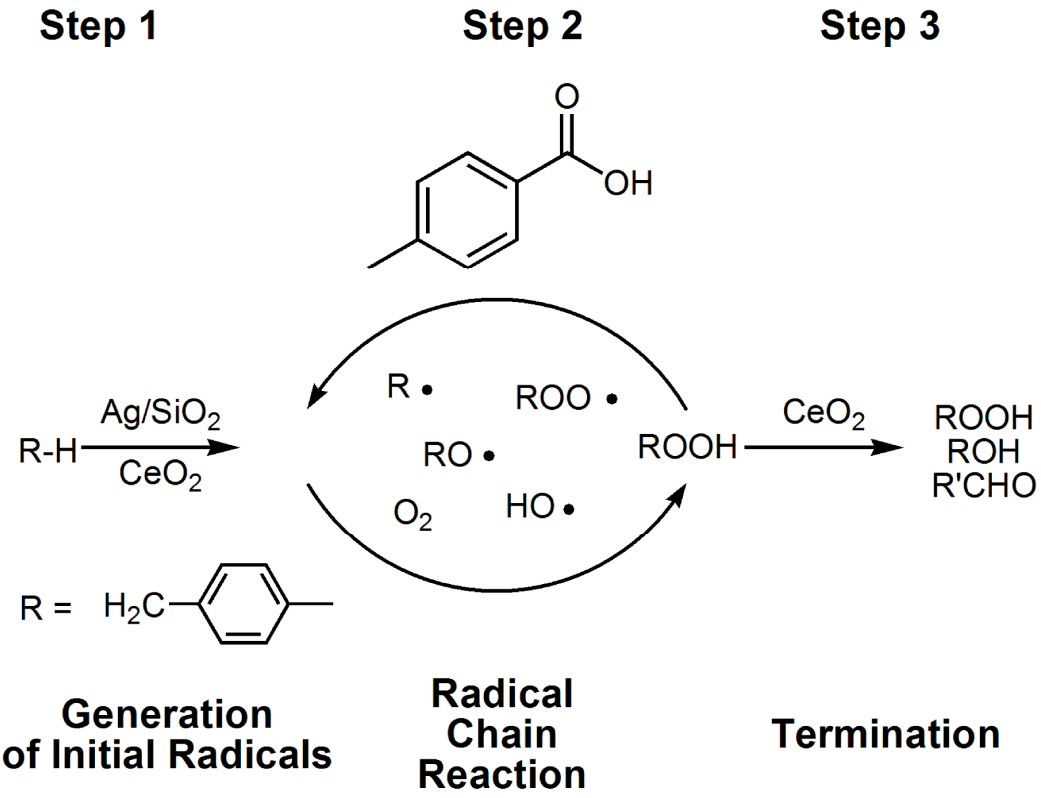

Scheme 4-2: Schematic reaction sequence in the radical autoxidation of *p*-xylene and potential roles of Ag, CeO_2 and *p*-toluic acid promoters.

Additionally, the latter more stable peroxo radicals [59] might have a longer half life which makes quenching by scavengers, which CeO_2 is, more likely. Molecular oxygen does not play a dominant role in the radical chain reaction since the reaction of alkyl radicals with molecular oxygen is fast [57]. Addition of carboxylic acid did not only increase the overall yield but also influenced the product distribution and hence changed the overall mechanism either directly *via* the propagation mechanism [54] (Scheme 4-2, step 2) or *via* destabilization of the termination product, i.e. the hydroperoxide, in the presence of radicals [60]. Indeed, in the case of *p*-xylene, ethylbenzene and cumene oxidation the hydroperoxide exhibited transient behavior. A higher degree of hydroperoxide dissociation would also result in a higher radical concentration which explains why not only the product distribution was shifted but also a higher overall yield was obtained. The higher O-H bond dissociation energies (BDE) of benzoic acid and toluic acid compared to the C-H BDE of alkyl aromatic compounds and the O-H BDE of the corresponding peroxides [59] makes the presence of carboxyloxo radical species generated from the added carboxylic acid unlikely. Thus, the carboxylic acids presumably promote the peroxide dissociation. Additionally, the capability of carboxylic acids to act as an H-bond acceptor can stabilize ·OH radicals

[61]. This lowers the activation energy for e.g. peroxide dissociation thereby generating a higher radical concentration and promoting the chain initiation.

Cumene oxidation with FSP synthesized CeO_2-SiO_2 supported catalysts proceeded with a low reaction rate and gave mainly acetophenone as a product. This was not the case when ^{imp}10%Ag/SiO_2-900 was used in the presence of ceria nanoparticles, but here leaching of silver is important. The initiation by homogeneous silver as observed with the impregnated catalyst is likely faster compared to the chain termination by a heterogeneous radical scavenger explaining the higher activity of the impregnated catalyst as compared to the FSP catalysts. In both cases the product distribution differs from typical cumene autoxidations for which the main product is cumene hydroperoxide. Thermal decomposition of the hydroperoxide alone cannot be the reason since in the absence of ceria and benzoic acid, cumene hydroperoxide was by far the dominating product. Ceria was used before as a catalyst for alkyl aromatics oxidation with bromate affording the carbonyl compound as the main product [58]. Acetophenone can be formed from cumene hydroperoxide either by reaction with a reducing agent [62] or generation of a hydroxyl radical *via* cleavage of the oxygen-oxygen bond [57] resulting an intermediate *α*,*α*-dimethylbenzyloxy radical. According to Bhattacharya et al. [57] this radical preferably reacts to form acetophenone which could be supported by ceria.

4.5 Conclusions

Silver particles supported on silica effectively promoted the side chain oxidation of toluene, *p*-xylene, ethylbenzene and cumene without any solvent. Except for toluene, no elevated pressures were needed to facilitate the reaction. Addition of a carboxylic acid considerably enhanced the reaction rate. CeO_2 had an ambivalent influence on the reaction and could both promote and inhibit product formation depending on substrate and reaction conditions. Except for cumene oxidation silver catalysts prepared *via* impregnation were inferior to flame-made catalysts which gave TONs up to 2000. In addition, the flame-synthesized catalysts were significantly less prone to leaching compared to the impregnated catalyst. This may be exploited in the future to prepare more stable catalysts for liquid phase reactions where leaching should be circumvented. In order to be active, silver is required to be metallic as suggested by EXAFS analysis. The oxidation reaction is most likely based on a radical mechanism where CeO_2 possibly assists silver as a chain initiator, while the carboxylic acid influences the dissociation of peroxides to radical species to initiate radical chains. Ceria as a radical scavenger additionally induces chain termination.

4.6 References

[1] J.M. Thomas, R. Raja, Chem. Commun. (2001) 675.

[2] J.M. Bregeault, Dalton Trans. (2003) 3289.

[3] T. Punniyamurthy, S. Velusamy, J. Iqbal, Chem. Rev. 105 (2005) 2329.

[4] A.K. Suresh, M.M. Sharma, T. Sridhar, Ind. Eng. Chem. Res. 39 (2000) 3958.

[5] F. Ullmann, "Ullmann's encyclopedia of industrial chemistry", 6th edition, Wiley-VCH, Weinheim, 2003.

[6] H.J. Rozie, M.L.C. Dsinter, J.B. Dakka, A. Zoran, Y. Sasson, PCT Int. Appl., 9,520,560 (1995).

[7] M.L. Kantam, B.M. Choudary, P. Sreekanth, K.K. Rao, K. Naik, T.P. Kumar, A.A. Khan, Eur. Pat. Appl., 1,088,810 (2001).

[8] S. Park, J.S. Yoo, K. Jun, D.B. Raju, Y. Kim, U.S. Patent, 6,476,257 (2002).

[9] W. Partenheimer, Catal. Today 23 (1995) 69.

[10] V. Kumar, P.D. Grover, Ind. Eng. Chem. Res. 30 (1991) 1139.

[11] G. Busca, J. Chem. Soc. Faraday 89 (1993) 753.

[12] J.S. Yoo, J.A. Donohue, M.S. Kleefisch, P.S. Lin, S.D. Elfline, Appl. Catal. A 105 (1993) 83.

[13] P.A. Hamley, T. Ilkenhans, J.M. Webster, E. Garcia-Verdugo, E. Venardou, M.J. Clarke, R. Auerbach, W.B. Thomas, K. Whiston, M. Poliakoff, Green Chem. 4 (2002) 235.

[14] T. Seki, M. Baiker, Chem. Rev. 109 (2009) 2409.

[15] H.V. Borgaonkar, S.R. Raverkar, S.B. Chandalia, Ind. Eng. Chem. Prod. Res. Dev. 23 (1984) 455.

[16] M. Hronec, Z. Hrabe, Ind. Eng. Chem. Prod. Res. Dev. 25 (1986) 257.

[17] M. Ilyas, M. Sadiq, Catal. Lett. 128 (2009) 337.

[18] B. Chou, J. Tsai, S. Cheng, Microporous Mesporous Mater. 48 (2001) 309.

[19] F. Wang, J. Xu, X. Li, J. Gao, L. Zhou, R. Ohnishi, Adv. Synth. Catal. 347 (2005) 1987.

[20] R. Raja, J.M. Thomas, V. Dreyer, Catal. Lett. 110 (2006) 179.

[21] R. Raja, J.M. Thomas, Solid State Sci. 8 (2006) 326.

[22] M.J. Beier, T.W. Hansen, J.-D. Grunwaldt, J. Catal. 266 (2009) 320.

[23] R. Strobel, A. Baiker, S.E. Pratsinis, Adv. Powder Technol. 17 (2006) 457.

[24] R. Kydd, W.Y. Teoh, K. Wong, Y. Wang, J. Scott, Q. Zeng, A. Yu, J. Zou, R. Amal, Adv. Funct. Mater. 19 (2009) 369.

[25] S. Hannemann, J.-D. Grunwaldt, P. Lienemann, D. Guenther, F. Krumeich, S.E. Pratsinis, A. Baiker, Appl. Catal. A 316 (2007) 226.

[26] H. Schulz, L. Mädler, R. Strobel, R. Jossen, S.E. Pratsinis, T. Johannessen, J. Mater. Res. 20 (2005) 2568.

[27] J. Yuan, X. Liao, H. Wang, G. Yang, M. Tang, J. Phys. Chem. B. 113 (2009) 1418.

[28] T. Ressler, J. Synchrotron Radiat. 5 (1998) 118.

[29] S.I. Zabinsky, J.J. Rehr, A. Ankudinov, R.C. Albers, M.J. Eller, Phys. Rev. B 52 (1995) 2995.

[30] R.J. Hill and C.J. Howard, AAEC (now ANSTO), *Australian Atomic Commission Report No. M112*, 2nd ed., Lucas Heights Research Laboratories, New South Wales, Australia, 1986; winpow was obtained from http://struktur.kemi.dtu.dk/kenny/powder_programs.html, last accessed on April, 16th, 2010.

[31] K. Ohkubo, S. Fukuzumi, Org. Lett. 2 (2000) 3647.

[32] G. Sereda, V. Rajpara, Tetrahedron Lett. 48 (2007) 3417.

[33] C. Rehren, G. Isaac, R. Schlögl, G. Ertl, Catal. Lett. 11 (1991) 253.

[34] X. Bao, G. Lehmpfuhl, G. Weinberg, R. Schlögl, G. Ertl, J. Chem. Soc. Faraday 88 (1992) 865.

[35] Z.P. Qu, M.J. Cheng, W.X. Huang, X.H. Bao, J. Catal. 229 (2005) 446.

[36] Z.P. Qu, W.X. Huang, M.J. Cheng, X.H. Bao, J. Phys. Chem. B. 109 (2005) 15842.

[37] S. Babu, A. Velez, K. Wozniak, J. Szydlowska, S. Seal, Chem. Phys. Lett. 442 (2007) 405.

[38] P. Trogadas, J. Parrondo, V. Ramani, Electrochem. Solid-State Lett. 11 (2008) B113.

[39] A. Trovarelli, G.J. Hutchings (Ed.), "Catalysis by ceria and related materials", Imperial College Press, London, 2002.

[40] A. Abad, P. Concepcion, A. Corma, H. Garcia, Angew. Chem. Int. Edit. 44 (2005) 4066.

[41] T. Vogler, A. Studer, Synthesis (2008) 1979.

[42] S. Hannemann, J.-D. Grunwaldt, F. Krumeich, P. Kappen, A. Baiker, Appl. Surf. Sci. 252 (2006) 7862.

[43] H. Schulz, L. Maedler, S.E. Pratsinis, P. Burtscher, N. Moszner, Adv. Funct. Mater. 15 (2005) 830.

[44] A. Teleki, S.E. Pratsinis, K. Wegner, R. Jossen, F. Krumeich, J. Mater. Res. 20 (2005) 1336.

[45] B. Medasani, Y.H. Park, I. Vasiliev, Phys. Rev. B 75 (2007) 235436-1.

[46] P. Niggli, Z. Kristallogr., Kristallgeom., Kristallphys. Kristallchem. 57 (1922) 253.

[47] F. Liebau, Acta Crystallogr. 14 (1961) 537.

[48] M. Jansen, H.L. Keller, Angew. Chem. 91 (1979) 500.

[49] K. Heidebrecht, M. Jansen, Z. Anorg. Allg. Chem. 597 (1991) 79.

[50] W. Klein, M. Jansen, Z. Anorg. Allg. Chem. 634 (2008) 1077.

[51] O.A. Yeshchenko, I.M. Dmitruk, A.A. Alexeenko, A.V. Kotko, Nanotechnology 21 (2010) 045203/1.

[52] I. Hermans, J. Peeters, L. Vereecken, P.A. Jacobs, ChemPhysChem. 8 (2007) 2678.

[53] T.V. Bukharkina, O.S. Grechishkina, N.G. Digurov, N.V. Krukovskaya, Org. Process Res. Dev. 3 (1999) 400.

[54] Y. Kamiya, M. Kashima, Bull. Chem. Soc. Jpn. 46 (1973) 905.

[55] Q. Jiang, Y. Xiao, Z. Tan, Q. Li, C. Guo, J. Mol. Catal. A 285 (2008) 162.

[56] P.P. Toribio, A. Gimeno-Gargallo, M.C. Capel-Sanchez, M.P. de Frutos, J.M. Campos-Martin, J.L.G. Fierro, Appl. Catal. A. 363 (2009) 32.

[57] A. Bhattacharya, Chem. Eng. J. 137 (2008) 308.

[58] I. Hermans, J. Peeters, P.A. Jacobs, J. Org. Chem. 72 (2007) 3057.

[59] E.T. Denisov, E.V. Tumanov, Russ. Chem. Rev. 74 (2005) 905.

[60] C. Wang, H. Chen, C. Chen, Polym. Adv. Technol. 17 (2006) 579.

[61] I. Hermans, J. Peeters, P.A. Jacobs, ChemPhysChem 7 (2006) 1142.

[62] H. Boardman, J. Am. Chem. Soc. 75 (1953) 4268.

Chapter 5

Experimental Determination, Modeling and Utilization of the Phase Behavior in the Selective Oxidation of Alcohols in Pressurized CO_2

Abstract

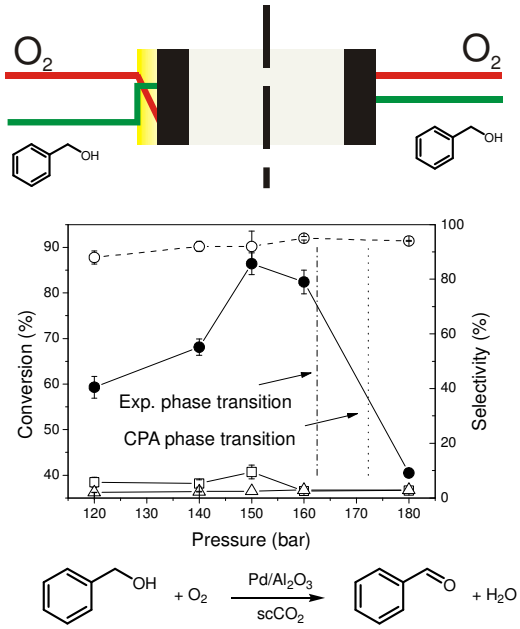

Alcohol oxidation in "supercritical" CO_2.

The catalytic oxidation of benzyl alcohol to benzaldehyde with molecular oxygen in "supercritical" CO_2 is significantly influenced by the phase behavior where either all substrates are present in a single phase or two phases are formed, one rich in CO_2 and the other in benzyl alcohol. The Cubic plus Association Equation of State was used in order to predict the phase behavior of ternary mixtures relevant to the catalytic oxidation of benzyl alcohol. Model predictions were compared to experimental phase behavior data. The usefulness of the model predictions was validated by catalytic studies in a continuous reactor over a commercial Pd catalyst under different conditions. The catalytic activity was studied both under biphasic and single phase conditions under different flows, compositions and with different oxygen concentrations. In general, biphasic conditions resulted in the highest reaction rate. On transition to the single phase, the oxygen availability at the catalyst surface increases potentially causing catalyst deactivation. Preliminary results

suggest that the substrate transport through the continuous reactor under biphasic conditions is complex.

5.1 Introduction

The selective oxidation of alcohols to aldehydes or ketones in the liquid phase has been intensively investigated in the recent years [1, 2]. Toxic and expensive oxidizing agents were replaced by oxygen being environmentally benign [3]. Besides the coinage metals described in Chapter 2, other noble metal based heterogeneous catalysts have been used successfully, especially those based on ruthenium, platinum and palladium. A problem associated with the aerobic alcohol oxidation is the low oxygen solubility and diffusion coefficient in organic solvents frequently used for these reactions. Thus, the use of gaseous oxygen introduces an additional phase boundary to the liquid/solid reaction system inducing further mass transport limitations. These limitations could be overcome by using pressurized CO_2 as an alternative solvent having a high solubility for oxygen where Pd as a catalytically active metal has received high attention [4-10]. The performance of other frequently used metals like gold [11, 12], platinum and ruthenium [10] did not profit from the use of pressurized CO_2 giving poor conversions. This might be connected to overoxidation of the metal due to the high oxygen availability or blocking of surface sites [10]. In general, dense CO_2 features the advantage of being environmentally benign, safer in combination with organics and oxygen and being chemically stable with respect to oxidation [13-15]. The balance between liquid and gas-like properties results in a fast mass and heat transfer and a high solubility for low-functionalized organic molecules. A unique feature is the tunability of the solvent properties of CO_2 by adjusting the pressure and temperature. Exploiting the beneficial properties of CO_2, higher reaction rates were observed in alcohol oxidation than in standard solvents [6, 15-17]. Work especially from the Baiker group and co-workers demonstrated the potential of tuning of the solvent properties using the same catalyst (0.5% Pd/Al_2O_3), temperature and continuous experimental setup: thus, in one catalytic study, benzyl alcohol was oxidized with a surface TOF of 430 h^{-1} [16]. By adjusting the pressure in a later study, TOFs close to 2000 h^{-1} were achieved [6, 7]. In order to optimize catalytic processes involving CO_2 as a solvent, knowledge about the phase behavior is important [15, 18]. At conditions relevant to catalysis, two different scenarios can occur: (1) all the compounds (except the solid catalyst) are in a single phase at high pressures and (2) formation of two phases, one being rich in CO_2 and another consisting mainly of the organic substrate. The reaction rate may differ greatly when working under single phase or two phase conditions [7, 8]. Determining optimal reaction conditions in CO_2 is experimentally elaborate and requires special equipment

such as a high pressure view cell. Therefore, catalytic reactions in supercritical CO_2 reported in the literature are often only optimized to a small extend for a very limited set of reaction parameters. This may result in missing close-to-optimal reaction conditions. In contrast to this trial-and-error approach, modeling the phase behavior offers a great chance of conducting experiments in a more controlled way.

The most important compounds involved in the oxidation of benzyl alcohol in CO_2 are benzyl alcohol and oxygen as substrates as well as benzaldehyde and water as products, with CO_2 as the solvent. These compounds associate strongly *via* hydrogen bonds. Thus, a sophisticated model is necessary accounting both for the polar nature of the compounds and the strong association between them. Cubic equation of states (the most well-known being the van-der-Waals equation of state) are in selected cases capable of modeling highly non-ideal systems when advanced mixing rules for multi-component mixtures are used. Modifying the models by an association term further enables phase behavior predictions for systems with strong hydrogen-bonds. Here, applicable Equation of State (EoS) models are the Statistically Associating Fluid Theory (SAFT) variants [19], the Non Random Hydrogen Bonding (NRHB) model [20] and the Cubic plus Association (CPA) model [21-23].

In this study, the CPA EoS will be used to predict the phase behavior of ternary systems relevant to the oxidation of benzyl alcohol, i.e. substrate mixtures consisting of O_2, benzyl alcohol and CO_2 and product mixtures consisting of water, benzaldehyde and CO_2. The model predictions will be compared to experimental data obtained by monitoring the phase behavior in a high pressure view cell. It has been shown in the past that phase behavior is critical for alcohol oxidation. Hence, the usefulness of the model will be validated by the oxidation of benzyl alcohol over a commercial shell-impregnated 0.5 wt.-% Pd/Al_2O_3 catalyst in pressurized CO_2 (Scheme 5-1) using a continuous fixed bed reactor. The catalytic activity in the oxidation of benzyl alcohol will be monitored in between pressures where the phase transition is predicted to occur.

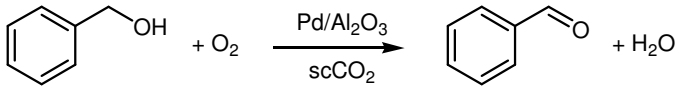

Scheme 5-1: Palladium-catalyzed oxidation of benzyl alcohol by molecular oxygen.

5.2 Experimental

5.2.1 Experimental setups

5.2.1.1 View cell for phase behavior measurements

Phase experiments were performed in a high pressure view cell (15-65 mL, SITEC, Switzerland) with variable volume which was custom-designed from a screw-type manual pump similar to the system described by Crampon et al. [24]. Temperature and pressure measurements, respectively, were performed with a J type thermocouple and a Dynisco pressure sensor (MDT422H-1/2-2C-15/46). The cell was equipped with a CO_2 and a gas (O_2/N_2) inlet as well as a rupture disc for preventing overpressures. Stirring was achieved by a magnetic stir bar in connection with a magnetic stirrer (Heidolph MR 2002). Heating of the cell was accomplished by means of an oil-containing heating jacket controlled by a thermo-/cryostat (Julabo F25 HD). A sapphire window covering the whole diameter of the cell (26 mm) allowed optical identification of phases. A cold light source applied from the front illuminated the cell. Construction details and the flowchart of the cell can be found in ref. [25]. In this project phase identification was performed without the previously described CCD camera by direct optical identification giving more accurate results when the light source is used in the viewing direction.

5.2.1.2 Continuous reactor for catalytic reactions in pressurized CO_2

The setup was based on the design of previous studies [6, 16] with some modifications (Figure 5-1). Connecting tubes and valves were obtained from Swagelok. CO_2 pressurized with a compressor (NWA Loerrach, Germany) to ca. 200-250 bar was down-regulated to the desired system pressure by an interconnected reducing valve (TESCOM, stainless steel, P/N 44-1165-24). Accordingly, an O_2 compressor (NWA Loerrach) supplied O_2 *via* a reducing valve (TESCOM, brass, P/N44-1115-24) to a six-port-dosing valve (NWA Loerrach). The six-port-dosing valve consisted of two coils (V_{coil} = $61 \cdot 10^{-6}$ L) which were alternating filled with oxygen and unloaded to the system. A switching time could be set between 0.1 s - 9.9 s allowing different O_2 dosing rates. The pressure difference between the oxygen feed and the system was measured by two pressure gauges (both Yokogawa DPharp transmitter EJX530A, readout VEGAMET 381; accuracy ± 0.5 bar). Risk of back-flowing of organic compounds into an oxygen-rich atmosphere was minimized by a check valve. The liquid alcohol was fed to the system by a GILSON 305 HPLC pump. A view cell autoclave (NWA Loerrach) equipped with heating (controlled by a Eurotherm 2216e temperature controller) and stirrer was interconnected in order to monitor the phase behavior of the feed at conditions close to the reactor. The view cell could be set on bypass in order to avoid

long equilibration times, which was usually done. The reactor consisted of a 30 cm long 8 mm (e.d.) Swagelok tube equipped with external heating (controlled by a Eurotherm 2216e temperature controller). The reactor was filled with 1.25 g catalyst particles corresponding to a bed length of ca. 15 cm (0.5 % Pd/Al_2O_3 [shell impregnated], sieve fraction 250 µm - 425 µm, Engelhard 4586, BET surface area 106 $m^2 g^{-1}$, pore volume 24.3 $cm^3 g^{-1}$, average pore diameter by BET 9.6 nm, metal dispersion 0.29; data taken from [7]). Note that the Pd-containing impregnated shell of the catalyst appeared more brittle, so that the crushing and sieving procedure caused an uncertainty with respect to the actual Pd amount in the catalyst bed. Therefore, the use of TOFs in this study will be avoided. Top and bottom of the reactor were filled with inert particles (e.g. Al_2O_3) of the same size fraction. Two reduction valves after the reactor allowed stepwise decreasing of the system pressure. The first reduction valve was heatable (controlled by a Eurotherm 2216e temperature controller) in order to avoid freezing due to the Joule-Thomson effect. The effluent gas flow was cooled in a coil immersed in an NaCl/ice bath after which sampling was possible. The gas/liquid separator consisted of a stainless steel reactor (NWA Loerrach, 300 bar pressure rating). A downstream needle valve allowed fine tuning of the overall system gas flow which was measured with a flowmeter calibrated on a daily basis.

5.2.2 Experimental procedures

5.2.2.1 Experimental determination of the phase behavior

Leak checks of the view cell were performed weekly. Prior to experiments the cell was thoroughly cleaned with acetone and CO_2 and dried in a N_2 stream. For experiments the cell was charged with the desired amounts of benzyl alcohol (Aldrich, 99 %+, freshly distilled, stored under argon atmosphere), benzaldehyde (Fluka, 99.5 %+, redistilled, stored under argon atmosphere) and/or water (Fluka, >2 µS/cm) at 288 K. The sealed cell was carefully flushed several times with either O_2 or N_2 (both PanGas, 5.0) or CO_2 (PanGas, 3.0) to remove air and filled with the appropriate amount of O_2 or N_2 (calculated using data from NIST [26]). CO_2 was added by means of a CO_2 compressor (NWA Loerrach, Germany) and quantified with a mass flow transmitter (Rheonik Messgeräte GmbH, Germany) at a constant pressure of 100 bar provided by an interconnected reducing valve. The cell was heated to the desired temperature and a pressure significantly higher than the dew point applied by adjusting the cell volume. Under these conditions the cell was equilibrated for an appropriate amount of time (min. 2 h - overnight). After a first rough investigation of the respective system, dew points were determined by changing the pressure in intervals of 0.5 - 2 bar, equilibration (15 min - 2 h) and visual

inspection. Accordingly, a pressure interval between a high and a low pressure limit in between which phase separation occurred was noted. Usually, dew points were determined by following the dissolution of droplets. Prior to formation of drops by decreasing the pressure the feed lines were heated by means of a heat gun. The dew point pressures were usually measured three times for each composition and temperature from which a standard deviation was obtained. The uncertainty of the high and low pressure limit around the dew point was then determined by twice the standard deviation plus the uncertainty due to the pressure sensor (± 0.5 bar). The dew point was calculated as the center of the thus obtained pressure interval in which phase separation occurred and the maximum error was considered in order to describe the interval boundaries. Further experimental uncertainties are estimated to be ± 0.02 mol-% for the molar fraction of each component and ± 0.5 K for the temperature. Batch experiments were conducted in the same cell by adding 0.5 % Pd/Al_2O_3.

5.2.2.2 Catalytic studies

Prior to each run the catalytic setup was flushed with CO_2 (AGA A/S; grade 3.0). The reactor was heated to the desired temperature (usually 80 °C). Benzyl alcohol (Sigma-Aldrich, anhydrous, 99.8 %) was introduced to the system by means of the HPLC pump. The CO_2 pressure of the compressor was set to ca. 200-250 bar and fine-tuned to the desired pressure by the interconnected reducing valve. O_2 (AGA A/S; grade 3.5) was compressed to ca. 200 bar (or higher if necessary) and regulated to a pressure 10-20 bar higher than the system pressure by the respective reducing valve. The desired oxygen molar flow F_{O2} was applied by setting a shifting time t_S (between 2-5 s pulses) for the 6-port-dosing valve and calculated from the coil volume V_{coil} and the difference between the system pressure P_{sys} and the oxygen feed pressure P_{O2} according to Eq. 5-1.

(Eq. 5-1) $$F_{O2} = \frac{\left(P_{O2} - P_{sys}\right) \cdot V_{coil}}{24.4 \frac{l \cdot bar}{mol} \cdot t_S}$$

The total flow of gaseous compounds (i.e. CO_2 at low O_2 concentrations) was regulated at the exit of the setup by means of the expansion unit: with the first (heatable) reduction valve the system pressure was decreased to ca. 15 bar, the second reduction valve was set to ca. 5 bar. The flow was fine-tuned with the needle valve after the gas-liquid separator and measured with the ball flowmeter being calibrated daily. Samples were taken where indicated in Figure 5-1 collected in ca. 2-4 mL of ethyl acetate cooled to -18 °C every 20 min. GC analysis was carried out with an Agilent 6890 N gas chromatograph equipped with a 7683 B series autosampler, a flame ionization detector, and a DB-FFAP column (Agilent, 30 m x 0.25 mm x 0.25 µm). Conversions and selectivities were calculated from the relative amounts of benzyl alcohol, benzaldehyde, benzoic acid, toluene and benzyl

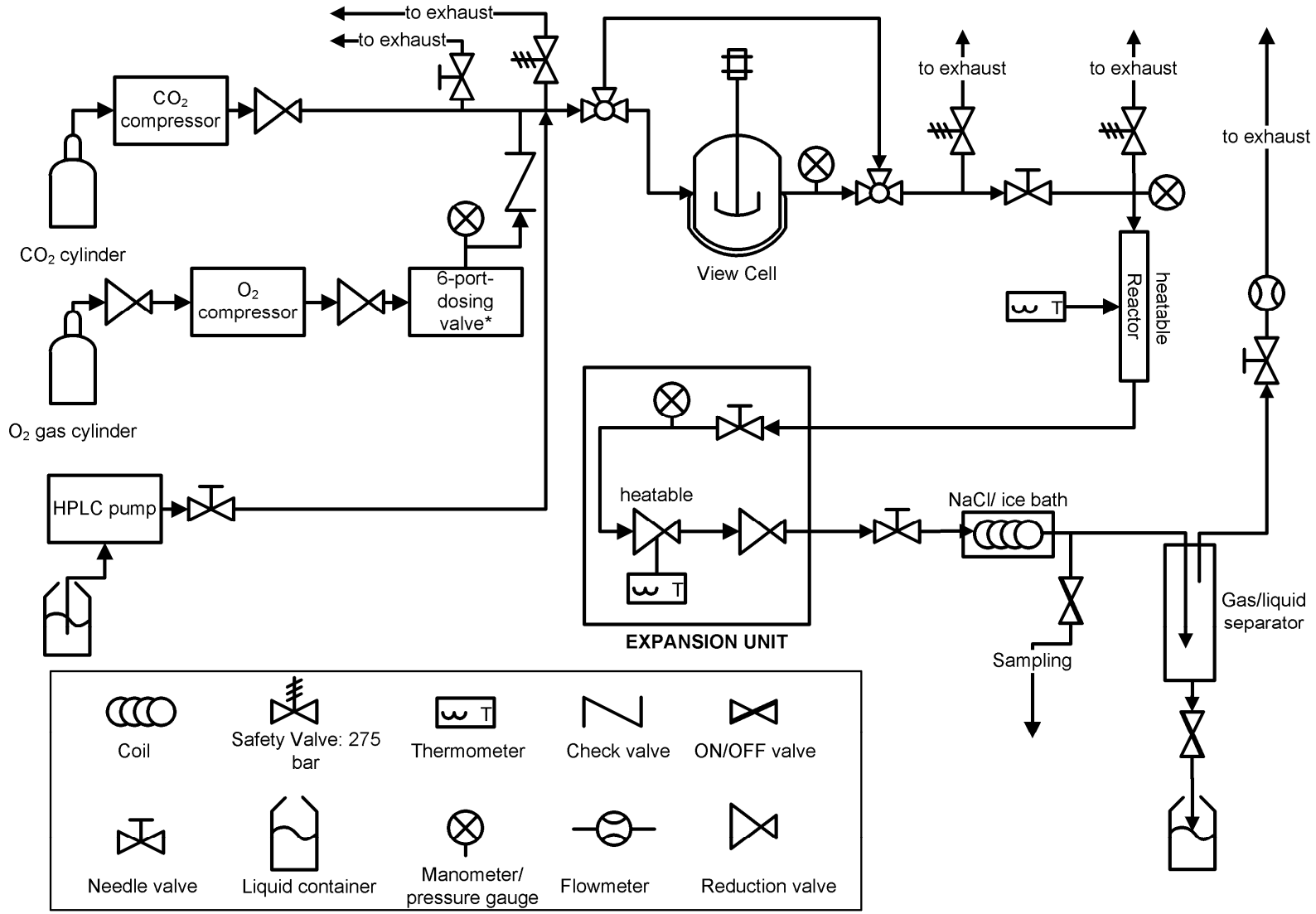

Figure 5-1: Schematic view of the experimental setup for continuous high pressure catalytic alcohol oxidation.

benzoate. The mass balance was checked by comparing inlet and outlet flow masses and found to be >96 % assuming that one molecule of water is formed per benzaldehyde molecule. Using an internal standard gave unsatisfactory results especially in the two phase region. Samples were taken until the obtained conversion stabilized; the conversion was then calculated by averaging 5-10 samples taken at steady-state. Uncertainties were calculated as twice the standard deviation. The catalyst bed was exchanged from time to time in order to stabilize the catalytic activity.

Batch reactions were conducted in the view cell previously used for phase behavior investigation. 200 mg of 0.5 % Pd/Al_2O_3 (as pellets, ca. 5 mm in diameter), benzyl alcohol (336 µL, 3.2 mmol) and ca. 10 µL of *tert*.-butylbenzene were introduced to the cell. Maintaining the cell at 10 °C, the cell was flushed several times with oxygen of which 40 NmL (1.6 mmol) were added followed by 15.6 g of CO_2. The cell was then heated up to 80 °C while stirring. By changing the cell volume, the system was kept in a single phase during the heat-up phase. After the heating jacket reached the desired temperature, the mixture was allowed to react for 1 h at the desired pressure and then cooled down to 10 °C. The reactor was carefully vented and a sample for GC analysis was taken.

5.2.3 Phase behavior modeling

Modeling of the phase behavior of relevant systems was done using the Cubic plus Association (CPA) Equation of State (EoS, Eq. 5-2) [21-23]:

(Eq. 5-2)
$$P = \frac{RT}{V_m - b} - \frac{\alpha(T)}{V_m(V_m + b)} - \frac{1}{2}\frac{RT}{V_m}\left(1 + \rho\frac{\partial \ln g}{\partial \rho}\right)\sum_i x_i \sum_{A_i}(1 - X_{A_i})$$

P system pressure

R ideal gas constant

T temperature

b co-volume parameter

$\alpha(T)$ temperature dependent energy parameter

V_m molar volume

$g(\rho)$ radial distribution function

ρ molar density

x_i molar fraction of compound i

X_{Ai} association term (fraction of A-sites on compound i which are unassociated, “monomer fraction”)

The first two terms are identical to the Soave-Redlich-Kwong EoS; three substance specific parameters are needed, i.e. b and for calculation of $\alpha(T)$ according to Eq. 5-3 both a_0 and c_1.

(Eq. 5-3) $$\alpha(T) = \alpha_o \left[1 + c_1(1 - \sqrt{T_r})\right]^2$$

T_r reduced temperature

α_0, c_1 energy parameters

The third term describes the association of molecules, the critical part being the association term X_{Ai} (Eq. 5-4).

(Eq. 5-4) $$X_{A_i} = \frac{1}{1 + \rho \sum_j x_j \sum_{B_j} X_{B_j} \Delta^{A_i B_j}}$$

The association term can be simplified depending on the type of association scheme, i.e. the number of association sites on the molecules and the cross association [27]. The association strength $\Delta^{A_i B_j}$ is calculated according to Eq. 5-5.

(Eq. 5-5) $$\Delta^{A_i B_j} = g(\rho)\left[\exp\left(\frac{\varepsilon^{A_i B_j}}{RT}\right) - 1\right] b_{ij} \beta^{A_i B_j}$$

$\varepsilon^{A_i B_j}$ association energy (measure for the hydrogen bond strength)

$\beta^{A_i B_j}$ association volume

b_{ij} co-volume of the mixture; $b_{ij} = 0.5(b_i + b_j)$

$\varepsilon^{A_i B_j}$ and $\beta^{A_i B_j}$ are additional substance specific parameters necessary when association between molecules occurs. The radial distribution function $g(\rho)$ is obtained from Eq. 5-6.

(Eq. 5-6) $$g(\rho) = \frac{1}{1 - 1.9 \cdot (0.25 \cdot b\rho)}$$

Within this study, the conventional mixing rules for determining the co-volume and energy parameter were employed, i.e.

(Eq. 5-7) $$b = \sum_i x_i b_i$$

(Eq. 5-8) $$\alpha = \sum_i \sum_j x_i x_j \alpha_{ij} \text{ with } \alpha_{ij} = \sqrt{\alpha_i \alpha_j}\,(1 - k_{ij})$$

where k_{ij} is a binary interaction parameter.

The binary interaction parameter k_{ij} was fitted to experimental data of binary systems for use in ternary systems and is the only required parameter for non-associating compounds. The CR-1 combining rule was used for determining the cross-association energy (Eq. 5-9) and cross association volume (Eq. 5-10) for mixtures where both compounds are self-associating.

(Eq. 5-9) $$\varepsilon^{A_i B_j} = \varepsilon_{cross} = \frac{\varepsilon^{A_i B_i} + \varepsilon^{A_j B_j}}{2}$$

(Eq. 5-10) $$\beta^{A_i B_j} = \beta_{cross} = \sqrt{\beta^{A_i B_i} \beta^{A_j B_j}}$$

The cross-association, i.e. associative interaction between different kinds of molecules, can alternatively be calculated from the modified CR-1 combining rule (Eq. 5-11) for systems with only one self-associating compound (i.e. the other is inert); β_{cross} was fitted from binary systems data [28].

(Eq. 5-11) $$\varepsilon^{A_i B_j} = \varepsilon_{cross} = \frac{\varepsilon_{associating}}{2}$$

First, the respective binary parameters were obtained from fitting to experimental data for binary mixtures. Having obtained the binary interaction parameters and parameters for pure compounds, the phase behavior of two ternary systems, i.e. benzyl alcohol – O_2 – CO_2 and benzaldehyde – water – CO_2 was modeled. Modeling was done by Ioannis Tsivintzelis [29].

5.3 Results

5.3.1 CPA parameters of pure compounds

Pure compound parameters, i.e. a, b and c_1 were obtained from vapor pressures and liquid densities, respectively from DIPPR correlations [30] and can be found in Table 5-1.

5.3.2 CPA of binary mixtures

The binary parameters required for the ternary systems were obtained by fitting of experimental data (Figure 5-2). There were not sufficient data points for the systems benzyl alcohol – CO_2 and benzaldehyde – O_2, so new

Table 5-1: CPA parameters for pure compounds [29].

Association Scheme[a]	T_c (K)	a_o (L bar mol^{-2})	b (L mol^{-1})	c_1	ε (bar Lmol^{-1})	β
Benzyl alcohol (0.4T_c – 0.9 T_c)[b]						
3B	720.15	29.141	0.0973	0.7533	205.41	0.0024
Benzaldehyde (0.4T_c – 0.9T_c)[b]						
-	695.0	27.836	0.0932	0.8814	-	-
CO_2 (T_m – 0.9T_c)[b]						
-	304.21	3.508	0.0272	0.7602	-	-
O_2 *(0.5T_c – 0.9 T_c)*[b]						
-	154.58	1.390	0.0216	0.4754	-	-
Water [22]						
4C	647.13	1.228	0.0145	0.6736	166.55	0.0692

[a]3B and 4C association schemes according to the notation of Huang and Radosz [27]; [b]The temperature range of the regression is given in parenthesis, T_c: critical temperature, T_m melting point.

Table 5-2: Bubble points for benzaldehyde – N_2 and benzyl alcohol – CO_2 measured between 60-80 °C.

Temperature (°C)	P_{high}[a]	P_{low}[b]	P_{sep}[c]
98.00 ± 0.02 mol-% benzaldehyde and 2.00 ± 0.02 mol-% N_2			
60 ± 0.5	54.6 ± 2.1	50.5 ± 1.9	52.7 ± 4.0
80 ± 0.5	53.5 ± 2.5	49.8 ± 1.7	52.1 ± 4.0
99.60 ± 0.02 mol-% benzyl alcohol and 0.40 ± 0.02 mol-%CO_2			
80 ± 0.5	137.0 ± 1.5	136.0 ± 1.5	136.5 ± 2.0

[a]Average high pressure limit; [b]Average low pressure limit; [c]Pressure interval for phase separation.

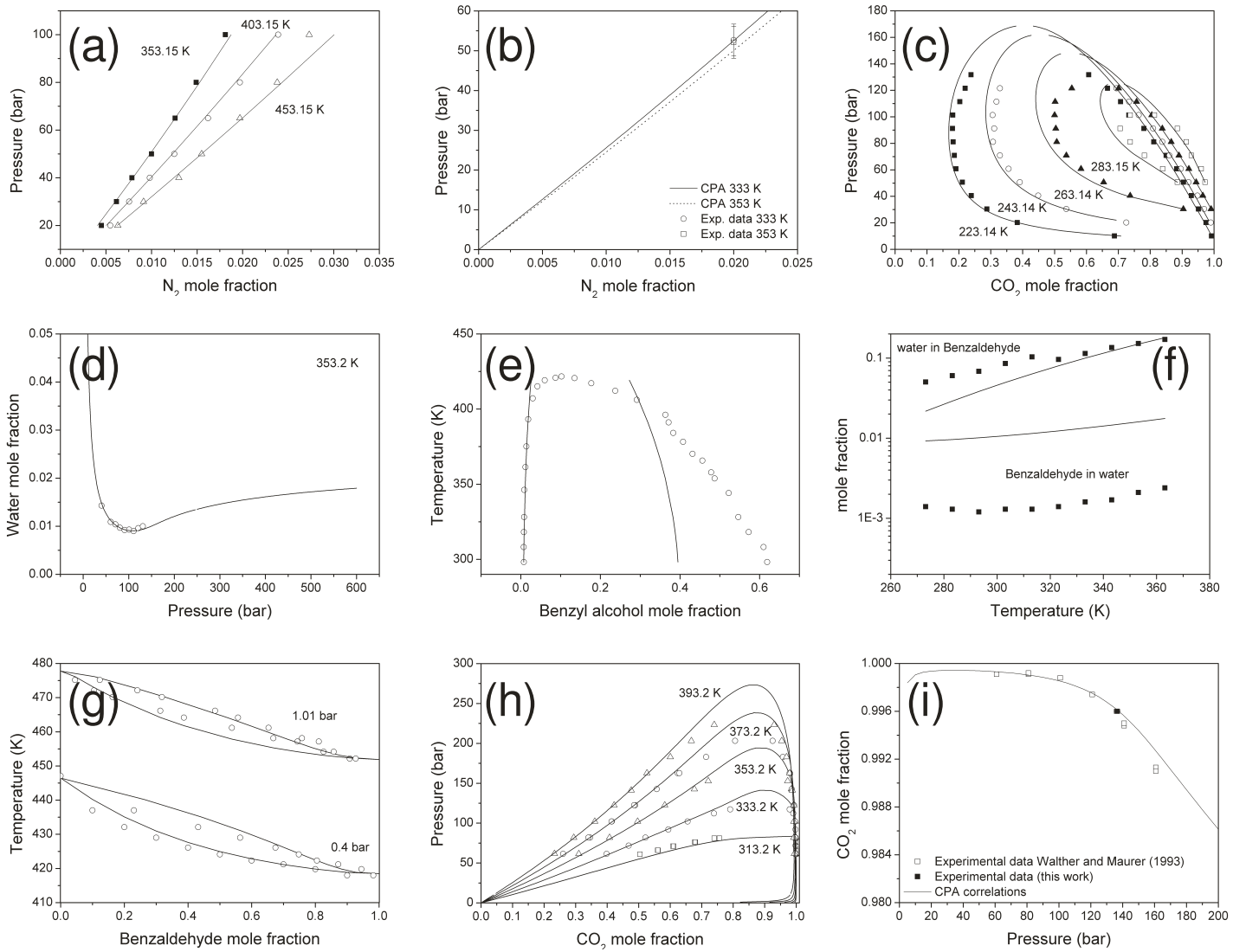

Figure 5-2: Experimental data (points) and CPA fits for binary systems; (a) N_2 solubility in benzyl alcohol, data from ref. [31]; (b) N_2 solubility in benzaldehyde, data from this work; (c) CO_2-O_2 VLE, data from ref. [32]; (d) CO_2 – water phase compositions (80 °C), data from ref. [33-35]; (e) benzyl alcohol – water LLE, data from ref. [36]; (f) benzaldehyde – water LLE, data from ref [37]; (g) benzyl alcohol – benzaldehyde VLE, data from ref. [28, 38]; (h) CO_2 – benzaldehyde VLE, data from ref. [39]; (i) CO_2 – benzyl alcohol vapor phase composition (80 °C), data from ref. [40] and this work (solid symbols).

measurements were carried out in this study. Since oxygen may react with benzaldehyde, experiments were conducted with N_2 instead. Results obtained from triplicate measurements are reported in Table 5-2. The systems $O_2(N_2)$ – benzyl alcohol (Figure 5-2a), O_2 (N_2) – benzaldehyde (Figure 5-2b) and $CO_2 – O_2$ (Figure 5-2c) as well as benzyl alcohol – benzaldehyde (Figure 5-2g) and CO_2 – benzaldehyde (Figure 5-2h) could be satisfactorily fitted without associating interactions. Fitted k_{ij} values can be found in Table 5-3.

Table 5-3: Fitted k_{ij} values for binary systems with no cross association.

Entry	Compound 1	Compound 2	k_{ij}
1	Benzyl alcohol	N_2 (O_2)	0.20701
2	Benzaldehyde	N_2 (O_2)	0.00535
3	CO_2	O_2	0.08971
4	Benzyl alcohol	benzaldehyde	0.02338
5	CO_2	benzaldehyde	0.04284

Table 5-4: Fitted k_{ij} and β_{cross} values for binary systems with cross association.

Entry	Compound 1	Compound 2	k_{ij}	β_{cross}	Temperature range (°C)
1	CO_2	H_2O	0.15476	0.02362	80
2	H_2O	Benzyl alcohol	0.00841	0	20 – 150
3	H_2O	Benzaldehyde	-0.06387	0.13074	25 – 147
4	CO_2	Benzyl alcohol	$-0.063819 + 8.353 \cdot 10^{-4} \cdot T\,(K)$	0.26337	60 – 180

On the other hand, the binary systems $CO_2 – H_2O$ (Figure 5-2d), H_2O – benzyl alcohol (Figure 5-2e), H_2O – benzaldehyde (Figure 5-2f) and CO_2 – benzyl alcohol (Figure 5-2i) required the assumption of suitable association schemes for obtaining satisfactory results. Fitted parameters can be found in Table 5-4. The $CO_2 – H_2O$ system was modeled assuming one association site on CO_2 which only interacts with water (entry 1). The cross association energy for the system benzyl alcohol – water was estimated from the CR-1 combining rule; accordingly, the model tended to overestimate the saturation concentration of water in benzyl alcohol (entry 2). For benzaldehyde – H_2O (entry 3), two association sites on

benzaldehyde were estimated capable of cross-associating with water only. The cross association parameters were estimated with the modified CR-1 combining rule. Finally, one cross-association site was estimated on CO_2 to only cross-associate with benzyl alcohol for the last system (entry 4). Further details can be found in ref. [29]. Since the model performed satisfactorily for binary systems, ternary systems were modeled in the next step.

5.3.3 Application of the CPA equation of state for phase behavior modeling

The binary interaction parameters between the relevant compounds allowed the prediction of the phase behavior of ternary mixtures, i.e. benzyl alcohol – O_2 – CO_2 representing the substrate mixture and benzaldehyde – H_2O – CO_2 representing the product mixture at 100 % conversion and 100 % selectivity. The phase behavior predictions were accompanied by measuring dew points experimentally.

Table 5-5: Experimental dew points for relevant ternary mixtures between 60-80 °C.

Temperature (°C)	P_{high}[a]	P_{low}[b]	P_{sep}[c]
0.45 ± 0.02 mol-% benzyl alcohol, 0.16 ± 0.02 mol-% oxygen and 99.39 ± 0.02 mol-% CO_2			
60 ± 0.5	123.0 ± 1.9	122.0 ± 1.9	122.5 ± 2.4
70 ± 0.5	133.0 ± 4.1	132.0 ± 3.9	132.6 ± 4.5
80 ± 0.5	140.0 ± 2.5	139.0 ± 3.1	139.2 ± 3.3
0.60 ± 0.02 mol-% benzyl alcohol, 0.30 ± 0.02 mol-% oxygen and 99.10 ± 0.02 mol-% CO_2			
60 ± 0.5	151.5 ± 1.7	150.5 ± 2.3	150.7 ± 2.5
0.91 ± 0.02 mol-% benzyl alcohol, 0.43 ± 0.02 mol-% oxygen and 98.66 ± 0.02 mol-% CO_2			
60 ± 0.5	133.0 ± 3.3	132.0 ± 3.5	132.4 ± 3.9
70 ± 0.5	150.0 ± 3.3	149.0 ± 3.9	149.2 ± 4.1
80 ± 0.5	163.0 ± 3.5	162.0 ± 3.5	162.5 ± 4.0
0.45 ± 0.02 mol-% benzaldehyde, 0.45 ± 0.02 mol-% H_2O and 99.10 ± 0.02 mol-% CO_2			
60 ± 0.5	105.0 ± 1.7	104.0 ± 1.3	104.7 ± 2.0
80 ± 0.5	110.0 ± 1.1	109.0 ± 2.1	109.0 ± 2.1
0.90 ± 0.02 mol-% benzaldehyde, 0.90 ± 0.02 mol-% H_2O and 98.20 ± 0.02 mol-% CO_2			
60 ± 0.5	112.0 ± 2.5	111.0 ± 2.5	111.5 ± 3.0
80 ± 0.5	133.0 ± 2.5	131.0 ± 1.5	132.5 ± 3.0

[a]Average high pressure limit; [b]Average low pressure limit; [c]Pressure interval for phase separation.

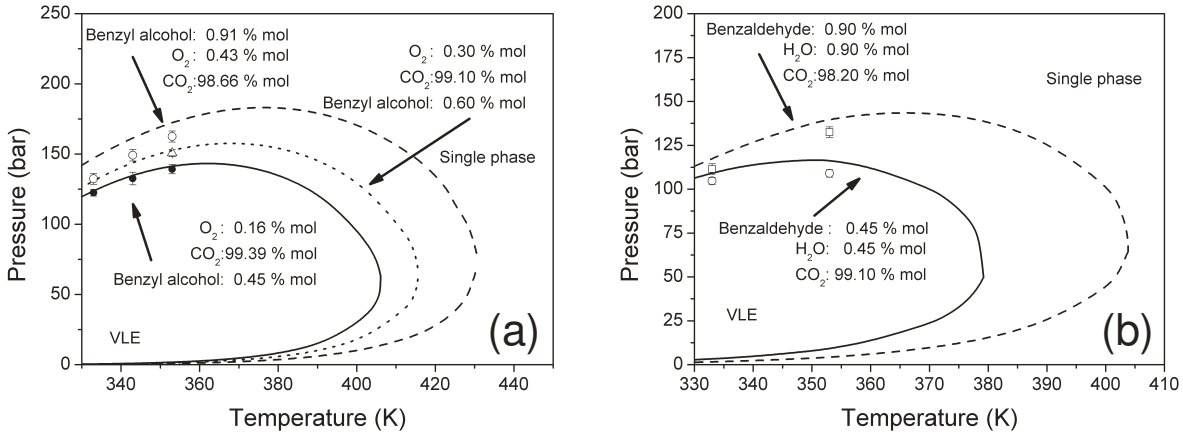

Figure 5-3: CPA Equation of State predictions (lines) and experimental data (points) for the phase transitions of the ternary systems benzyl alcohol – O_2 – CO_2 (a) and benzaldehyde – H_2O – CO_2 at catalysis-relevant conditions and compositions.

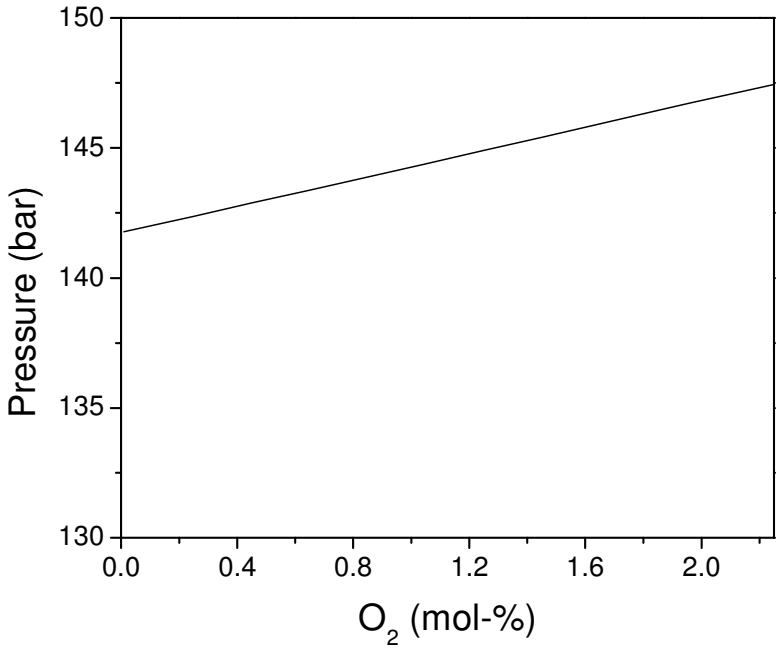

Figure 5-4: Influence of the oxygen concentration on the dew point (conditions: 0.45 mol-% benzyl alcohol, O_2 as indicated, rest CO_2; 80 °C).

The results are shown in Table 5-5. Comparing the experimental data with the model (Figure 5-3a) showed that the dew point pressures were slightly overestimated. Nevertheless, especially at low benzyl alcohol concentrations, the model was in reasonable agreement with the experimental data. Similar observations were made for the ternary mixture representing the product mixture (Figure 5-3b). In general, the pressure required for the reaction mixture to exist as a single phase is higher for the mixture corresponding to 0 % conversion. At an assumed conversion of 50 % (with 100 % selectivity) the dew point of the mixture also occurred at a lower pressure. The role of oxygen was further studied being both the oxidant and influencing the dew point (Figure 5-4). With increasing oxygen concentration, the dew point is increasing. Within a range relevant for the catalytic oxidation reaction, the influence of oxygen on the dew point is much smaller compared to the influence of the benzyl alcohol concentration.

5.3.4 Benzyl alcohol oxidation as a function of pressure

The oxidation of benzyl alcohol was studied with pressurized CO_2 as the solvent with a commercial shell-impregnated 0.5 wt.-% Pd/Al_2O_3 catalyst in a fixed bed reactor. By using a shell-impregnated catalyst, internal mass transport effects were minimized. Due to the tunability of the CO_2 solvent properties, the pressure plays an important role in this type of reaction. Figure 5-5 shows the dew points of substrate and product mixtures obtained from CPA modeling at 80 °C with different benzyl alcohol/benzaldehyde concentrations in stoichiometric mixtures with oxygen and water, respectively. Accordingly, the catalytic activity of different stoichiometric compositions as a function of the pressure was studied maintaining

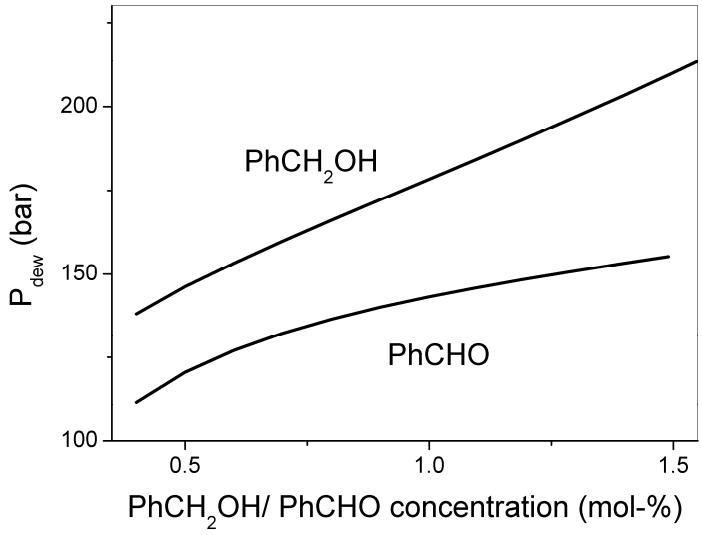

Figure 5-5: Dew points of stoichiometric benzyl alcohol (benzaldehyde) – O_2 (water) in CO_2 mixtures at 80 °C.

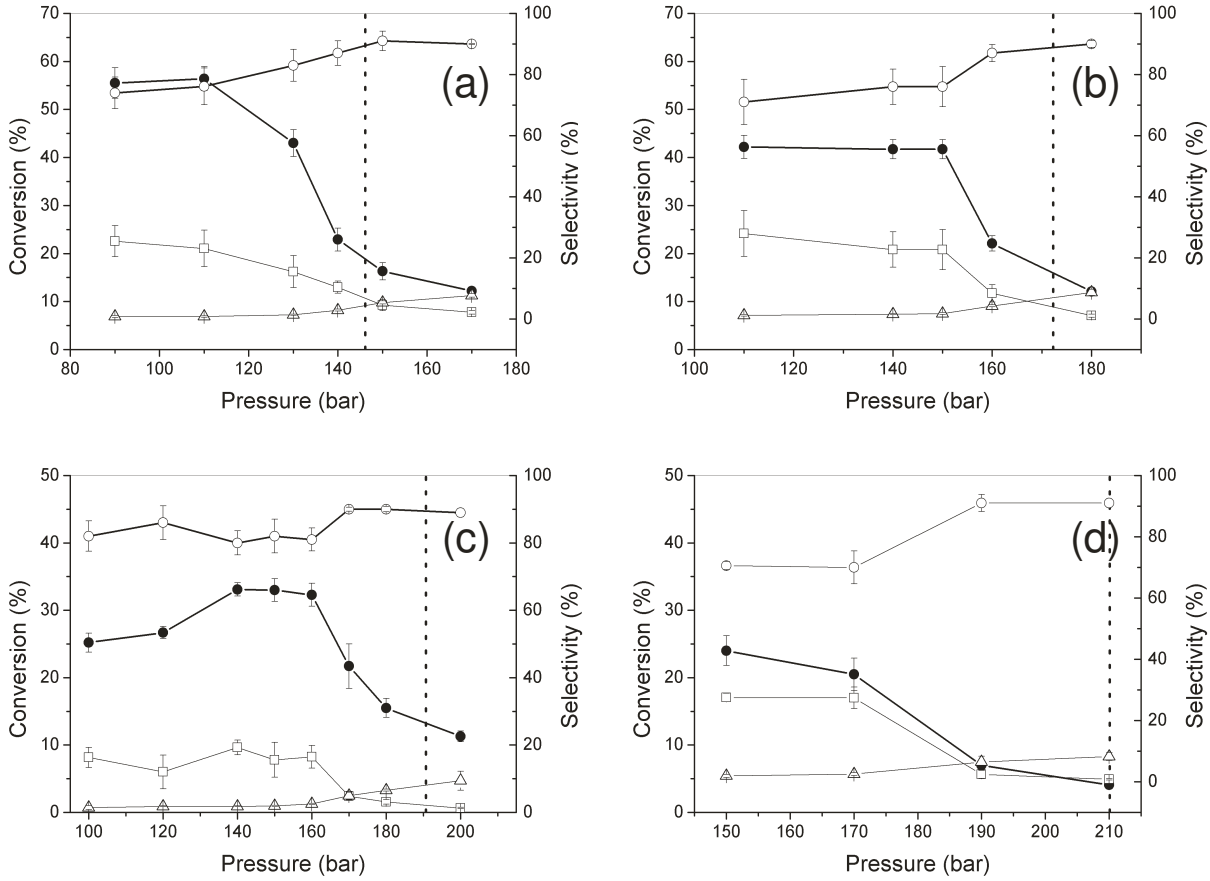

Figure 5-6: Catalytic oxidation of benzyl alcohol as a function of the system pressure. The dotted line represents the phase transition prediction from CPA modeling. Conditions: 80 °C, total flow 0.177 mol/min, 1.25 g 0.5%Pd/Al_2O_3 in a fixed bed reactor; feed composition: (a) 0.5 mol-% benzyl alcohol, 0.25 mol-% O_2, rest CO_2; (b) 0.9 mol-% benzyl alcohol, 0.45 mol-% O_2, rest CO_2; (c) 1.2 mol-% benzyl alcohol, 0.6 mol-% O_2, rest CO_2; (d) 1.5 mol-% benzyl alcohol, 0.75 mol-% O_2, rest CO_2; (●) conversion, (○) benzaldehyde selectivity, (□) toluene selectivity, (∆) selectivity to overoxidation products.

an overall constant molar flow (Figure 5-6). In general, higher conversions were obtained at lower pressures where – on the other hand – the benzaldehyde selectivity was low (70-80 %). The main side product was toluene. Raising the pressure caused a significant decrease in the selectivity to toluene and an overall shift to high benzaldehyde selectivities (>90 %). Overoxidation products, i.e. benzoic acid and benzyl benzoate, became the main side-products. Noticeably, the reaction rate dropped significantly (measured under steady-state conditions) when exceeding a certain pressure. The pressure at which the conversion dropped was increasing with the benzyl alcohol concentration suggesting that the phase transition from two phases to a single phase is the origin of the change in reactivity and selectivity. The dew points obtained from the CPA model (Figure 5-5 and dotted lines in Figure 5-6) are slightly

overestimated (*vide supra*), but give a good indication of the pressure around which the catalytic performance of the system changes critically. The influence of the phase behavior was additionally supported by visual inspection of the feed mixture in the inter-connectable view cell of the setup. Thus, for the feed mixture consisting of 0.9 mol-% benzyl alcohol (Figure 5-6b), clearly two phases were observable at 150 bar, while only one was existing at 170 bar. At an intermediate pressure of 160 bar,

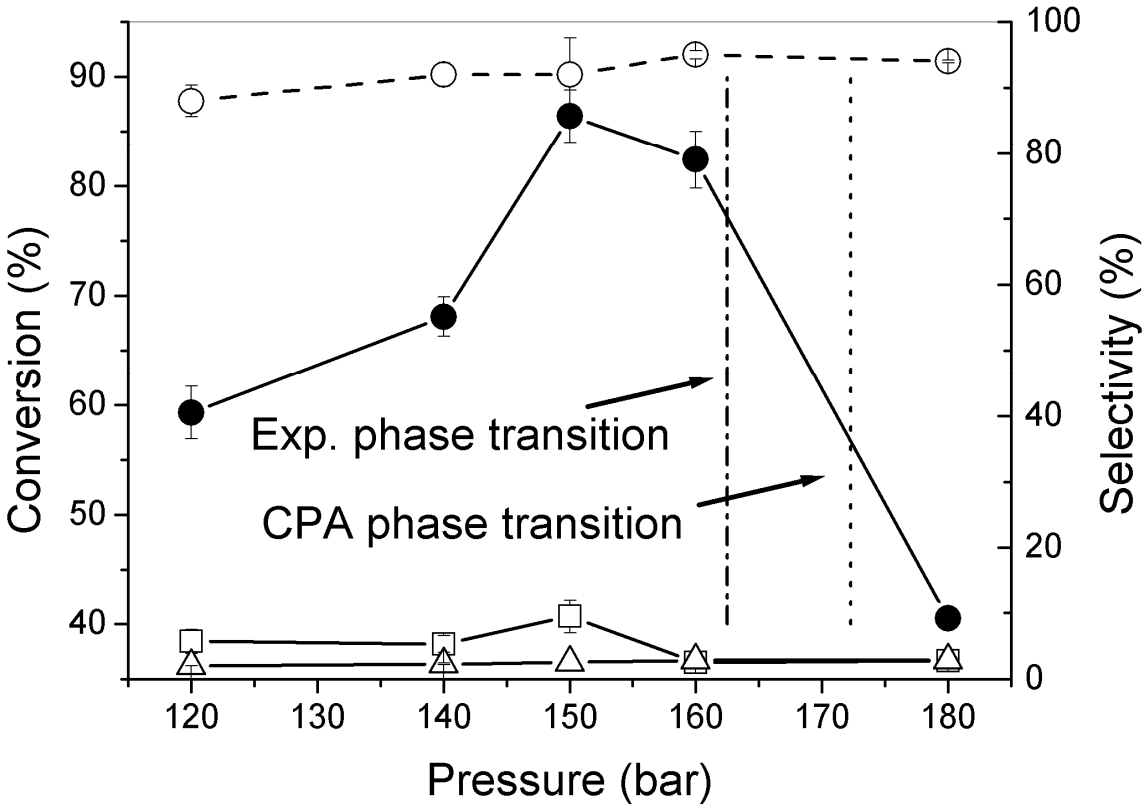

Figure 5-7: Oxidation of benzyl alcohol at a molar flow of 0.118 mol/min; conditions: 80 °C, 1.25 g 0.5%Pd/Al_2O_3 in a fixed bed reactor; feed composition: 0.9 mol-% benzyl alcohol, 0.45 mol-% O_2, rest CO_2; (●) conversion, (○) benzaldehyde selectivity, (□) toluene selectivity, (Δ) selectivity to overoxidation products.

no clear conclusion on the number of phases could be drawn from simple phase monitoring under flow conditions. Decreasing the overall molar flow showed that the pressure at which the decrease in reaction rate occurred remained almost the same (Figure 5-7) matching again well with the experimental data and the CPA predictions. Compared to the previously described experiments, the selectivity was always higher than 90 %. A significant increase in conversion was found between 140 and 150 bar which was also reported under similar conditions [7]. Again, at both pressures the system exists

as two phases by visual inspection. Thus, the observed increase in reaction rate is not due to a phase transition. The increased toluene selectivity indicates a faster transport of benzaldehyde to the catalyst surface compared to O_2. When changing from two phase conditions to single phase conditions, the time until a steady-state was reached was very long and a continuous decrease in catalytic activity occurred. Note that in this study a steady-state was assumed when the conversion was stable within the experimental uncertainty during a few hours, so it cannot be unambiguously excluded that further long-term deactivation might occur.

5.3.5 Macroscopic mass transport in the two phase region

One observation made during the phase behavior measurements was that the alcohol-rich phase is only small in volume and viscous compared to the CO_2 phase. This might hamper the transport of the alcohol-rich phase through the reactor. In a simple experiment under non-reactive (i.e. oxygen-free) conditions the effluent mass flow was compared to the feed flow (Figure 5-8) under definite single (200 bar) and two phase (100 bar) conditions by measuring the weight increase of the accumulated benzyl alcohol as a function of time at the system exit and comparison with the feed flow. Starting with a system pressure of 200 bar, the effluent flow was constant and the catalyst particles only in contact with the CO_2-dominated phase. Upon change to 100 bar (~20 min), the effluent benzyl alcohol flow was decreasing to zero before it reached a constant level as high as at 200 bar again (~70-80 min). Thus, the organic substrate was deposited in the system including the reactor and the catalyst particles. Increasing the pressure to 200 bar caused an intermediate massive increase in the flow which reached again the value observed before (after roughly 20 min). Thus, under single phase conditions previously deposited substrate is removed from the reactor (and the catalyst particles). The deposition of substrate in the biphasic pressure region has two important consequences, i.e. a higher concentration of the substrate in the reactor as compared to the feed and accordingly a longer residence time of benzyl alcohol in the reactor. Thus, a direct comparison of continuous and batch experiments is not possible offhand which is additionally complicated by a pressure-dependent induction phase observed under batch conditions [7]. Therefore, catalytic batch experiments were performed in the view cell previously used for phase behavior determination. Also here, two phase conditions resulted in a higher catalytic activity than single phase conditions. In contrast to the continuous experiments, selectivities close to 100 % were observed. Due to conversion of benzyl alcohol to the more readily soluble benzaldehyde, a phase transition from two phases to a single phase was observed at low pressure (Figure 5-9).

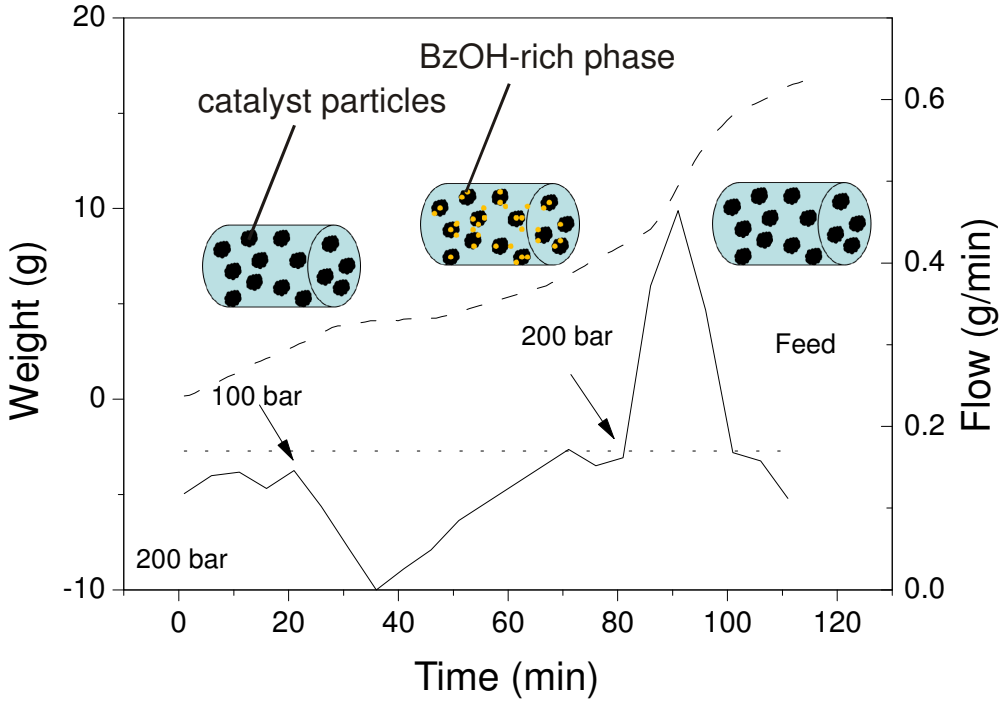

Figure 5-8: Comparison of feed (dotted line) and effluent flow (solid line) depending on the pressure (conditions: 0.9 mol-% benzyl alcohol, rest CO_2, 80 °C). The dashed line shows the accumulated increase in benzyl alcohol mass measured by a balance placed at the reactor exit. Note that the initial difference between feed and effluent flow is due to drag-out of benzyl alcohol at the exit due to the high gas flow.

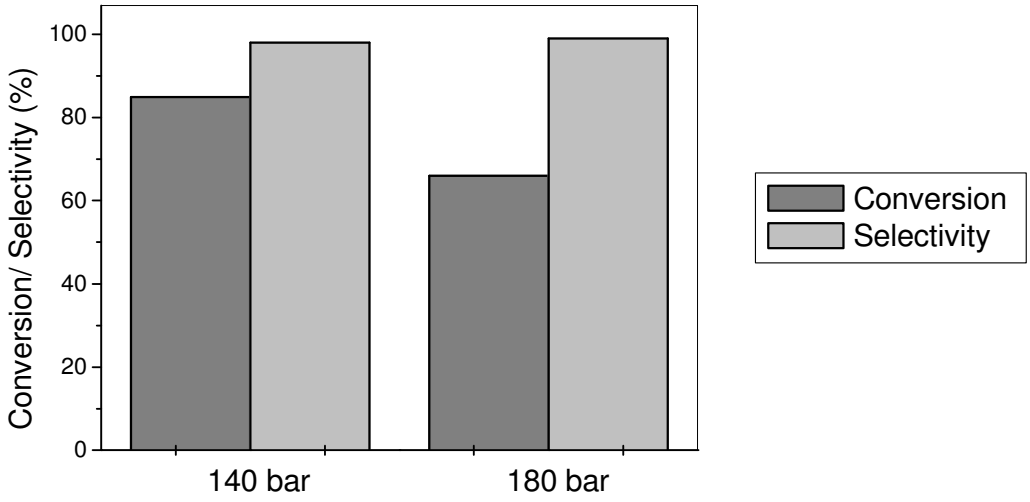

Figure 5-9: Catalytic activity under batch conditions at 140 bar (two phases) and 180 bar (single phase). Conditions: 3.2 mmol BzOH, 1.6 mmol O_2, 354 mmol CO_2 (0.9 mol-% BzOH, 0.45 mol-% O_2), 200 mg 0.5%Pd/Al_2O_3 (as pellets), 80 °C, pressure as indicated, 1 h reaction time.

5.3.5 Influence of oxygen in the single phase and two phase region

The time required to reach a steady state was usually short within the pressure region of high conversion (2-4 h) but became very long (1-2 days) when changing from the low- to the high-pressure region indicating that the low conversion is also a cause of gradual (reversible) catalyst deactivation. This would additionally limit the comparability of (short-term) batch experiments with continuous experiments as described here. Interestingly, the catalyst recovered slightly during overnight shutdown phases. The concentration of oxygen can both increase the reaction rate and deactivate the catalyst due to oxidation of palladium [41, 42]. Studying the influence of O_2 in higher than stoichiometric amounts caused a decrease in conversion both under single and two phase conditions (Figure 5-10). In general, the selectivity to toluene decreased and the amount of benzoic acid and benzyl benzoate increased with increasing oxygen concentrations though still under two phase conditions a relatively high amount of toluene prevailed. Under single phase conditions, the conversion decreased continuously over two subsequent days indicating catalyst deactivation. After 2 days, the conversion was stable over a few hours though a further decrease over a longer period cannot be excluded. The deactivation was reversible; after 7 days under high oxygen concentrations and single phase conditions (i.e. measuring Figure 5-10a), a conversion of 89.7 % ± 1.4 % was found when switching back to two phase conditions compared to 86.4 % ± 2.4 % obtained before (for conditions see Figure 5-7). Note that some long-term deactivation was, however, observed.

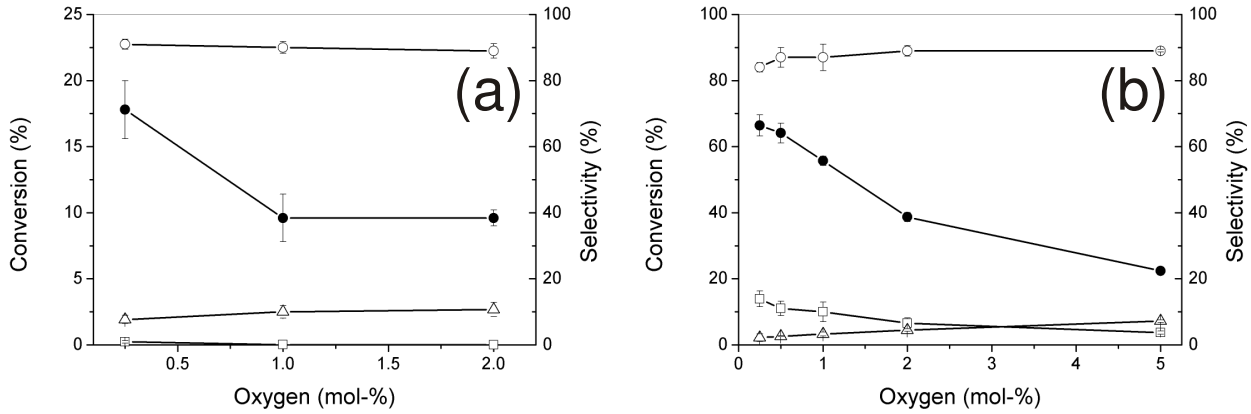

Figure 5-10: Benzyl alcohol oxidation with different oxygen concentrations under single phase (a) and two phase conditions (b); reaction conditions: 80 °C, 1.25 g 0.5%Pd/Al_2O_3 in a fixed bed reactor; feed composition: 0.5 mol-% benzyl alcohol, O_2 as indicated, rest CO_2, total flow 0.177 mol/min, (a) 180 bar, (b) 140 bar; (●) conversion, (○) benzaldehyde selectivity, (□) toluene selectivity, (Δ) selectivity to overoxidation products.

5.3.6 Higher reaction temperature

So far, the reaction was studied at a temperature of 80 °C and a clear influence of the phase behavior was observed. Performing the reaction at 100 °C, a different reaction profile was found (Figure 5-11). While still a decrease in reaction rate was found at higher pressures there was no abrupt change in conversion although CPA modeling suggests a phase transition to occur in the investigated pressure range. The decrease in toluene selectivity observed between 130 and 140 bar might be due to a change in the number of phases but no clear conclusions can be drawn here. In contrast to the catalytic reactions performed at 80 °C, the time required to reach a steady-state was always short (2-3 h).

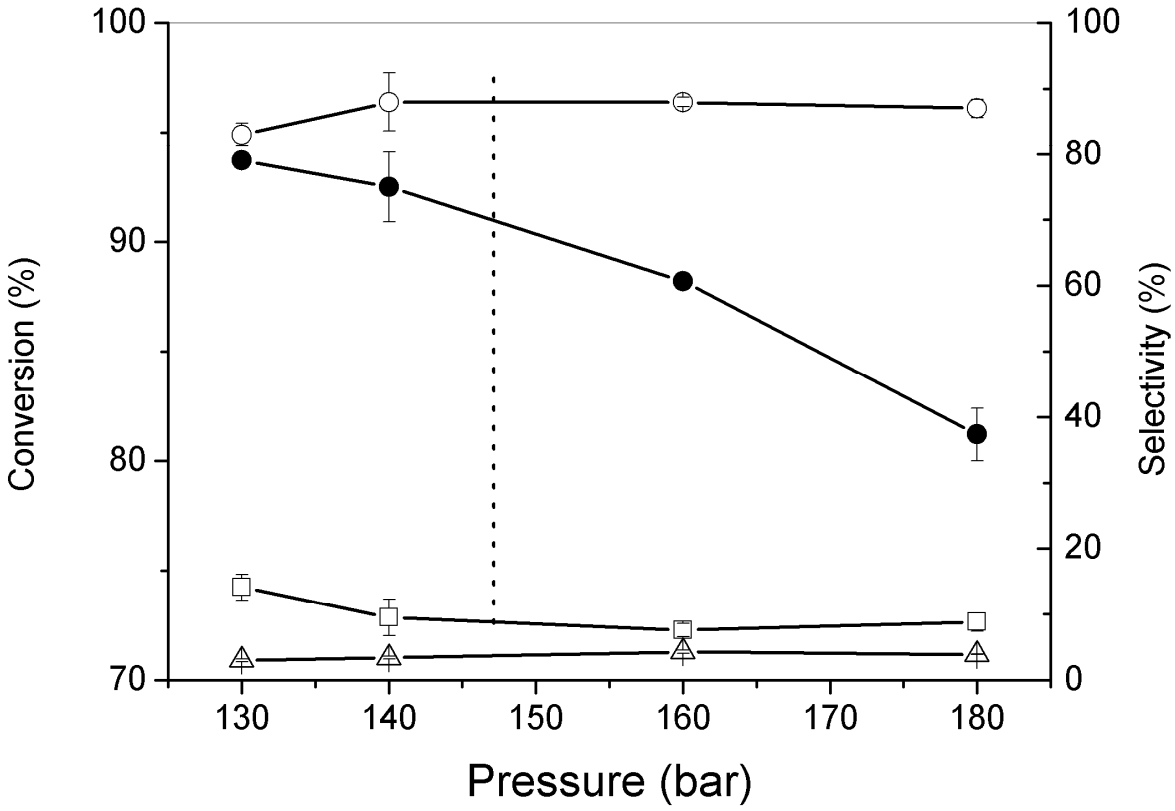

Figure 5-11: Pressure dependency of the benzyl alcohol oxidation at 100 °C. Reaction conditions: 100 °C, 1.25 g 0.5%Pd/Al_2O_3 in a fixed bed reactor; feed composition: 0.5 mol-% benzyl alcohol, 0.25 mol-% O_2, rest CO_2, total molar flow 0.177 mol/min. The dotted line indicates the phase transition from CPA modeling; (●) conversion, (○) benzaldehyde selectivity, (□) toluene selectivity, (Δ) selectivity to overoxidation products.

5.4 Discussion

Previous studies on alcohol oxidation in "supercritical" CO_2 often found a pronounced influence of the pressure on the observed catalytic activity [6, 15, 43] which was connected to the phase behavior [7]. Since reactions in pressurized CO_2 are often carried out in closed reactors, the phase behavior cannot easily be monitored though it is essential for the catalytic reaction. The CPA Equation of State used in this study proved useful in predicting the pressure dependency of the phase behavior of systems containing CO_2, O_2, H_2O, benzyl alcohol and benzaldehyde, respectively. With parameters of pure compounds and fitted binary interaction parameters, the pressure at which the phase transition occurs was found to be only slightly over-predicted, especially at low concentrations of the organic substrate. The pressure of the dew points for the substrate mixture are higher than for the product mixture, thus, a phase transition can occur during the reaction in a certain pressure range as was also experimentally observed in the batch experiments. This flexible approach can predict the phase behavior for a broad range of conditions and thus offers an alternative to often laborious experimental phase behavior determination requiring special equipment. The model predictions for the phase transition furthermore fell in the pressure regime where a considerable change in catalytic activity was observed and gave a good indication of the optimal system pressure. Thus, the CPA EoS allows for a more effective reaction optimization. This can be especially useful where little is known about the phase behavior. In the present case, the phase behavior modeling suggested that the catalytic reaction should be studied at higher pressures than previously done in order to reach a single phase. Under very similar conditions as in ref. [7] also an increase in reaction rate between 140 bar and 150 bar (0.9 % benzyl alcohol, 0.45 % O_2, rest CO_2, *cf.* Figure 5-7) was found here. Only when extending the studies to pressures >160 bar a decrease in reaction rate was concurring with the system being in a single phase which is similar to results reported for the oxidation of cinnamyl alcohol [8]. Both at 140 bar and at 150 bar the mixture was biphasic though the phase behavior in the catalyst pores may be different as indicated by infrared spectroscopic studies [7].

Pd catalysts used in alcohol oxidation are sensitive to the availability of oxygen [41, 44]. A low availability of oxygen causes blocking of surface sites by adsorbed hydrogen and strongly adsorbing CO which are both removed by oxidation. High amounts of oxygen favor overoxidation of Pd which is connected to a lower catalytic activity [41, 44, 45]. Hence, a general recommendation is to operate the reactor in the oxygen mass-transport limited regime [3]. The lower catalytic activity observed under single phase conditions might be connected to the oxidative deactivation of the palladium particles on the catalyst surface which underlines that the oxygen mass transport to the catalyst surface is improved

compared to the biphasic situation. This is further corroborated by the significantly higher selectivity to overoxidation products. Note that oxidized palladium can be re-reduced by the alcohol [46] so no permanent (short-term) deactivation is caused by oxygen treatment. Under biphasic conditions, XAS measurements showed that Pd was mainly reduced [41, 42] but analogue measurements under single phase conditions are still missing. If the oxidation state of the active metal is the primary reason for the pronounced response to the phase behavior, then the results made at 100 °C where no sudden change in conversion was observed might indicate that palladium is always reduced at that temperature.

The oxidation of palladium occurs rapidly [6, 41] and does not explain the long time required for reaching a steady-state when operating in a single phase. A side product in the oxidation of primary alcohols is the corresponding carboxylic acid which is only poorly soluble in CO_2. Hence, adsorption of benzoic acid on alumina and/or Pd during single phase conditions could cause deactivation and was previously suggested from IR investigations [7]. In the presence of two phases, the benzyl alcohol rich layer around the catalyst particles has a higher eluting power than the corresponding CO_2-rich single phase cleaning the catalyst surface from overoxidation products. In addition, less benzoic acid is formed under biphasic conditions.

The phase transition was accompanied by a change in the product distribution; the major side product at low pressures was toluene while benzoic acid and benzyl benzoate were the preferred side products at high pressures. Cleavage of the C-O bond in benzyl alcohol is caused by surface adsorbed hydrogen on palladium [47] and thus the difference in selectivity is related to a low availability of oxygen which first has to diffuse through a layer of the second benzyl alcohol (or benzaldehyde) rich phase covering the catalyst particles. Under single phase conditions, the availability of oxygen is obviously improved. Though more data are necessary to corroborate this trend, the selectivity also appeared to depend on the flow. At high flows, the selectivity to benzaldehyde was ca. 70 %, while the composition studied at the same pressure at a lower flow oxidized benzyl alcohol with ca. 90 % selectivity. Additionally, the system exhibited only a small response to the pressure within the two phase region at high flow. With lower flow, however, a maximum in conversion was observed at the high pressure end of the two phase region. At this point, the amount of data allow no clear definition of this trend and so the explanation sketched in Figure 5-12 remains highly speculative: at very low pressures the solubility of benzyl alcohol is poor and the catalyst particles are covered in a layer of substrate which is intensified by the observed accumulation of the substrate in the reactor and the additional low solubility of the benzaldehyde product (*cf.* Figure 5-5). The layer protects the catalyst particles keeping Pd in its active state. The low availability of oxygen causes significant formation of toluene and may also hinder the

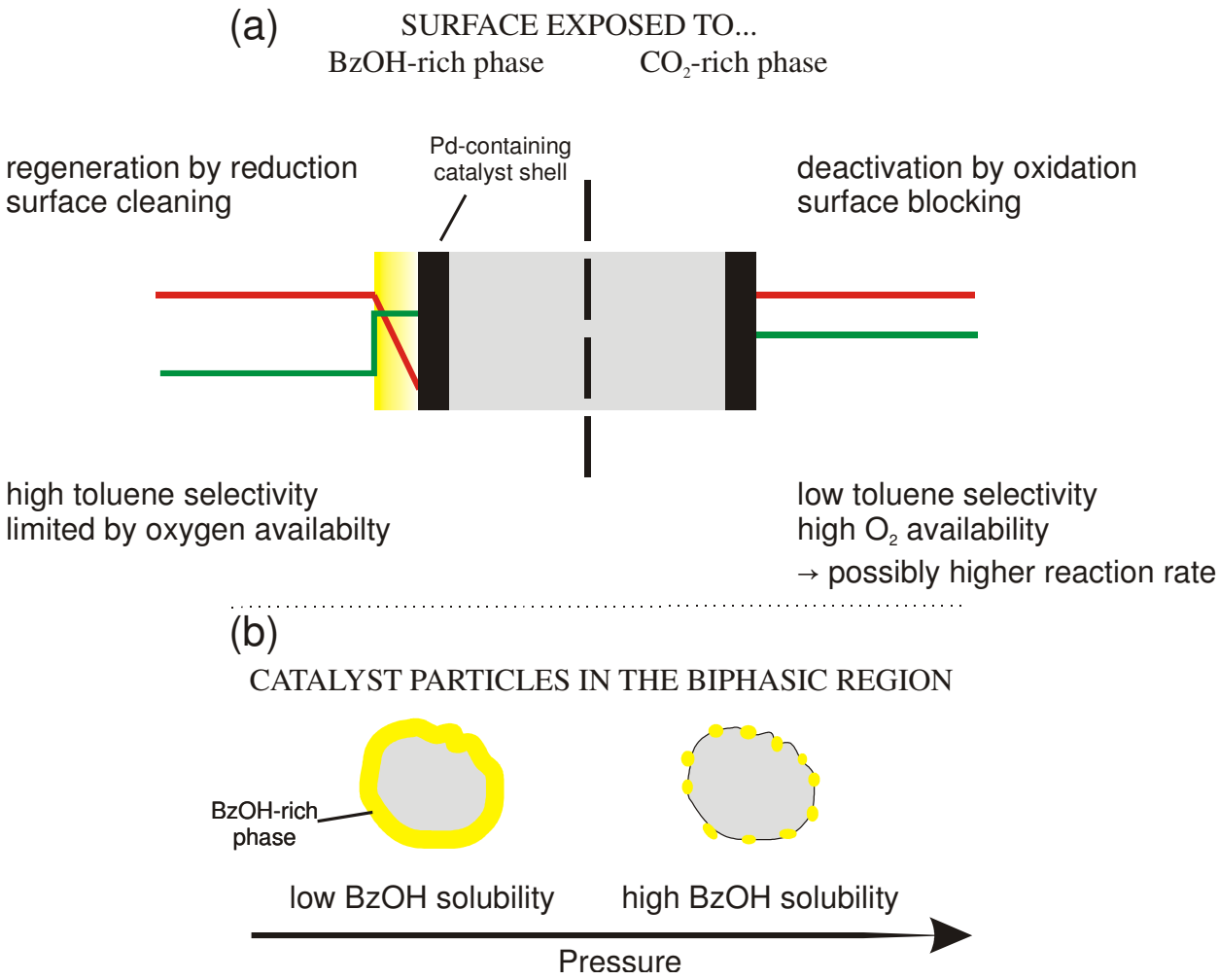

Figure 5-12: Schematic catalytic processes at the catalyst interface depending on the pressure; (a) left: situation on the catalyst surface upon exposure to the benzyl alcohol-rich phase, right: exposure to the CO_2-rich phase; (b) distribution of benzyl alcohol-rich phase on catalyst particles depending on the solvent power of CO_2. Note that the extensive pore system of the catalyst has been omitted for clarity reasons.

conversion of substrate. When the catalyst surface is exposed directly to the CO_2-rich phase, the selectivity to toluene is low and the high availability of oxygen may in principal afford higher reaction rates over the catalyst in its active state, but the catalyst (gradually) deactivates. At high pressures in the biphasic region both scenarios may coexist, if the flow (and therefore the substrate accumulation) in the reactor is not too high. Additionally, the solubility for benzaldehyde is high which is rapidly extracted to the CO_2-rich phase. The advantages of contact with both phases may add up: droplets of benzyl alcohol maintain the catalyst in its active state while a high benzaldehyde selectivity and potentially also a higher conversion is obtained from catalyst sites directly in contact with the supercritical phase. Note that due to deactivation, the reaction rate over *not* deactivated palladium under single phase conditions

was not accessible. The difference in conversion in short-time (i.e. low deactivation) batch experiments between biphasic and single phase conditions was however low. Previous IR studies further indicated that the phase transition might be (slightly) different within the pore system [7] hinting at the possible coexistence of single and biphasic conditions. Once again, more data and extensive ATR-IR as well as EXAFS studies are necessary to corroborate these speculations.

Due to the high viscosity and polarity and the small amounts as compared to the CO_2-rich phase, the phase rich in organic substrate was apparently accumulating in the reactor (and the overall system) resulting in a higher benzyl alcohol/benzaldehyde concentration as compared to the feed and consequently a longer residence time. Applying conditions where the feed composition is in a single phase causes the subsequent dissolution of excess benzyl alcohol (or benzaldehyde etc.) in the reactor. The complex transport of the phase rich in organic substrate is one reason why no direct comparison of batch and continuous experiments is possible and needs further investigation. Still, both under batch and continuous flow, biphasic conditions gave the highest reaction rate. The accumulation is noticeable by an intermediate change in the exit flow of the substrate during the phase transition. The measurement is tedious though it does not require further equipment. This method could potentially be exploited to (automatically) determine phase transitions for this and similar systems.

5.5 Conclusions

The phase behavior of ternary systems consisting of benzyl alcohol – O_2 – CO_2 and benzaldehyde – H_2O – CO_2 was modeled using the Cubic plus Association Equation of State. The predicted dew points were validated against experimental data measured at conditions relevant to the selective catalytic oxidation of benzyl alcohol in pressurized CO_2 as a solvent. A good agreement between model and experimental dew point measurements was found. The pressure of dew points for substrate mixtures are in general higher than for the corresponding product mixtures implying that the optimal pressure is defined by the former mixtures. Since the dew point plays a crucial role in catalytic studies with pressurized CO_2, the model was applied in the catalytic oxidation of benzyl alcohol. The reaction rate was found to depend on the number of phases present in the reactor, the model thus supplying valuable information towards the optimal reaction conditions. The model further indicated that catalytic data especially at higher pressures than in previous studies are required. Biphasic conditions at pressures close to the dew point resulted in the highest reaction rate with toluene formed as a side product in noticeable amounts. When operated in a single phase, products from overoxidation became the dominating side products and long

equilibration times where observed presumably due to surface blocking by benzoic acid. Under biphasic conditions, the organic substrate accumulated in the reactor (and also in the system in general) causing an enhanced substrate concentration and a longer residence time which needs to be investigated more thoroughly in the future.

5.6 References

[1] M. Besson, P. Gallezot, Catal. Today 57 (2000) 127.

[2] J.H.J. Kluytmans, A.P. Markusse, B.F.M. Kuster, G.B. Marin, J.C. Schouten, Catal. Today 57 (2000) 143.

[3] T. Mallat, A. Baiker, Chem. Rev. 104 (2004) 3037.

[4] A.M. Steele, J. Zhu, S.C. Tsang, Catal. Lett. 73 (2001) 9.

[5] Z. Hou, N. Theyssen, W. Leitner, DGMK Tagungsber. 2005-2 (2005) 61.

[6] M. Caravati, J.-D. Grunwaldt, A. Baiker, Catal. Today 91-2 (2004) 1.

[7] M. Caravati, J.-D. Grunwaldt, A. Baiker, Phys. Chem. Chem. Phys. 7 (2005) 278.

[8] M. Caravati, D.M. Meier, J.-D. Grunwaldt, A. Baiker, J. Catal. 240 (2006) 126.

[9] G. Jenzer, M.S. Schneider, R. Wandeler, T. Mallat, A. Baiker, J. Catal. 199 (2001) 141.

[10] M. Caravati, J.-D. Grunwaldt, A. Baiker, Catal. Today 126 (2007) 27.

[11] X. Wang, H. Kawanami, S.E. Dapurkar, N.S. Venkataramanan, M. Chatterjee, T. Yokoyama, Y. Ikushima, Appl. Catal. A 349 (2008) 86.

[12] B. Kimmerle, J.-D. Grunwaldt, A. Baiker, Top. Catal. 44 (2007) 285.

[13] G. Musie, M. Wei, B. Subramaniam, D.H. Busch, Coord. Chem. Rev. 219 (2001) 789.

[14] J.-D. Grunwaldt, R. Wandeler, A. Baiker, Catal. Rev. Sci. Eng. 45 (2003) 1.

[15] T. Seki, M. Baiker, Chem. Rev. 109 (2009) 2409.

[16] G. Jenzer, T. Mallat, A. Baiker, Catal. Lett. 73 (2001) 5.

[17] R. Glaser, R. Jos, J. Williardt, Top. Catal. 22 (2003) 31.

[18] A. Baiker, Chem. Rev. 99 (1999) 453.

[19] I.G. Economou, Ind. Eng. Chem. Res. 41 (2002) 953.

[20] C. Panayiotou, I.C. Sanchez, Macromolecules 24 (1991) 6231.

[21] G.M. Kontogeorgis, E.C. Voutsas, I.V. Yakoumis, D.P. Tassios, Ind. Eng. Chem. Res. 35 (1996) 4310.

[22] G.M. Kontogeorgis, M.L. Michelsen, G.K. Folas, S. Derawi, N. von Solms, E.H. Stenby, Ind. Eng. Chem. Res. 45 (2006) 4855.

[23] G.M. Kontogeorgis, M.L. Michelsen, G.K. Folas, S. Derawi, N. von Solms, E.H. Stenby, Ind. Eng. Chem. Res. 45 (2006) 4869.

[24] C. Crampon, G. Charbit, E. Neau, J. Supercrit. Fluid. 16 (1999) 11.

[25] R. Wandeler, N. Kunzle, M.S. Schneider, T. Mallat, A. Baiker, J. Catal. 200 (2001) 377.

[26] NIST Standard Reference Database, available at http://www.nist.org/news.php, last accessed 12/2010.

[27] S.H. Huang, M. Radosz, Ind. Eng. Chem. Res. 29 (1990) 2284.

[28] M. Chiu, S. Chen, H. Hsu, C. Lee, T. Chiu, J. Chin. Inst. Chem. Eng. 3 (1972) 113.

[29] I. Tsivintzelis, M.J. Beier, J.-D. Grunwaldt, A. Baiker, G.M. Kontogeorgis, Fluid Phase Equilib., available at DOI: 10.1016/j.fluid.2010.10.001.

[30] DIPPR DIADEM- The DIPPR Information and Data Evaluation Manager for the Design Institute for Physical Properties. 2006, Version1.1.0. (Computer Program).

[31] J. Chen, M. Lee, Fluid Phase Equilib. 130 (1997) 231.

[32] A. Fredenslund, G.A. Sather, J. Chem. Eng. Data 15 (1970) 17.

[33] A. Bamberger, G. Sieder, G. Maurer, J. Supercrit. Fluid. 17 (2000) 97.

[34] J.A. Nighswander, N. Kalogerakis, A.K. Mehrotra, J. Chem. Eng. Data 34 (1989) 355.

[35] J. Kiepe, S. Horstmann, K. Fischer, J. Gmehling, Ind. Eng. Chem. Res. 41 (2002) 4393.

[36] H.N. Sólimo, M.B. Gramajo de Doz, Fluid Phase Equilib. 107 (1995) 213.

[37] R.M. Stephenson, J. Chem. Eng. Data 38 (1993) 630.

[38] P.S. Pavlova, D.M. Popov, V.M. Olevskii, Tr. Gos. Nauch. Issled. Proekt. Inst. Azotn. Prom. Prod. Org. Sin. No. 15 (1972) 89.

[39] D. Walther, G. Maurer, Phys. Chem. Chem. Phys. 96 (1992) 981.

[40] D. Walther, G. Maurer, J. Chem. Eng. Data 38 (1993) 247.

[41] J.-D. Grunwaldt, M. Caravati, M. Ramin, A. Baiker, Catal. Lett. 90 (2003) 221.

[42] J.-D. Grunwaldt, M. Caravati, A. Baiker, J. Phys. Chem. B 110 (2006) 25586.

[43] Y. Xie, Z. Zhang, S. Hu, J. Song, W. Li, B. Han, Green Chem. 10 (2008) 278.

[44] C. Keresszegi, T. Burgi, T. Mallat, A. Baiker, J. Catal. 211 (2002) 244.

[45] C. Keresszegi, J.-D. Grunwaldt, T. Mallat, A. Baiker, J. Catal. 222 (2004) 268.

[46] J.-D. Grunwaldt, C. Keresszegi, T. Mallat, A. Baiker, J. Catal. 213 (2003) 291.

[47] C. Keresszegi, D. Ferri, T. Mallat, A. Baiker, J. Phys. Chem. B 109 (2005) 958.

Chapter 6

Aerobic Epoxidation of Olefins Catalyzed by the Cobalt-Based Metal-Organic Framework STA-12(Co)

Abstract

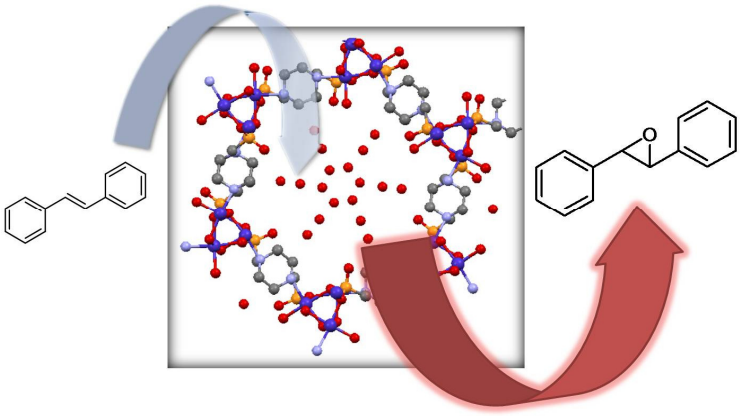

Epoxidation of stilbene by a Co-based metal-organic framework.

A Co-based metal-organic framework (MOF) was investigated as a catalyst material in the aerobic epoxidation of olefins in DMF and exhibited, based on catalyst mass, a remarkably higher catalytic activity compared to Co-doped zeolite catalysts typically used. The structure of STA-12(Co) is similar to STA-12(Ni) as evidenced by XRD Rietveld refinement and stable up to 270 °C. For the epoxidation reaction, significantly different selectivities were obtained depending on the substrate. Whereas styrene was epoxidized with low selectivity due to oligomerization, (*E*)-stilbene was converted with high selectivities between 80-90 %. Leaching of Co was low and the reaction was found to proceed mainly heterogeneously. The catalyst was reusable with only a small loss in activity. The catalytic epoxidation of stilbene with the MOF featured an induction phase. Interestingly, the induction phase was considerably shortened by styrene co-epoxidation. This could be traced back to benzaldehyde promoting the reaction. Detailed parameter and catalytic studies including *in situ* EPR and EXAFS were performed to obtain a first insight into the reaction mechanism.

6.1 Introduction

Among the broad class of oxidation reactions, the epoxidation of olefins plays a prominent role. Epoxides are highly reactive and therefore frequently used as intermediates in industry [1]. Ethylene oxide one of the world's most high demand chemicals with a production of $2.9 \cdot 10^6$ tons in 2008 in the US alone [2]. Ethylene oxide leads to ethylene glycols *via* hydrolysis [1] and thus forms the basis for many everyday products like anti-freezing agents, cosmetics etc. In contrast to ethylene the (catalytic) epoxidation of more complex olefins frequently requires oxygen in an activated form [3]. As an example, isolated Ti centers in a silica matrix have been shown to be ideal heterogeneous catalysts for epoxidations using simple peroxides such as TBHP and hydrogen peroxide [3-5]. In recent years, catalytic systems have been developed to use molecular oxygen as the least expensive oxidant for epoxidation reactions in liquid phase. Heterogeneous gold catalysts were reported to be catalytically active in the aerobic epoxidation of a number of olefins with [6] and without radical initiators [7]. The formation of secondary byproducts from oxygen was not reported in these cases while other aerobic gold based epoxidations require the activation of oxygen *via* an intermediate organic peroxide [8, 9]. The Mukaiyama epoxidation is a general protocol that facilitates the epoxidation of an olefin with oxygen by using a sacrificial aldehyde in the presence of various transition metals [10-12]. The aldehyde is transformed *in situ* to a carboxylperoxo radical facilitating oxygen transfer to the olefin. As a stoichiometric side product the carboxylic acid is formed.

Several papers report on the successful epoxidation of olefins with molecular oxygen in the absence of additional sacrificial reductants or radical initiators in DMF. Mainly heterogeneous Co catalysts were used in these investigations [13-22]. The use of amide solvents is mandatory for obtaining catalytic activity. This is mostly interpreted in terms of the formation of a Co-DMF complex reacting with oxygen to a Co superoxo species transferring oxygen to the olefin. To the best of the author's knowledge, only one study reported that the olefin transformation is accompanied by significant DMF oxidation [23] to *N*-formyl-*N*-methylformamide (FMF) which might alternatively explain the epoxidation on the basis of a solvent co-oxidation mechanism. Based on experiments with radical scavengers, the mechanism was suggested to be of radical nature. Co-substituted zeolites turned out to be the most effective catalysts and a general conclusion is that isolated Co species are most active. Since isolated species can only be obtained with low Co loadings in zeolites, rather high absolute catalyst amounts are required. Metal-organic frameworks feature, like zeolites, isolated metal-centers that are well-distributed and well-defined. Their main advantage compared to zeolites consists in their substantially higher metal loading which offers the opportunity to reduce the overall amount of catalyst significantly.

MOFs usually have high porosity and specific surface areas which makes them adequate candidates for catalytic applications both as high-surface area supports and as an intrinsic catalyst [24, 25]. MOFs have been used as catalysts for various types of oxidation reactions in the liquid phase, e.g. alcohol oxidation [26], epoxidation [27, 28], hydrocarbon oxidation [29, 30], hydroquinone oxidation [31], oxidation of organic sulfides [32] or the oxidation of aromatics [33]. Especially for these oxidation reactions, a certain degree of deactivation is frequently observed. Co-based MOFs were used previously for the oxidation of cyclohexene with TBHP resulting mainly in allylic oxidation products [34, 35].

In the present study the epoxidation of styrene and stilbene by molecular oxygen is investigated using DMF as solvent and the MOF catalyst STA-12(Co). The MOF structure has been resolved by Rietveld refinement featuring an analogous structure to STA-12(Ni) [36] and is therefore a high metal containing alternative to the frequently used zeolites. The influence of important reaction parameters is examined in detail in order to clarify the role of the Co-MOF and the role of various activating and deactivating additives on the catalytic reaction were investigated. *In situ* electron paramagnetic resonance (EPR) and X-ray absorption spectroscopy (XAS) studies provided additional valuable mechanistic information.

6.2 Experimental

6.2.1 Materials

(*E*)-stilbene (97 %), 4-*tert.*-butyl catechol (≥98 %), Cobalt (>99.8 %), dimethylacetamide (puriss.) and PPh_3 (≈99 %) were obtained from Fluka. Benzaldehyde (99.5 %, redist.) was obtained from Acros Organics, biphenyl (99.5 %) and 2,6-di-*tert.*-butyl-4-methylphenol (≥99 %) from Sigma-Aldrich, and *N*,*N*-dimethylformamide (99.8 %) from VWR. Oxygen was used from PanGas (grade 5.0). Styrene (Sigma-Aldrich, 99.5 %, stabilized) was distilled prior to use. Synthesis of *N*-formyl-*N*-methylformamide (FMF): For the preparation of *N*-formyl-*N*-methylformamide 12.5 ml (0.2 mol) of iodomethane (ABCR, 99 %) and 22.8 g (0.24 mol) of sodium diformylamide (Acros) were added to a flask containing 50 mL of acetonitrile (Sigma-Aldrich, ≥ 99.5 %) [37]. The mixture was stirred for 4 hours under reflux. After cooling the solution was concentrated with a rotary evaporator until sodium iodide precipitated. The mixture was filtered and the process was repeated with the filtrate until no further precipitation occurred. Acetonitrile was removed by evacuation to afford *N*-formyl-*N*-methylformamide sufficiently pure for GC analysis. The synthesis of FMF was done by Bertram Kimmerle (ETH Zürich).

6.2.2 MOF synthesis

STA-12(Co) was synthesized hydrothermally by reaction of cobalt(II) acetate and *N*,*N*'-piperazinebis(methylenephosphonic acid) (H_4**L**), prepared by the method reported by Mowat *et al.* [38]. In a typical synthesis cobalt(II) acetate tetrahydrate (Sigma), H_4**L**, potassium hydroxide solution (freshly prepared, 1 mol/L) and water were mixed, to give a reaction ratio of 2.0:1.0:2.12:900, in a 40 mL Teflon lined autoclave, using 20 mL of water. The reaction was stirred for 30 minutes and an initial pH of 8 recorded. The autoclave was then sealed and heated at 220 °C for 72 hours. The resulting purple powder was collected by vacuum filtration, washed with water and dried overnight at 40 °C. Phase purity was confirmed by powder X-ray diffraction, using a Stoe STADI P powder diffractometer with an Fe $K_{\alpha1}$ radiation source (λ = 1.930642 Å). The composition of STA-12(Co) was determined jointly by elemental analysis, using a CEInstruments EA1110 CHNS analyzer; thermo-gravimetric analysis (TGA), using a Netzsch TG 209, and energy dispersive X-ray spectroscopy (EDX) using a JEOL JSM-5600 scattered electron microscope (SEM) fitted with an Oxford Instruments INCA Energy 200 EDX system. Porosimetry measurements were made gravimetrically using a Hiden Isochema IGA at 77 K. Synthesis and *ex situ* characterization of the freshly synthesized MOF material was done by Michael T. Wahrmby and Paul A. Wright from the University of St. Andrews (UK).

6.2.3 Catalytic test reactions

Catalytic test reactions were performed in a 25 mL three-necked flask equipped with reflux condenser, magnetic stirrer and gas inlet. Since the system was sensitive to minute amounts of Co, cleaning the flask with aqua regia prior to each experiment was necessary. In a typical reaction, the flask was charged with 30 mL DMF and immersed in an oil bath kept at 100 °C under vigorous stirring. Oxygen was fed to the reaction mixture *via* the gas inlet with 50 mL/min. After a short time (15-30 min), 100 mg biphenyl as internal standard, 2.0 mg STA-12(Co) and 2.00 mmol of the olefin ((*E*)-, (*Z*)-stilbene or styrene) were added. Samples for GC analysis were taken in regular intervals. GC analysis was performed with a HP 6000 series gas chromatograph equipped with an FID detector and a HP-5 GC column (Agilent Technologies Inc.). Used catalyst for recycling experiments was obtained from an experiment where 20 mg instead of 2.0 mg were employed because of difficulties in recovering the small catalyst amount used in the standard experiment. Autoclave reactions were carried out in a 100 mL stainless steel autoclave with a PTFE inset. The reactor was charged with the same amounts of DMF, (*E*)-stilbene, biphenyl and STA-12(Co) as described above. A magnetic stirrer was added, the autoclave sealed, purged several times with oxygen and finally pressurized to the desired oxygen pressure. The autoclave

was immersed in an oil bath heated at ca. 110 °C so that the internal temperature in the autoclave was 100 °C. After the reaction, the autoclave was cooled to room temperature and carefully vented to prevent loss of material. Product analysis was done by GC as described above.

6.2.4 Catalyst characterization after reaction

Powder X-ray diffraction patterns were recorded on a Siemens D5000 diffractometer equipped with a Ni filter using Cu K_α-radiation. Measurements were performed in the 2Θ range from 5 to 55° with a step size of 0.01° and a step time of 2 s. Scanning Electron Microscopy (SEM) was measured with a Gemini 1530 (Zeiss) instrument.

6.2.5 Flame atomic absorption spectroscopy (F-AAS)

For leaching experiments, 15 mL of the reaction solution were concentrated and the remaining solid transferred into a crucible and treated at 700 °C in air for 4 h. The remainder was dissolved in aqua regia and diluted to 10.0 mL with distilled water. The Co concentration was measured on a Varian SpectrAA 220FS equipped with a cobalt SpectrAA lamp (Varian; λ = 240.7 nm). Concentrations were determined *vs.* standard solutions prepared from cobalt metal dissolved in HNO_3.

6.2.6 X-ray absorption spectroscopy (XAS)

Ex situ samples were measured at the ANKA XAS beamline at the ANKA synchrotron facility at the Karlsruhe Institute of Technology (Karlsruhe, Germany). The synchrotron ring was operated at 2.5 GeV and a typical ring current of 85-180 mA. Measurements were conducted in transmission mode at the Co K-edge around 7.7 keV with a Si(111) double monochromator in step scanning mode. The beam intensity was measured by means of three ionization chambers placed before and after the sample as well as after the reference (Co foil). *In situ* experiments were conducted at the X1 beamline at the Hamburger Synchrotronstrahlungslabor (HASYLAB) at the Deutsche Elektronen-Synchrotron (DESY, Hamburg, Germany). XAS spectra were recorded in transmission mode at the Co K-edge around 7.7 keV with a Si(111) double monochromator in step scanning mode in a specially designed spectroscopic liquid phase cell applicable up to 200 bar [39, 40]. The beam intensity was measured with ion chambers before and after the sample. Co foil for referencing was measured extra. Prior to the experiment a thin catalyst pellet (30 mg) was pressed and adjusted to the X-ray path. DMF (3 mL) and (*E*)-stilbene (20 mg) were added, the cell was closed, pressurized with oxygen (2 bar) and heated to 100 °C. XANES spectra were processed by energy calibration, deglitching where necessary, background subtraction, and normalization using the WinXAS 3.1 software [41]. EXAFS spectra were extracted from the XAS spectra

after analogous treatment and Fourier-transformation and fitted in R-space. Phase shifts were calculated with the FEFF 7.0 code [42].

6.2.7 Electron paramagnetic resonance (EPR)

The spectrometer used was an X-band Bruker EMX continuous wave instrument equipped with a TM type cavity. The microwave power applied was 20 mW. The sample temperature in the cavity was controlled with a Eurotherm liquid nitrogen evaporator and heater. *In situ* experiments were carried out in 1 mm quartz tubes at a temperature of 100 °C with the same substrate concentrations as in the batch experiments over several hours. The DMF solutions of (*E*)-stilbene were kept saturated with dioxygen by passing a continuous stream of the gas from a Teflon capillary over the DMF. 40 spectra were accumulated from each sample to obtain enough sensitivity. In addition, 60 mg of dry catalyst was measured in 5 mm quartz tubes (also with accumulation). The formation of products under these conditions was checked by GC. EPR measurements were done in collaboration with Reinhard Kissner (ETH Zürich).

6.3 Results

6.3.1 Synthesis of the MOF and characterization

Powders obtained from the reaction of cobalt(II) acetate with H_4**L** were characterised by powder X-ray diffraction and were found, as previously reported [43], to have a similar characteristic diffraction pattern as observed for STA-12(Ni) (Figure 6-1) [36]. Optimization of the reaction conditions indicated that a cobalt acetate to H_4**L** ratio of 2:1 at a starting pH of 8 yields phase pure samples of STA-12(Co). Powder diffraction data were analysed by Le Bail fitting, using the routines within the GSAS suite of programs [44] and with the unit cell of as-prepared STA-12(Ni) [36] as the starting point. Refinement of the unit cell parameters indicated as-prepared STA-12(Co) crystallized in the same rhombohedral space group as STA-12(Ni), but with a slightly larger cell (space group: R-3, hexagonal setting: a = 28.0942(19) Å; c = 6.2846(3) Å). Thermo-gravimetric analysis (TGA) in air, with a ramp rate of 1.5 °C min^{-1} up to 900 °C, showed two weight loss events (not shown). The first weight loss of 18.3 wt.-% (20-85 °C) was assigned to the removal of physisorbed water from the pores. This was immediately followed by an increase in gradient of the TGA plot, marking a second weight loss of 6.8 wt.-% (85-108 °C), assigned to the loss of chemisorbed water from the Co^{2+} cations. There were no further weight losses up to 270 °C, above which the structure began to collapse underlining the stability of the MOF for

high-temperature reactions. Energy dispersive X-ray spectroscopy (EDX) indicated a Co:P ratio of 1.0 and in combination with the TGA data, a composition for STA-12(Co) of $Co_2(H_2O)_2$**L**.$5H_2O$, where **L** = $C_6H_{12}N_2P_2O_6$, was postulated. This hypothetical composition shows reasonable agreement with obtained elemental analysis data (expected: C = 14.0 %, N = 5.5 %; found: C = 14.53 %, N = 4.95 %).

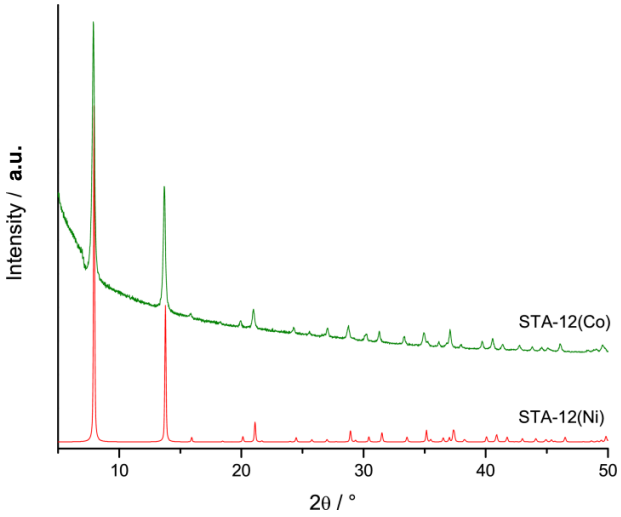

Figure 6-1: Characteristic XRD pattern of the newly synthesized STA-12(Co) MOF compared to STA-12(Ni) [36] in the as-prepared state.

The structure of STA-12(Co) was refined by the Rietveld method, using the GSAS suite of programs [44], against laboratory powder X-ray diffraction data (Fe $K_{\alpha 1}$, λ = 1.930642 Å). The structure of as-prepared STA-12(Ni) was used as the starting model, with the cell derived from Le Bail fitting. Positions of physisorbed water molecules were retained from STA-12(Ni) and the reduced amount of physisorbed water accounted for by changes in the occupancies of water sites. The final profile fit shows good agreement with the observed diffraction pattern indicating STA-12(Co) to be isostructural (Figure 6-2) with STA-12(Ni).

The porosity of STA-12(Co) was confirmed by N_2 adsorption at 77 K on dehydrated samples of STA-12(Co). Samples were activated at 140 °C for 180 minutes and found to have a pore volume of 0.10 $cm^3\ g^{-1}$ (at p/p_0 = 0.4). Synthesis and the characterization of the MOF material was done by Michael T. Wahrmby and Paul A. Wright from the University of St. Andrews (UK).

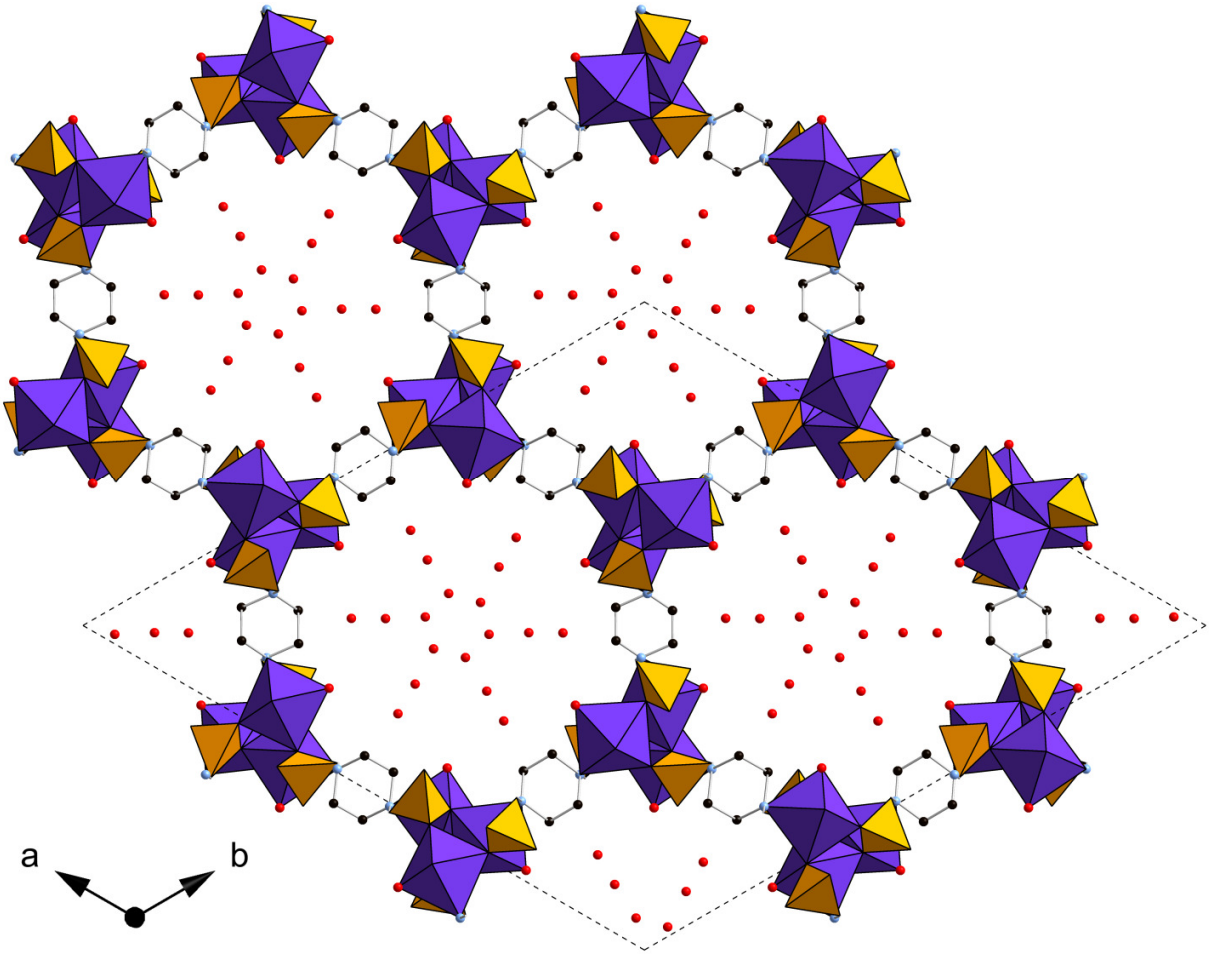

Figure 6-2: Structure of STA-12(Co) as obtained from Rietveld refinement.

6.3.2 STA-12(Co) as heterogeneous epoxidation catalyst in DMF

The Co-based metal-organic framework was used as an epoxidation catalyst in DMF with molecular oxygen as the oxidant. In a first set of experiments, the epoxidation of styrene was investigated giving styrene oxide, benzaldehyde and benzoic acid as the major products detectable by GC accounting for roughly 60 % of the mass balance. The rate of product formation increased steadily in the beginning of the reaction comprising a noticeable induction phase of ca. 30 min (Figure 6-3). The reaction was complete after 5 h and exhibited only a very low selectivity of 21 % to styrene oxide. Roughly twice the amount of *N*-formyl-*N*-methylformamide (FMF) was formed during the reaction with respect to converted styrene. The incomplete mass balance obtained from GC analysis throughout the reaction might be accounted for by styrene oligomerization. Thus, (*E*)-stilbene was used being less prone to oligomerization for further studies. (*E*)-stilbene was readily converted to *trans*-stilbene oxide (Figure

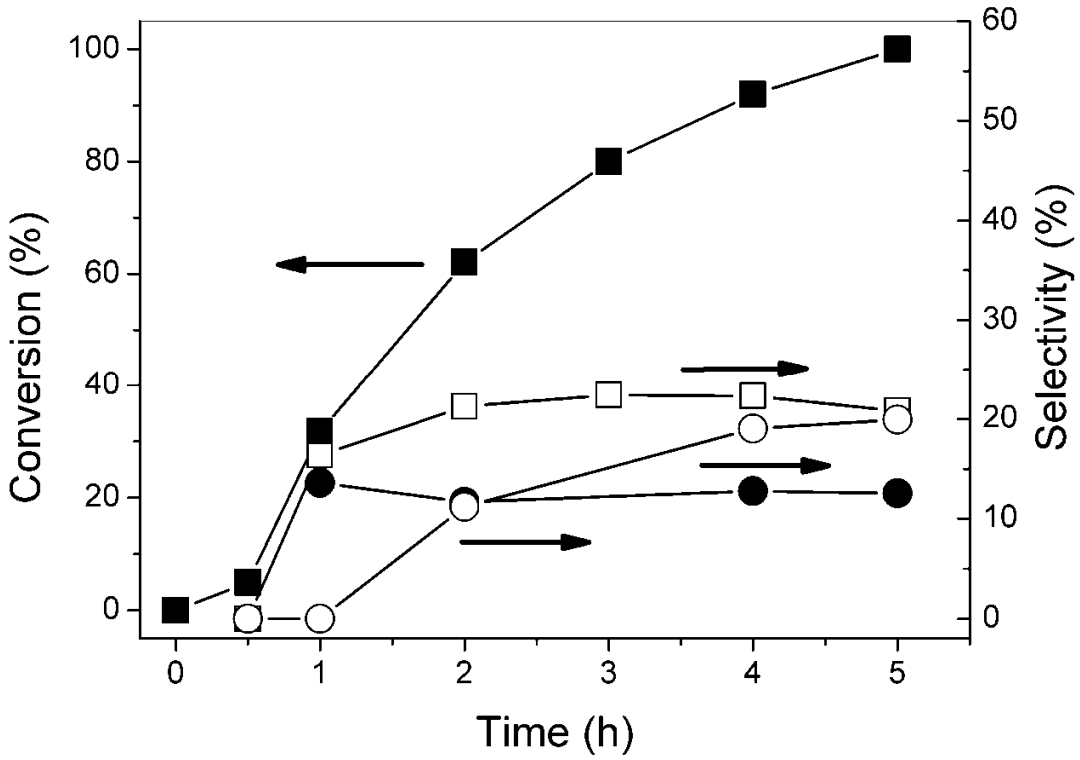

Figure 6-3: Epoxidation of styrene with the Co-based metal-organic framework material STA-12(Co) with (■) styrene conversion (□) styrene oxide selectivity, (●) benzaldehyde selectivity, (○) benzoic acid selectivity. Reaction conditions: 2.0 mmol styrene, 100 mg biphenyl, 30 mL DMF, 50 mL min^{-1} O_2, 2.0 mg STA-12(Co), 100 °C.

6-4) the mass balance from GC analysis being close to 100 %. Almost full conversion was obtained after 12 h and an FMF amount of about 1.6 times the converted stilbene was found. Note that the formation of a slightly higher amount of FMF in the case of styrene epoxidation took only 5 h. Apparently, FMF formation depends on the type of olefin and correlates with the conversion. FMF was also formed in the absence of a substrate but in significantly lower amounts. The selectivity to *trans*-stilbene oxide was close to 90 % and a low selectivity towards benzaldehyde of ca. 5 % was found assuming that two molecules of benzaldehyde are formed from one (*E*)-stilbene molecule. Co_3O_4 also exhibited some catalytic activity (Table 6-1) while essentially no product formation was found in the absence of a catalyst. An analogous mixed metal STA-12(Co,Ni) (in 1:3 ratio) was virtually not catalytically active (3 % conversion after 12 h) suggesting that the organic backbone of the MOF is inactive. In comparison to the (*E*)-isomer, (*Z*)-stilbene was epoxidized very slowly giving also *trans*-stilbene oxide (*cf.* Table 6-3, entry1). Isomerization of (*Z*)- to (*E*)-stilbene was not observed. In order to assess its stability, the catalyst was tested for reusability. Some deactivation was observed that caused mainly a longer induction phase

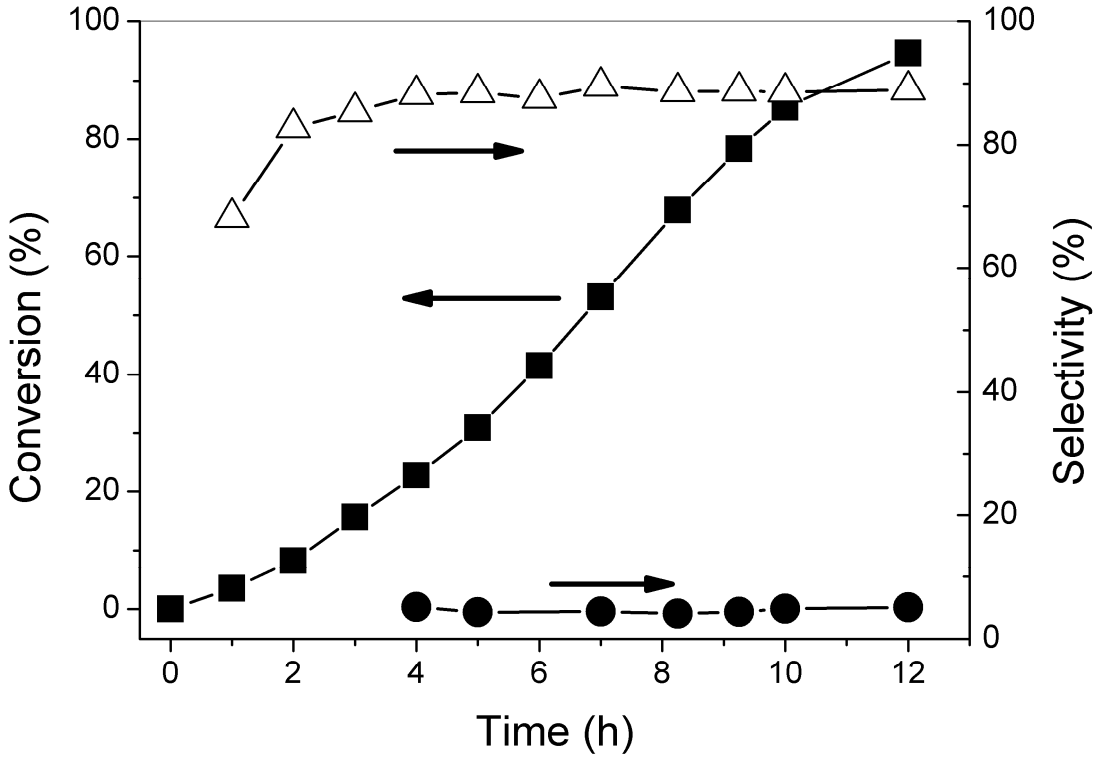

Figure 6-4: Epoxidation of (*E*)-stilbene over STA-12(Co) with (■) (*E*)-stilbene conversion, (Δ) *trans*-stilbene oxide selectivity, (●) benzaldehyde selectivity. Reaction conditions: 2.0 mmol (*E*)-stilbene, 100 mg biphenyl, 30 mL DMF, 50 mL min^{-1} O_2, 2.0 mg STA-12(Co), 100 °C.

Table 6-1: Aerobic epoxidation of (*E*)-stilbene in DMF. Reaction conditions: 2.0 mmol (*E*)-stilbene, 6.8 µmol Co, 100mg biphenyl, 30 mL DMF, 50 mL min^{-1} O_2.

Catalyst	Time (h)	Conversion (%)	Selectivity (%)
-	10	<1	-
Co_3O_4	12	15	68
STA-12(Co)	12	95	89
STA-12(Co:Ni 1:3)	12	3	60

after which the reaction proceeded with comparable rate (not shown). SEM and XRD analysis of a fresh and a used catalyst did not show any significant difference suggesting that the MOF remained in its initial crystalline state (Figure 6-5). A reason for the observed deactivation might be blocking of pore entrances or poisoning of free Co sites by amines formed from DMF during the reaction (*vide infra*).

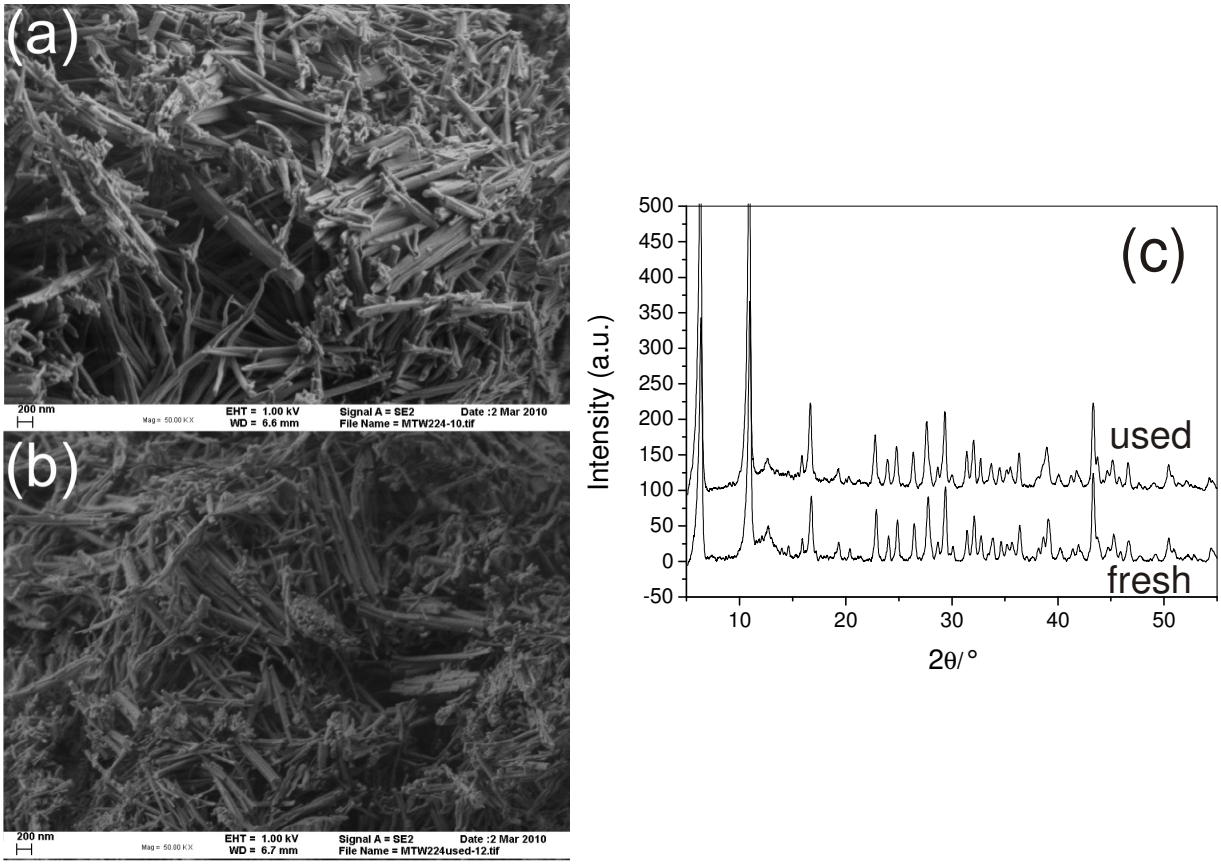

Figure 6-5: Comparison of fresh and used STA-12(Co) catalyst. (a) SEM image of fresh catalyst; (b) SEM image of used catalyst; (c) XRD of fresh and used catalyst.

6.3.3 Heterogeneous *vs.* homogeneous catalysis

A key in MOF catalysis is to assess whether catalysis proceeds mainly homogeneously or heterogeneously [24, 45] since dissolvable impurities or MOF degradation might also account for any observed catalytic activities. Thus, the catalyst was removed by filtration after the induction phase (Figure 6-6). As can be seen, the reaction proceeds after catalyst removal, but with a significantly lower reaction rate. AAS analysis of the reaction mixture indeed showed some Co leaching of 0.40 ppm amounting to ca. 3 % of the employed Co. Subsequent dissipation of the MOF during reaction as a cause for the catalytic activity and the induction phase can, however, be excluded: addition of (*E*)-stilbene to an oxygen-pretreated mixture of the Co-MOF and DMF (100 °C over 12 h) did not result in a higher

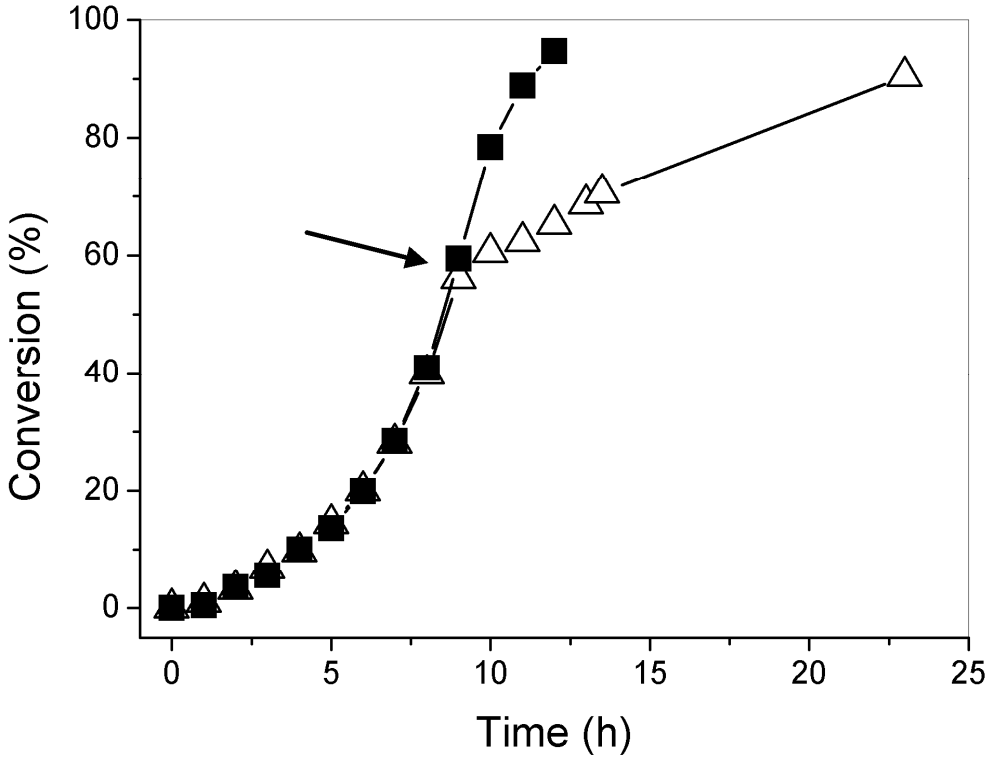

Figure 6-6: Comparison of the epoxidation with and without catalyst removal (removal of catalyst after 9 h as indicated by the arrow). (■) (*E*)-stilbene conversion with STA-12(Co), (Δ) (*E*)-stilbene conversion and STA-12(Co) separation; Reaction conditions: 4.0 mmol (*E*)-stilbene, 100 mg biphenyl, 30 mL DMF, 50 mL min^{-1} O_2, 2.0 mg STA-12(Co), 100 °C.

reaction rate. In fact, the induction took even longer due to catalyst deactivation. Similar leaching was found (0.44 ppm). Overall this indicates that the main catalytic route is heterogeneous in nature though minor homogeneous contributions cannot be excluded. Homogeneously dissolved Co salts (cobalt(III) acetyl acetonate and cobalt(II) acetate) indeed showed considerable activity. Using the same amount of Co as in the heterogeneous experiments, both (*E*)- and (*Z*)-stilbene were converted faster (Figure 6-7) exhibiting no induction phase. The conversion of (*E*)-stilbene occurred in two kinetically distinct phases: in the first phase the reaction was (pseudo-)zero-order with respect to the substrate concentration. Towards the end of the reaction the substrate was limiting and so the reaction became (pseudo-)first order. On the contrary, the conversion of (*Z*)-stilbene always proceeded as a (pseudo-)first order reaction (after the short initial induction phase). The selectivities were similar to the MOF catalyst being in the range of 90 % for (*E*)- and 80 % for (*Z*)-stilbene. Interestingly, both Co^{II} and Co^{III} salts were equally active at the same concentration meaning that the Co oxidation/reduction occurs rapidly and is not a limiting factor for the homogeneous catalyst. The difference in induction between homogeneous and

heterogeneous catalysts might result from pore diffusion limitations due to the extensive microporous system. However, a simple initial inhibition because of slow stilbene diffusion into the microspores of the MOF can be ruled out as a reason: treating the MOF catalyst and (*E*)-stilbene in DMF under a high N_2 flow for 12 h and then switching to O_2 did not shorten the induction phase.

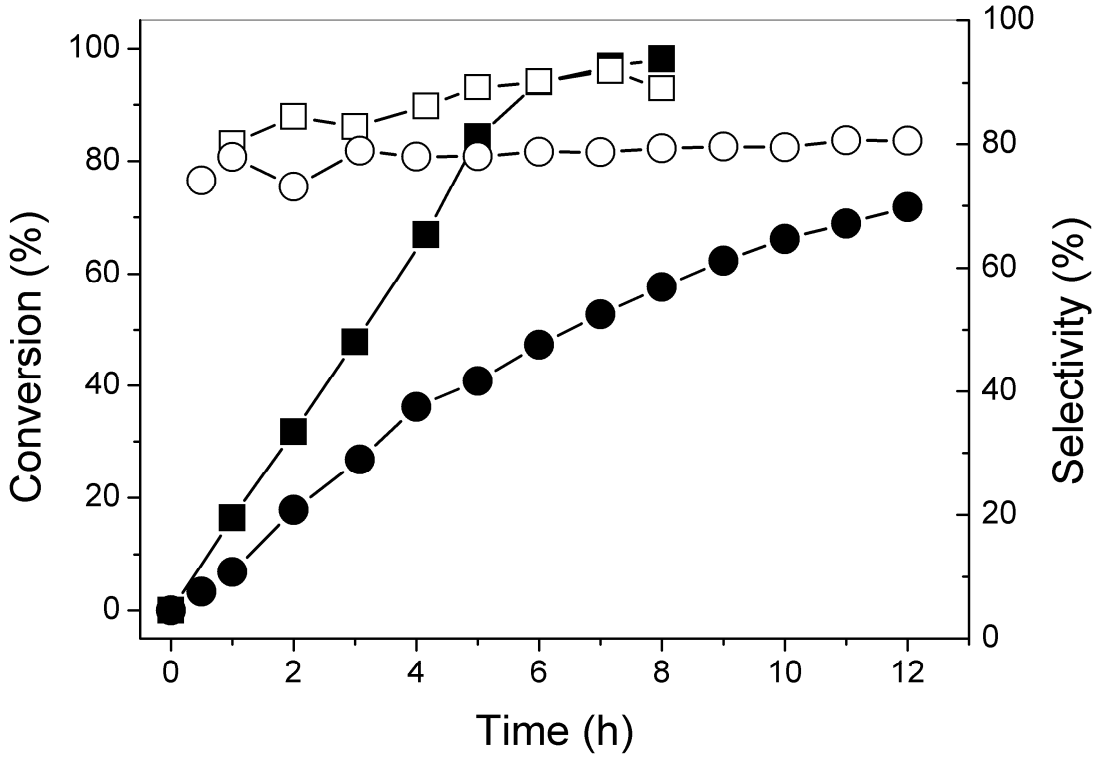

Figure 6-7: Comparison of the catalytic epoxidation of (*E*)- and (*Z*)-stilbene with homogeneous cobalt complexes; (■) (*E*)-stilbene conversion (□) trans-stilbene oxide selectivity from (*E*)-stilbene; (●) (*Z*)-stilbene conversion (○) trans-stilbene oxide selectivity from (*Z*)-stilbene; reaction conditions: 2.0 mmol stilbene, 100 mg biphenyl, 30 mL DMF, 50 mL min^{-1} O_2, 2.4 mg $Co(acac)_3$.

6.3.4 Influence of reaction parameters

As a next step the effects of temperature, catalyst amount, substrate concentration and oxygen flow rate were studied. Higher temperatures enhanced the reaction rate (Figure 6-8a). At 60 °C the conversion was only 7 % after 10 h while at 120 °C the reaction was almost complete (95 % conversion). Interestingly, also the selectivity to the epoxide was lowest at 60 °C (48 %). Low epoxide selectivity was on the other hand always obtained at low conversions. Above 80 °C the temperature had little influence on the epoxide selectivity being close to 90 %. The reaction rate was highly dependent on the oxygen flow rate (Figure 6-8b). This is interesting, since the overall reaction rate is small and the consumption of

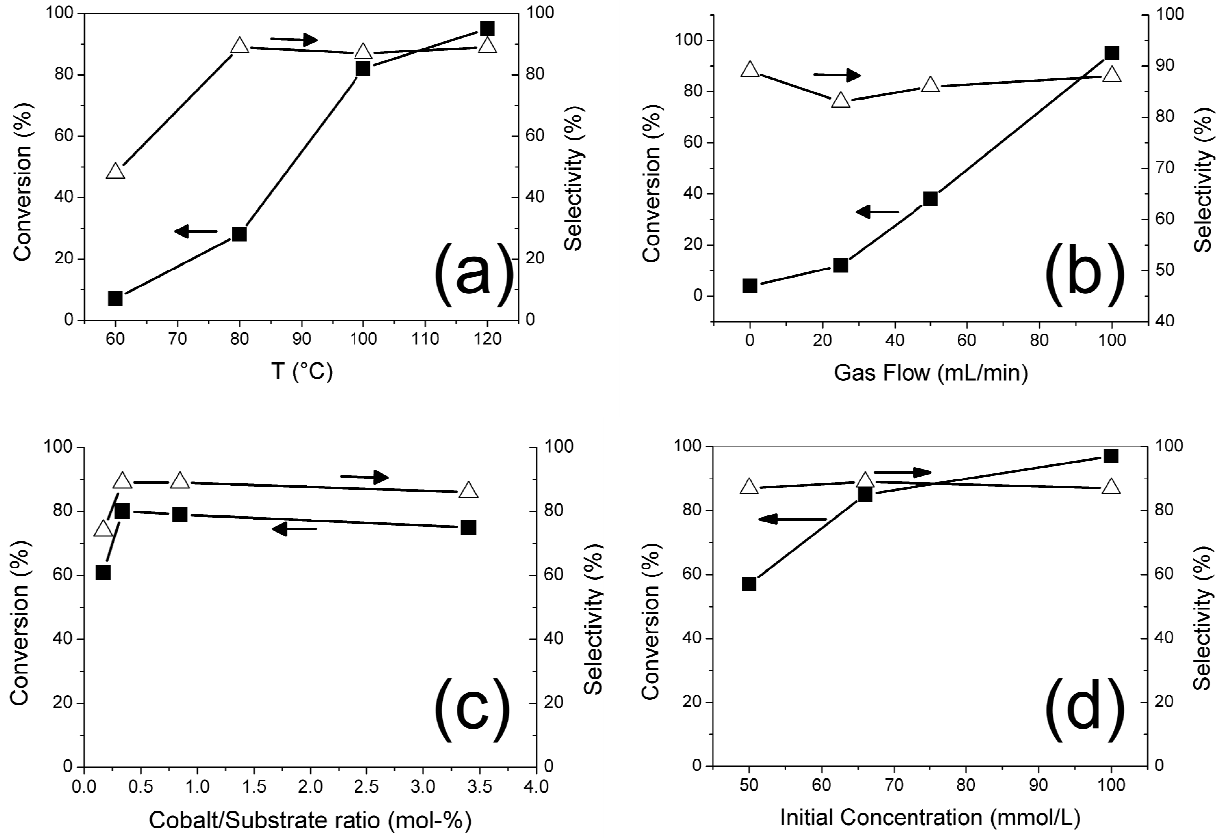

Figure 6-8: Influence of temperature (a), oxygen flow (b), catalyst amount (c) and reactant concentration (d) on the epoxidation of (*E*)-stilbene. Reaction conditions: 2.0 mmol (*E*)-stilbene, 100 mg biphenyl, 30 mL DMF, 50 mL min^{-1} O_2, 2.0 mg STA-12(Co), 100 °C, 10 h reaction time; variations: (a) temperature: 60-120 °C; (b) oxygen flow 0-100 mL min^{-1}, reaction time 6 h; (c) Substrate to catalyst ratio 30-600; (d) DMF 20-40 mL (■) (*E*)-stilbene conversion; (Δ) epoxide selectivity.

oxygen should be overcompensated already by small gas flows. Epoxidations with gold catalysts proceed at similar rates [6] and were conducted in an open reaction vessel without any additional oxygen flow. In the present study, faster removal of volatile catalyst poisons such as amines (*vide infra*) might be the cause of a beneficial high gas flow. Consequently, reaction mixtures became considerably darker after 12 h when the flow was low potentially due to amine oxidation products. This was, however, not the sole reason for the observed effect. Using air instead of pure oxygen with the same flow rate resulted in smaller conversions. After 6 h the conversion was 8 % with an air flow of 50 mL/min compared to 38 % with 50 mL/min oxygen. Thus, high oxygen availability is crucial. The reaction rate did not increase steadily with the amount of catalyst (Figure 6-8c) but rather exhibited an optimal cobalt to substrate ratio of 0.34 mol-% (80 % conversion after 10 h) whereas a higher cobalt amount did not significantly influence the conversion under the chosen conditions as also found previously [17] and might indicate

that the reaction is limited by mass transfer. Also the substrate concentration had a peculiar influence on the catalytic process (Figure 6-8d). With a higher initial concentration of the reactants, a higher conversion was found after 10 h keeping the catalyst/substrate ratio constant, i.e. using different solvent amounts. In this way, also the solvent-to-catalyst ratio changes. This effect was, however, only seen for long reaction times and variation in the concentration *via* the solvent amount. Varying the amount of substrate leaving the catalyst and solvent amount the same, the reaction rate was almost not sensitive to the substrate concentration at sufficiently high concentrations (Figure 6-9) as also observed with the homogeneous Co catalyst (*vide supra*). Thus, the heterogeneous reaction rate is (initially) (I) not

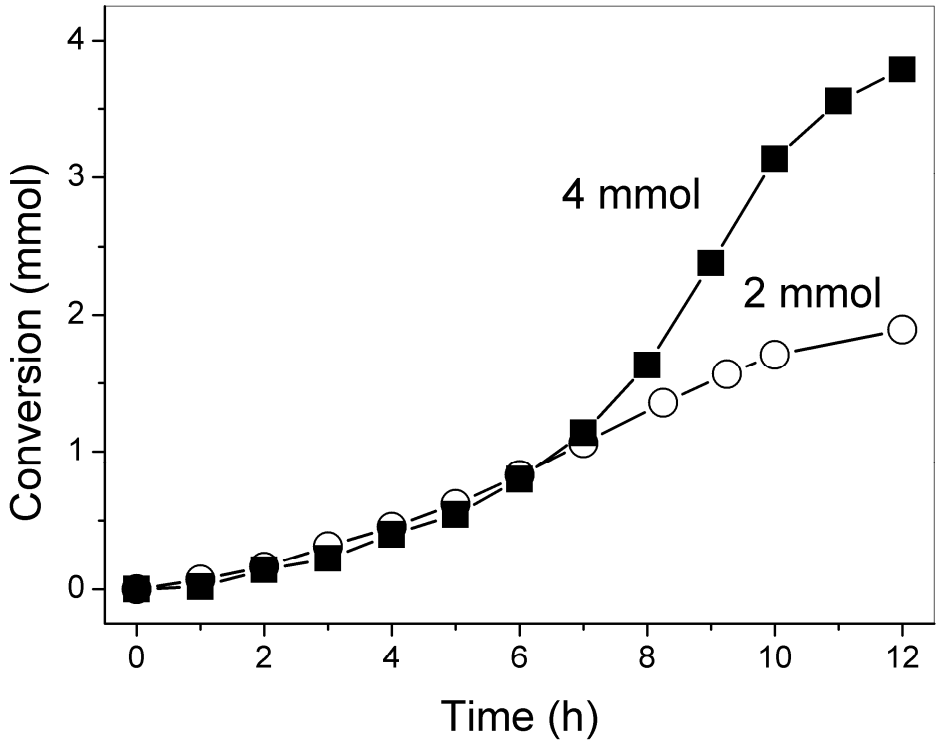

Figure 6-9: Conversion (in mmol)-time profile at different substrate/catalyst ratios. Reaction conditions: 2.0/ 4.0 mmol (*E*)-stilbene, 100 mg biphenyl, 30 mL DMF, 50 mL min^{-1} O_2, 2.0 mg STA-12(Co), 100 °C.

depending on the substrate concentration, and (II) at the same time steadily increasing. The choice of solvent played a vital role. Toluene did not yield any epoxidation products while mixtures of toluene and DMF exhibited some catalytic activity. *N*,*N*-Dimethylacetamide (DMAc) as another amide solvent also proved to be a suitable solvent affording an even higher reaction rate (Table 6-2, entry 1,2). With similar conditions as used previously, full conversion (97 %) was achieved already after 8.5 h compared to 12 h

with DMF. On the other hand, the selectivity to *trans*-stilbene oxide was markedly lower, i.e. around 60 % compared to approximately 90 % with DMF. The generally higher selectivity to benzaldehyde in DMAc might explain the higher reactivity in this solvent (*vide infra*). No reaction was observed in pure (*E*)-stilbene at 130 °C in contrast to a Co^{II} exchanged heteropoly acid catalyst tested in the oxidation of styrene to benzaldehyde [46]. Likewise no reaction was observed in a 1:1 mixture of DMF and water the latter thus being an inhibitor in high concentrations.

6.3.5 Amines as inhibitors

In a closed reactor system (i.e. an autoclave), the selectivity and conversion dropped significantly even though relatively high oxygen pressures were applied (Table 6-2, entry 3) resulting in a high oxygen availability which had proved beneficial in experiments performed in an open reactor. Reference [23] also states a lower conversion observed in closed reactors while other studies investigated the epoxidation in a closed reactor under elevated oxygen pressure and found only small differences [17]. A reason for the higher conversion in open reactor systems might be the formation of amines from DMF decomposition which coordinate at free Co sites. The high volatility of the amines assures a quick

Table 6-2: Influence of solvent, closed/open system and additives. Reaction conditions: 2.0 mmol (*E*)-stilbene, 2.0 mg STA-12(Co), 100 mg biphenyl, 30 mL DMF, oxygen flow/pressure as indicated.

Entry	Solvent	O_2-flow[a]/pressure[b]	Additive	Time (h)	Conv. (%)	Sel. (%)
1	DMF	50 mL/min	-	12	95	89
2	DMAc	50 mL/min	-	8.5	97	64
3	DMF	7.5 bar	-	10	25	52
4	DMAc	7.5 bar	-	10	73	41
5	DMF	7.5 bar	NaH_2PO_4	10	6	64
6	DMF	7.5 bar	CH_3COOH	10	49	68

[a]Flowing oxygen in an open glass reactor system. [b]Oxygen pressure applied in a closed reactor system.

removal in an open reactor which is not possible in an autoclave. Additionally, in a closed system epoxidation with DMAc as the solvent gave a significantly higher conversion (entry 4). DMAc is more stable towards decomposition [47] and thus the amine concentration should be lower. This also explains at least part of the lower observed catalytic activity in DMF compared to DMAc in an open system. Addition of NaH_2PO_4 as an amine scavenger did have a negative effect on the epoxidation reaction

(entry 5) while acetic acid (entry 6) doubled the conversion. In an open system, both the MOF catalyst as well as dissolved Co species could be completely inactivated by constant addition of diethylamine. This underlines that a free coordination site at the Co centers is required for catalytic activity.

6.3.6 Involvement of radical species

DMF promoted epoxidations are widely assumed to occur *via* a radical reaction pathway. Indeed, the reaction rate was significantly decreased upon addition of two different radical scavengers, i.e. 4-*tert.*-butylcatechol and 2,6-di-*tert*-butyl-4-methylphenol. Radical reactions usually feature an induction period – as observed in the present study – in order to form a steady-state radical concentration. However, radical initiators such as azo-bis(isobutyronitrile) (AiBN) had no effect on the initial reaction rate. The initial conversion was fast with 5 mol-% *tert.*-butylhydroperoxide (TBHP) but then continued as in the other experiments. TBHP can thus be regarded as an epoxidizing reagent being rapidly consumed in the beginning and not as an initiator. In order to further shed light into the possible involvement of radicals the reaction mixture was investigated with EPR under *in situ* conditions where, however, free organic radicals could not be detected. Potential free radicals could be EPR inactive due to coupling or their concentration is below the limit of detection. The inhibiting effect of radical scavengers might also be due to adsorption or coordination to free Co sites [48]. A signal at g = 2.0076 was found which can be ascribed to Co^{III}-O_2*$^-$ (superoxo-) species formed from reaction of Co^{II} with oxygen [49]. These can already be found in the solid catalyst measured *ex situ* and thus are not formed specifically under reaction conditions. Hence, their formation is likely not connected to the induction phase. Note that Co^{III}-peroxo-species, which might also form from reaction of Co^{II} with O_2, are not EPR active [50].

6.3.7 Co-epoxidation of styrene and (*E*)-stilbene

Driven by the observation that styrene epoxidation does not only proceed faster but also features a shorter induction phase, the co-epoxidation of styrene and (*E*)-stilbene was investigated thus doubling the substrate/catalyst ratio (Figure 6-10a). Although the catalyst amount was not increased, styrene induced a much faster conversion of (*E*)-stilbene. At the same time, the conversion of styrene became only slightly but significantly slower at medium conversions. Co-epoxidation with styrene had the strongest effect on the conversion of (*Z*)-stilbene which increased from 11 % to 58 % with styrene (Table 6-3, entry 1,2). This effect was not observed for the homogeneous Co catalysts neither for (*E*)- nor (*Z*)-stilbene epoxidation (Table 6-3, entry 3, 4) and might be an effect related to the special features of the

MOF. Styrene being smaller than (*E*)-stilbene can diffuse more easily into the micropores of the MOF. However, a transfer-epoxidation from styrene oxide to (*E*)-stilbene does not account for the styrene promotion since styrene oxide as an additive did not have any promoting effect even in large quantities. Oxygen transfer from styrene oxide as the potential oxidizing agent to (*E*)-stilbene was also not observed under reaction conditions with flowing N_2 instead of O_2.

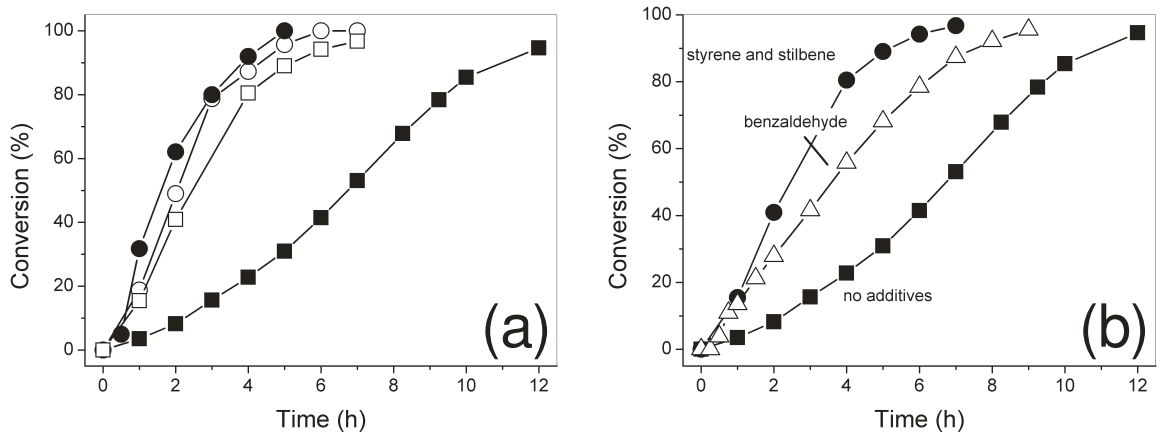

Figure 6-10: Co-epoxidation of styrene and (*E*)-stilbene and the effect of benzaldehyde. (a) Comparison of only styrene and (*E*)-stilbene conversion (solid symbols) with co-epoxidation of styrene and (*E*)-stilbene (open symbols), (■,□) (*E*)-stilbene; (•,○) styrene conversion; (b) effect of benzaldehyde addition (0.2 mmol) on (*E*)-stilbene conversion. Reactions conditions: 2.0 mmol (*E*)-stilbene and/or styrene, 100 mg biphenyl, 30 mL DMF, 50 mL min^{-1} O_2, 2.0 mg STA-12(Co), 100 °C.

Table 6-3: Epoxidation of (*Z*)-stilbene with heterogeneous and homogeneous Co catalysts. Reaction conditions: 2.0 mmol (*Z*)-stilbene, 6.8 µmol Co as catalyst, 100 mg biphenyl, 30 mL DMF, 10 h, 50 mL min^{-1} O_2. Optional styrene addition: 2.0 mmol.

Entry	Catalyst	Styrene Promotion	Conversion (%)	Selectivity (%)
1	STA-12(Co)	NO	11	92
2	STA-12(Co)	YES	58	86
3	$Co(acac)_3$	NO	66	80
4	$Co(acac)_3$	YES	65	92
5	Co_3O_4	NO	9.4	53

Two major differences between MOF-catalyzed styrene and (*E*)-stilbene conversion are the higher reaction rate and the higher benzaldehyde selectivity (styrene ca. 12 %; (*E*)-stilbene ca. 5 %) for the former. Thus, styrene conversion affords a comparably high benzaldehyde concentration already in the beginning of the reaction. Indeed, benzaldehyde as the major by-product can explain the observed

promoting effect – as with styrene, the (*E*)-stilbene reaction rate was enhanced by addition of small substoichiometric amounts of benzaldehyde (Figure 6-10b). In analogy to the previous observations, benzaldehyde did not have a promoting effect on homogeneous Co catalysts.

6.3.8 Formation of oxidizing species

Triphenylphosphine is frequently used to scavenge thermally unstable peroxides for GC analysis. Also in the present study, triphenylphosphine oxide was found when PPh_3 was added to the samples taken for GC analysis indicating the presence of peroxides. Over time the amount of peroxides increased steadily. Similar to FMF-formation, peroxides also formed in lower amounts in the absence of substrate. With homogeneous catalysts, the formation of peroxides proceeded at a higher rate which correlates with the higher product formation rate. Peroxides can in general serve as epoxidizing agents as e.g. shown for gold catalysts [9, 51]. In the present case, however, peroxides proved to be almost irrelevant for the epoxidation, since an oxygen pretreated (i.e. peroxide containing) mixture of DMF and Co-MOF did not affect (*E*)-stilbene epoxidation after substrate addition under N_2-atmosphere – after 12 h a conversion of only 3 % was found with a low epoxide selectivity of 60 % representing only a minor reaction pathway. This is principally in accordance with the lower epoxidation activity of H_2O_2 in DMF with respect to O_2 described previously [16, 19]. In the present study, addition of PPh_3 to the reaction mixture inhibited the formation of products and only small amounts of $OPPh_3$ were formed. PPh_3 likely coordinates free Co sites and thus acts as a catalyst poison.

6.3.9 EXAFS investigations under reaction conditions

In order to understand the complex catalytic process more thoroughly, XAS experiments were conducted. The Co K-edge FT EXAFS spectra of fresh and used catalyst were very similar (Figure 6-11a). Fit results suggest that the structure of STA-12(Co) is close to hydrated STA-12(Ni) [36] with a Co-O/N coordination number of 6 and an additional Co-Co and Co-P shell (Table 6-4). Note that during fitting no distinction between Co-N and Co-O contributions was made. The large Debye-Waller factor indicates a low symmetry of the Co-N/O polyhedral. In addition, the similar distances of the Co-Co and Co-P backscattering paths complicate their differentiation and leads to inaccurate coordination numbers. The fitted Co-Co and Co-P distances are in reasonable agreement with XRD data. The catalyst was also investigated *in situ* with X-ray absorption spectroscopic measurements in a closed autoclave (due to safety considerations). Upon addition of DMF to the catalyst pellet, the white-line intensity dropped and

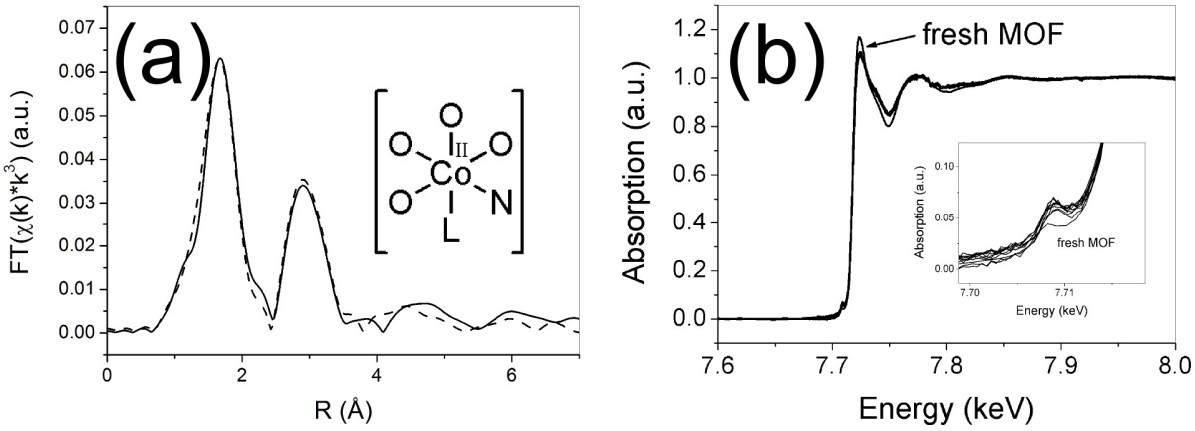

Figure 6-11: EXAFS and XANES investigations of as-prepared and in use/used STA-12(Co). (a) Fourier transformed Co K-edge EXAFS data of the fresh (dashed line) and used catalyst (solid line); (b) *in situ* Co K-edge XANES spectra of STA-12(Co) before and during the epoxidation in DMF; inset: pre-edge region.

Table 6-4: Fit results for STA-12(Co) fresh (*ex situ*), used (*ex situ*) and under reaction conditions (*in situ*). The damping factor S_o^2 was set to 0.8 in all fits.

Fresh STA-12(Co)[a]				
Shell	N	R (Å)	σ^2	ΔE_0 (eV)
Co-O	5.9	2.10	0.0085	-3.1
Co-Co	4.1	3.23	0.0049	-3.1
Co-P	4.7	3.23	0.0032	-3.1
Used STA-12(Co)[b]				
Shell	N	R (Å)	σ^2	ΔE_0 (eV)
Co-O	5.4	2.09	0.0077	-4.1
Co-Co	1.1	3.23	0.0023	-4.1
Co-P	4.4	3.28	0.010	-4.1
STA-12(Co) in DMF (*in situ*)[c]				
Shell	N	R (Å)	σ^2	ΔE_0 (eV)
Co-O	2.5	2.04	0.0077	-5.2
Co-Co	2.0[d]	3.18	0.0097	-5.2
Co-P	3.3	3.20	0.013	-5.2

[a]Fitted in k = 2.5-13 $Å^{-1}$; R = 1.2-3.8 Å; residual 5.1. [b]Fitted in k = 2.5-13 $Å^{-1}$; R = 1.2-3.6 Å; residual 7.7. [c]Fitted in k = 2.5-12 $Å^{-1}$; R = 1.2-3.2 Å; residual 3.9.[d]Fixed during refinement.

the pre-edge peak became more pronounced (Figure 6-11b + inset). The latter is usually ascribed to a reduction in symmetry which might be caused by incorporation of DMF into the pores of the catalyst. Heating the catalyst and the reaction mixture to 100 °C did not induce further structural changes of the catalyst over 8 h thus showing no major catalyst decomposition. The data quality was too poor for individual data fitting of each spectrum but required averaging of all the similar spectra in DMF (Table 6-4). Apparently, the Co-O/N coordination number decreased significantly due to a decrease in symmetry as also suggested by the pre-edge feature.

6.4 Discussion

The presented STA-12(Co) catalyst effectively catalyzed the epoxidation of olefins in DMF media as it combines a high dispersion of well-defined metal sites with a high metal content. Thereby the absolute amount of catalyst necessary for a reasonable conversion could be decreased by two orders of magnitude compared to reports in the literature on zeolite catalysts [22]. The conversion of styrene occurred quickly but with only a very low selectivity around 20 % and accompanied by formation of unknown (presumably oligomeric) side products as suggested by the incomplete mass balance. This is likely a general side reaction for styrene in DMF at elevated temperatures. Various examples in the literature on aerobic epoxidations in DMF with Co-based solid catalysts (e.g. [20, 52]) report styrene oxide selectivities of higher than 60 % which are, however, calculated on the basis of benzaldehyde and styrene oxide being the only products. Using the same estimation matrix for this study would also result in selectivities well above 60 %. Additionally, styrene was distilled prior to use in this study so that stabilizers were removed. On the contrary, the MOF catalyst converted (*E*)-stilbene with a high selectivity between 80-90 %. Average turn-over frequencies were higher in the present study being around 20 h^{-1} compared to maximal 8 h^{-1} in [22] under similar conditions calculated based on the overall Co amount. Alongside the epoxidation reaction large amounts of byproducts not directly attributable to the olefin were formed in over- and near-stoichiometric amounts, i.e. *N*-formyl-*N*-methylformamide (FMF) as a solvent oxidation product and presumably free peroxides, both hinting at the complexity of the reaction mechanism.

A side-by-side comparison of the MOF catalyst with the homogeneous catalysts employed here is difficult due to the different ligand sphere. Better homogeneous analogues of the MOF would bear a *N,N*'-piperazinebis(methylenephosphonate) ligand but due to the pronounced Co network in the MOF would still not allow for conclusions by analogy. Differences show, however, that many effects seen for

the MOF cannot be generalized for other Co catalysts. A major difference is the induction phase found only with the MOF. One reason for the induction phase could be traced back to the gradual formation of benzaldehyde which was found to be connected to the MOF catalytic activity and served as an explanation for the unexpected promoting role of another substrate, styrene, on the conversion of the investigated stilbene isomers. Other reasons for the induction phase were also investigated; e.g it seems unlikely that pore diffusion had an effect. The micropores of the MOF (ca. 1 nm) are similar in size to the stilbene isomers (ca. 1 nm) and therefore diffusion should influence the induction and reaction rate – if epoxidation takes place in the pores. Since benzaldehyde will hardly influence stilbene diffusion and MOF-pretreatment with stilbene under N_2 did not shorten the induction phase, the MOF is likely active *via* its outer surface only. The efficacy of the MOF catalyst is therefore still limited by diffusion issues causing the inaccessibility of the MOF micropores. Opre *et al.* [23] suggest that epoxidation might occur *via* a DMF-derived peroxide which would need to be formed prior to product formation. While indeed DMF oxidation is the cause of the pronounced solvent effect, a link between conversion and formed peroxides could not be established in the present case. Subsequent leaching of the MOF to release catalytically active Co species is also not responsible for the initial increase in the reaction rate. The reaction was shown to be primarily heterogeneous and pretreatment of the MOF in DMF did not shorten the induction although leaching could be found. Further *in situ* EPR investigations suggested that the formation of Co-O_2* species is not at the origin of the induction phase since these are already present in fresh STA-12(Co). Also the formation of a steady-state radical concentration could at least not be corroborated as a cause for the induction and reaction. Note that it cannot be excluded that the radical concentration was below the limit of detection by EPR. Thus, the primary reason for the induction phase appears to be the formation of benzaldehyde promoting the reaction. The exact role of benzaldehyde is unclear at this point but its influence is not similar to the Mukaiyama epoxidation since only minute amounts of benzoic acid were detected and the mass balance was closed for the epoxidation of the stilbene isomers. Since no reaction was observed in the beginning of the reaction, benzaldehyde might activate the MOF catalyst and increase the availability of active sites. Benzaldehyde concentration as a limiting factor for the catalyst activity might serve as an explanation for the small influence of the amount of MOF used on the catalytic reaction but it might also be conceivable that mass transport limitations dominate the reaction at high catalyst loadings. Clearly, further studies are necessary to elucidate the effect of benzaldehyde. With respect to the actual epoxidizing agent three species are conceivable from which free peroxides found in high concentrations can be excluded. Reaction of Co^{II} with O_2 can result in two different species namely Co-superoxo species and (mostly)

binuclear Co-peroxo species [53]. These species are interrelated as Co^{III}-O_2*$^-$ can (possibly reversibly) bind to Co^{II} with one available coordination site as shown for Co complexes in water [54-57]. Binuclear Co-peroxo complexes also form in DMF [58]. In the cited studies, the formation of peroxo-species was favored over the formation of superoxo-species. From the MOF structure, the formation of peroxides cannot be excluded. Typical Co-Co distances in binuclear Co-peroxo complexes are around 4.5 Å [58, 59] similar to Co-Co distances in the MOF of 4.87 Å. Still, the formation of Co-peroxo species would require some rearrangement in the ligand sphere around the active site, potentially induced by benzaldehyde. Co-superoxo species were found both in untreated STA-12(Co) and under *in situ* conditions by EPR hence their formation should not cause an induction phase. μ-Peroxo complexes are diamagnetic [59] and homogeneous complexes were found to be active in oxidation reactions [60]. Peroxides with electron-deficient oxygen as in percarboxylic acids are effective epoxidizing agents which is also plausible for Co-peroxides. The very low activity of STA-12(Co,Ni) might indeed be interpreted by a synergistic effect of adjacent Co sites. Due to the 1:3 ratio of Co:Ni enough Co single sites should be available for an appreciable catalytic activity while the amount of adjacent Co-Co sites would be greatly decreased assuming a homogeneous distribution of the metals. Of course, Ni could also have an inhibiting effect on the reaction. This is less likely since Ni catalysts promoted similar epoxidation reactions [61-63]. Thus, both Co-peroxo as well as radical superoxo species appear to be responsible for the epoxidation activity of the MOF material, especially since these two species are interrelated given that the formation of binuclear Co species is possible.

With the assumption that epoxidation occurs *via* two Co-oxygen species a feasible preliminary mechanism as in Scheme 6-1 is proposed. The role of benzaldehyde in the MOF-catalyzed reaction was clearly observed and is interpreted in terms of an activation of the catalyst (step 1). The exact way of this presumed activation is unknown at this time but a control of the catalyst activity by the benzaldehyde concentration would explain the limited influence of the catalyst amount on the reaction rate. Activated Co^{II} sites react with molecular oxygen from which the formation of Co-superoxo and binuclear Co-peroxo species is conceivable (step 2). A competition for the free Co coordination site between ligands present in solution (e.g. DMF or amines) and oxygen would explain the beneficial influence of high oxygen flows (step 2a). In step 3, the reaction between stilbene and Co activated oxygen affords an intermediate complex. The number of oxygen atoms in this intermediate complex depends on the interaction of the stilbene isomers with the Co oxygen species. Formation of the epoxide is not concerted since both (*E*)- and (*Z*)-stilbene afforded *trans*-stilbene oxide. Since the same product is formed from the stilbene isomers their difference in reactivity cannot be from desorption

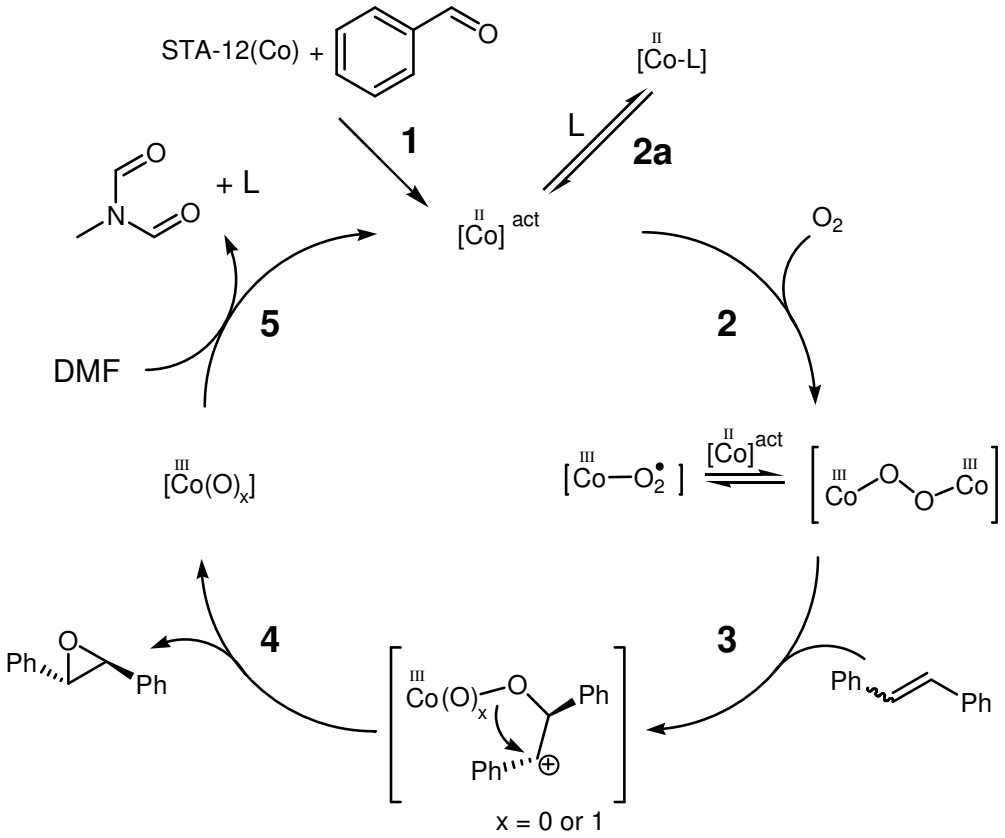

Scheme 6-1: Proposed reaction mechanism for the epoxidation of stilbene assuming an activated Co-center as active species.

(step 4), thus not being rate-limiting. The remaining Co^{III} species requires regeneration *via* oxidation of the solvent (step 5) explaining the strong solvent influence and the observed solvent oxidation. Regeneration of the catalyst would be fast compared to the other steps since the reaction rate clearly depends on the type of substrate. Although the proposed reaction mechanism is speculative, it explains the observations made in this paper. Nevertheless, more data is needed to provide evidence for the postulated intermediates.

6.5 Conclusions

The metal-organic framework STA-12(Co) featured high activity in the aerobic epoxidation of various olefins in DMF. Due to the defined Co distribution and high loading of the MOF the total catalyst amount that was necessary to obtain similar conversions could be markedly reduced compared to commonly used zeolite type catalysts. The structure of STA-12(Co) is similar to the previously reported STA-12(Ni).

The selectivity in styrene epoxidation was low due to substrate oligomerization. In contrast, both (*E*)- and (*Z*)-stilbene were epoxidized with high selectivities between 80-90 % featuring an induction phase of a few hours. Within the catalytic reaction the solvent served as a sacrificial reductant. Free peroxides formed in considerable amounts but could not be connected to the epoxidation reaction. The reaction rate increased with oxygen flow rate, higher temperatures and substrate concentration (by varying solvent amounts). The substrate-to-catalyst ratio exhibited an optimum at ca. 0.3 mol-% (with 50 mL/min O_2). The catalyst was reusable with only minor deactivation though no major structural changes were observed with SEM, XRD and EXAFS underlining the stability of the MOF under reaction conditions. The reaction proceeded mainly heterogeneously with minor contributions from leached Co and a corresponding Co-Ni-MOF was considerably less active. Homogeneous Co was indeed found to be very active for the epoxidation exhibiting no induction phase. The substrate-dependent induction phase of the Co-based MOF catalyst and the beneficial effect of styrene on stilbene epoxidation could be linked to the promoting effect of benzaldehyde only observable for the Co-MOF catalyst and not with homogeneous Co catalysts. Both the reaction catalyzed by homogeneous Co and STA-12(Co) were (pseudo-)zero order with respect to the substrate at high concentrations. A feasible catalytic cycle accounting for the observations made in this study was proposed that should further be substantiated in future studies also on other Co-based catalysts.

6.6 References

[1] F. Ullmann, "Ullmann's encyclopedia of industrial chemistry", 6th edition, Wiley-VCH, Weinheim, 2003.

[2] M. McCoy, M.S. Reisch, A.H. Tullo, J. Tremblay, M. Voith, Chem. Eng. News 87 (2009) 51.

[3] M. Dusi, T. Mallat, A. Baiker, Catal. Rev. Sci. Eng. 42 (2000) 213.

[4] R. Murugavel, H.W. Roesky, Angew. Chem. Int. Edit. 36 (1997) 477.

[5] A. Corma, H. Garcia, Chem. Rev. 102 (2002) 3837.

[6] M.D. Hughes, Y.J. Xu, P. Jenkins, P. McMorn, P. Landon, D.I. Enache, A.F. Carley, G.A. Attard, G.J. Hutchings, F. King, E.H. Stitt, P. Johnston, K. Griffin, C.J. Kiely, Nature 437 (2005) 1132.

[7] M. Turner, V.B. Golovko, O.P.H. Vaughan, P. Abdulkin, A. Berenguer-Murcia, M.S. Tikhov, B.F.G. Johnson, R.M. Lambert, Nature 454 (2008) 981.

[8] P. Lignier, S. Mangematin, F. Morfin, J. Rousset, V. Caps, Catal. Today 138 (2008) 50.

[9] C. Aprile, A. Corma, M.E. Domine, H. Garcia, C. Mitchell, J. Catal. 264 (2009) 44.

[10] F. Loeker, W. Leitner, Chem. Eur. J. 6 (2000) 2011.

[11] D. Dhar, Y. Koltypin, A. Gedanken, S. Chandrasekaran, Catal. Lett. 86 (2003) 197.

[12] E. Angelescu, R. Ionescu, O.D. Pavel, R. Zavoianu, R. Birjega, C.R. Luculescu, M. Florea, R. Olar, J. Mol. Catal. A 315 (2010) 178.

[13] Q.H. Tang, Y. Wang, J. Liang, P. Wang, Q.H. Zhang, H.L. Wan, Chem. Commun. (2004) 440.

[14] M. Salavati-Niasari, S. Abdolmohammadi, M. Oftadeh, J. Coord. Chem. 61 (2008) 2837.

[15] M.V. Patil, M.K. Yadav, R.V. Jasra, J. Mol. Catal. A 277 (2007) 72.

[16] M.L. Kantam, B.P.C. Rao, R.S. Reddy, N.S. Sekhar, B. Sreedhar, B.M. Choudary, J. Mol. Catal. A 272 (2007) 1.

[17] X. Zhang, C. Zeng, L. Zhang, N. Xu, Kinet. Catal. 50 (2009) 199.

[18] X. Lu, Q. Xia, S. Fang, B. Xie, B. Qi, Z. Tang, Catal. Lett. 131 (2009) 517.

[19] Q.H. Tang, Q.H. Zhang, H.L. Wu, Y. Wang, J. Catal. 230 (2005) 384.

[20] J. Jiang, R. Li, H. Wang, Y. Zheng, H. Chen, J. Ma, Catal. Lett. 120 (2008) 221.

[21] K.M. Jinka, J. Sebastian, R.V. Jasra, J. Mol. Catal. A 274 (2007) 33.

[22] X. Quek, Q. Tang, S. Hu, Y. Yang, Appl. Catal. A 361 (2009) 130.

[23] Z. Opre, T. Mallat, A. Baiker, J. Catal. 245 (2007) 482.

[24] J. Lee, O.K. Farha, J. Roberts, K.A. Scheidt, S.T. Nguyen, J.T. Hupp, Chem. Soc. Rev. 38 (2009) 1450.

[25] A.U. Czaja, N. Trukhan, U. Mueller, Chem. Soc. Rev. 38 (2009) 1284.

[26] F.X. Llabres i Xamena, A. Abad, A. Corma, H. Garcia, J. Catal. 250 (2007) 294.

[27] K. Brown, S. Zolezzi, P. Aguirre, D. Venegas-Yazigi, V. Paredes-Garcia, R. Baggio, M.A. Novak, E. Spodine, Dalton Trans. (2009) 1422.

[28] J. Perles, N. Snejko, M. Iglesias, M.A. Monge, J. Mater. Chem. 19 (2009) 6504.

[29] M.H. Alkordi, Y. Liu, R.W. Larsen, J.F. Eubank, M. Eddaoudi, J. Am. Chem. Soc. 130 (2008) 12639.

[30] D. Jiang, T. Mallat, D.M. Meier, A. Urakawa, A. Baiker, J. Catal. 270 (2010) 26.

[31] Y. Wu, L. Qiu, W. Wang, Z. Li, T. Xu, Z. Wu, X. Jiang, Transition Met. Chem. 34 (2009) 263.

[32] F. Gandara, A. de Andres, B. Gomez-Lor, E. Gutierrez-Puebla, M. Iglesias, M.A. Monge, D.M. Proserpio, N. Snejko, Cryst. Growth Des. 8 (2008) 378.

[33] S. Bhattacharjee, J. Choi, S. Yang, S.B. Choi, J. Kim, W. Ahn, J. Nanosci. Nanotechnol. 10 (2010) 135.

[34] Y. Lu, M. Tonigold, B. Bredenkoetter, D. Volkmer, J. Hitzbleck, G. Langstein, Z. Anorg. Allg. Chem. 634 (2008) 2411.

[35] M. Tonigold, Y. Lu, B. Bredenkoetter, B. Rieger, S. Bahnmueller, J. Hitzbleck, G. Langstein, D. Volkmer, Angew. Chem. Int. Ed. 48 (2009) 7546.

[36] S.R. Miller, G.M. Pearce, P.A. Wright, F. Bonino, S. Chavan, S. Bordiga, I. Margiolaki, N. Guillou, G. Ferey, S. Bourrelly, P.L. Llewellyn, J. Am. Chem. Soc. 130 (2008) 15967.

[37] Y.L. Han, H.W. Hu, Synthesis (1990) 122.

[38] J.P.S. Mowat, J.A. Groves, M.T. Wharmby, S.R. Miller, Y. Li, P. Lightfoot, P.A. Wright, J. Solid State Chem. 182 (2009) 2769.

[39] J.-D. Grunwaldt, M. Ramin, M. Rohr, A. Michailovski, G.R. Patzke, A. Baiker, Rev. Sci. Instrum. 76 (2005) 054104.

[40] F. Jutz, J.-D. Grunwaldt, A. Baiker, J. Mol. Catal. A. 297 (2009) 63.

[41] T. Ressler, J. Synchrotron Radiat. 5 (1998) 118.

[42] S.I. Zabinsky, J.J. Rehr, A. Ankudinov, R.C. Albers, M.J. Eller, Phys. Rev. B 52 (1995) 2995.

[43] G.M. Pearce, Ph.D. Thesis, University of St. Andrews 2009.

[44] A.C. Larson, R.B. Von Dreele, General Structure Analysis System (Computer software) 1994.

[45] D. Jiang, A. Urakawa, M. Yulikov, T. Mallat, G. Jeschke, A. Baiker, Chem. Eur. J. 15 (2009) 12255.

[46] P. Shringarpure, A. Patel, J. Mol. Catal. A 321 (2010) 22.

[47] I.Z. Éifer, G.A. Rudova, O.N. Semenikhina, O.M. Bochkareva, Fibre Chem. 13 (1981) 23.

[48] H.K. Lee, C.H. Lam, S.L. Li, Z.Y. Zhang, T.C.W. Mak, Inorg. Chem. 40 (2001) 4691.

[49] E. Giamello, Z. Sojka, M. Che, A. Zecchina, J. Phys. Chem. 90 (1986) 6084.

[50] C. Comuzzi, A. Melchior, P. Polese, R. Portanova, M. Tolazzi, Inorg. Chem. 42 (2003) 8214.

[51] Wang Ya-Li, Sun Jian-Hong, Xiang Dan, Wang Lu, Sun Jian-Min, Xiao Feng-Shou, Chem. J. Chin. Univ. Chin. 29 (2008) 135.

[52] J. Sebastian, K.M. Jinka, R.V. Jasra, J. Catal. 244 (2006) 208.

[53] A.F. Holleman, E. Wiberg, "Lehrbuch der Anorganischen Chemie", 101th edition, De Gruyter, Berlin, New York, 1995.

[54] J. Simplici, R.G. Wilkins, J. Am. Chem. Soc. 89 (1967) 6092.

[55] F. Miller, J. Simplici, R.G. Wilkins, J. Am. Chem. Soc. 91 (1969) 1962.

[56] F. Miller, R.G. Wilkins, J. Am. Chem. Soc. 92 (1970) 2687.

[57] M. Maeder, H.R. Macke, Inorg. Chem. 33 (1994) 3135.

[58] H. Furutachi, S. Fujinami, M. Suzuki, H. Okawa, J. Chem. Soc. Dalton (1999) 2197.

[59] M. Mori, J.A. Weil, J. Am. Chem. Soc. 89 (1967) 3732.

[60] A. Sobkowiak, D.T. Sawyer, J. Am. Chem. Soc. 113 (1991) 9520.

[61] R.I. Kureshy, N.H. Khan, S.H.R. Abdi, S.T. Patel, P. Iyer, E. Suresh, P. Dastidar, J. Mol. Catal. A 160 (2000) 217.

[62] M.R. Maurya, A.K. Chandrakar, S. Chand, J. Mol. Catal. A 274 (2007) 192.

[63] V. Mirkhani, M. Moghadam, S. Tangestaninejad, I. Mohammadpoor-Baltork, E. Shams, N. Rasouli, Appl. Catal. A 334 (2008) 106.

Chapter 7

Concluding Remarks

7.1 Conclusions and summary

This thesis covered several topics related to the oxidation of organic compounds over heterogeneous catalysts in the liquid phase. Special focus was put on using oxygen as the least expensive oxidizing agent. Within the coinage metals the dominating role of gold catalysts was compared to the performance of silver and copper catalysts for the most widely studied liquid-phase oxidation reactions. Synthesis strategies are important; for gold, standard impregnation techniques are unsuited, while silver catalysts might require the incorporation of subsurface-oxygen species to be active. Copper catalysts are widely active for different reactions both in the metallic form and oxidized form. In the latter case, isolated copper species usually give the best performance in terms of conversion, selectivity and stability when compared to oxidic copper nanoparticles. A pronounced difference in the reactivity between gold on the one hand and copper and silver on the other hand is that the latter two can catalyze the anaerobic oxidation of alcohols which gives rise to new applications in catalysis. Gold catalysts appear to be less efficient in oxidizing hydrocarbons which usually proceeds *via* a radical (aut)oxidation mechanism though there is some discrepancy in the open literature. Here, either copper (e.g. for benzene hydroxylation) or silver (e.g. for the side-chain oxidation of alkyl aromatic compounds) are better suited candidates. The potential of silver catalysts for alcohol oxidation was thoroughly investigated. By using a simple screening approach, silver supported on SiO_2 in combination with CeO_2 nanoparticles was found to be an effective catalyst for the aerobic oxidation of alcohols. The calcination procedure for the silver catalyst had a strong influence on the catalytic performance: relatively short calcination times at 500 °C gave the best catalyst. This might be due to incorporation of silver-oxygen species as suggested by EXAFS, TEM and XRD measurements. The collaborative effect between Ag/SiO_2 and CeO_2 was not related to leaching but likely to direct physical contact, CeO_2 showing to be well-dispersed on the SiO_2

support after the reaction. Interestingly, both Pd as well as Au catalysts were also promoted by the simple addition of CeO_2 nanoparticles when applied under the same reaction conditions. When used in combination with CeO_2 and a carboxylic acid, Ag/SiO_2 also was an effective heterogeneous catalyst for the selective side-chain oxidation of alkyl aromatic compounds such as toluene, *p*-xylene, ethylbenzene and cumene. Ceria played an ambivalent role promoting the oxidation of *p*-xylene but (partially) inhibiting the oxidation of ethylbenzene and cumene. In the absence of a carboxylic acid, ceria completely inhibited the conversion of substrate which additionally explains why no solvent oxidation was observed in the alcohol oxidation study. Silver catalysts prepared by impregnation tended to leach significantly. When synthesized by flame-spray pyrolysis, the catalysts were more stable towards leaching. CeO_2 incorporated during the flame synthesis additionally afforded an apparent higher dispersion of the silver nanoparticles resulting in a more efficient catalyst. The reaction most likely proceeded *via* a radical autoxidation.

A widely used metal for catalyzing the oxidation of alcohols is palladium. Previous studies showed that the use of pressurized CO_2 as a solvent is promising. Due to the tunability of the solvent properties of CO_2 by pressure and temperature, mixtures relevant in alcohol oxidation can both be present as a single phase and in two phases. By using the Cubic plus Association Equation of State, a model predicting the phase behavior of two ternary mixtures, i.e. benzyl alcohol – O_2 – CO_2 and benzaldehyde – H_2O – CO_2 was established and found to be in reasonable agreement to experimental data. The model was tested in the aerobic oxidation of benzyl alcohol over a commercial palladium catalyst in continuous mode and was found useful in localizing the pressure region with optimal catalytic performance. The highest catalytic activity was obtained under biphasic conditions close to the dew point of the system. Under single phase conditions the high availability of oxygen at the catalyst surface probably partially oxidized the Pd surface and led to deactivation. The selectivity to the desired product benzaldehyde was not only found to be dependent on the pressure (i.e. the phase behavior) but also on the flow. Substrate accumulation in the reactor was found under biphasic conditions which might serve as a preliminary explanation.

Besides the use of pressurized CO_2 in oxidation catalysis, metal-organic frameworks are a thriving field of research. The Co-based metal-organic framework STA-12(Co) (for which a crystal structure was presented) was found to be an effective catalyst in the epoxidation of (*E*)- and (*Z*)-stilbene in DMF as a solvent. Compared to previously published catalysts, the absolute amount of catalyst necessary to obtain high conversions was significantly lower. Styrene was epoxidized faster though with poor selectivity which is most likely related to oligomerization. SEM, XRD and EXAFS measurements as

well as leaching studies showed that the MOF catalyst is highly stable and reusable with only a minor decrease in activity. Temperature, oxygen flow rate and substrate concentration were found to have a significant influence on the reaction rate. At the same time, the amount of catalyst influenced the reaction rate only to a limited extent. The reaction featured an induction period of a few hours. *In situ* EPR investigations found no radical species other than Co-superoxo species which were already present in the fresh catalyst and thus could not be linked to the induction phase. An interesting observation was made when co-epoxizing styrene and (*E*)-stilbene: stilbene was converted faster which could be traced back to the catalyst activating side product benzaldehyde (which is formed in larger quantities from styrene) explaining also the observed induction period. Neither the induction period nor the activating effect of benzaldehyde was observed when using homogeneously dissolved Co salts as catalysts suggesting that the influence of benzaldehyde is MOF-related.

7.2 Final remarks and outlook

In many cases, the catalytic performance of gold catalysts seems to be better compared to copper or silver which might either be connected to the better suitability of gold or to the high efforts which were put into developing gold catalysts. The interesting case of cyclohexane oxidation may underline that the performance of gold also can be overestimated. The chance of silver and copper certainly is a different chemoselectivity compared to gold. Different reactivities to e.g. aliphatic and aromatic alcohols will not necessarily result in a profound chemoselectivity for either group when combined in one molecule. It would e.g. also be conceivable that the aromatic moiety is required for the molecule to adsorb on the catalyst surface or that the catalyst is activated by one moiety. The effect observed in Chapter 6 co-epoxidizing styrene and stilbene is a good example where a substrate plays a more complex role than simply being converted. Therefore, future catalytic studies should ideally also investigate the oxidation of molecules with several oxidizable moieties. The investigations with silver reported in this thesis have shown that silver has potential as an oxidation catalyst. Prepared by simple impregnation, Ag/SiO_2 exhibited considerable catalytic activity in alcohol oxidation though the (required) reaction temperatures were still high. The poor dispersion of the reported silver catalyst indicates that there is substantial potential for improvement. The involvement of silver-oxygen species as a necessary feature of silver also for several liquid phase oxidations as well as CO oxidation was suggested previously and should be further investigated. The generation of these oxygen species would then also have to be

implemented in suitable catalyst synthesis strategies. Consequently, the necessary high-temperature treatment might complicate the synthesis of very small silver nanoparticles.

The general usefulness of nano-sized ceria for promoting gold, palladium and silver catalysts in aerobic alcohol oxidation applied simply by addition is promising and hopefully might be useful in future studies. Addition of ceria (in the form of a precursor) also had a beneficial effect on the silver particle size when Ag/CeO_2-SiO_2 was produced by flame spray pyrolysis. Using this preparation technique silver leaching could be limited, a feature which has rarely been described for flame synthesized catalysts.

Reactions in pressurized CO_2 are popular within catalysis and the high reaction rates for the oxidation of alcohols over palladium catalysts are one example justifying the considerable research efforts in this field. Phase behavior indeed can be important and should therefore in general be considered in CO_2 related studies. This can be done experimentally in a relatively simple way when the equipment – i.e. mainly a view cell – is already present. The modeling approach is an alternative when the equipment is not available and is also more flexible but of course requires substantial familiarization with the overall modeling process. The results presented here are a good starting point but more studies should follow investigating whether the proposed model can replace simple semi-quantitative phase behavior studies in a reliable way. The catalytic results reported here differ from previously reported conclusions stating that biphasic conditions – though still close to the pressure at which phase transition occurs – result in a faster catalytic conversion. At high pressure the oxygen mass transport to the Pd surface appears to be too high. The process is very complex, phase behavior being only one parameter and is far from being completely understood. The influence of the flow on the activity and selectivity as well as the comparability between batch and continuous experiments should be investigated more carefully in order to obtain an understanding of the flow properties. Further extensive X-ray absorption and infrared spectroscopic studies under single and two phase conditions might give insights into the origin of the pronounced response to the phase behavior.

Catalysis by metal-organic frameworks (MOFs) is a new research direction and so far the performance of many MOFs has been interesting as a property of a new material but was often inferior to established catalyst materials. Contrary to this, the MOF used in the epoxidation study investigated here showed a very promising performance though the observed solvent co-oxidation limits the attractiveness of the studied process under economical viewpoints. Still, the broad distribution of especially homogeneous cobalt catalysts for oxidation reactions makes the MOF studied in here an interesting candidate for further catalytic studies.

Acknowledgements

This thesis and I received a lot of support during the last three years and I therefore owe many people sincere thanks. Jan-Dierk Grunwaldt “lured” me to Denmark making this thesis possible and initiated a big step forward in my life. He supported me constantly though without dictating my work. I always had the very productive feeling that he was more of an experienced collaborator than my boss. This allowed me to develop my independence as a researcher and to fully feel responsible for this thesis with all the flaws it certainly contains though being greatly minimized by his swift proof-reading. Many thanks! I would like to thank Anker D. Jensen who took over as my principal supervisor after Jan-Dierk left for Karlsruhe. He helped me a lot with his engineering point of view and I appreciated his constant interest in my work. I would furthermore like to thank both Anker and Jan-Dierk for the very important support during the writing of my research proposal. I would like to acknowledge Georgios M. Kontogeorgis for supervising me during the phase behavior study making this interesting study actually possible. I owe thanks to Alfons Baiker for allowing me to work in his group at the ETH where I certainly learned a lot. Kim Dam-Johansen supported me in coming to Denmark and created a fruitful working environment in his department which is very much appreciated. Teaching can be cumbersome but also rewarding. I profited especially from courses taught by Kenny Ståhl, Ingmar Persson, Peter Glarborg, Jan-Dierk Grunwaldt, Anders Riisager and Rasmus Fehrmann. Furthermore thanks to Martin Muhler, Konrad Herbst and Anders Riisager for taking over the time-consuming task of evaluating a Ph.D. thesis.

A Ph.D. study is expensive and therefore I would like to thank Haldor Topsoe A/S, DTU, MP_2T and FTP for their financial support and also the European Community (within the FP-6 Infrastructure Action “Integrating Activity on Synchrotron and Free Electron Laser Science”) and DANSCATT for granting financial help during the XAS trips. I am grateful for the possibility to measure XAS at the Swiss Light Source in Switzerland, the Angströmquelle Karlsruhe, the Hamburger Synchrotronstrahlungslabor at DESY (both Germany) and the MAX-lab in Sweden and of course I would like acknowledge the beamline scientists for providing professional support during the measurements.

Collaborating with other researchers made my work output far more efficient and so I would like to thank (in alphabetical order) Jens Enevold Thaulov Andersen (for providing ICP-MS equipment and support during the measurements), Thomas W. Hansen (for measuring TEM), Bertram Kimmerle (for synthesis of FMF, very fruitful discussions and introducing me to equipment at ETH), Reinhard

Kissner (for measuring and evaluating EPR data), Wolfgang Kleist (for discussion and coordination of the MOF project), Björn Schimmöller and Sotiris E. Pratsinis (for FSP synthesis and very fruitful discussion in the side-chain oxidation project), Samira Telschow (for determining BET surfaces), Ioannis Tsivintzelis (for phase behavior modeling and advice) and finally Michael T. Wharmby and Paul A. Wright (for MOF synthesis and characterization). Furthermore I would like to thank Alexander Gese and Søren Mikkelsen for performing experiments for me as part of their studies.

I would like to acknowledge my colleagues from ETH Zürich and DTU for integrating me so quickly and for the frequent Friday afternoon “meetings”. I enjoyed being a part of both groups! I would like to especially highlight Bertram Kimmerle, Jean-Michel Andason, Stefan Marx, Fabian Jutz (all ETH), Jacob Brix, Jakob Munkholdt, Nikolaj Musko, Anne Juul Pedersen and Martin Høj (all DTU). Special thanks to Tobias Dokkedal Elmøe and Jacob Brix for translating the summary and the abstract to Danish. I was very much supported by the technicians at DTU especially by Mette Larsen and Anders Tiedje. Mette ordered chemicals and therefore received more than 100 APVs from me. Anders was always at hand when I had technical problems, supported me with ordering equipment and last but not least encouraged me strongly in using the Danish language. The tool shop helped out swiftly when repairs where necessary. Charly Pickel supported me with details and tricks for the “supercritical” setup.

A Ph.D. study is nothing without social life. Sincere thanks to my departmental colleagues for fun spare time activities, the members of the Staff Club and to my friends, especially Per and Jacob who were there for me when life was tough. I would like to thank my family, Petra, my mother, Manfred, my father, my grandparents, my girlfriend Samira and my brother Manuel for supporting me during these three years. Without you my life would be so dull! I would like to highlight my mother who was always there for me during the past 28 years of my life and brought me to where I am now!

I did my best not to forget anyone and apologize if I should have done so.

Curriculum Vitae

Matthias Josef Beier

Date of Birth	June, 26th, 1982
Place of Birth	Braunschweig, Germany
Nationality	German
Parents	Petra Schellhorn-Beier, Social pedagogue
	Dr. Manfred Beier, Physicist
Academic Education	B. Sc. (Chemistry), University of Leipzig, Germany, 2005
	M. Sc. (Chemistry), University of Leipzig, Germany, 2007
Present Employment	02/2008 – 02/2011: Ph.D. student, Department of Chemical and Biochemical Engineering, Technical University of Denmark